2016

The effects of exposure to the environmental neurotoxicant manganese on α-synuclein and its cell-to-cell transmission via exosomes

Dilshan Shanaka Gurunnaselage Don
Iowa State University

The effects of exposure to the environmental neurotoxicant manganese on α-synuclein and its cell-to-cell transmission via exosomes

by

Dilshan Gurunnanselage Don

A dissertation submitted to the graduate faculty

in partial fulfillment of the requirements for the degree of

DOCTOR OF PHILOSOPHY

Major: Toxicology

Program of Study Committee:
Dr. Anumantha Kanthasamy, Major Professor
Dr. Arthi Kanthasamy
Dr. Wilson Rumbeiha
Dr. Stephanie Hansen
Dr. Sanjeevi Sivasankar

Iowa State University

Ames, Iowa

2016

To my father G.D. Harischandra and mother Priyani Jayamanna,

thank you for allowing me to follow my ambitions throughout my childhood

TABLE OF CONTENTS

ABSTRACT

Parkinson's disease (PD) is a chronic multifaceted neurodegenerative condition caused by a complex interplay of genetic and environmental factors that affects about 1% of people over the age of 60. Although the progressive loss of dopaminergic neurons and accumulation of aggregated α-Synuclein (αSyn) protein in Lewy bodies are considered key pathophysiological features of the disease, the physiological function of αSyn and the molecular mechanisms leading to protein aggregation and propagation remain unknown. Manganese (Mn) is considered a key inhaled pollutant implicated in environmentally-linked PD as evidenced by epidemiological studies done on humans exposed to Mn during mining, welding metals, and dry battery manufacturing. However, the exact molecular mechanisms underlying Mn-induced protein aggregation are not well understood. Considering the role of the divalent metal Mn in PD-like neurological disorders, we conducted a comprehensive characterization of the role of αSyn in Mn-induced dopaminergic neurotoxicity, cell-to-cell spreading of αSyn protein aggregates and aberrant miRNA delivery via exosomes. Using an αSyn-expressing dopaminergic cell model, we show that wildtype αSyn significantly attenuates Mn-induced neurotoxicity during the early stages of exposure while prolonged Mn exposure promotes αSyn aggregation and dampens its neuroprotective effect. Our subsequent studies show that upon Mn exposure, misfolded αSyn-containing exosomes are released to its extracellular milieu, which may in turn induce neuroinflammatory, and neurodegenerative responses in cell culture and animal models of PD. We also found enhanced accumulation of misfolded αSyn species in serum exosomes of welders exposed to Mn indicating the possibility of using exosomes as biomarkers of Mn-

neurotoxicity. To further elucidate the regulatory role of exosomes in Mn-induced miRNA dysregulation, we performed next-generation miRNA sequencing and identified multiple differentially expressed miRNAs in Mn-stimulated exosomes in contrast to control exosomes. Herein, our results suggest that Mn induces a novel mechanism of cell injury through modulating the protein and miRNA cargo in exosomes and altering gene expression. This may contribute to the cell-to-cell transmission of the aggregated αSyn protein and progression on neurodegeneration.

CHAPTER I: GENERAL INTRODUCTION

Dissertation Organization

The alternative format was chosen for this thesis and consists of manuscripts that have been published, or are being prepared for submission. The dissertation contains a general introduction, two book chapters, three research papers and a conclusions/future directions section that briefly discusses the overall findings from all chapters. The references for each manuscript chapter are listed at the end of that specific section. References pertaining to the background and literature review as well as those used in general conclusion section are listed at the end of the dissertation. The introduction section under Chapter 1 provides a brief background and overview of Parkinson's disease (PD), manganese (Mn) neurotoxicity and exosomes which this thesis is heavily based upon. The Background and Literature Review-I section covers in depth review on the recent advances on elucidating cellular and molecular mechanisms of Mn-induced protein misfolding, mitochondrial dysfunction and consequent neuroinflammation and neurodegeneration; this section will be submitted to *Pharmacology and Therapeutics* for publication. In the background and literature review II section, authors discuss and summarize current literature on exosome composition, biogenesis and their potential function as intercellular messengers in cell-to-cell transmission of proteins and small-RNA species.

The manuscript from Chapter 2 was recently published in the *Toxicological Science*. It demonstrates a potential neuroprotective role of wild-type α-Syn against Mn-induced neurotoxicity during the early stages of exposure in a dopaminergic neuronal

model of PD. Chapter 3 explores how aggregated α-synuclein, the major component of PD-associated Lewy bodies and a gene linked to the development of familial PD, can transfer from one to another through exosomes leading to inflammation and neurodegeneration in experimental models on Mn-toxicity. Chapter 4 studies how exosomes contributes to cell-to-cell transmission of miRNAs and thereby manipulate recipient cell gene expression. Chapters 3 and 4 are in the process of being submitted for publication.

This dissertation also contains three appendix sections. Appendix I is a book chapter that was recently published in *Manganese in Health and Disease* summerizeing role of manganese in Prion disease. Appendix II is published in the *Jornal Prion* evaluating the role of oxidative stress-sensitive, pro-apoptotic protein kinase Cδ (PKCδ) in prion-induced neuronal cell death using cerebellar organotypic slice cultures (COSC) and mouse models of prion diseases. Appendix III is a book chapter that was recently published in the *Inflammation, Oxidative Stress and Age-Related Disease* summarizing the recent discoveries of antioxidant therapeutics, including mitochondria-targeted antioxidants for modulating oxidative damage in PD and its potential as a possible treatment for PD.

This dissertation contains the experimental data and results obtained by the author during his Ph.D. study under the supervision of his major professor Dr. Anumantha G. Kanthasamy at Iowa State University, Department of Biomedical Sciences.

.

Introduction

Parkinson's disease

Parkinson's disease (PD) is the second most common neurodegenerative disorder after Alzheimer's disease, and is the most common movement disorder in people over the age of 65. PD also recognized as one of the most common neurologic disorders, affecting approximately 1% of individuals older than 60 years causing progressive disability characterized by severe motor symptoms including uncontrollable tremor, postural imbalance, slowness of movement and rigidity (Lotharius and Brundin, 2002). Pathologically, this disease is characterized by a progressive degeneration of dopaminergic neurons projecting from the substantia nigra pars compacta (SNpc) to the striatum resulting in pronounced loss of neurotransmitter dopamine resulting above mentioned extrapyramidal features. Disease also often associated with abnormal accumulation of misfolded proteins in cytoplasmic inclusions called Lewy bodies (LB) and Lewy neurites, association between Lewy pathology and pathogenesis of the disease is poorly understood. Although aging appears to be the greatest risk for the development of PD, pathogenesis of the disease remains incompletely understood and remains to be elucidated. Recent evidence has implicated several genes such as α-synuclein (PARK1), Parkin (PARK-2), PINK1(PARK6), DJ-1(PARK7), ATP13A2 (PARK9), and SLC30A10 with early-onset Parkinson's whereas LRRK2 (PARK8) and VPS35 (PARK-17) are accounted for late-onset PD (Dawson et al., 2010; Roth, 2014). While major emphasis has been given to the familial PD caused by gene mutations, more than 90% of PD occurrences count for the sporadic form of PD which is likely caused by a complex interplay of genetic and environmental factors. During the last couple of decades a

number of epidemiological and clinical studies have suggested potential environmental risk factors for PD. These include: repeated head injury, heavy metal exposure, excess body weight, exposure to pesticides and some surrogate measures such as living in rural areas, drinking well water, farming etc (Dick et al., 2007; Priyadarshi et al., 2001). Although PD is classically defined as a movement disorder associated with degeneration of neurons in the nigrostriatal system, non-motor symptoms have been recognized in recent years. During the early stages of the disease or the presymptomatic phase, patients develop non-motor deficits including cognitive changes, behavioral/neuropsychiatric changes autonomic nervous system failure, olfactory impairment and sleep disturbances. Non-motor symptoms can represent some of the greatest challenges to quality of life and appropriate management in PD since they usually do not respond to dopamine therapy as well as motor symptoms.

α-Synuclein

α-Synuclein (α-Syn) is a small, acidic protein of 14.5kDa and 140-amino acids that highly is conserved in vertebrates and predominantly expressed presynaptically in neurons throughout the mammalian brain and cerebrospinal fluid (CSF). Physiological functions of a-Syn are poorly understood, but evidence has suggested a role for it in synaptic plasticity, dopamine regulation, and membrane trafficking. α-Syn is belongs to the synuclein family composed of α-, β-, and γ-synuclein. Structurally, α-Syn is a natively unfolded protein which lacks defined secondary structure and therefore belongs to the intrinsically unstructured protein family. The α-Syn protein has three distinct structural domains. The amphipathic N-terminal region (residues 1 to 60) contains 11 amino acid repeats including the consensus sequence KTKEGV, which is important in α-
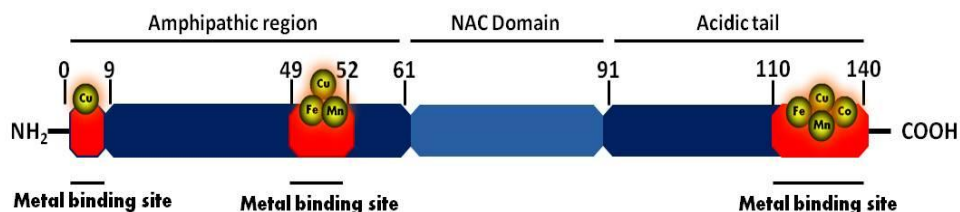
Figure 1: Structure of α-synuclein protein indicating its metal binding sites

helix formation. The central hydrophobic region (residues 61 to 91) contains the nonamyloid component region (NAC), which is important in protein aggregation. Finally, the C-terminal region (residues 91 to 140) is highly acidic proline rich and is responsible for the intrinsically disordered nature of αSyn (Harischandra et al., 2015). The a-Syn protein has three metal binding sites: one at N- terminus, one at central region and one at C-terminus of the protein. The metal binding sites near 49–52 and 110–140 are known to interact with divalent metals including manganese (Uversky et al., 2001).

The link between αSyn and PD pathogenesis is based on case studies of familial PD and the observation that misfolded αSyn is a major constituent of Lewy bodies and Lewy neurites in both familial and sporadic PD. Also, there is compelling evidence that mutations in the gene encoding αSyn directly linked to the onset of PD. The overexpression of αSyn due to duplication or triplication of the SNCA gene or single nucleotide polymorphisms in the SNCA gene resulting Ala53Thr, Ala30Pro, and Glu46Lys mutations are linked to causes rare familial forms of PD. The idea that αSyn can pathologically propagate throughout the CNS recently gained much attention with the finding of αSyn species in human plasma and CSF (El-Agnaf et al., 2003; Kordower et al., 2008) and host-to-graft propagation of αSyn-positive Lewy bodies in fetal ventral

mesencephalic and embryonic nigral neurons transplanted in human PD patients. (Kordower *et al.*, 2008; Li *et al.,* 2008). Even though several models have postulated the cell-to-cell transmission of pathological propagating αSyn species (Desplats et al., 2009; Dunning et al., 2013; Lee et al., 2008), the exact mechanism of PD pathogenesis and related synucleinopathies largely remains unknown. Growing evidence indicates that extracellular αSyn induces pathogenic actions by activating neuroinflammatory and neurodegenerative responses *in vitro* (Emmanouilidou et al., 2010; Su et al., 2008).

Manganese neurotoxicity

Manganese is considered a key inhaled pollutant in the environment and recently gained importance as a putative risk factor for environmentally linked PD and related neurodegenerative disorders. Being the 12th most abundant element which composes approximately 0.1% of the earth crust, makes manganese ubiquitously present in the environment (Martinez-Finley et al., 2012). In trace amounts, manganese is an essential metal found in all body tissues as it is essential for many ubiquitous enzymatic reactions, including synthesis of amino acids, lipids, proteins, and carbohydrates. It also plays a key nutritional role in bone formation, fat and carbohydrate metabolism, blood sugar regulation, and calcium absorption in the body (Bowman et al., 2011b). Primary route of manganese exposure in humans is through diet, as it is present in whole grains, rice, nuts, tea, leafy green vegetables and manganese-containing nutritional supplements. However, chronic excessive exposure by occupational or environmental sources of manganese cause a neurodegenerative disorder known as Manganism, characterized by severe neurological deficit that often resembles the involuntary extrapyrimydal symptoms

associated with PD. Manganese is also highly present in the environment through common human uses, such as use of methylcyclopentadienyl manganese tricarbonyl (MMT) as an antiknock gasoline additive, use in fertilizers, use in paint and cosmetics known as manganese violet (Martinez-Finley et al., 2012). The other major anthropogenic sources of environmental manganese include municipal wastewater discharges, welding, mining and mineral processing, emissions from alloy, steel, and iron production, combustion of fossil fuel and dry-cell manufacturing. Although exact mechanisms through which manganese is absorbed into the body are not fully understood, it has been shown to accumulate in the brain, specifically in the basal ganglia region, exerting its neurotoxic effects. Despite the prevalence and potential risk to human health, the mechanisms by which manganese exerts its neurotoxic effects are not well understood and mechanisms by which manganese cause neuronal dysfunction and death are yet to be elucidated. However, manganese neurotoxicity suggested exerting nigrostriatal cell death by causing oxidative damage, protein misfolding, and neuroinflammation mediated apoptotic cell death

Exosomes

Exosomes are cell-derived vesicles of 50-200nm in size with endosomal origin. They are released into the extracellular space as a result of fusion of multivesicular bodies (MVBs) with plasma membrane. Exosomes were initially thought to serve simply as "garbage bags" for cells to get rid of unwanted constituents. However, an increasing body of evidence indicates that they play a pivotal role in cell-to-cell communication and influence both physiological and pathological processes. Exosome could directly

stimulate target cells by receptor-mediated interactions or may transfer from the cell of origin to various bioactive molecules including membrane receptors, proteins, mRNAs and microRNAs. Importantly, recent studies have shown that exosomes carry misfolded protein cargo which could induce deleterious effects on targets cells in neurodegenerative disorders (Arellano-Anaya et al., 2015; Grey et al., 2015; Kong et al., 2014) suggesting that exosomes may be involved in cell-to-cell transmission of pathogenic proteins in pathogenesis of progressive neurodegenerative disorders. Since central pathophysiological mechanism of many neurodegenerative diseases including Alzheimer's disease, Parkinson's disease, Huntington's disease and Prion Disease involves protein aggregation and its transmission, exosomes may play central role in progression of these protein misfolding diseases.

Background and Literature Review – I

Manganese; its role and significance in Parkinsonism Spectrum Disorders

A review to be submitted to *Pharmacology and Therapeutics*

Dilshan S. Harischandra, Shivani Ghaisas, Huajun Jin, Arthi Kanthasamy, Vellareddy Anantharam, Anumantha G. Kanthasamy*

Department of Biomedical Sciences, Iowa Center for Advanced Neurotoxicology, Iowa State University, Ames, Iowa 50011

Abstract

Metal ions (zinc, copper, magnesium, manganese, etc.) are important components of various metalloenzymes that function in many biological processes, such as synaptic

communication, respiration, free radical generation and hypoxia detection. Most of these ions are required in minute doses that are frequently met by proper nutrition. However, if present in large amounts, they can inhibit different enzymatic reactions as well as interfere with metabolic processes. Manganese is a co-factor of manganese superoxide dismutase, an enzyme that efficiently removes reactive oxygen species from cells. In contrast, high concentrations of manganese are known to impair cellular antioxidant mechanisms thus exacerbating oxidative damage in cells, particularly astrocytes and neurons. Growing evidence also suggests that manganese can bind to α-synuclein, a presynaptic protein that plays a central role in the pathogenesis of Parkinson's disease (PD), causing conformational changes in this protein thus leading to protein aggregation and subsequent mitochondrial toxicity and cell death. Chronic manganese exposure by either ingestion or inhalation can lead to neurological symptoms similar to idiopathic PD. While there have been recent advances in the understanding of its pathophysiology, manganese neurotoxicity is still poorly understood. The aim of this review is to concisely accrue what we know about its effect primarily on the nervous system with respect to its role in protein misfolding, mitochondrial dysfunction and consequently neuroinflammation and neurodegeneration.

Metals in biology

At least 13 metals have been identified as essential for life, and four of these (sodium, potassium, magnesium and calcium) are present in large quantities. The remaining nine trace metals (manganese, iron, cobalt, vanadium, chromium, molybdenum, nickel, copper and zinc) assume vital roles in building organic biomolecules. In the last couple of

decades, the importance of metal ions in protein biology has been an increasingly attractive research subject given their association with many human diseases, for which metals have been identified as the causative or stimulatory agent. Metals are essential because of their integral role in enzymes that catalyze the basic metabolic or biochemical processes shared by all forms of life on earth. It has been estimated that a third of all proteins require metal ions to carry out their biological functions (Holm et al., 1996).

When considering all six classes of enzymes - oxidoreductases, transferases, hydrolases, lyases, isomerases, ligases, over 40% of all enzymes contain metals (Andreini et al., 2008). Moreover, the chemistry of metals allows for a broader set of protein-metal reactions. For instance, redox-active metal ions are often interchangeable depending on the metal concentration and their affinities to protein. The affinities of proteins for the different trace metals are substantially determined by universal series, which for divalent metals is the Irving-Williams series ($Mn^{2+} < Fe^{2+} < Co^{2+} < Ni^{2+} < Cu^{2+} > Zn^{2+}$), wherein Cu^{2+} is highly competitive and can replace lower order metals (Tottey et al., 2008).

These "metalloproteins" are involved in many key biological processes, such as gas transport, photosynthesis, cell respiration, antioxidant defense and many other vital redox reactions driven by their interaction with metals. Well-characterized examples for redox active metalloprotein systems are blue-copper proteins, heme-binding proteins and iron-sulfur-cluster proteins. Moreover, recent advances in synthetic chemistry have focused on the study of metal sites in metalloproteins and metalloenzymes to influence biological processes in the battle against many daunting human diseases. Advanced medicinal chemistry approaches have given us new, innovative medicinal applications of metal

complexes and organometallic agents. Prime examples for such uses of metals include the platinum-containing anticancer drugs (e.g., Cisplatin), lithium-containing depression drugs (e.g., Camcolit), and manganese-containing anticancer drugs (e.g., SOD mimics; Farrell, 2003).

Presumably, all metalloproteins would bind to their desired metal ligands, and this binding can regulate their folding. However, despite the wealth of structural information, the coupled protein folding-metal binding pathways for metalloproteins remain largely unknown (Wittung-Stafshede, 2002). Proper protein folding is critical to the conformational integrity and function of proteins. However, metal ligand binding can also induce undesirable structural transitions in proteins that eventually lead to the formation of protein aggregates associated with several diseases. The pathologies of Alzheimer's disease (AD), PD, and prion diseases are linked to abnormal misfolding of otherwise harmless neural proteins. For example, in AD it has been shown that increased levels of metals such as Cu^{2+} and Zn^{2+} are linked to the aggregation of Aβ protein *in vitro* (Kenche and Barnham, 2011). The theory of metal-induced aggregation has gained credence following numerous studies tying metal concentrations in the brain with AD, PD and amyotrophic lateral sclerosis (ALS) in *in vivo* and *in vitro* studies employing recombinant proteins (Brown, 2011; Brown et al., 2005).

In this review we will focus on α-Synuclein, one of the major proteins implicated in PD, and its interactions with metals; specifically its interaction with manganese in oxidative stress, protein aggregation and neurodegeneration.

Parkinson's disease

PD is the second most common neurodegenerative disorder after Alzheimer's disease, and is the most common movement disorder in people over the age of 65, causing progressive disability characterized by severe motor symptoms including uncontrollable tremor, postural imbalance, slowness of movement and rigidity (Lotharius and Brundin, 2002). Pathologically, this disease is characterized by a progressive degeneration of dopaminergic neurons projecting from the substantia nigra pars compacta (SNpc) to the striatum, resulting in a pronounced loss of the neurotransmitter dopamine and hence the above-mentioned extrapyramidal symptoms. Even though the disease is also often associated with the abnormal accumulation of misfolded proteins in cytoplasmic inclusions called Lewy bodies (LB) and Lewy neurites, the association between Lewy pathology and disease pathogenesis is poorly understood. Similar neuropathological lesions involving the deposition of abnormal proteins also characterize other neurological disorders (Ross and Poirier, 2004), including AD (Kotzbauer et al., 2001; Uchikado et al., 2006), Lewy body dementia (LBD) (McKeith et al., 2004), Huntington's disease (HD) (Davis et al., 2014), multiple system atrophy (MSA) (Shoji et al., 2000) and some prion diseases (Aguzzi and Calella, 2009; Aguzzi and O'Connor, 2010).

Although aging appears to be the greatest risk factor for developing PD, its pathogenesis remains incompletely understood. Recent evidence has implicated several genes to the onset of PD, such as *α-synuclein* (PARK1), *parkin* (PARK-2), *PINK1*(PARK6), *DJ-1*(PARK7), *ATP13A2* (PARK9) and *SLC30A10* associated with early-onset PD as well as the genes *LRRK2* (PARK8) and *VPS35* (PARK-17) (Dawson et al., 2010; Roth, 2014)

linked with late onset of the disorder. While major emphasis has been given to the familial PD caused by gene mutations, the sporadic form of PD accounts for more than 90% of PD occurrences whose onsets were likely caused by a complex interplay of genetic and environmental factors. A growing number of epidemiological and clinical studies have identified potential environmental risk factors for PD, including repeated head injury, heavy metal exposure, excess body eight, exposure to pesticides and some surrogate measures such as rural living, drinking well water and farming (Dick et al., 2007; Priyadarshi et al., 2001). Interestingly, some of these environmental triggers and toxins induce pathophysiological features that mimic PD when they are administered in experimental animal settings. One such toxin is methyl-4-phenyl-1,2,3,6-tetrahydropyridine (MPTP), a compound produced as an impurity during the illicit synthesis of the narcotic Desmethylprodine. MPTP causes chronic and severe Parkinsonism by selectively damaging the substantia nigra, resulting in all the motor features of PD (Appendino et al., 2014; Ballard et al., 1985; Langston et al., 1983). Other compounds widely used in experimental models to study the etiopathogenesis of PD include the narcotic methamphetamine, the dopamine derivative 6-hydroxydopamine, and pesticides such as rotenone, paraquat and dieldrin. These neurotoxins cause nigrostriatal cell death by interfering with mitochondrial function, inducing oxidative stress, inducing protein aggregation and modifying proteasomal function (Ghosh et al., 2013; Jin et al., 2015b; Kanthasamy et al., 2008; Latchoumycandane et al., 2011). In addition, exposure to heavy metals such as iron, lead, mercury, cadmium, arsenic and manganese, as well as exposure to metal-based nanoparticles, has been shown to increase the risk of PD through the neurotoxic accumulation of metals in the SNpc and by increasing oxidative stress-

mediated apoptosis (Aboud et al., 2014; Afeseh Ngwa et al., 2009; Afeseh Ngwa et al., 2011; Harischandra et al., 2015; Kanthasamy et al., 2012; Milatovic et al., 2009).

Manganese

Manganese is considered a key inhaled pollutant in the environment and recently gained importance as a putative risk factor for environmentally-linked PD and related neurodegenerative disorders. Being the 12th most abundant element, composing approximately 0.1% of the earth's crust, manganese is ubiquitously present in the environment (Martinez-Finley et al., 2012). Although the earth's crust is the major source pool of manganese in the environment, other sources include direct atmospheric deposition, wash-off from plant and other surfaces, leaching from plant tissues, ocean spray, and volcanic activity. Manganese occurs in trace amounts in all body tissues as it is an essential trace metal for many ubiquitous enzymatic reactions, including the synthesis of amino acids, lipids, proteins, and carbohydrates. It also plays a key nutritional role in bone formation, fat and carbohydrate metabolism, blood sugar regulation, and calcium absorption in the body (Bowman et al., 2011). Being present in whole grains, rice, nuts, tea, leafy green vegetables and manganese-containing nutritional supplements, the primary route of manganese exposure in humans is through dietary intake. The abundance of manganese-enriched food in the typical daily diet makes it relatively easy to accrue the daily reference intake (DRI) of 2.3 mg/day for men and 1.8 mg/day for women (Aschner and Aschner, 2005), thereby minimizing the risk of manganese deficiency-related birth defects, impaired fertility, osteoporosis and enhanced

susceptibility to seizures (Aschner and Aschner, 2005; Dendle, 2001; Sarban et al., 2007).

Despite its nutritional benefits, prenatal and postnatal exposure to high levels of manganese affects infant neurodevelopment, exemplifying the role of manganese as both an essential nutrient and a toxicant (Claus Henn et al., 2010; Zota et al., 2009). High manganese exposure in early life is associated with poorer cognitive performance, especially in the verbal domain of children (Menezes-Filho et al., 2011). In older cohorts, chronic excessive exposure by occupational or environmental sources of manganese causes a neurodegenerative disorder known as Manganism, which is characterized by a severe neurological deficit that often resembles the involuntary extrapyramidal symptoms associated with PD. In 1837, Dr. John Couper at the University of Glasgow reported the first case of manganese-induced neurotoxicity, which was discovered in employees of Charles Tennant and Co., a manufacturer of bleaching powder (Couper, 1837). Later, public awareness of manganese neurotoxicity arose as more clinical studies identified a PD-like syndrome in workers employed at a manganese ore crushing plant and a ferromanganese factory (Cook et al., 1974; Huang et al., 1989). Manganese also enters human-impacted environments through its use as an antiknock gasoline additive (methylcyclopentadienyl manganese tricarbonyl, MMT), in fertilizers, and in paint and cosmetics known as manganese violet (Martinez-Finley et al., 2012). Manganese neurotoxicity has often been found in agricultural workers exposed to organic manganese-containing pesticides, such as manganese ethylene-bis-dithiocarbamate (Maneb) and in chronic abusers of the street drug called 'Bazooka', a cocaine-based drug contaminated with manganese carbonate (Ensing, 1985). The other major anthropogenic

sources of environmental manganese include municipal wastewater discharges, welding, mining and mineral processing, emissions from alloy, steel and iron production, combustion of fossil fuel and dry-cell manufacturing. Although the precise mechanisms through which manganese is absorbed into the body are not fully understood, it has been shown that it accumulates in the brain's basal ganglia region. Although manganism shares many commonalities with PD, it is also worth pointing out the differences. Behaviorally, manganism is mainly characterized by milder and less frequent resting tremor that tends to be postural or actional, a propensity to fall backward, excessive salivation and frequent dystonia consisting of facial grimacing, hand dystonia and/or plantar flexion of the foot (Calne et al., 1994). Patients were also reported to have symptoms of irritability, emotional lability, illusion, hallucinations and psychoses, referred to as "manganese madness" (Huang, 2007). Pathologically, manganese neurotoxicity affects primarily neurons in both the globus pallidus and striatum, whereas PD predominantly affects dopaminergic neurons in the SNpc (Roth, 2014). Therefore, in fact, the PD-like behavior deficits in manganism result from manganese's capability to suppress dopamine release from the striatum, thus generating fundamental behavioral dysfunctions common to both PD and manganism (Fitsanakis et al., 2006; Kim et al., 2002; Racette et al., 2005; Roth et al., 2013).

Manganese in oxidative stress and neurodegeneration

Although the mechanisms by which manganese induces nigrostriatal cell death are not well defined, its neurotoxicity appears to be regulated by a number of factors, including oxidative injury, mitochondrial dysfunction, protein misfolding and neuroinflammation.

Manganese is a redox-active metal with high reduction potential, giving it an important role in oxygen chemistry. As a cofactor forming manganese superoxide dismutase (MnSOD), it aids the removal of harmful byproducts of oxygen metabolism such as superoxide ($O_2^{.-}$) and hydrogen peroxide (H_2O_2). However, when allowed to accumulate, manganese exacerbates oxidative damage. At just 2% of body weight while consuming 20% of the total oxygen and calories, the brain is highly metabolically active and hence highly susceptible to oxidative damage. As mentioned before, manganese is known to accumulate in the globus pallidus and striatum. These regions are especially vulnerable to oxidative injury because of their intense oxygen consumption, significant dopamine content and their high content of non-heme iron. A recent study evaluating the effect of Mn on DAT transfected and non-transfected HEK cells showed that Mn prevents dopamine reuptake in the transfected cells and also mobilize DAT receptors, from the cell surface to the intracellular compartments. Consequently, dopamine-induced cell toxicity is observed (Roth et al., 2013). Studies conducted with N27 mesencephalic dopaminergic neuronal cells have shown that manganese treatment increases reactive oxygen species (ROS) production (Harischandra et al., 2015). This ROS production resulted in the sequential activation of mitochondrial-dependent proapoptotic events, including cytochrome *c* release, caspase-3 activation and DNA fragmentation, but not caspase-8 activation, indicating that the mitochondrial-dependent apoptotic cascade primarily triggers manganese-induced apoptosis as shown in Figure 1 (Latchoumycandane et al., 2005). Moreover, protein kinase C delta (PKCδ), a redox-sensitive kinase involved in neurodegenerative disorders such as Alzheimer's disease, prion disease and PD (Ciccocioppo et al., 2008; Harischandra et al., 2014; Jin et al., 2011; Kanthasamy et al.,

2006), is reported to be a key mediator in manganese-induced apoptosis (Anantharam et al., 2002; Latchoumycandane et al., 2005). Later studies in differentiated N27 cells also demonstrated that chronic low-dose manganese exposure impairs tyrosine hydroxylase (TH), the rate-limiting enzyme in dopamine synthesis, through activation of PKCδ and protein phosphatase-2A (PP2A) activity (Zhang et al., 2011). Notably, *in vitro* and *in vivo* studies conducted with the hydrophilic antioxidant vitamin E analog, Trolox (6-hydroxy-2,5,7,8-tetramethylchroman-2-carboxylic acid) reversed manganese-induced neurotoxicity and rescued dysfunctional dopaminergic transmission and manganese-induced motor coordination deficits (Cordova et al., 2013; Milatovic et al., 2011), further emphasizing the relationship between oxidative stress and manganese-related neurodegeneration.

Dopamine belongs to the catecholamine and phenethylamine families and serves as a neurotransmitter under physiological conditions. However, the chemical structure of catecholamines predisposes them to oxidation, and their well-characterized metabolic routes can yield quinones and free radicals providing evidence that dopamine may also serve as a neurotoxin contributing to the neurodegenerative process through oxidative metabolism. By promoting dopamine auto-oxidation, manganese as a transition metal potentiates dopamine toxicity in high manganese-accumulating areas of the brain (globus pallidus and striatum). Under normal physiological conditions, dopamine is oxidized enzymatically through monoamine oxidases (MAO) to dihydroxyphenylacetic acid (DOPAC) and subsequently methylated by catechol-O-methyltransferase (COMT) to homovanillic acid (HVA) or else dopamine is converted to 3-methoxytyramine (3-MT) via COMT and then further oxidized to HVA through MOA. During this MAO-mediated

dopamine turnover process, hydrogen peroxide (H_2O_2) is a byproduct of the deamination of dopamine, generating inherent oxidative stress conditions in nigrostriatal system. Dopamine can also be non-enzymatically oxidized by molecular oxygen, yielding quinones and H_2O_2. These quinones also undergo intramolecular cyclization, which is immediately followed by a cascade of oxidative reactions culminating in a black, insoluble polymeric pigment known as neuromelanin (Graham, 1978; Hermida-Ameijeiras et al., 2004). Neuromelanin in dopaminergic neurons augments the vulnerability to auto-oxidation through quinone modification of dopamine leading to high basal levels of oxidative stress in the SN (Graham, 1978). Therefore, the degradation of dopamine, either enzymatically or non-enzymatically, produces H_2O_2. Two prominent manganese valence states, Mn^{2+} and Mn^{3+}, are found in biological systems. In the presence of high levels of divalent manganese (Mn^{2+}), H_2O_2 can convert via the Fenton reaction to highly toxic hydroxyl radicals ($\bullet OH$). But because of its higher oxidative state, Mn^{3+} was an order of magnitude more cytotoxic than Mn^{2+} in studies conducted in rats dosed with manganese (Ali et al., 1995). In fact, oxidation of dopamine by Mn^{3+}, generating quinones and H_2O_2, has been shown to be independent of oxygen and far more rapid than that mediated by Mn^{2+} (Archibald and Tyree, 1987). Since Mn^{2+} can readily oxidize to Mn^{3+} in the human brain via superoxides, the autoxidation of catecholamines can only further potentiate oxidative stress.

Impairment of the cellular antioxidant machinery, causing an imbalance between ROS generation and its elimination, plays a major role in the development of certain neurodegenerative processes. The antioxidant glutathione (GSH), present in both neurons and astrocytes, provides the first line of cellular defense against ROS. GSH actively

disposes off exogenous peroxides by acting as a co-substrate in reactions catalyzed by glutathione peroxidase (GPx), thus playing important functional roles in the central nervous system (CNS). Altered striatal concentrations of GSH, glutathione disulfide (GSSG), ascorbic acid (AA), malondialdehyde (MDA), and the activities of glutathione reductase (GR) and GPx have been previously reported with manganese neurotoxicity, suggesting that impairment in the neuronal antioxidant system renders the brain susceptible to manganese-induced neurotoxicity (Chen and Liao, 2002; Dukhande et al., 2006; Maddirala et al., 2015). Moreover, inhibition of GSH synthesis potentiated the manganese-induced increase in inosine, hypoxanthine, xanthine and uric acid levels in the striatum and brainstem of aged rats (Desole et al., 2000), indicating that manganese-induced cytotoxicity was mediated through mitochondrial dysfunction. Therefore, the specific vulnerability of dopamine neurons to manganese plays a pivotal role in the impairment of cellular antioxidant defenses, wherein disruption of the mitochondrial oxidative energy metabolism cascade leads to dopaminergic cell death. Excessive production of ROS induces the oxidation of membrane polyunsaturated fatty acids (PUFA), yielding a multitude of lipid peroxidation products including reactive aldehydes such as 4-hydroxy-trans-2-nonenal (4-HNE), 4-oxo-trans-2-nonenal (4-ONE), malondialdehyde (MDA) acrolein, F_2-isoprostanes (F_2-IsoPs), and isofurans (Aluru et al., 2015; Esterbauer et al., 1991). These markers are derived from free radical-mediated peroxidation of arachidonic acid (ARA), which is released from neural membrane glycerophospholipids through the activation of cytosolic phospholipases A_2 ($cPLA_2$), which are enzymes coupled to NMDA receptors through a G-protein independent mechanism (Farooqui and Horrocks, 2007; Farooqui and Farooqui, 2011). Since most

biological membranes of cells and organelles are composed of PUFA, lipid peroxidation is considered as the main molecular mechanisms involved in the oxidative damage to cell structures and in the toxicity process that leads to cell death. Consistent with these observations, primary rat cortical neurons exposed to a very high manganese dose (500 μM) for 6 hours showed structural damage to neurons and a significant increase in F_2-IsoPs levels (roughly 50%) compared to controls (Milatovic and Aschner, 2009). Likewise, in primary astrocyte cultures exposed to the same experimental conditions, F_2-IsoPs levels increased 51% compared to control cultures (Milatovic et al., 2007). However, the direct role of manganese in CNS toxicity associated with lipid peroxidation remains debatable as some investigators argue that *in vivo* administration of manganese alters cellular Ferrous (Fe^{2+}), which plays a permissive role in increasing lipid peroxidation and augmenting neuronal vulnerability (Chen et al., 2006; Chen et al., 2000; Shukla and Chandra, 1981).

Moreover, dopamine quinones have been shown to bind and modify several proteins implicated in PD pathophysiology such as α-synuclein, DJ-1 and parkin (Conway et al., 2001; Girotto et al., 2012; LaVoie et al., 2005). However, among the multitude of cellular macromolecules prone to oxidative damage, damaged nucleic acids are particularly hazardous due to compromised genetic information. Among the five nucleobases, namely uracil, thymine, cytosine, adenine and guanine, guanine is the most susceptible to oxidation by hydroxyl radicals (Cerchiaro et al., 2009; Cooke et al., 2003). Hydroxyl radical-mediated insults to DNA strands produce 8-hydroxyguanosine (8-OHG), presently the most studied oxidized DNA product. Interestingly, DNA damage in PD also involves 8-OHG as well as 8-hydroxyl-2-deoxyguanosine (8-OHdG) as elevated 8-OHG

and reduced 8-OHdG have been observed in the SN and cerebrospinal fluid (CSF) of PD patients (Isobe et al., 2010; Zhang et al., 1999). In contrast, *in vitro* studies of manganese toxicity reported increased 8-oxo-7,8-dihydro-2'-deoxyguanosine (8-oxodG) content in the DNA of PC12 cells treated with dopamine (Oikawa et al., 2006). Stephenson and colleagues have also shown that manganese catalyzes the auto-oxidation of catecholamines in SH-SY5Y cells with the ensuing oxidative damage to thymine and guanine DNA bases, further indicating the effect of manganese-induced semi-quinone radical ions and ROS production on DNA damage (Stephenson et al., 2013).

Manganese and neuroinflammation

Although much emphasis has been placed on oxidative stress in the manganese-induced dysfunction of dopaminergic neurons, the activation of glial cells also plays an important role in potentiating manganese neurotoxicity by inducing the release of non-neuronal-derived ROS and inflammatory mediators such as proinflammatory cytokines. The state of glial activation is defined by its morphology and by the proliferation, migration and expression of immune modulatory molecules. The two major types of glial cells in the CNS are astrocytes and microglia with the latter constituting about 10% of all glial cells in CNS.

It is now well documented that glial activation is prominent in the brains of humans exposed to manganese, as well as in non-human primate and rodent models of manganese neurotoxicity (Cordova et al., 2013; Erikson and Aschner, 2006; Huang, 2007; Perl and Olanow, 2007). Neuroinflammation is regarded as a key mediator in mechanisms leading to the loss of dopaminergic neurons in PD. The activation of microglia plays a major role

in the response to environmental stresses and immunological challenges by scavenging excess neurotoxins, removing dying cells and cellular debris, and releasing proinflammatory cytokines (Carson et al., 2007; Tansey et al., 2008). Inducible nitric oxide synthase (iNOS), which produces large amounts of nitric oxide (NO), is released by microglia in response to inflammatory mediators such as LPS and cytokines. The levels of NO are reported to be higher in the CNS of human PD cases and in animal models of PD (Mogi et al., 1994). Consistent with this finding, iNOS knockout animals were resistant to MPTP-induced dopaminergic neuronal loss in the substantia nigra (Przedborski and Vila, 2003). Recent reports suggest that NF-κB, a transcription factor required for transcribing proinflammatory molecules, is also activated in the substantia nigra of PD patients and MPTP-treated mice (Ghosh et al., 2007). In contrast to microglia, astrocytes do not attack any pathological targets, but instead produce factors that are important in inflammatory reactions seen in the SN of PD brains (Miklossy et al., 2006). Activated astroglial cells were recently found in human PD brains and in the MPTP mouse model of PD (Ghosh et al., 2007; Ghosh et al., 2009).

In terms of manganese toxicity, astrocytes play a major role in neuroinflammation as they represent a "sink" for brain manganese (Wedler and Denman, 1984), with concentrations 10–50 fold greater in these cells than neurons, making them more susceptible to manganese toxicity than other cell types. Since astrocytes have transferrin receptors, which readily bind to Tf-Mn^{3+}, it is not surprising to find higher levels of manganese in astrocytes than in any other neural cell type (Aschner et al., 1999; Erikson and Aschner, 2006). It is thought that excess glutamate, which leads to glutamate-induced

excitotoxicity, abruptly increases intracellular Ca^{2+} levels. This increase in Ca^{2+} blocks Mn^{2+} uptake, prompting a release of mitochondrial Mn^{2+} into the cytosol. Finally, high levels of cytosolic Mn^{2+} in astrocytes activates glutamine synthetase, which removes excess glutamate (Wedler et al., 1994). However, excessive extracellular Mn^{2+} can disrupt intracellular Ca^{2+} signaling in astrocytes by competitively occupying Ca^{2+} binding sites, thus interfering with mitochondrial Ca^{2+} homeostasis (Farina et al., 2013). Loss of Ca^{2+} homeostasis leads to astrogliosis. In addition, Mn^{3+} causes astrocyte swelling via oxidative/nitrosative pathways (Rama Rao et al., 2007). Increased manganese levels in astrocytes elevate the expression of proinflammatory signals such as iNOS and IL-6 (Moreno et al., 2008). *In vitro* studies have shown that manganese-treated astrocytes use larger amounts of L-arginine, which is a substrate for nitric oxide (NO) (Hazell and Norenberg, 1998). While timely expression of these signals is necessary in response to neuronal stress or cellular damage, excessive production is counter-productive, often exacerbating the toxic insult. Microarray gene expression profiling of primary human astrocytes exposed to manganese showed an upregulation of genes encoding proinflammatory cytokines with a concurrent downregulation of genes involved in cell cycle regulation and DNA replication and repair (Sengupta et al., 2007).

The Glutamate-GABA cycle (GGC) is important especially in the context of astrocyte-neuron metabolism. The amino acid glutamine is a precursor for the production of Glutamate and GABA (Bak et al., 2006). Deamidation of neuronal glutamine to glutamate produces ammonia, which is then transferred to astrocytes and utilized in the amidation of glutamate. Glutamine released by astrocytes is taken up by Glutamatergic and GABAergic neurons that incidentally show projections in the basal ganglia among

other brain regions and are involved in the regulation of voluntary movements (Sidoryk-Wegrzynowicz and Aschner, 2013). However, in response to elevated levels of manganese in the brain, there is a rapid entry of manganese into the astrocytic mitochondria. As mentioned in the previous section, high levels of mitochondrial manganese impair cellular respiration and prevent the production and activation of glutathione peroxidase. Taken together, astrocytes appear to be particularly affected by a disruption of manganese homeostasis in the brain. This in turn could have a negative impact on the GABAergic and Glutamatergic projections in the basal ganglia leading to the motor deficits characterizing manganese neurotoxicity.

Manganese and α-synuclein protein misfolding

Belonging to a family that includes β- and γ-synuclein, α-synuclein (α-Syn) is a small, 14.5-kDa acidic protein comprising 140 amino acids. Encoded by a single gene consisting of seven exons located on Chromosome 4, it is highly conserved in vertebrates. α-Syn is predominantly expressed presynaptically in neurons throughout the mammalian brain and CSF and is estimated to account for as much as 1% of total protein in soluble cytosolic brain fractions. The physiological functions of α-Syn are poorly understood, but evidence suggests a role for it in synaptic plasticity, dopamine regulation, and membrane trafficking. The link between α-Syn and PD pathogenesis is based on case studies of familial PD as well as the observation that misfolded α-Syn is a major constituent of Lewy bodies and Lewy neurites in both familial and sporadic PD (Roth et al., 2013). Also, compelling evidence demonstrates that mutations in the gene encoding α-Syn are directly linked to the onset of PD (Liu et al., 2012). Furthermore, rare familial

forms of PD also have been linked to the overexpression of α-Syn due to duplication or triplication of the *SNCA* gene.

The aggregation and fibrillation of α-Syn, forming intracellular proteinaceous aggregates, have been implicated in several other neurodegenerative disorders besides PD, including LBD, Lewy body variant of AD, MSA and Hallervorden-Spartz disease. The study of synucleinopathies and the idea that α-Syn aggregates can pathologically propagate throughout the CNS recently gained much attention with the finding of α-Syn species in human plasma and CSF (El-Agnaf et al., 2003; Kordower et al., 2008) and the host-to-graft propagation of α-Syn-positive Lewy bodies in fetal ventral mesencephalic and embryonic nigral neurons transplanted in human PD patients (Kordower et al., 2008; Li et al., 2008). Even though several models have postulated the pathological cell-to-cell transmission of propagating α-Syn species (Desplats et al., 2009; Dunning et al., 2013; Lee et al., 2008), its exact mechanistic role in PD pathogenesis and related synucleinopathies largely remains unknown. Available *in vitro* evidence thus far indicates that extracellular α-Syn induces pathogenic actions by activating neuroinflammatory and neurodegenerative responses (Emmanouilidou et al., 2010; Su et al., 2008).

The natively unfolded α-Syn protein lacks a defined secondary structure, and therefore, belongs to the intrinsically unstructured protein family. However, upon interaction with lipid membranes, it adopts an α-helical conformational change, and under conditions that trigger aggregation, α-Syn undertakes the characteristic crossed β-conformation and self-aggregates into soluble oligomers, which gradually form insoluble amyloid-like fibrils.

As shown in Figure 2, the α-Syn protein has three distinct structural domains. The amphipathic N-terminal region (residues 1-60) contains 11 amino acid repeats including the consensus sequence KTKEGV, which is important in α-helix formation. The central hydrophobic region (residues 61-91) contains the hydrophobic and three additional KTKEGV repeats and the highly amyloidogenic nonamyloid component (NAC) region, which is important in protein aggregation. Specifically, within this region a hydrophobic GAV motif (residues 66-74) mainly consisting of glycine, alanine and valine residues has been identified as the critical core for the fibrillization and cytotoxicity of α-Syn (Du et al., 2006). Finally, the highly acidic C-terminal region (residues 91-140) is proline-rich and is responsible for the intrinsically disordered nature of α-Syn (Harischandra et al., 2015). The N-terminal and NAC regions form a membrane-binding domain, whereas the C-terminal tail is thought to contain protein–protein and protein–small molecule interaction sites.

Importantly, α-Syn protein has three metal binding sites providing its metalloprotein properties: one at the N-terminus, one in the central region and one at the C-terminus. A systematic analysis of mono-, di- and trivalent metal ligands (Li^+, K^+, Na^+, Cs^+, Ca^{2+}, Co^{2+}, Cd^{2+}, Cu^{2+}, Fe^{2+}, Mg^{2+}, Mn^{2+}, Zn^{2+}, Co^{3+}, Al^{3+} and Fe^{3+}) revealed that conformational changes occur upon metal binding that cause normally benign α-Syn protein to aggregate (Uversky et al., 2001). Out of the 15 metal cations studied, Uversky et al determined Al^{3+} to be the most effective stimulator of protein fibril formation followed by Cu^{2+}, Fe^{2+}, Co^{3+} and Mn^{2+}, with each causing conformational changes detectable by intrinsic protein fluorescence and far UV-circular dichroism (Uversky et

al., 2001). Furthermore, Uversky et al also showed that Mn^{3+} induced immediate di-tyrosine formation, suggesting that manganese is responsible for the metal-induced oxidation of α-Syn protein. Among the three metal binding sites, binding sites located at the N-terminal domain, specifically the [1]MDVFMKGLS[9] and [48]VAHGV[52] regions, demonstrated high-affinity binding for Cu^{2+} ($K_d \sim 0.1$ μM) (Rasia et al., 2005) whereas metal binding sites near 49–52 and 110–140 are known to interact with divalent metals including manganese (Binolfi et al., 2008; Binolfi et al., 2006; Uversky et al., 2001). In a detailed study, the metal ions Mn^{2+}, Fe^{2+}, Co^{2+} and Ni^{2+} bound preferentially to the [119]DPDNEA[124] motif, in which Asp121 acted as the main anchoring site with low affinity (mM) to metal ligands (Binolfi et al., 2006). These findings regarding the structural basis of metal interaction with α-Syn provide a tighter link with PD and suggest that perturbations in metal homeostasis may constitute a more widespread element in neurodegenerative disorders than previously recognized (Binolfi et al., 2006).

How manganese affects the expression of α-synuclein and induces cytotoxicity has been studied in *in vitro*, *in vivo* and *ex-vivo* models of PD (Gitler et al., 2009; Verina et al., 2013; Xu et al., 2013). Figure 3 provides a pictorial representation of the impact that acute and prolonged exposure to Mn have on α-synuclein. Our previous studies have shown that physiological levels of human wild-type α-Syn protein attenuate manganese-induced dopaminergic neuronal degeneration in cell culture models during early stages of manganese toxicity. However, prolonged manganese exposure promotes α-Syn aggregation and dampens its neuroprotective effect (Harischandra et al., 2015). Furthermore, using a genetically modified *Caenorhabditis elegans* model system,

Borhorst and colleagues have shown enhanced manganese accumulation and oxidative stress in the pdr1 and djr1.1 mutants, which were reduced by α-Syn expression (Bornhorst et al., 2014). Taken together, these studies uncover a novel, neuroprotective role for human wild-type α-Syn in attenuating acute manganese toxicity. This observed neuroprotective role of α-Syn may be a direct effect of its metal binding capability. In biological environments, free roaming manganese cations could induce oxidative stress, free radical formation and downstream mitochondria-dependent apoptotic signaling.

Manganese preferentially accumulates in the mitochondria via the mitochondrial Ca^{2+} uniporter. In the mitochondria, it is mainly bound to the membrane or matrix proteins (Gavin et al., 1999). Succinate, malate as well as glutamate are important substrates for mitochondrial respiration. At high concentrations, manganese (Mn^{2+}) binds to these substrates effectively inhibiting mitochondrial respiration (Gavin et al., 1999). Interference in oxidative phosphorylation triggers the downstream release of inflammatory signals leading ultimately to apoptosis. Recent evidence sheds light on manganese-induced endoplasmic reticular (ER) stress and ER-mediated cellular apoptosis. Rats given three different doses of manganese for four weeks showed a dose-dependent increase in apoptotic cells in the striatum, as evidenced by chromatin condensation, as well as up-regulation of markers of mitochondrial and ER stress-mediated apoptosis (Wang et al., 2015). Furthermore, manganese induces the transcriptional and translational up-regulation of α-Syn (Li et al., 2010), promoting susceptibility to manganese-induced neurotoxicity through ERK1/2 MAPK activation,

NF-κB nuclear translocation and activation of apoptotic signaling cascades leading to dopaminergic cell death (Cai et al., 2010; Prabhakaran et al., 2011).

Manganese affects not only cellular viability but also affects various factors involved in neurotransmitter regulation. Acetylcholine esterase (AChE) is an enzyme that hydrolyses acetylcholine (ACh) thus regulating its availability in the synaptic cleft (Pohanka, 2012; Whittaker, 1990). Chronic exposure to high levels of manganese inhibited the activity of AChE, thereby allowing ACh to accumulate in the synaptic cleft and subsequently overstimulating muscarinic and nicotinic ACh receptors. While the precise mechanism has not been determined, inhibiting AChE increases levels of ROS and RNS (Milatovic et al., 2006; Santos et al., 2012), which further lead to lipid peroxidation as well as production of citrulline, a marker of RNS activity. It has been reported that manganese overexposure in rats on a low protein diet reduces the level of GABA in the brain while increasing the animals' susceptibility to seizures (Ali et al., 1983). However, the changes in brain GABA levels depended on the treatment regime and age of animals used. For instance, low-dose manganese given thrice weekly for five weeks increased GABA levels (Takagi et al., 1990). Additional mechanistic studies need to be conducted to understand the role played by manganese in GABA dysregulation. In the case of glutamate, high levels of manganese in the brain may lead to constitutive NMDA activation leading to excitotoxic-related neuronal death. Once released into the synaptic cleft, most of the glutamate is removed by astrocytes via the glutamate:aspartate transporter (GLAST). However, high levels of extracellular Mn^{2+} decrease the expression of GLAST and induce astrocyte apoptosis (Erikson et al., 2002). Chronic exposure to manganese can

also increase the amplitude of excitatory postsynaptic potentials (EPSPs) in striatal neurons. With respect to the neurotransmitter dopamine, Ingersoll et al. (1999) demonstrated manganese transport to dopaminergic neurons via the Dopamine transporter (DAT) (Ingersoll et al., 1999). Another study done on DAT -\- mice administered high doses of manganese reported a lower amount of manganese in the striatum compared to wild type mice given the same dose. Interestingly, only the normally DAT-rich region of the striatum showed this contrasting pattern, which was not seen in areas that do not express DAT (Erikson et al., 2005). Young non-human primates exposed to a low dose of Mn twice weekly for about nine weeks showed retracted microglial processes even while initially dopaminergic neurons remained unchanged (Verina et al., 2011). Perhaps a prolonged study would give us more information on the effect of this microglial disturbance on nigrostriatal neurons.

To conclude, manganese influx and efflux are tightly controlled in the body by various receptors and ion channels. However overexposure of manganese can lead to the toxic accumulation of manganese in the brain especially in the basal ganglia. High levels of manganese in the brain cause hyperactivity of cortico-striatal neurons. While contradictory evidence arises from different dose regimens, in general Mn also affects the regulation of neurotransmitters such as dopamine, glutamate and GABA. Manganese inhibits the activity of various enzymes involved in regulating optimum neurotransmitter levels. High levels of glutamate and/or acetylcholine in the synaptic cleft overstimulate NMDA receptors leading to excitotoxic neuronal death. Mn may get transported into dopaminergic neurons via DAT. Excess cellular Mn^{2+} disrupts Ca^{2+} homeostasis in cells, leading to decreased dopamine production and neuronal death. Manganese also causes

ER and mitochondrial stress leading to neuronal apoptosis and/or gliosis. Thus there is mounting evidence of the deleterious effects of Mn on neurons and glia. Various studies have been conducted on the use of metal chelators and antioxidants as therapeutic interventions against manganism.

Manganese homeostasis

The homeostasis of manganese and other metal ions is maintained through tightly regulated mechanisms of uptake, storage and secretion that strictly limit their abundance in the cellular compartment. The distribution and neurotoxicity of manganese is governed largely by the routes of exposure, which are primarily ingestion and inhalation. In humans, the primary route of exposure is through manganese-enriched food and well water. However, the molecular mechanisms of oral manganese absorption are not well understood. Roughly 3-5% of the manganese ingested gets absorbed into the body from the gastrointestinal tract (Finley et al., 1994). Under normal physiological conditions, manganese enters the portal circulation through either passive diffusion (Bell et al., 1989) or active transport via Divalent metal transporter 1 (DMT1) (Erikson and Aschner, 2006; Fitsanakis et al., 2007). DMT1 (formerly known as Nramp2 and DCT1) is the first mammalian transmembrane iron transporter to be identified. It is a 12-transmembrane domain protein responsible for the uptake of various divalent metals including Fe^{2+}, Mn^{2+}, Zn^{2+}, Co^{2+} and Ni^{2+}, and it transfers ions across the apical surface of intestinal cells and out via transferrin (Tf)-cycle endosomes (Andrews, 1999). Besides using a mechanism similar to that for iron, there are no known metal transporters specific for transporting manganese into cells. In plasma, approximately 80% of manganese in the 2+ oxidation state (Mn^{2+}) is bound to α-macroglobulin or albumin, while only a small

fraction (<1%) of Mn^{3+} is bound to Tf. It has been proposed that, like iron, manganese in plasma is oxidized from the Mn^{2+} to the Mn^{3+} valence state by the ferroxidase enzyme ceruloplasmin and loaded onto plasma Tf for circulating into tissues (Davidsson et al., 1989). Circulating manganese diffuses throughout the body including bone, kidney, pancreas, liver and brain (Martinez-Finley et al., 2012).

Once in the brain, manganese (Mn^{3+}) entry into neurons occurs by Tf-Mn^{3+} complex binding to the transferring receptor (TfR) and it becomes localized in endosomes. Subsequent recruitment of v-ATPases acidifies endosomes and dissociates Mn^{3+} from the Tf/TfR complex, reducing it to Mn^{2+}, which is quite stable at physiological pH, and thereafter neuronal transport occurs via DMT1 independent of the Tf pathway. In the brain, DMT1 is highly expressed in the DA-rich basal ganglia, putamen, cortex and substantia nigra (Huang et al., 2004; Salazar et al., 2008), which may account for manganese's pattern of accumulation and neurotoxicity. Other primary transport mechanisms for manganese are through capillary endothelial cells of the blood-brain-barrier (BBB) (Crossgrove et al., 2003) or through the CSF via the choroid plexus (Murphy et al., 1991). Since manganese neurotoxicity primarily occurs through occupational exposure, such as inhalation of manganese fumes or dust in welding, dry-cell battery manufacturing and the smelting industry, the nasal space through the olfactory epithelium to the olfactory nerve is another major manganese transport mechanism in to the brain (Tjalve et al., 1996). In fact, DMT1 is highly expressed in the olfactory epithelium and is required for manganese transport across the olfactory epithelium as has been shown in the rat (Thompson et al., 2007). Evidence also exists for

transport of manganese into the CNS through store-operated calcium channels (Crossgrove and Yokel, 2005), ionotrophic glutamate receptor calcium channels (Kannurpatti et al., 2000) and manganese citrate transporters (Crossgrove et al., 2003).

Another mechanism regulating manganese homeostasis in the brain involves manganese being transferred with high affinity into cells by the Zinc transporters ZIP-8 and ZIP-14, Zrt-/Irt-related protein (ZIP) family metal transporters encoded by SLC39A8 and SLC39A14, respectively. These transporters are highly expressed in the liver, duodenum, kidney, testis, and are localized on apical surfaces of brain capillaries (Girijashanker et al., 2008; Wang et al., 2012). Taking advantage of its particular magnetic properties, Aoki and colleagues showed that manganese uptake also occurs through the choroid plexus as visualized by magnetic resonance imaging (MRI) (Aoki et al., 2004). One day after they systemically administered Mn^{2+} to rats, the distribution of manganese in the brain extended to the olfactory bulb, cortex, basal forebrain, and basal ganglia, overlapping specific brain structures vulnerable to manganese-induced neurotoxicity (Aoki et al., 2004). In cells, toxic accumulations of manganese are found primarily in the mitochondria, heterochromatin and nucleoli in both neurons and astrocytes (Lai et al., 1999; Morello et al., 2008).

Manganese also shares the Ca^{2+} uniporter mechanism and the *rapid mode* (*RaM*) of Ca^{2+} *uptake* of mitochondrial calcium influx, resulting in manganese sequestration in mitochondria, which is cleared only very slowly from the brain (Gavin et al., 1990). This manganese accumulation inhibits the efflux of calcium, decreases MAO activity and

inhibits the respiratory chain and ATP production (Zhang et al., 2003), which may partly explain the role of mitochondrial dysfunction in manganese neurotoxicity. Previously, manganese detoxification and efflux from cells was thought to be primarily regulated by ferroportin (Fpn), also known as HFE4, MTP1, IREG1, encoded by the SLC40A1 gene. Although Fpn was initially identified as the iron exporter, recent data suggest that Fpn also interacts with manganese, zinc and cobalt to export them from the cell (Madejczyk and Ballatori, 2012; Troadec et al., 2010; Yin et al., 2010). Furthermore, manganese exposure increases Fpn mRNA levels in mouse bone marrow macrophages (Troadec et al., 2010) and it significantly increases Fpn protein levels in HEK293T cells (Yin et al., 2010). Increasing Fpn levels were linked to reduced manganese accumulation in both the cerebellum and cortex of mice treated with manganese (Yin et al., 2010), further confirming that Fpn removes manganese and reduces manganese-induced neurotoxicity.

Recently, the secretory pathway of the Ca^{2+}/Mn^{2+} ATPases SPCA1 and SPCA2, which are localized at the Golgi, was suggested as an alternative way of cytosolic manganese detoxification by sequestering into the Golgi lumen (Sepulveda et al., 2009). Overexpressing SPCA1 in HEK293T cells conferred tolerance of manganese (Mn^{2+}) toxicity by facilitating Mn^{2+} accumulation in the Golgi, thereby increasing cell viability (Leitch et al., 2011). However, the degree to which SPCA1 and SPCA2 regulates manganese homeostasis has yet to be determined. Another mode for manganese egress through Golgi has been attributed to SLC30A10 in humans (Tuschl et al., 2012). Recently, SLC30A10 was shown to be localized on the cell surface where it acted as a manganese efflux transporter to reduce cellular manganese levels and protect against

manganese-induced toxicity (Leyva-Illades et al., 2014). Mutations in the SLC30A10 gene have been associated with hepatic cirrhosis, dystonia, polycythemia, Parkinsonian-like gate disturbances and hypermanganesemia in cases unrelated to environmental manganese exposure (Tuschl et al., 2012). Importantly, these recent discoveries involving SLC30A10 and its mutations reinforce its crucial role as a manganese transporter in humans, shedding further light on our understanding of familial Parkinsonism as a result of mutations in SLC30A10.

The p-type transmembrane ATPase protein ATP13A2 (also known as PARK9) located at the lysosome also protects cells from manganese-induced toxicity (Tan et al., 2011). Although the physiological function of ATP13A2 in mammalian cells remains elusive, loss-of-function mutations in ATP13A2 cause an autosomal recessive form of early-onset Parkinsonism with pyramidal degeneration and dementia called Kufor-Rakeb Syndrome (KRS) (Ramirez et al., 2006). Overexpression of wild-type ATP13A2, but not the KRS pathogenic ATP13A2 mutants, protected mammalian cell lines and primary rat neuronal cultures from Mn^{2+}-induced cell death by reducing intracellular manganese concentrations and cytochrome c release, suggesting a role of ATP13A2 in manganese detoxification and homeostasis (Tan et al., 2011). A summary of the above-mentioned receptors and channels that play a part in cellular Mn homeostasis is shown in Figure 4.

Manganese in other diseases

Until the last decade, manganese neurotoxicity was mainly associated with Parkinsonism and very little attention had been given to its potential role in other neurodegenerative

diseases. However, with growing interest in the neurobiology of heavy metals, manganese has now been linked to other major neurodegenerative diseases such as Huntington's disease (HD) and Prion disease (Choi et al., 2010; Kumar et al., 2015; Martin et al., 2011). Furthermore, gene expression studies in the frontal cortex of *cynomolgus macaques* exposed to various manganese doses indicated that Amyloid-β (Aβ) precursor-like protein 1 (APLP1), a member of the amyloid precursor family, was highly up-regulated, providing an association between manganese exposure and AD (Guilarte et al., 2008). Along with this gene array analysis, immunochemistry revealed the presence of Amyloid-β plaques and α-Syn aggregates, which have been linked to PD as well as AD, and which have also been seen in the gray and white matter of manganese-exposed animals (Guilarte, 2010).

In contrast to manganese-induced Parkinsonism, a deficiency in manganese transport has been implicated in the pathogenesis of HD, an autosomal dominant neurodegenerative disorder characterized by the loss of medium spiny neurons in the striatum (Kumar et al., 2015). Recent experiments carried out with immortalized mutant HD cell lines (SThdh$^{Q7/Q7}$ and SThdh$^{Q111/Q111}$) showed reduced TfR levels and substantial deficits in net manganese uptake, even under basal conditions (Williams et al., 2010). In follow-up studies, YAC128 HD transgenic mice accumulated less manganese in their basal ganglia, including the striatum, which is a common target for both HD neuropathology and manganese accumulation (Madison et al., 2012). Furthermore, transition metal analysis of HD patients has shown significantly increased iron together with significantly decreased

cortical copper and manganese (Rosas et al., 2012), further supporting the role of manganese in HD.

Prion protein is also widely known for its association with transmissible spongiform encephalopathies (TSE), a class of neurodegenerative diseases caused by the accumulation of an abnormal isoform of the prion protein known as PrP^{Sc} (Jin et al., 2015a). The cellular prion protein PrP^{C} has a high binding affinity to divalent metals and plays an important role in the biological function and pathogenesis of prion diseases. Interestingly, increased manganese content has been observed in the blood and brains of humans infected with Creutzfeldt–Jakob disease (CJD), in mice infected with scrapie, and in cattle infected with bovine spongiform encephalopathy (BSE) (Hesketh et al., 2008; Hesketh et al., 2007; Wong et al., 2001). The binding of manganese to prion protein mitigates against Mn's neurotoxicity during the early acute phase of manganese exposure (Choi et al., 2007). In contrast, prolonged manganese exposure alters the stability of prion proteins without any change in gene transcription (Choi et al., 2010), suggesting manganese may play a role in prion protein misfolding and prion disease pathogenesis. Interestingly, exposure to manganese in a soil matrix significantly increases prion protein survival (Davies and Brown, 2009). Thus, manganese is an environmental risk factor for both the survival of the PrP^{Sc} and its transmissibility. The role of manganese in TSE was further validated with the findings that it enhances the ability of the pathogenic PrP^{Sc} isoform to regulate manganese homeostasis (Martin et al., 2011) and that it increases the infectivity of scrapie-infected cells (Davies and Brown, 2009). Therefore, understanding the interaction of metals with disease-specific proteins may provide further insight to the pathogenesis of neurodegenerative diseases.

Conclusion

Chronic exposure to large amounts of manganese has been shown to induce various neurological and psychiatric symptoms. While the body especially the gut and liver can efficiently remove excess manganese, the brain cannot. Inhalation of large doses of manganese can lead to its accumulation in the basal ganglia in the brain. Astrocytes are particularly sensitive to manganese toxicity and may compound neuroinflammation by releasing pro-inflammatory cytokines in response to excess manganese. Manganese can also bind to substrates of oxidative phosphorylation thus inhibiting mitochondrial respiration. Chronic exposure to manganese causes benign α-synuclein monomers, which are present in all neurons, to undergo a conformational change to the toxic oligomeric structures that are toxic to neurons. Taken together, we can effectively conclude that manganese toxicity impairs key biochemical events necessary for neuronal survival. Elsewhere in the body, excess manganese also interferes with the body's iron metabolism and can cause kidney failure. Early detection and chelation therapy can effectively reverse the harmful effects caused by this metal; however, if it progresses untreated, it can cause severe neurological and physiological defects. As with any metal, there is a possibility of bioaccumulation and teratogenic effects of manganese. However this aspect has not been studied in detail. Similarly, an in-depth study on the role of manganese in protein misfolding and upregulation of genetic markers for various neurological diseases in humans must be conducted. By combining the results of epidemiological surveys, human case studies as well as mechanistic studies done in *in* vitro and animal models of manganese toxicity, we can better understand the causes and symptoms as well as determine effective therapeutic strategies to treat early and advanced states of

neurodegeneration caused by manganese toxicity.
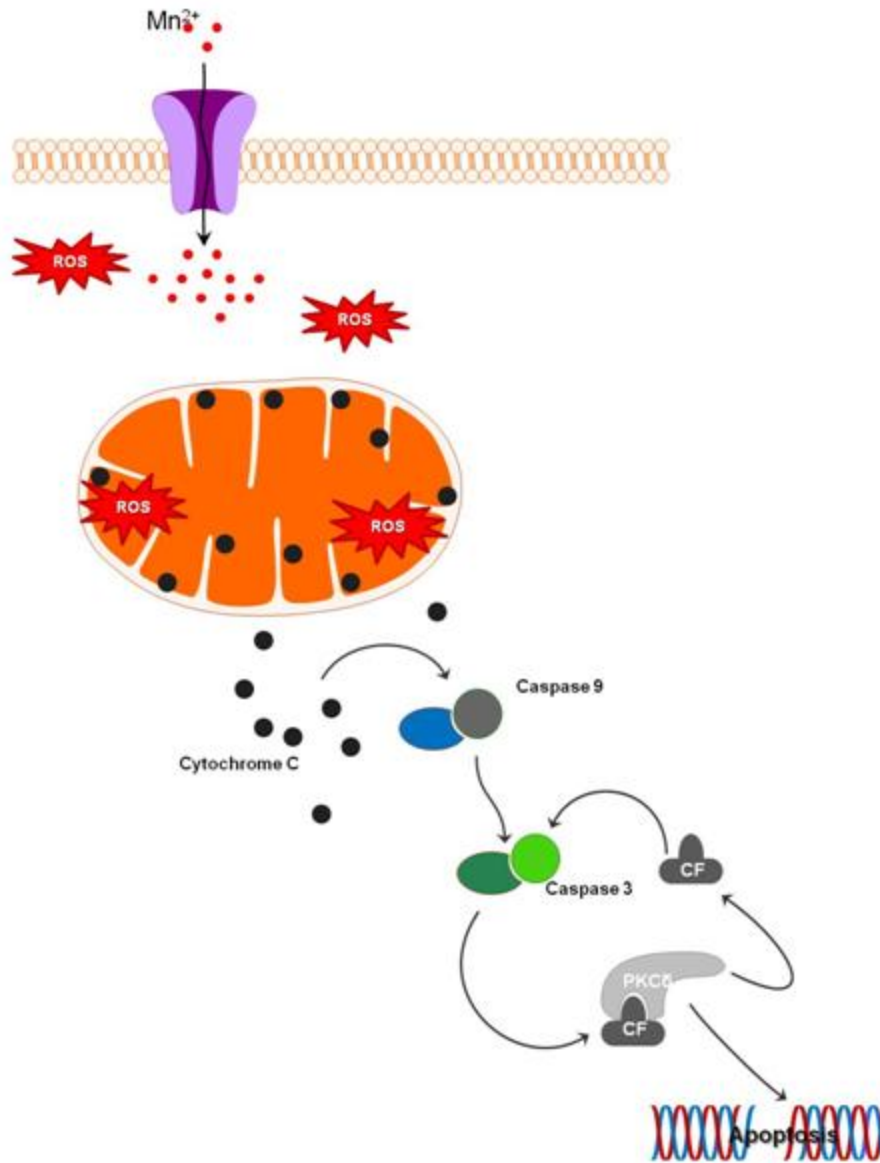
Figure 1: Molecular mechanisms of Mn-induced cell death: Cellular Mn homeostasis is dependent upon efficient uptake, retention and excretion by various cell receptors and/or ion channels. Under normal conditions, in the presence of excess Mn, the receptors involved in the uptake of this metal are down-regulated while those involved in its release from the cell are up-regulated. However, during chronic exposure to high

concentrations of Mn, these system checks are not maintained. Increased uptake of Mn under these conditions increases the production of reactive oxygen species (ROS) leading to mitochondrial dysfunction. Impaired mitochondrial function leads to release of cytochrome C that activates the apoptosis initiator caspase-9 which in turn cleaves caspase-3. The cleaved fragment of caspase-3 interacts with Protein kinase delta, a pro-apoptotic protein. Caspase-3 mediated proteolytic cleavage of PKCd leads to DNA fragmentation and apoptosis.
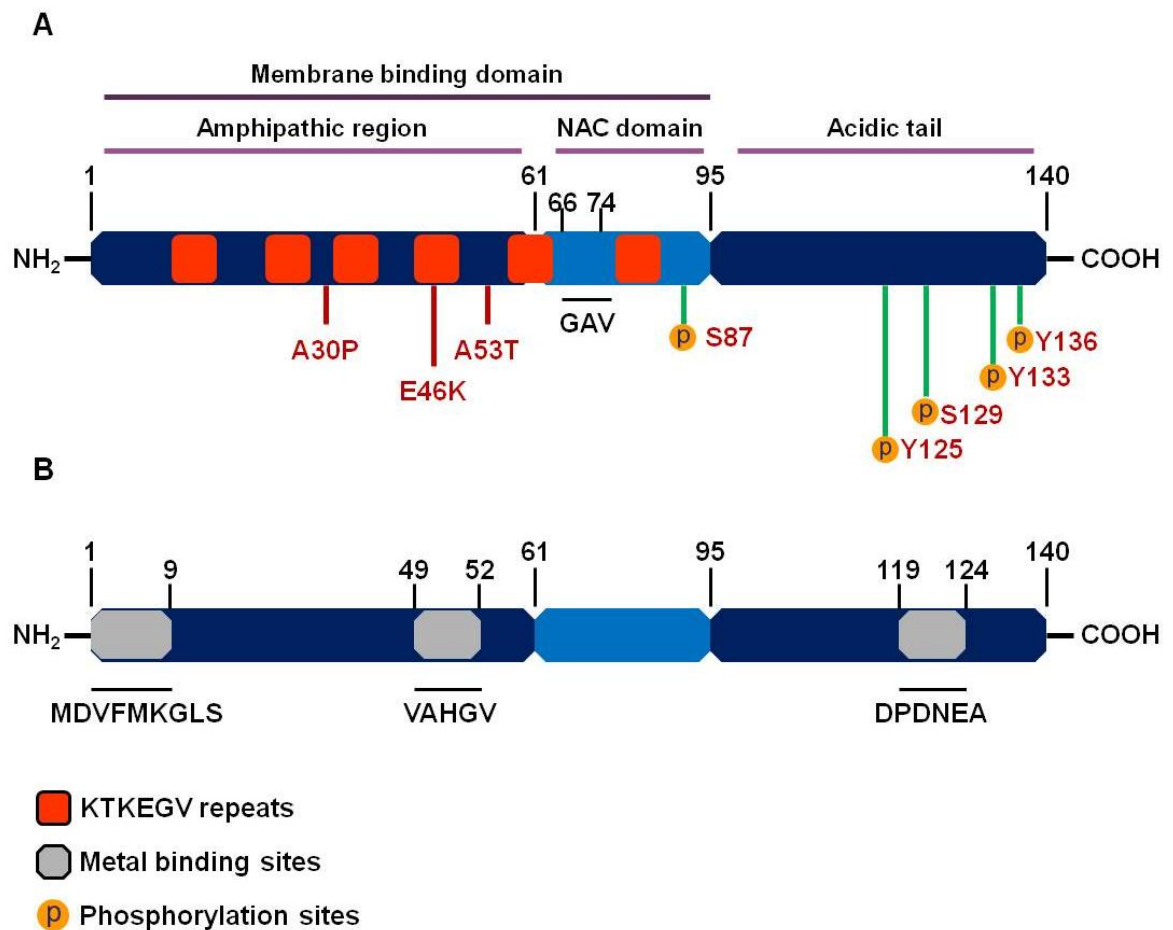
Figure 2: **Structure of the α-synuclein protein**
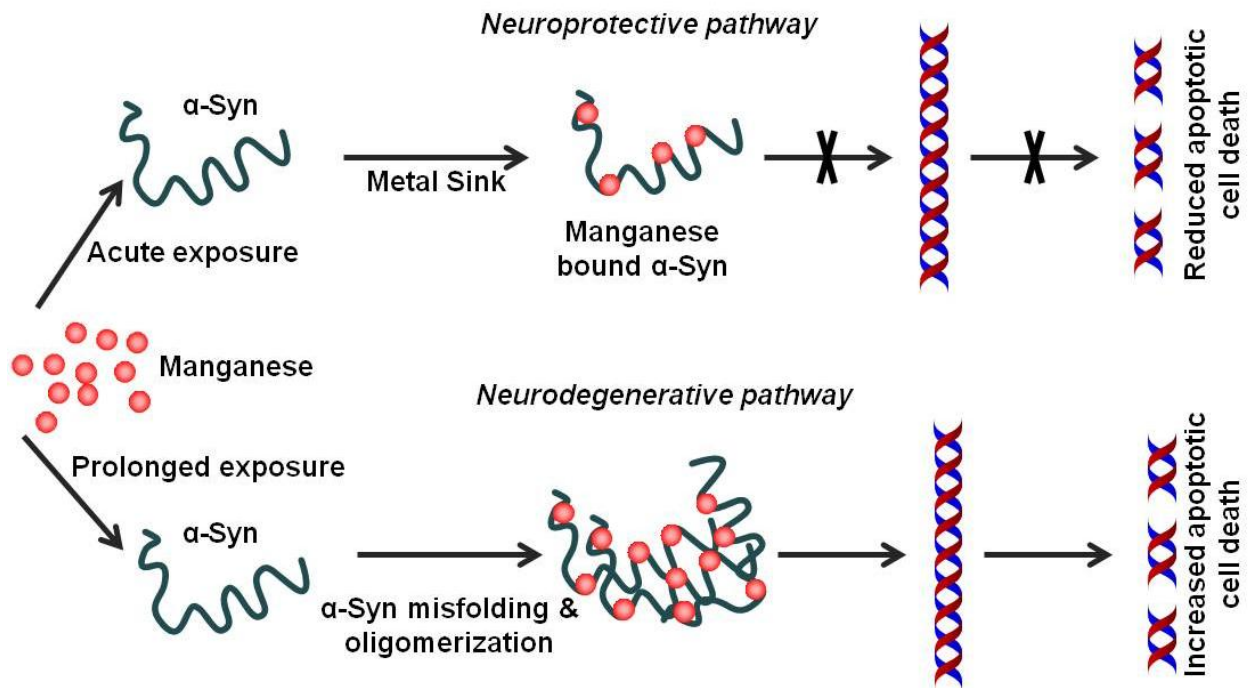
Figure 3**: Effect of chronic Mn overexposure on α-synuclein misfolding**. Metal binding sites on a-synuclein allow it to become a metal sink for free roaming metals in the cells. During an acute exposure to Mn, free-roaming Mn binds to the metal binding sites on the C-terminus of this protein. In this way a-synuclein effectively works as a chelator for different metal ions including Mn. However continued exposure to Mn can lead to saturation of this chelating property. Following additional binding of Mn to the C-terminus, the natively conformed protein misfolds. Misfolded a-synuclein leads to the production of pro-inflammatory factors. Thus Mn overexposure leads to progressive protein misfolding in the neurons and induces inflammation and finally neurodegeneration.
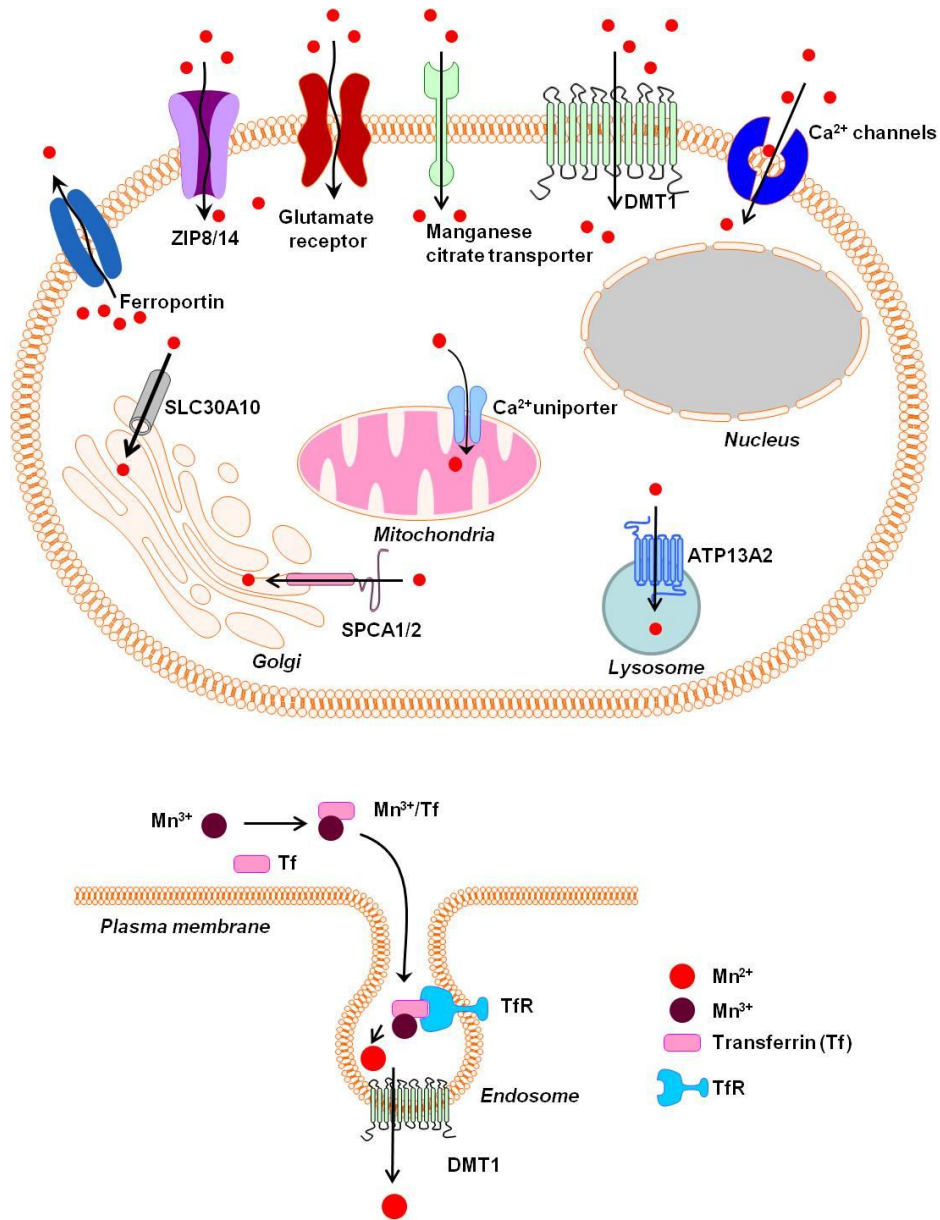
Figure 4: Receptors/ Channels involved in Mn hoemostasis: Various cellular receptors such as divalent metal transporter 1 (DMT1) and transferrin receptor (Tfr R) as well as ion channels such as store operated Ca^{+2} channels (SOCC) or voltage gated Ca^{+2} channels (VGCC) facilitate the entry of divalent Mn into the cells whereas SLC40A (ferroportin) and Ca^{+2} facilitate its expulsion from the cell and mitochondria respectively. Mn^{+2} is

passively transported via VGCC and glutamate activated ionic channels while Mn^{+3} entry is facilitated via transferri.

References

Aboud, A. A., et al., 2014. PARK2 patient neuroprogenitors show increased mitochondrial sensitivity to copper. Neurobiol Dis. 73C**,** 204-212.

Afeseh Ngwa, H., et al., 2009. Vanadium induces dopaminergic neurotoxicity via protein kinase Cdelta dependent oxidative signaling mechanisms: relevance to etiopathogenesis of Parkinson's disease. Toxicol Appl Pharmacol. 240**,** 273-85.

Afeseh Ngwa, H., et al., 2011. Manganese nanoparticle activates mitochondrial dependent apoptotic signaling and autophagy in dopaminergic neuronal cells. Toxicol Appl Pharmacol. 256**,** 227-40.

Aguzzi, A., Calella, A. M., 2009. Prions: protein aggregation and infectious diseases. Physiol Rev. 89**,** 1105-52.

Aguzzi, A., O'Connor, T., 2010. Protein aggregation diseases: pathogenicity and therapeutic perspectives. Nat Rev Drug Discov. 9**,** 237-48.

Ali, M. M., et al., 1983. Effect of low protein diet on manganese neurotoxicity: II. Brain GABA and seizure susceptibility. Neurobehav Toxicol Teratol. 5**,** 385-9.

Ali, S. F., et al., 1995. Manganese-induced reactive oxygen species: comparison between Mn+2 and Mn+3. Neurodegeneration. 4**,** 329-34.

Aluru, N., et al., 2015. Targeted mutagenesis of aryl hydrocarbon receptor 2a and 2b genes in Atlantic killifish (Fundulus heteroclitus). Aquat Toxicol. 158**,** 192-201.

Anantharam, V., et al., 2002. Caspase-3-dependent proteolytic cleavage of protein kinase Cdelta is essential for oxidative stress-mediated dopaminergic cell death after

exposure to methylcyclopentadienyl manganese tricarbonyl. J Neurosci. 22, 1738-51.

Andreini, C., et al., 2008. Metal ions in biological catalysis: from enzyme databases to general principles. J Biol Inorg Chem. 13, 1205-18.

Andrews, N. C., 1999. The iron transporter DMT1. Int J Biochem Cell Biol. 31, 991-4.

Aoki, I., et al., 2004. In vivo detection of neuroarchitecture in the rodent brain using manganese-enhanced MRI. Neuroimage. 22, 1046-59.

Appendino, G., et al., 2014. Recreational drug discovery: natural products as lead structures for the synthesis of smart drugs. Nat Prod Rep. 31, 880-904.

Archibald, F. S., Tyree, C., 1987. Manganese poisoning and the attack of trivalent manganese upon catecholamines. Arch Biochem Biophys. 256, 638-50.

Aschner, J. L., Aschner, M., 2005. Nutritional aspects of manganese homeostasis. Mol Aspects Med. 26, 353-62.

Aschner, M., et al., 1999. Manganese uptake and distribution in the central nervous system (CNS). Neurotoxicology. 20, 173-80.

Bak, L. K., et al., 2006. The glutamate/GABA-glutamine cycle: aspects of transport, neurotransmitter homeostasis and ammonia transfer. J Neurochem. 98, 641-53.

Ballard, P. A., et al., 1985. Permanent human parkinsonism due to 1-methyl-4-phenyl-1,2,3,6-tetrahydropyridine (MPTP): seven cases. Neurology. 35, 949-56.

Bell, J. G., et al., 1989. Higher retention of manganese in suckling than in adult rats is not due to maturational differences in manganese uptake by rat small intestine. J Toxicol Environ Health. 26, 387-98.

Binolfi, A., et al., 2008. Site-specific interactions of Cu(II) with alpha and beta-synuclein: bridging the molecular gap between metal binding and aggregation. J Am Chem Soc. 130, 11801-12.

Binolfi, A., et al., 2006. Interaction of alpha-synuclein with divalent metal ions reveals key differences: a link between structure, binding specificity and fibrillation enhancement. J Am Chem Soc. 128, 9893-901.

Bornhorst, J., et al., 2014. The effects of pdr1, djr1.1 and pink1 loss in manganese-induced toxicity and the role of alpha-synuclein in C. elegans. Metallomics. 6, 476-90.

Bowman, A. B., et al., 2011. Role of manganese in neurodegenerative diseases. J Trace Elem Med Biol. 25, 191-203.

Brown, D. R., 2011. Metals in neurodegenerative disease. Metallomics. 3, 226-8.

Brown, R. C., et al., 2005. Neurodegenerative diseases: an overview of environmental risk factors. Environ Health Perspect. 113, 1250-6.

Cai, T., et al., 2010. Manganese induces the overexpression of alpha-synuclein in PC12 cells via ERK activation. Brain Res. 1359, 201-7.

Calne, D. B., et al., 1994. Manganism and idiopathic parkinsonism: similarities and differences. Neurology. 44, 1583-6.

Carson, M. J., et al., 2007. A rose by any other name? The potential consequences of microglial heterogeneity during CNS health and disease. Neurotherapeutics. 4, 571-9.

Cerchiaro, G., et al., 2009. Hydroxyl radical oxidation of guanosine 5'-triphosphate (GTP): requirement for a GTP-Cu(II) complex. Redox Rep. 14, 82-92.

Chen, C. J., Liao, S. L., 2002. Oxidative stress involves in astrocytic alterations induced by manganese. Exp Neurol. 175**,** 216-25.

Chen, M. T., et al., 2006. Effects of acute manganese chloride exposure on lipid peroxidation and alteration of trace metals in rat brain. Biol Trace Elem Res. 110**,** 163-78.

Chen, M. T., et al., 2000. Protective effects of manganese against lipid peroxidation. J Toxicol Environ Health A. 61**,** 569-77.

Choi, C. J., et al., 2010. Manganese upregulates cellular prion protein and contributes to altered stabilization and proteolysis: relevance to role of metals in pathogenesis of prion disease. Toxicol Sci. 115**,** 535-46.

Choi, C. J., et al., 2007. Normal cellular prion protein protects against manganese-induced oxidative stress and apoptotic cell death. Toxicol Sci. 98**,** 495-509.

Ciccocioppo, F., et al., 2008. Expression and phosphorylation of protein kinase C isoforms in Abeta(1-42) activated T lymphocytes from Alzheimers disease. Int J Immunopathol Pharmacol. 21**,** 23-33.

Claus Henn, B., et al., 2010. Early postnatal blood manganese levels and children's neurodevelopment. Epidemiology. 21**,** 433-9.

Conway, K. A., et al., 2001. Kinetic stabilization of the alpha-synuclein protofibril by a dopamine-alpha-synuclein adduct. Science. 294**,** 1346-9.

Cook, D. G., et al., 1974. Chronic manganese intoxication. Arch Neurol. 30**,** 59-64.

Cooke, M. S., et al., 2003. Oxidative DNA damage: mechanisms, mutation, and disease. FASEB J. 17**,** 1195-214.

Cordova, F. M., et al., 2013. Manganese-exposed developing rats display motor deficits and striatal oxidative stress that are reversed by Trolox. Arch Toxicol. 87, 1231-44.

Couper, J., 1837. On the effects of black oxide of manganese when inhaled into the lungs. Br Ann Med Pharm Vital Stat Gen Sci. 1, 41–2.

Crossgrove, J. S., et al., 2003. Manganese distribution across the blood-brain barrier. I. Evidence for carrier-mediated influx of managanese citrate as well as manganese and manganese transferrin. Neurotoxicology. 24, 3-13.

Crossgrove, J. S., Yokel, R. A., 2005. Manganese distribution across the blood-brain barrier. IV. Evidence for brain influx through store-operated calcium channels. Neurotoxicology. 26, 297-307.

Davidsson, L., et al., 1989. Identification of transferrin as the major plasma carrier protein for manganese introduced orally or intravenously or after in vitro addition in the rat. J Nutr. 119, 1461-4.

Davies, P., Brown, D. R., 2009. Manganese enhances prion protein survival in model soils and increases prion infectivity to cells. PLoS One. 4, e7518.

Davis, M. Y., et al., 2014. The co-occurrence of Alzheimer's disease and Huntington's disease: a neuropathological study of 15 elderly Huntington's disease subjects. J Huntingtons Dis. 3, 209-17.

Dawson, T. M., et al., 2010. Genetic animal models of Parkinson's disease. Neuron. 66, 646-61.

Dendle, P., 2001. Lupines, manganese, and devil-sickness: an Anglo-Saxon medical response to epilepsy. Bull Hist Med. 75, 91-101.

Desole, M. S., et al., 2000. Glutathione deficiency potentiates manganese-induced increases in compounds associated with high-energy phosphate degradation in discrete brain areas of young and aged rats. Aging (Milano). 12**,** 470-7.

Desplats, P., et al., 2009. Inclusion formation and neuronal cell death through neuron-to-neuron transmission of alpha-synuclein. Proc Natl Acad Sci U S A. 106**,** 13010-5.

Dick, F. D., et al., 2007. Environmental risk factors for Parkinson's disease and parkinsonism: the Geoparkinson study. Occup Environ Med. 64**,** 666-72.

Du, H. N., et al., 2006. Acceleration of alpha-synuclein aggregation by homologous peptides. FEBS Lett. 580**,** 3657-64.

Dukhande, V. V., et al., 2006. Manganese-induced neurotoxicity is differentially enhanced by glutathione depletion in astrocytoma and neuroblastoma cells. Neurochem Res. 31**,** 1349-57.

Dunning, C. J., et al., 2013. What's to like about the prion-like hypothesis for the spreading of aggregated alpha-synuclein in Parkinson disease? Prion. 7**,** 92-7.

El-Agnaf, O. M., et al., 2003. Alpha-synuclein implicated in Parkinson's disease is present in extracellular biological fluids, including human plasma. FASEB J. 17**,** 1945-7.

Emmanouilidou, E., et al., 2010. Cell-produced alpha-synuclein is secreted in a calcium-dependent manner by exosomes and impacts neuronal survival. J Neurosci. 30**,** 6838-51.

Ensing, J. G., 1985. Bazooka: cocaine-base and manganese carbonate. J Anal Toxicol. 9**,** 45-6.

Erikson, K. M., Aschner, M., 2006. Increased manganese uptake by primary astrocyte cultures with altered iron status is mediated primarily by divalent metal transporter. Neurotoxicology. 27, 125-30.

Erikson, K. M., et al., 2005. Manganese accumulation in striatum of mice exposed to toxic doses is dependent upon a functional dopamine transporter. Environ Toxicol Pharmacol. 20, 390-4.

Erikson, K. M., et al., 2002. Glutamate/aspartate transporter (GLAST), taurine transporter and metallothionein mRNA levels are differentially altered in astrocytes exposed to manganese chloride, manganese phosphate or manganese sulfate. Neurotoxicology. 23, 281-8.

Esterbauer, H., et al., 1991. Chemistry and biochemistry of 4-hydroxynonenal, malonaldehyde and related aldehydes. Free Radic Biol Med. 11, 81-128.

Farina, M., et al., 2013. Metals, oxidative stress and neurodegeneration: a focus on iron, manganese and mercury. Neurochem Int. 62, 575-94.

Farooqui, A. A., Horrocks, L. A., 2007. Glycerophospholipids in brain : phospholipase A2 in neurological disorders. Springer, New York, N.Y.

Farooqui, T., Farooqui, A. A., 2011. Lipid-mediated oxidative stress and inflammation in the pathogenesis of Parkinson's disease. Parkinsons Dis. 2011, 247467.

Farrell, N., Metal Complexes as Drugs and Chemotherapeutic Agents. In: J. A. M. J. Meyer, (Ed.), Comprehensive Coordination Chemistry II. Pergamon, Oxford, 2003, pp. 809-840.

Finley, J. W., et al., 1994. Sex affects manganese absorption and retention by humans from a diet adequate in manganese. Am J Clin Nutr. 60, 949-55.

Fitsanakis, V. A., et al., 2006. The effects of manganese on glutamate, dopamine and gamma-aminobutyric acid regulation. Neurochem Int. 48**,** 426-33.

Fitsanakis, V. A., et al., 2007. Putative proteins involved in manganese transport across the blood-brain barrier. Hum Exp Toxicol. 26**,** 295-302.

Gavin, C. E., et al., 1990. Manganese and calcium efflux kinetics in brain mitochondria. Relevance to manganese toxicity. Biochem J. 266**,** 329-34.

Gavin, C. E., et al., 1999. Manganese and calcium transport in mitochondria: implications for manganese toxicity. Neurotoxicology. 20**,** 445-53.

Ghosh, A., et al., 2007. Selective inhibition of NF-kappaB activation prevents dopaminergic neuronal loss in a mouse model of Parkinson's disease. Proc Natl Acad Sci U S A. 104**,** 18754-9.

Ghosh, A., et al., 2009. Simvastatin inhibits the activation of p21ras and prevents the loss of dopaminergic neurons in a mouse model of Parkinson's disease. J Neurosci. 29**,** 13543-56.

Ghosh, A., et al., 2013. The peptidyl-prolyl isomerase Pin1 up-regulation and proapoptotic function in dopaminergic neurons: relevance to the pathogenesis of Parkinson disease. J Biol Chem. 288**,** 21955-71.

Girijashanker, K., et al., 2008. Slc39a14 gene encodes ZIP14, a metal/bicarbonate symporter: similarities to the ZIP8 transporter. Mol Pharmacol. 73**,** 1413-23.

Girotto, S., et al., 2012. Dopamine-derived quinones affect the structure of the redox sensor DJ-1 through modifications at Cys-106 and Cys-53. J Biol Chem. 287**,** 18738-49.

Gitler, A. D., et al., 2009. Alpha-synuclein is part of a diverse and highly conserved interaction network that includes PARK9 and manganese toxicity. Nat Genet. 41, 308-15.

Graham, D. G., 1978. Oxidative pathways for catecholamines in the genesis of neuromelanin and cytotoxic quinones. Mol Pharmacol. 14, 633-43.

Guilarte, T. R., 2010. APLP1, Alzheimer's-like pathology and neurodegeneration in the frontal cortex of manganese-exposed non-human primates. Neurotoxicology. 31, 572-4.

Guilarte, T. R., et al., 2008. Increased APLP1 expression and neurodegeneration in the frontal cortex of manganese-exposed non-human primates. J Neurochem. 105, 1948-59.

Harischandra, D. S., et al., 2015. alpha-Synuclein protects against manganese neurotoxic insult during the early stages of exposure in a dopaminergic cell model of Parkinson's disease. Toxicol Sci. 143, 454-68.

Harischandra, D. S., et al., 2014. Role of proteolytic activation of protein kinase Cdelta in the pathogenesis of prion disease. Prion. 8, 143-53.

Hazell, A. S., Norenberg, M. D., 1998. Ammonia and manganese increase arginine uptake in cultured astrocytes. Neurochem Res. 23, 869-73.

Hermida-Ameijeiras, A., et al., 2004. Autoxidation and MAO-mediated metabolism of dopamine as a potential cause of oxidative stress: role of ferrous and ferric ions. Neurochem Int. 45, 103-16.

Hesketh, S., et al., 2008. Elevated manganese levels in blood and CNS in human prion disease. Mol Cell Neurosci. 37, 590-8.

Hesketh, S., et al., 2007. Elevated manganese levels in blood and central nervous system occur before onset of clinical signs in scrapie and bovine spongiform encephalopathy. J Anim Sci. 85, 1596-609.

Holm, R. H., et al., 1996. Structural and Functional Aspects of Metal Sites in Biology. Chem Rev. 96, 2239-2314.

Huang, C. C., 2007. Parkinsonism induced by chronic manganese intoxication--an experience in Taiwan. Chang Gung Med J. 30, 385-95.

Huang, C. C., et al., 1989. Chronic manganese intoxication. Arch Neurol. 46, 1104-6.

Huang, E., et al., 2004. Distribution of divalent metal transporter-1 in the monkey basal ganglia. Neuroscience. 128, 487-96.

Ingersoll, R. T., et al., 1999. Central nervous system toxicity of manganese. II: Cocaine or reserpine inhibit manganese concentration in the rat brain. Neurotoxicology. 20, 467-76.

Isobe, C., et al., 2010. Levels of reduced and oxidized coenzyme Q-10 and 8-hydroxy-2'-deoxyguanosine in the cerebrospinal fluid of patients with living Parkinson's disease demonstrate that mitochondrial oxidative damage and/or oxidative DNA damage contributes to the neurodegenerative process. Neurosci Lett. 469, 159-63.

Jin, H., et al., Chapter 23 Manganese and Prion Disease. Manganese in Health and Disease. The Royal Society of Chemistry, 2015a, pp. 574-603.

Jin, H., et al., 2011. Transcriptional regulation of pro-apoptotic protein kinase Cdelta: implications for oxidative stress-induced neuronal cell death. J Biol Chem. 286, 19840-59.

Jin, H., et al., 2015b. Targeted toxicants to dopaminergic neuronal cell death. Methods Mol Biol. 1254**,** 239-52.

Kannurpatti, S. S., et al., 2000. Calcium sequestering ability of mitochondria modulates influx of calcium through glutamate receptor channel. Neurochem Res. 25**,** 1527-36.

Kanthasamy, A. G., et al., 2006. A novel peptide inhibitor targeted to caspase-3 cleavage site of a proapoptotic kinase protein kinase C delta (PKCdelta) protects against dopaminergic neuronal degeneration in Parkinson's disease models. Free Radic Biol Med. 41**,** 1578-89.

Kanthasamy, A. G., et al., 2012. Effect of divalent metals on the neuronal proteasomal system, prion protein ubiquitination and aggregation. Toxicol Lett. 214**,** 288-95.

Kanthasamy, A. G., et al., 2008. Environmental neurotoxin dieldrin induces apoptosis via caspase-3-dependent proteolytic activation of protein kinase C delta (PKCdelta): Implications for neurodegeneration in Parkinson's disease. Mol Brain. 1**,** 12.

Kenche, V. B., Barnham, K. J., 2011. Alzheimer's disease & metals: therapeutic opportunities. Br J Pharmacol. 163**,** 211-9.

Kim, Y., et al., 2002. Dopamine transporter density is decreased in parkinsonian patients with a history of manganese exposure: what does it mean? Mov Disord. 17**,** 568-75.

Kordower, J. H., et al., 2008. Lewy body-like pathology in long-term embryonic nigral transplants in Parkinson's disease. Nat Med. 14**,** 504-6.

Kotzbauer, P. T., et al., 2001. Lewy body pathology in Alzheimer's disease. J Mol Neurosci. 17**,** 225-32.

Kumar, K. K., et al., 2015. Untargeted metabolic profiling identifies interactions between Huntington's disease and neuronal manganese status. Metallomics. 7**,** 363-70.

Lai, J. C., et al., 1999. Manganese mineral interactions in brain. Neurotoxicology. 20**,** 433-44.

Langston, J. W., et al., 1983. Chronic Parkinsonism in humans due to a product of meperidine-analog synthesis. Science. 219**,** 979-80.

Latchoumycandane, C., et al., 2011. Dopaminergic neurotoxicant 6-OHDA induces oxidative damage through proteolytic activation of PKCdelta in cell culture and animal models of Parkinson's disease. Toxicol Appl Pharmacol. 256**,** 314-23.

Latchoumycandane, C., et al., 2005. Protein kinase Cdelta is a key downstream mediator of manganese-induced apoptosis in dopaminergic neuronal cells. J Pharmacol Exp Ther. 313**,** 46-55.

LaVoie, M. J., et al., 2005. Dopamine covalently modifies and functionally inactivates parkin. Nat Med. 11**,** 1214-21.

Lee, H. J., et al., 2008. Assembly-dependent endocytosis and clearance of extracellular alpha-synuclein. Int J Biochem Cell Biol. 40**,** 1835-49.

Leitch, S., et al., 2011. Vesicular distribution of Secretory Pathway Ca(2)+-ATPase isoform 1 and a role in manganese detoxification in liver-derived polarized cells. Biometals. 24**,** 159-70.

Leyva-Illades, D., et al., 2014. SLC30A10 is a cell surface-localized manganese efflux transporter, and parkinsonism-causing mutations block its intracellular trafficking and efflux activity. J Neurosci. 34**,** 14079-95.

Li, J. Y., et al., 2008. Lewy bodies in grafted neurons in subjects with Parkinson's disease suggest host-to-graft disease propagation. Nat Med. 14**,** 501-3.

Li, Y., et al., 2010. alpha-Synuclein overexpression during manganese-induced apoptosis in SH-SY5Y neuroblastoma cells. Brain Res Bull. 81**,** 428-33.

Liu, G., et al., 2012. alpha-synuclein, LRRK2 and their interplay in Parkinson's disease. Future Neurol. 7**,** 145-153.

Lotharius, J., Brundin, P., 2002. Pathogenesis of Parkinson's disease: dopamine, vesicles and alpha-synuclein. Nat Rev Neurosci. 3**,** 932-42.

Maddirala, Y., et al., 2015. N-acetylcysteineamide protects against manganese-induced toxicity in SHSY5Y cell line. Brain Res. 1608**,** 157-66.

Madejczyk, M. S., Ballatori, N., 2012. The iron transporter ferroportin can also function as a manganese exporter. Biochim Biophys Acta. 1818**,** 651-7.

Madison, J. L., et al., 2012. Disease-toxicant interactions in manganese exposed Huntington disease mice: early changes in striatal neuron morphology and dopamine metabolism. PLoS One. 7**,** e31024.

Martin, D. P., et al., 2011. Infectious prion protein alters manganese transport and neurotoxicity in a cell culture model of prion disease. Neurotoxicology. 32**,** 554-62.

Martinez-Finley, E. J., et al., 2012. Cellular transport and homeostasis of essential and nonessential metals. Metallomics. 4**,** 593-605.

McKeith, I., et al., 2004. Dementia with Lewy bodies. Lancet Neurol. 3**,** 19-28.

Menezes-Filho, J. A., et al., 2011. Elevated manganese and cognitive performance in school-aged children and their mothers. Environ Res. 111**,** 156-63.

Miklossy, J., et al., 2006. Role of ICAM-1 in persisting inflammation in Parkinson disease and MPTP monkeys. Exp Neurol. 197**,** 275-83.

Milatovic, D., Aschner, M., 2009. Measurement of isoprostanes as markers of oxidative stress in neuronal tissue. Curr Protoc Toxicol. Chapter 12**,** Unit12 14.

Milatovic, D., et al., 2006. Anticholinesterase toxicity and oxidative stress. ScientificWorldJournal. 6**,** 295-310.

Milatovic, D., et al., 2011. Protective effects of antioxidants and anti-inflammatory agents against manganese-induced oxidative damage and neuronal injury. Toxicol Appl Pharmacol. 256**,** 219-26.

Milatovic, D., et al., 2007. Manganese induces oxidative impairment in cultured rat astrocytes. Toxicol Sci. 98**,** 198-205.

Milatovic, D., et al., 2009. Oxidative damage and neurodegeneration in manganese-induced neurotoxicity. Toxicol Appl Pharmacol. 240**,** 219-25.

Mogi, M., et al., 1994. Interleukin-1 beta, interleukin-6, epidermal growth factor and transforming growth factor-alpha are elevated in the brain from parkinsonian patients. Neurosci Lett. 180**,** 147-50.

Morello, M., et al., 2008. Sub-cellular localization of manganese in the basal ganglia of normal and manganese-treated rats An electron spectroscopy imaging and electron energy-loss spectroscopy study. Neurotoxicology. 29**,** 60-72.

Moreno, J. A., et al., 2008. Manganese potentiates nuclear factor-kappaB-dependent expression of nitric oxide synthase 2 in astrocytes by activating soluble guanylate cyclase and extracellular responsive kinase signaling pathways. J Neurosci Res. 86**,** 2028-38.

Murphy, V. A., et al., 1991. Saturable transport of manganese(II) across the rat blood-brain barrier. J Neurochem. 57**,** 948-54.

Oikawa, S., et al., 2006. Mechanism for manganese enhancement of dopamine-induced oxidative DNA damage and neuronal cell death. Free Radic Biol Med. 41**,** 748-56.

Perl, D. P., Olanow, C. W., 2007. The neuropathology of manganese-induced Parkinsonism. J Neuropathol Exp Neurol. 66**,** 675-82.

Pohanka, M., 2012. Alpha7 nicotinic acetylcholine receptor is a target in pharmacology and toxicology. Int J Mol Sci. 13**,** 2219-38.

Prabhakaran, K., et al., 2011. alpha-Synuclein overexpression enhances manganese-induced neurotoxicity through the NF-kappaB-mediated pathway. Toxicol Mech Methods. 21**,** 435-43.

Priyadarshi, A., et al., 2001. Environmental risk factors and Parkinson's disease: a metaanalysis. Environ Res. 86**,** 122-7.

Przedborski, S., Vila, M., 2003. The 1-methyl-4-phenyl-1,2,3,6-tetrahydropyridine mouse model: a tool to explore the pathogenesis of Parkinson's disease. Ann N Y Acad Sci. 991**,** 189-98.

Racette, B. A., et al., 2005. [18F]FDOPA PET and clinical features in parkinsonism due to manganism. Mov Disord. 20**,** 492-6.

Rama Rao, K. V., et al., 2007. Manganese induces cell swelling in cultured astrocytes. Neurotoxicology. 28**,** 807-12.

Ramirez, A., et al., 2006. Hereditary parkinsonism with dementia is caused by mutations in ATP13A2, encoding a lysosomal type 5 P-type ATPase. Nat Genet. 38, 1184-91.

Rasia, R. M., et al., 2005. Structural characterization of copper(II) binding to alpha-synuclein: Insights into the bioinorganic chemistry of Parkinson's disease. Proc Natl Acad Sci U S A. 102, 4294-9.

Rosas, H. D., et al., 2012. Alterations in brain transition metals in Huntington disease: an evolving and intricate story. Arch Neurol. 69, 887-93.

Ross, C. A., Poirier, M. A., 2004. Protein aggregation and neurodegenerative disease. Nat Med. 10 Suppl, S10-7.

Roth, J. A., 2014. Correlation between the biochemical pathways altered by mutated parkinson-related genes and chronic exposure to manganese. Neurotoxicology. 44, 314-25.

Roth, J. A., et al., 2013. The effect of manganese on dopamine toxicity and dopamine transporter (DAT) in control and DAT transfected HEK cells. Neurotoxicology. 35, 121-8.

Salazar, J., et al., 2008. Divalent metal transporter 1 (DMT1) contributes to neurodegeneration in animal models of Parkinson's disease. Proc Natl Acad Sci U S A. 105, 18578-83.

Santos, D., et al., 2012. The inhibitory effect of manganese on acetylcholinesterase activity enhances oxidative stress and neuroinflammation in the rat brain. Toxicology. 292, 90-8.

Sarban, S., et al., 2007. Relationship between synovial fluid and plasma manganese, arginase, and nitric oxide in patients with rheumatoid arthritis. Biol Trace Elem Res. 115**,** 97-106.

Sengupta, A., et al., 2007. Gene expression profiling of human primary astrocytes exposed to manganese chloride indicates selective effects on several functions of the cells. Neurotoxicology. 28**,** 478-89.

Sepulveda, M. R., et al., 2009. Silencing the SPCA1 (secretory pathway Ca2+-ATPase isoform 1) impairs Ca2+ homeostasis in the Golgi and disturbs neural polarity. J Neurosci. 29**,** 12174-82.

Shoji, M., et al., 2000. Accumulation of NACP/alpha-synuclein in lewy body disease and multiple system atrophy. J Neurol Neurosurg Psychiatry. 68**,** 605-8.

Shukla, G. S., Chandra, S. V., 1981. Manganese toxicity: lipid peroxidation in rat brain. Acta Pharmacol Toxicol (Copenh). 48**,** 95-100.

Sidoryk-Wegrzynowicz, M., Aschner, M., 2013. Manganese toxicity in the central nervous system: the glutamine/glutamate-gamma-aminobutyric acid cycle. J Intern Med. 273**,** 466-77.

Stephenson, A. P., et al., 2013. Manganese-induced oxidative DNA damage in neuronal SH-SY5Y cells: attenuation of thymine base lesions by glutathione and N-acetylcysteine. Toxicol Lett. 218**,** 299-307.

Su, X., et al., 2008. Synuclein activates microglia in a model of Parkinson's disease. Neurobiol Aging. 29**,** 1690-701.

Takagi, H., et al., 1990. [Evaluation of non-surgical treatments of hepatocellular carcinoma--investigation of the cases with long and short survivals after treatment]. Nihon Gan Chiryo Gakkai Shi. 25**,** 757-69.

Tan, J., et al., 2011. Regulation of intracellular manganese homeostasis by Kufor-Rakeb syndrome-associated ATP13A2 protein. J Biol Chem. 286**,** 29654-62.

Tansey, M. G., et al., 2008. Neuroinflammation in Parkinson's disease: is there sufficient evidence for mechanism-based interventional therapy? Front Biosci. 13**,** 709-17.

Thompson, K., et al., 2007. Olfactory uptake of manganese requires DMT1 and is enhanced by anemia. FASEB J. 21**,** 223-30.

Tjalve, H., et al., 1996. Uptake of manganese and cadmium from the nasal mucosa into the central nervous system via olfactory pathways in rats. Pharmacol Toxicol. 79**,** 347-56.

Tottey, S., et al., 2008. Protein-folding location can regulate manganese-binding versus copper- or zinc-binding. Nature. 455**,** 1138-42.

Troadec, M. B., et al., 2010. Induction of FPN1 transcription by MTF-1 reveals a role for ferroportin in transition metal efflux. Blood. 116**,** 4657-64.

Tuschl, K., et al., 2012. Syndrome of hepatic cirrhosis, dystonia, polycythemia, and hypermanganesemia caused by mutations in SLC30A10, a manganese transporter in man. Am J Hum Genet. 90**,** 457-66.

Uchikado, H., et al., 2006. Alzheimer disease with amygdala Lewy bodies: a distinct form of alpha-synucleinopathy. J Neuropathol Exp Neurol. 65**,** 685-97.

Uversky, V. N., et al., 2001. Metal-triggered structural transformations, aggregation, and fibrillation of human alpha-synuclein. A possible molecular NK between Parkinson's disease and heavy metal exposure. J Biol Chem. 276, 44284-96.

Verina, T., et al., 2011. Manganese exposure induces microglia activation and dystrophy in the substantia nigra of non-human primates. Neurotoxicology. 32, 215-26.

Verina, T., et al., 2013. Manganese exposure induces alpha-synuclein aggregation in the frontal cortex of non-human primates. Toxicol Lett. 217, 177-83.

Wang, C. Y., et al., 2012. ZIP8 is an iron and zinc transporter whose cell-surface expression is up-regulated by cellular iron loading. J Biol Chem. 287, 34032-43.

Wang, T., et al., 2015. ER stress and ER stress-mediated apoptosis are involved in manganese-induced neurotoxicity in the rat striatum in vivo. Neurotoxicology. 48, 109-19.

Wedler, F. C., Denman, R. B., 1984. Glutamine synthetase: the major Mn(II) enzyme in mammalian brain. Curr Top Cell Regul. 24, 153-69.

Wedler, F. C., et al., 1994. Effects of Ca(II) ions on Mn(II) dynamics in chick glia and rat astrocytes: potential regulation of glutamine synthetase. Neurochem Res. 19, 145-51.

Whittaker, V. P., 1990. The contribution of drugs and toxins to understanding of cholinergic function. Trends Pharmacol Sci. 11, 8-13.

Williams, B. B., et al., 2010. Altered manganese homeostasis and manganese toxicity in a Huntington's disease striatal cell model are not explained by defects in the iron transport system. Toxicol Sci. 117, 169-79.

Wittung-Stafshede, P., 2002. Role of cofactors in protein folding. Acc Chem Res. 35**,** 201-8.

Wong, B. S., et al., 2001. Aberrant metal binding by prion protein in human prion disease. J Neurochem. 78**,** 1400-8.

Xu, B., et al., 2013. Oxidative stress involvement in manganese-induced alpha-synuclein oligomerization in organotypic brain slice cultures. Toxicology. 305**,** 71-8.

Yin, Z., et al., 2010. Ferroportin is a manganese-responsive protein that decreases manganese cytotoxicity and accumulation. J Neurochem. 112**,** 1190-8.

Zhang, D., et al., 2011. Effects of manganese on tyrosine hydroxylase (TH) activity and TH-phosphorylation in a dopaminergic neural cell line. Toxicol Appl Pharmacol. 254**,** 65-71.

Zhang, J., et al., 1999. Parkinson's disease is associated with oxidative damage to cytoplasmic DNA and RNA in substantia nigra neurons. Am J Pathol. 154**,** 1423-9.

Zhang, S., et al., 2003. Effect of manganese chloride exposure on liver and brain mitochondria function in rats. Environ Res. 93**,** 149-57.

Zota, A. R., et al., 2009. Maternal blood manganese levels and infant birth weight. Epidemiology. 20**,** 367-73.

Background and Literature Review II

Exosomes: Nanoscale dumpsters or delivery trucks?

Brief History

Exosomes, previously considered as microvesicles (MV) were first identified in the mid 40's as one of the pro-coagulant components in blood (Chargaff and West, 1946). Between 1960 to 1980, MV's were identified in epiphyseal cartilage as plasma-membrane derived vesicles (Wuthier, 1975) as a part of blood serum (Dalton, 1975) or seminal plasma (Ronquist et al., 1978) as well as an important pool of vesicles generated from various cancerous cells including hepatoma cells (Davidova and Shapot, 1970), rectal adenomas (De Broe et al., 1975), melanomas and gliomas (Trams et al., 1981). In fact, Trams *et al* first used the term "exosomes" in describing the microvesicles released from various neoplastic cell lines. They also hypothesized that these membrane vesicles might serve a physiological function rather than simply being waste baskets or excess cellular material exfoliated from a cell (Trams et al., 1981). This hypothesis gained more credence when Harding and colleagues showed that distinct from endosomes and other MV's, exosomes collected from the media in which reticulocytes were grown, had the transferrin receptor – a marker of intracellular vesicles (endosomes) present on its surface (Harding et al., 1983; Pan et al., 1985). Time-dependent electron microscopic images and pulse-chase experiments showed these vesicles fusing with the plasma membrane leading to their secretion in the medium. Peters *et al* also showed presence of intercellular clefts into which internal vesicles were present awaiting extracellular release (Peters et al., 1989). In 1996 Raposo, G. *et al* showed that B lymphoblastoid cells released exosomes

containing MHC class II molecules, inducing antigen-specific MHC class II –restricted T cell responses (Raposo et al., 1996). This was a novel form of antigen presentation and provided an insight into the role it can play in immune cell activation and cell-to-cell transmission of biologically active components. Another type of immune cell- the dendritic cell was found to release exosomes that contained tumor specific antigens that could promote anti-tumor responses in mice (Zitvogel et al., 1998). While exosomes were primarily studied in immune cells in the context of antigen presentation, they were soon found to play an important role in disease pathogenesis and progression in various diseases notably leishmaniasis (Silverman et al., 2010), malaria (Coltel et al., 2006; Mantel et al., 2013), trichomoniasis (Twu et al., 2013), trypanosomiasis (Cestari et al., 2012; Goncalves et al., 1991), schistosomiasis (Wang et al., 2015) as well as infections caused by fungi such as *Cryptococcus neoformans* (Rodrigues et al., 2008a)*, Paracoccidioides brasiliensi* (Vallejo et al., 2011) and *Candida albicans* (Rodrigues et al., 2008b)*.* Since then, exosomes have been implicated in other diverse diseases such as AIDS, Alzheimer's (Rajendran et al., 2006)*,* Parkinson's (Tomlinson et al., 2015), prion diseases (Fevrier et al., 2004) etc. At present, exosomes have been identified in all biological fluids including blood (Caby et al., 2005), urine (Pisitkun et al., 2004), saliva (Keller et al., 2011) and breast milk (Admyre et al., 2007).

Difference between microvesicles, endosomes and exosomes

There is some confusion over the appropriate terminology to discern exosomes from other microvesicles. As shown in Fig.1 based on their approximate size, origin and cargo the different vesicles can be differentiated into endosomes, microvesicles, exosomes and apoptotic bodies. For the purpose of this review we will only delineate the properties of exosomes.

Most recent papers agree that exosomes range in size between 40 – 150 nm in diameter. A common way of isolating and selectively enriching exosomes from different biological fluids or cell supernatants is by filtering the sample through a 0.22 μm filter followed by differential ultracentrifugation using a sucrose gradient (Thery et al., 2001). The initial filtration removes most extracellular proteins, intact cells and larger cell debris. Having a high content of lipid, the exosomes float on the sucrose and can be differentiated from multivesicular bodies (MVB's) that are larger in size (~ 1000 nm in diameter) or apoptotic bodies, which are much smaller in size (~ 10 – 50 nm in diameter)(Aalberts et al., 2012; Escola et al., 1998). However, the size and density of most exosomes is similar to intraluminal vesicles (ILV's) and some extracellular microvesicles thus contaminating a supposedly enriched pool of exosomes. An alternative is to immunoselect exosomes by using a antibody targeted to a common exosomal protein such as CD63 (Escola et al., 1998). By immunoselection, it is possible to isolate exosomes with greater purity. However, the flip side to using this method is that depending on how ubiquitously is the target molecule expressed in these vesicles, it might exclude other exosomes not rich in the target protein. Another important factor that distinguishes exosomes from endosomes

or intra luminal vesicles are the contents present in these vesicles. Exosomes usually have cytosolic or plasma membrane proteins and are devoid of mitochondria, endoplasmic reticulum or nuclear material (Raposo and Stoorvogel, 2013; Thery et al., 2002). This is in direct contrast to endosomes that have the above-mentioned proteins too that are ultimately degraded during the lysosomal pathway. The cytosolic proteins present in exosomes also include those that are a part of the endocytic pathway including RAB proteins, GTPase, annexins, flotllin, alix, heat shock proteins (HSP's) etc (Gruenberg and Maxfield, 1995; van Niel et al., 2006). Compared to MVB's or apoptotic bodies, exosomes are enriched in cholesterol, sphingomyelin and ceramide (Thery et al., 2006). In contrast, apoptotic bodies usually contain a higher percentage of phosphatidylcholine and phosphatidylethanolamine while endosomes contain cholesterol, diacylglycerol and phosphatidylserine (Gasser et al., 2003; Thery et al., 2001).

Exosome Biogenesis

Biomolecules such as proteins, lipids as well as immunomodulatory molecules such as antigens are taken up by cells by phagocytosis, micro- or macropinocytosis as well as endocytosis. Phagocytosis is the main mode of uptake of immune cells such as macrophages and microglia. Non-immune cells mainly use endocytosis as the main route of intercellular uptake. Endocytosis is mainly through clathrin coated vesicles although caveolin mediated vesicular internalization are also known to occur. Following internalization via clathrin coated vesicles; these vesicles fuse to form the early endosome (EE). EE are characterized by presence of early endosomal antigen 1 (EEA1), Rab4, 5 and 14 as well as transferrin receptor (TfR) and have a mildly acidic pH (between 6.0 –

6.5). Since EE's lack degradative enzymes, the cargo in these vesicles such as receptors can be recycled back to the surface when the tubular endosome buds off during membrane recycling. The internalized proteins are also sorted with some fated to recycling while others are transported to late endosomes (LE) for degradation via the lysosomal pathway.

Switching of Rab5 for Rab7 leads to the transitioning of EE to LE (Poteryaev et al., 2010). LE's are circular and have a more acidic environment compared to early endosomes (pH = 4.9 − 6.0). In this environment recycling receptors are lost and the vesicular cargo is exclusively targeted for degradation. Acid hydrolases can begin protein degradation although the high pH allows only a small percentage of degradation to occur in the LE's. Incredibly, when LE formation is initialized, they begin moving from the peripheral cytoplasm to the perinuclear area. This movement is initiated by dynein-dynactin via the Rab7 interacting lysosomal protein (RILP) (Granger et al., 2014). Through bi-directional shuttling with the trans golgi network, lysosomal components are added to the LE while endosomal components such as RAb5 and other proteins associated with EE's are removed (Huotari and Helenius, 2011). An important aspect in the maturation of endosomes is the formation of intraluminal vesicles (ILV's). The endosomal sorting complex required for transport (ESCRT), Alix and Vps4 among other protein complexes are required for the formation of ILV's. Unlike endosomes that have a limiting membrane, which is highly glycosylated, ILV's do not have glycocalyx on their membrane. In this way the cargo that is fated for degradation is easily accessible to the acid hydrolases. A number of ILV's present together in the endosome forms what is known as multivesicular body (MVB).

Proteins required for the formation of lysosomes as well as those integral for its functioning are generated in the endoplasmic reticulum and transported via the trans golgi network to the LE's leading to the formation of lysosomes (Appelqvist et al., 2013). The pH in lysosomes is about 4.0 -4.5. This highly acidic environment provides an optimum condition for the action of acid hydrolases including cathepsins, peptidases, sulfatases, lipases, phosphatases, glycosidases etc, which results in the degradation of almost all molecules. The lysosomes themselves are resistant to this acidic degradation due to the presence of a heavily glycosylated membrane containing proteins such as lysosome associated membrane proteins (LAMP's), lysosomal integral protein (LIMP2) and CD63 (Eskelinen et al., 2003). Following the action of the various hydrolases, the end products are either reused by the cells or removed via exocytosis.

Besides transporting the endosomal cargo to the lysosome for degradation, MVB's can also fuse with the cell membrane and essentially release the IV's outside the cell. These exocytosed ILV's are now called exosomes. The mechanism by which exosomes are released has only become clear in the past few years. In particular switching of specific Rab proteins is thought to determine the fate of ILV's in the MVB's; Rab27b on the membrane of MVB's leads to lysosomal degradation pathway. Exosome secretion involves the presence of various Rab GTPases such as Rab27, Rab35 and Rab11. Importantly, switching of Rab27b to Rab27a is required for the release of exosomes in the intercellular environment. This was shown by Ostrowski *et al* who demonstrated that knockdown of Rab27a and Rab27b reduced exosome release while exogenous addition of Rab27a and Rab27b lead to greater numbers of peripheral vesicles or perinuclear endosomes respectively (Ostrowski et al., 2010; Pfeffer, 2010). A general scheme of

exosome release involves the concerted action of the following mechanisms: 1) Inward budding of LE's to form ILV's containing cytosolic, ubiquinated proteins. 2) A number of budding incidences leading to a number of ILV's in what is now called an MVB. 3) Recruitment of the ESCRT proteins ESCRT I (recognizes the ubiquinated cargo in developing MVB's), II (involved in membrane budding of the LE's to form ILV's in the MVB) and III (involved in cleavage of MVB to release their cargo) as well as Alix and Vps4 among other proteins during the formation of MVB's. 4) For most cell types recruitment of Rab11 and Alix as well as flotillin and glycosphingolipids or lipid rafts leads to the docking and fusion of the MVB to the inner membrane of the cell and finally release of the ILV's now - termed exosomes, outside the cell. (Colombo et al., 2013; Phuyal et al., 2014; Pisitkun et al., 2004; Savina et al., 2005) The above steps are an over simplified version of exosome formation and release, indeed studies carried out in different cell types report different sets of proteins involved in exosome biogenesis and release. However, in general the proteins from the ESCRT and retromer complexes and their associated effector molecules are the main components that drive this phenomenon. While the above-mentioned phenomenon can be considered constitutive, exosome release can also be caused by stress stimuli including lipopolysaccharide (LPS) stimulation, heat-shock, hypoxia etc (Chen et al., 2011; Malik et al., 2013; Momen-Heravi et al., 2015).

Role of exosomes in disease pathogenesis

Earlier, exosomes were mainly studied in immune cells such as T cells and monocytes mainly in the context of immunomodulation and cancer propagation (Farsad, 2002; Graves and Valente, 1991; Taylor and Gercel-Taylor, 2005). They have been implicated

in propagating tumor-causing or tumor-supressing proteins to distant cells and tissues as they move in the extra cellular milieu. For example, metastatic tumor cells released exosomes that suppressed the expression of class II MHC antigens by macrophages in a dose-dependent manner, while similar vesicles from early stage tumor cells did not (Taylor and Black, 1985; Taylor et al., 1988). Interestingly, these exocytosed vesicles contained anti-CD3 and concavalinA thus suppressing T cell activation. However, the molecular mechanism involved in the packaging of specific proteins and their release via exosomes had not been elucidated. Today, we know that Rab27 plays an important role in exosome release and propagation of tumorigenic proteins, leading to the propagation of cancer (Bobrie et al., 2012). Moreover, exosomes have been implicated in part in the development and progression of diverse pathological conditions including AD, PD, various cancers as well as cardiac diseases (Buzas et al., 2014; Emmanouilidou et al., 2010; Kahlert and Kalluri, 2013; Kharaziha et al., 2012; Record et al., 2014; Vingtdeux et al., 2012).

Cell-to-cell transfer of exosomes

Since exosomes contain a lipid membrane with moieties similar to those seen on the plasma membrane of various cells, it is easy for a distant cell to either engulf these extracellular vesicles or simply allow entry via plasma membrane fusion and diffusion into the cell cytosol. This cell-to-cell transfer of potential tumorigenic, immunomodulatory or aggregated proteins is thought to cause the progression of various metastatic cancers and neurodegenerative diseases.

In the case of pancreatic ductal adenocarcinomas (PDAC's), Costa-Silva and colleagues found that exosomes isolated from metastatic PDAC's showed high expression of macrophage migration inhibitory factor (MIF) compared to exosomes isolated from non-metastatic PDAC's. They also showed that Kupfer cells present in the liver were able to take up these PDAC-derived exosomes which lead to the development of a fibrotic environment due to heightened secretion of fibronectin and transforming growth factor β(Costa-Silva et al., 2015). By developing a fibrotic environment, the exosomes inherently made a "tumor- favorable" niche resulting in liver metastasis. Such a niche was not made by exosomes isolated from normal pancreatic cells thus proving that exosomes can prime the target organ/s to develop and propagate cancer. Curiously, despite being injected retro-orbitaly, the only organ affected was the liver. So how does this targeting and specific uptake take place?

It turns out that the transport of exosomes and their uptake is not as random as it seems and is mediated in some cells by the tetraspanin-integrin complex (Nazarenko et al., 2010; Rana et al., 2012). Exosome transfer of αvβ6 integrin to surrounding cells has shown to increase the probability of developing metastatic prostrate cancer (Fedele et al., 2015). Curiously, even tumor cell migration is dependent to a certain extent upon autocrine secretion and adhesion of exosomes. A recent study conducted by Sung *et al*, demonstrated that cancer cells required exosomes to provide the direction for cell migration. Disrupting exosome secretion caused constant directional switching leading to defective cell migration and consequently lowered incidence of metastasis. The same paper found that autocrine secretion of cancer cell derived exosomes and specifically the

73

presence of increased fibronectin in these vesicles promoted tumor cell migration in an efficient manner (Sung et al., 2015).

 Exosomes have been also linked in the transfer of aggregated proteins in various neurodegenerative diseases such as AD, PD and prion disease. Aggregated proteins are caused either by mutations in certain proteins that cause them to spontaneously misfold or due to cellular stress that may induce protein misfolding. Misfolded proteins typically acquire a β-sheet rich structure where-in the cell cannot degrade them and are instead accumulate in the cell interfering with cellular activities and ultimately leading to cell apoptosis. There have been a number of *in-vitro* studies that have shown that aggregated proteins can be transferred from one neuron to another via exosomes (Danzer et al., 2012; Saman et al., 2012; Vella et al., 2007). This "seeding" effect can cause widespread neuronal damage leading to neuroinflammation and neurodegeneration. Prion diseases are fatal, transmissible neurodegenerative disorders. These diseases develop when the prion protein, present in all tissues with the highest expression in the tissues of the central nervous system (CNS)

References

Aalberts, M., et al., 2012. Identification of distinct populations of prostasomes that differentially express prostate stem cell antigen, annexin A1, and GLIPR2 in humans. Biol Reprod. 86**,** 82.

Admyre, C., et al., 2007. Exosomes with immune modulatory features are present in human breast milk. J Immunol. 179**,** 1969-78.

Appelqvist, H., et al., 2013. The lysosome: from waste bag to potential therapeutic target. J Mol Cell Biol. 5**,** 214-26.

Bobrie, A., et al., 2012. Rab27a supports exosome-dependent and -independent mechanisms that modify the tumor microenvironment and can promote tumor progression. Cancer Res. 72**,** 4920-30.

Buzas, E. I., et al., 2014. Emerging role of extracellular vesicles in inflammatory diseases. Nat Rev Rheumatol. 10**,** 356-64.

Caby, M. P., et al., 2005. Exosomal-like vesicles are present in human blood plasma. Int Immunol. 17**,** 879-87.

Cestari, I., et al., 2012. Trypanosoma cruzi immune evasion mediated by host cell-derived microvesicles. J Immunol. 188**,** 1942-52.

Chargaff, E., West, R., 1946. The biological significance of the thromboplastic protein of blood. J Biol Chem. 166**,** 189-97.

Chen, T., et al., 2011. Chemokine-containing exosomes are released from heat-stressed tumor cells via lipid raft-dependent pathway and act as efficient tumor vaccine. J Immunol. 186**,** 2219-28.

Colombo, M., et al., 2013. Analysis of ESCRT functions in exosome biogenesis, composition and secretion highlights the heterogeneity of extracellular vesicles. J Cell Sci. 126**,** 5553-65.

Coltel, N., et al., 2006. Cell vesiculation and immunopathology: implications in cerebral malaria. Microbes Infect. 8**,** 2305-16.

Costa-Silva, B., et al., 2015. Pancreatic cancer exosomes initiate pre-metastatic niche formation in the liver. Nat Cell Biol. 17**,** 816-26.

Dalton, A. J., 1975. Microvesicles and vesicles of multivesicular bodies versus "virus-like" particles. J Natl Cancer Inst. 54**,** 1137-48.

Danzer, K. M., et al., 2012. Exosomal cell-to-cell transmission of alpha synuclein oligomers. Mol Neurodegener. 7**,** 42.

Davidova, S. Y., Shapot, V. S., 1970. Liporibonucleoprotein complex as an integral part of animal cell plasma membranes. FEBS Lett. 6**,** 349-351.

De Broe, M., et al., 1975. Letter: Membrane fragments with koinozymic properties released from villous adenoma of the rectum. Lancet. 2**,** 1214-5.

Emmanouilidou, E., et al., 2010. Cell-produced alpha-synuclein is secreted in a calcium-dependent manner by exosomes and impacts neuronal survival. J Neurosci. 30**,** 6838-51.

Escola, J. M., et al., 1998. Selective enrichment of tetraspan proteins on the internal vesicles of multivesicular endosomes and on exosomes secreted by human B-lymphocytes. J Biol Chem. 273**,** 20121-7.

Eskelinen, E. L., et al., 2003. At the acidic edge: emerging functions for lysosomal membrane proteins. Trends Cell Biol. 13**,** 137-45.

Farsad, K., 2002. Exosomes: novel organelles implicated in immunomodulation and apoptosis. Yale J Biol Med. 75**,** 95-101.

Fedele, C., et al., 2015. The alphavbeta6 integrin is transferred intercellularly via exosomes. J Biol Chem. 290**,** 4545-51.

Fevrier, B., et al., 2004. Cells release prions in association with exosomes. Proc Natl Acad Sci U S A. 101**,** 9683-8.

Gasser, O., et al., 2003. Characterisation and properties of ectosomes released by human polymorphonuclear neutrophils. Exp Cell Res. 285**,** 243-57.

Goncalves, M. F., et al., 1991. Trypanosoma cruzi: shedding of surface antigens as membrane vesicles. Exp Parasitol. 72, 43-53.

Granger, E., et al., 2014. The role of the cytoskeleton and molecular motors in endosomal dynamics. Semin Cell Dev Biol. 31, 20-9.

Graves, D. T., Valente, A. J., 1991. Monocyte chemotactic proteins from human tumor cells. Biochem Pharmacol. 41, 333-7.

Gruenberg, J., Maxfield, F. R., 1995. Membrane transport in the endocytic pathway. Curr Opin Cell Biol. 7, 552-63.

Harding, C., et al., 1983. Receptor-mediated endocytosis of transferrin and recycling of the transferrin receptor in rat reticulocytes. J Cell Biol. 97, 329-39.

Huotari, J., Helenius, A., 2011. Endosome maturation. EMBO J. 30, 3481-500.

Kahlert, C., Kalluri, R., 2013. Exosomes in tumor microenvironment influence cancer progression and metastasis. J Mol Med (Berl). 91, 431-7.

Keller, S., et al., 2011. Body fluid derived exosomes as a novel template for clinical diagnostics. J Transl Med. 9, 86.

Kharaziha, P., et al., 2012. Tumor cell-derived exosomes: a message in a bottle. Biochim Biophys Acta. 1826, 103-11.

Malik, Z. A., et al., 2013. Cardiac myocyte exosomes: stability, HSP60, and proteomics. Am J Physiol Heart Circ Physiol. 304, H954-65.

Mantel, P. Y., et al., 2013. Malaria-infected erythrocyte-derived microvesicles mediate cellular communication within the parasite population and with the host immune system. Cell Host Microbe. 13, 521-34.

Momen-Heravi, F., et al., 2015. Exosomes derived from alcohol-treated hepatocytes horizontally transfer liver specific miRNA-122 and sensitize monocytes to LPS. Sci Rep. 5**,** 9991.

Nazarenko, I., et al., 2010. Cell surface tetraspanin Tspan8 contributes to molecular pathways of exosome-induced endothelial cell activation. Cancer Res. 70**,** 1668-78.

Ostrowski, M., et al., 2010. Rab27a and Rab27b control different steps of the exosome secretion pathway. Nat Cell Biol. 12**,** 19-30; sup pp 1-13.

Pan, B. T., et al., 1985. Electron microscopic evidence for externalization of the transferrin receptor in vesicular form in sheep reticulocytes. J Cell Biol. 101**,** 942-8.

Peters, P. J., et al., 1989. Molecules relevant for T cell-target cell interaction are present in cytolytic granules of human T lymphocytes. Eur J Immunol. 19**,** 1469-75.

Pfeffer, S. R., 2010. Two Rabs for exosome release. Nat Cell Biol. 12**,** 3-4.

Phuyal, S., et al., 2014. Regulation of exosome release by glycosphingolipids and flotillins. FEBS J. 281**,** 2214-27.

Pisitkun, T., et al., 2004. Identification and proteomic profiling of exosomes in human urine. Proc Natl Acad Sci U S A. 101**,** 13368-73.

Poteryaev, D., et al., 2010. Identification of the switch in early-to-late endosome transition. Cell. 141**,** 497-508.

Rajendran, L., et al., 2006. Alzheimer's disease beta-amyloid peptides are released in association with exosomes. Proc Natl Acad Sci U S A. 103**,** 11172-7.

Rana, S., et al., 2012. Toward tailored exosomes: the exosomal tetraspanin web contributes to target cell selection. Int J Biochem Cell Biol. 44**,** 1574-84.

Raposo, G., et al., 1996. B lymphocytes secrete antigen-presenting vesicles. J Exp Med. 183**,** 1161-72.

Raposo, G., Stoorvogel, W., 2013. Extracellular vesicles: exosomes, microvesicles, and friends. J Cell Biol. 200**,** 373-83.

Record, M., et al., 2014. Exosomes as new vesicular lipid transporters involved in cell-cell communication and various pathophysiologies. Biochim Biophys Acta. 1841**,** 108-20.

Rodrigues, M. L., et al., 2008a. Extracellular vesicles produced by Cryptococcus neoformans contain protein components associated with virulence. Eukaryot Cell. 7**,** 58-67.

Rodrigues, M. L., et al., 2008b. Vesicular Trans-Cell Wall Transport in Fungi: A Mechanism for the Delivery of Virulence-Associated Macromolecules? Lipid Insights. 2**,** 27-40.

Ronquist, G., et al., 1978. An Mg2+ and Ca2+-stimulated adenosine triphosphatase in human prostatic fluid: part I. Andrologia. 10**,** 261-72.

Saman, S., et al., 2012. Exosome-associated tau is secreted in tauopathy models and is selectively phosphorylated in cerebrospinal fluid in early Alzheimer disease. J Biol Chem. 287**,** 3842-9.

Savina, A., et al., 2005. Rab11 promotes docking and fusion of multivesicular bodies in a calcium-dependent manner. Traffic. 6**,** 131-43.

Silverman, J. M., et al., 2010. An exosome-based secretion pathway is responsible for protein export from Leishmania and communication with macrophages. J Cell Sci. 123**,** 842-52.

Sung, B. H., et al., 2015. Directional cell movement through tissues is controlled by exosome secretion. Nat Commun. 6**,** 7164.

Taylor, D. D., Black, P. H., 1985. Inhibition of macrophage Ia antigen expression by shed plasma membrane vesicles from metastatic murine melanoma lines. J Natl Cancer Inst. 74**,** 859-67.

Taylor, D. D., Gercel-Taylor, C., 2005. Tumour-derived exosomes and their role in cancer-associated T-cell signalling defects. Br J Cancer. 92**,** 305-11.

Taylor, D. D., et al., 1988. Characterization of plasma membrane shedding from murine melanoma cells. Int J Cancer. 41**,** 629-35.

Thery, C., et al., 2006. Isolation and characterization of exosomes from cell culture supernatants and biological fluids. Curr Protoc Cell Biol. Chapter 3**,** Unit 3 22.

Thery, C., et al., 2001. Proteomic analysis of dendritic cell-derived exosomes: a secreted subcellular compartment distinct from apoptotic vesicles. J Immunol. 166**,** 7309-18.

Thery, C., et al., 2002. Exosomes: composition, biogenesis and function. Nat Rev Immunol. 2**,** 569-79.

Tomlinson, P. R., et al., 2015. Identification of distinct circulating exosomes in Parkinson's disease. Ann Clin Transl Neurol. 2**,** 353-61.

Trams, E. G., et al., 1981. Exfoliation of membrane ecto-enzymes in the form of micro-vesicles. Biochim Biophys Acta. 645**,** 63-70.

Twu, O., et al., 2013. Trichomonas vaginalis exosomes deliver cargo to host cells and mediate hostratioparasite interactions. PLoS Pathog. 9**,** e1003482.

Vallejo, M. C., et al., 2011. The pathogenic fungus Paracoccidioides brasiliensis exports extracellular vesicles containing highly immunogenic alpha-Galactosyl epitopes. Eukaryot Cell. 10**,** 343-51.

van Niel, G., et al., 2006. Exosomes: a common pathway for a specialized function. J Biochem. 140**,** 13-21.

Vella, L. J., et al., 2007. Packaging of prions into exosomes is associated with a novel pathway of PrP processing. J Pathol. 211**,** 582-90.

Vingtdeux, V., et al., 2012. Potential contribution of exosomes to the prion-like propagation of lesions in Alzheimer's disease. Front Physiol. 3**,** 229.

Wang, L., et al., 2015. Exosome-like vesicles derived by Schistosoma japonicum adult worms mediates M1 type immune- activity of macrophage. Parasitol Res. 114**,** 1865-73.

Wuthier, R. E., 1975. Lipid composition of isolated epiphyseal cartilage cells, membranes and matrix vesicles. Biochim Biophys Acta. 409**,** 128-43.

Zitvogel, L., et al., 1998. Eradication of established murine tumors using a novel cell-free vaccine: dendritic cell-derived exosomes. Nat Med. 4**,** 594-600.

CHAPTER II

α-SYNUCLEIN PROTECTS AGAINST MANGANESE NEUROTOXIC INSULT DURING THE EARLY STAGES OF EXPOSURE IN A DOPAMINERGIC CELL MODEL OF PARKINSON'S DISEASE

Dilshan S. Harischandra, Huajun Jin, Vellareddy Anantharam, Arthi Kanthasamy,

Anumantha G. Kanthasamy*

Department of Biomedical Sciences, Iowa Center for Advanced Neurotoxicology,

Iowa State University, Ames, Iowa 50011

Running title: α-Synuclein in manganese neurotoxicity

*To whom correspondence should be addressed: Dept. of Biomedical Sciences, Iowa

State University, 2062 College of Veterinary Medicine Building, Ames, IA 50011, USA.

Tel: 1-515-294-2516; Fax: 1-515-294-2315; Email: akanthas@iastate.edu

Email addresses:

DSH: dilshan@iastate.edu

HJ: egb761@iastate.edu

AK: arthik@iastate.edu

VA: anantram@iastate.edu

AGK: akanthas@iastate.edu

Abstract

The pathological role of alpha-synuclein (α-Syn) aggregation in neurodegeneration is well recognized, but the physiological function of normal α-Syn remains unknown. Since α-Syn protein contains multiple divalent metal binding sites, herein we conducted a comprehensive characterization of the role of α-Syn in manganese-induced dopaminergic neurotoxicity. We established transgenic N27 dopaminergic neuronal cells by stably expressing human wild-type α-Syn at normal physiological levels. Alpha-Syn-expressing dopaminergic cells significantly attenuated Mn-induced neurotoxicity for 24-h exposures relative to vector control cells. To further explore cellular mechanisms, we studied the mitochondria-dependent apoptotic pathway. Analysis of a key mitochondrial apoptotic initiator, cytochrome c, revealed that α-Syn significantly reduces the Mn-induced cytochrome c release into cytosol. The downstream caspase cascade, involving caspase-9 and caspase-3 activation, during Mn exposure was also largely attenuated in Mn-treated α-Syn cells in a time-dependent manner. Alpha-Syn cells also showed a dramatic reduction in the Mn-induced proteolytic activation of the pro-apoptotic kinase PKCδ. The generation of Mn-induced reactive oxygen species did not differ between α-Syn and vector control cells, indicating that α-Syn exerts its protective effect independent of altering ROS generation. Inductively coupled plasma-mass spectrometry (ICP-MS) revealed no significant differences in intracellular Mn levels between treated vector and α-Syn cells. Notably, the expression of wild-type α-Syn in primary mesencephalic cells also rescued cells from Mn-induced neurotoxicity. However, prolonged exposure to Mn promoted protein aggregation in α-Syn-expressing cells. Collectively, these results demonstrate that wild-type α-Syn exhibits

neuroprotective effects against Mn-induced neurotoxicity during the early stages of exposure in a dopaminergic neuronal model of PD.

Keywords: alpha-synuclein, protein aggregation, Parkinson's disease, metals, neuroprotection, neurotoxicity

Introduction

Parkinson's disease (PD) is a progressive neurodegenerative disorder characterized by the death of dopaminergic neurons projecting from the substantia nigra pars compacta (SNpc) to the striatum and by the presence of cytoplasmic eosinophilic inclusions, termed Lewy bodies and Lewy neurites (Gasser, 2009), throughout the nigrostriatal pathway. It is the second most common neurodegenerative disorder, affecting about 1.8% of the population over the age of 65 years. It is also characterized clinically by several extrapyramidal features such as bradykinesia, postural instability, resting tremor, and rigidity. Manifestation of non-motor symptoms at early stages of PD has been recognized in recent years. Although aging is the greatest risk for developing PD, pathogenesis of the disease remains unclear. Nevertheless, current etiological understanding suggests that PD likely results from genetic susceptibility combined with various environmental factors (Aschner et al., 2009).

Recent evidence has implicated several gene defects (*SNCA*, *PRKN*, *PINK1*, *DJ-1*, *MAPT*, *UCH-L1*, *LRRK2* and *ATP13A2*) directly contributing or enhancing susceptibility to PD (Dawson et al., 2010). The first gene identified as a genetic risk factor for autosomal-dominant PD was α-Syn (*PARK1/SNCA*), which strongly interacted with gene multiplications or three-point mutations (Gasser, 2009). Alpha-Syn is a 140-

amino acid protein predominantly expressed presynaptically in neurons throughout the mammalian brain and cerebrospinal fluid (CSF). Moreover, recent studies have shown that α-Syn is transported between neurons or from neurons to various glial cell types and that the blood-CSF barrier regulates α-Syn uptake from CSF, thus maintaining α-Syn homeostasis in the CSF and brain parenchyma (Bates and Zheng, 2014). However, physiological functions of α-Syn are poorly understood, but evidence has suggested a role for it in synaptic plasticity, dopamine regulation, and membrane trafficking (Auluck et al., 2010). The link between α-Syn and PD pathogenesis is based on case studies of familial PD and the observation that misfolded α-Syn is a major constituent of Lewy bodies and Lewy neurites in both familial and sporadic PD (Dawson et al., 2010). Despite this, there is a growing body of evidence that contradicts the current understanding of α-Syn, which suggests that wild-type α-Syn is perhaps neuroprotective rather than detrimental. In fact, some studies have shown α-Syn pathology in Lewy bodies and Lewy neurites to be neuroprotective (Tanaka et al., 2004), and findings of postmortem studies (Jellinger, 2004) done with aged individuals have shown formation of Lewy bodies without any signs of PD or any other neurodegenerative disorders, thus challenging the relevance of α-Syn as a classical neuropathological hallmark of PD. Moreover, recent studies have demonstrated neuroprotective effects of wild-type α-Syn against the classical Parkinsonian toxin MPP^+ (Kaul et al., 2005a), the oxidative stress inducer hydrogen peroxide (Lee et al., 2001), or the agro-chemicals (Choong and Say, 2011).

Although genes are an important risk factor, at least in many familial cases, exposure to toxins or other environmental factors may influence when symptoms of the disease appear and/or how the disease progresses. Manganese (Mn) is an essential trace

mineral vital for normal development and for biological functions of a number of enzymes (Aschner and Aschner, 2005; Karki et al., 2013). Manganese is essential in bone formation, fat and carbohydrate metabolism, blood sugar regulation, and calcium absorption (Bowman et al., 2011). Manganese deficiency can contribute to birth defects, impaired fertility, bone malformation and weakness, and enhanced susceptibility to seizures (Aschner and Aschner, 2005). However, excessive exposure to manganese is a well-recognized occupational and environmental neurotoxic hazard.

A link has been established between manganese exposure and PD or PD-related disorders (Cowan et al., 2009; Dydak et al., 2011; Guilarte, 2013), suggesting neurotoxic effects of manganese on the nigrostriatal system. Several mechanisms have been identified in manganese neurotoxicity, including mitochondrial impairment, oxidative and nitrative damage, astroglial- and microglial-mediated inflammation and dopamine metabolism impairment (Filipov and Dodd, 2012; Sidoryk-Wegrzynowicz and Aschner, 2013). We and others have shown that manganese can also interact with disease-specific proteins such as Huntington and prion proteins (Madison et al., 2012; Martin et al., 2011). Since the potential interaction of manganese with α-Syn is not well defined, herein, we systematically characterized the role of α-Syn in the early and late stages of manganese neurotoxicity in dopaminergic neuronal cells.

Materials and Methods

Reagents

Manganese chloride ($MnCl_2$) and mouse β-actin antibody were purchased from Sigma (St. Louis, MO). SYTOX Green nucleic acid dye was purchased from Molecular Probes (Eugene, OR). Cell Death Detection ELISA plus assay kit was purchased from Roche Molecular Biochemicals (Indianapolis, IN). Bradford protein assay kit was purchased from Bio-Rad Laboratories (Hercules, CA). RPMI 1640 medium, fetal bovine serum, L-glutamine, penicillin/streptomycin, hygromycin B, Lipofectamine Plus, LTX, and 2000 reagents and pCEP4 empty vector were purchased from Invitrogen (Carlsbad, CA). The pmaxGFP vector was purchased from Lonza. The primary antibodies against α-Synuclein 211, protein kinase Cδ (PKCδ), caspase-3, and transferrin (Tf) were purchased from Santa Cruz Biotechnology (Santa Cruz, CA). Divalent metal transporter (DMT-1) antibody was obtained from Alpha Diagnostic International (San Antonio, TX), and α-Synuclein monoclonal antibody (Syn-1) was purchased from BD Biosciences (San Diego, CA). Alexa Fluor 680-conjugated anti-mouse secondary antibody was purchased from Invitrogen. IR800-conjugated anti-rabbit secondary antibody was purchased from Rockland Immunochemicals (Gilbertsville, PA). Caspase-3 substrate (Ac-DEVD-AFC) was obtained from Bachem Biosciences (King of Prussia, PA). The $\{\gamma\text{-}^{32}P\}$ ATP was purchased from Perkin-Elmer Life Science (Boston, MA).

Cell culture and stable expression of α-synuclein

The immortalized rat mesencephalic dopaminergic cell line $1RB_3AN_{27,}$ also referred to as N27 cells, was a kind gift from Dr. Kedar N. Prasad (University of Colorado Health Sciences Center, Denver, CO). N27 cells were grown in RPMI 1640

medium containing 10% fetal bovine serum, 2 mM L-glutamine, 50 units of penicillin, and 50 μg/ml of streptomycin in a humidified atmosphere of 5% CO_2 at 37°C as described previously (Ghosh et al., 2013; Jin et al., 2011b; Kaul et al., 2005a; Kaul et al., 2003). Dr. Eliezer Masliah (University of California, San Diego, CA) kindly provided the pCEP4-α-Syn expression vector containing the full-length human α-synuclein sequence. The pCEP4-α-Syn and pCEP4 empty vector (Vec) were transfected into N27 cells using Lipofectamine 2000 reagent following the procedure recommended by the manufacturer and as described previously (Kaul et al., 2005a). The stable transfectants were selected 48 h post-transfection in 400 μg/ml of hygromycin B and further maintained in N27 growth media supplemented with 200 μg/ml of hygromycin B. Expression levels of α-Syn were confirmed by Western blot and immunocytochemistry.

DNA fragmentation assays

DNA fragmentation was measured using a Cell Death Detection ELISA Plus assay kit as described previously (Afeseh Ngwa et al., 2009; Jin et al., 2011a; Jin et al., 2011b). This method measures the amount of histone-associated low–molecular-weight DNA in the cytoplasm and is more sensitive than DNA ladder analysis. Briefly, cells were collected and lysed using the lysis buffer supplied with the kit. The lysate was spun down at 200 x g, and 20 μl of supernatant were then incubated for 2 h with the mixture of HRP-conjugated antibody that recognizes histones and single- and double-stranded DNA. After washing away the unbound components, the final reaction product was measured colorimetrically with 2,2′-azino-di-[3-ethylbenz-thiazoline sulfonate] as an HRP substrate using a spectrophotometer at 405 nm and 490 nm. The difference in absorbance between

405 and 490 nm was used to determine the amount of DNA fragmentation in each sample.

Sytox Green cytotoxicity assays

Cytotoxicity was assayed using Sytox Green, a membrane-impermeable DNA dye that enters dead cells *via* their damaged plasma membranes and intercalates with nucleic acids, as described previously (Afeseh Ngwa et al., 2009; Jin et al., 2011b; Martin et al., 2011). Excitation and emission wavelengths of 485 and 538 nm, respectively, were used to detect the DNA-bound Sytox Green using a fluorescence microplate reader (Synergy 2, BioTek Instruments, Winooski, VT). The fluorescence intensity is directly proportional to the number of dead cells. Equal numbers of subconfluent α-Syn and Vec cells were grown in 24-well plates for 16-18 h and then incubated with 1 µM Sytox Green and 300 µM manganese ($MnCl_2$) for the indicated time periods. Fluorescence intensity was monitored at appropriate time points during the experiments to quantify the resulting cell death, and fluorescence images were taken using an inverted fluorescence microscope (Nikon, Tokyo, Japan) equipped with a SPOT digital camera (Diagnostic Instruments, Sterling Heights, MI).

Immunofluorescence staining

Expression of human α-Syn in the stably-transfected N27 cells and transiently-transfected primary mesencephalic cultures was determined by immunocytochemistry. Briefly, the cells were seeded on a poly-D-lysine-coated cover slip. After 24 h, cells were washed with PBS and incubated in 4% paraformaldehyde (PFA) for 30 min at room temperature. After fixing, the cells were washed with PBS and blocked for 45 min with the blocking agent (2% BSA, 0.05% Tween-20, and 0.5% Triton X-100 in PBS). Cells

were then incubated overnight at 4°C with the mouse monoclonal antibody against human α-synuclein (α-Syn211 Santa Cruz, 1:1000) or GFP (ab6673 Abcam, 1:2000). The following day, cells were incubated for 90 min in the dark with Alexa Fluor 555-conjugated anti-mouse or Fluor 488-conjugated anti-goat secondary antibody (1:1500). Hoechst 44432 was used as a nuclear stain and the cover slips were then mounted on glass slides and viewed using a Nikon TE2000 microscope (Tokyo, Japan). Images were captured with a SPOT color digital camera (Diagnostic Instruments, Sterling Heights, MI).

Measurements of intracellular reactive oxygen species

The cytosolic levels of reactive oxygen species (ROS) were measured by dichlorofluorescein-diacetate (DCF-DA) (Molecular Probes) as previously described (Afeseh Ngwa et al., 2009). Briefly, 2×10^4 Vec and α-Syn cells were plated in 96-well plates. After roughly 18 h, the media was removed, and cells were then washed with PBS and co-treated with 300 μM $MnCl_2$ and 10 μM DCF-DA in Hank's buffered salt solution (HBSS) and fluorescence measurements were taken at time points up to 90 min. The DCF-DA dye is a cell permeable, non-fluorescent probe, but after cellular oxidation and removal of acetate groups by cellular esterases, it becomes fluorescent. Fluorescence of the cells was measured at various time points using the Synergy 2 fluorescence plate reader with 485 nm excitation and 538 nm emission filters.

Determinations of intracellular manganese concentrations

Intracellular manganese concentrations were measured by inductively coupled plasma-mass spectrometry (ICP-MS) as described in our recent publications (Afeseh Ngwa et al., 2009; Martin et al., 2011). Cells expressing α-Syn and Vec control cells were treated with 300 µM manganese for 24 h and washed three times with ice-cold PBS. ICP-MS was used to determine the concentrations of Mn at m/z 55 in each sample. The high-resolution double-focusing ICP-MS device (ELEMENT 1, Thermo Finnigan) was operated at medium resolution (m/Δm = 4,000) to resolve the isotopes of interest from any interferences. Each sample was placed in an acid-washed 5-ml Teflon vial and digested in 150 µl high purity nitric acid (Ultrex II, J.T. Baker). Following digestion, the samples were diluted to 5 ml with 18.2 MΩ deionized water to give a final acid concentration of approximately 3% nitric acid. The supernatant was analyzed with the ICP-MS. Gallium (Ga) was chosen as the internal standard because its m/z ratio of 69 is similar to that of the manganese, and it has no major spectroscopic interferences. A small spike of Ga standard solution was added to each sample for a final Ga concentration of 10 ppb and manganese standard (10-ppb) was prepared. The nitric acid blank, the Mn element standard, and each of the samples were introduced into the ICP-MS via a 100 µl/min self-aspirating PFA nebulizer (Elemental Scientific, Inc.). The nitric acid blank was used to rinse the nebulizer between each sample. The results for each sample were calculated using the integrated average background-subtracted peak intensities from 20 consecutive scans. To correct for differences in elemental ionization efficiency in the ICP, the manganese standard was used and concentrations of Mn were then calculated for each sample.

Measurements of caspase-3 and caspase-9 activities

After manganese exposure, cells were resuspended in caspase lysis buffer (50 mM Tris-HCl, pH 7.4, 1 mM EDTA, 10 mM EGTA, and 10 μM digitonin) at 37°C for 20 min. Lysates were centrifuged at 20,000 x *g* and the cell-free supernatants were incubated with 50 μM caspase-3 substrate (Ac-DEVD-AFC) or caspase-9 substrate (Ac-LEHD-AFC) at 37°C for 1 h (Afeseh Ngwa et al., 2009; Jin et al., 2011a). Formation of 7-amino-4-methylcoumarin (AFC), resulting from caspase-3 or caspase-9 activity, was measured at a 400 nm excitation and a 505 nm emission wavelength using a fluorescence plate reader. All fluorescence signals from the samples were normalized to protein concentration, as determined with the Bradford protein assay.

Western blot analysis

Whole cell lysates were prepared using modified RIPA buffer containing protease and phosphatase inhibitor cocktail (Thermo Scientific, Waltham, MA) as previously described (Ghosh et al., 2013; Kanthasamy et al., 2012). Mitochondrial and cytoplasmic extracts were isolated using the mitochondria isolation kit for cultured cells (Thermo Scientific, Waltham, MA). The protein concentrations were determined with the Bradford protein assay. Cell lysates containing equal amounts of protein were separated on a 10-to-15% SDS-polyacrylamide gel. After separation, proteins were transferred to a nitrocellulose membrane, and non-specific binding sites were blocked by treating with LI-COR blocking buffer. The membranes were then incubated overnight with primary antibodies directed against PKCδ (rabbit polyclonal; 1:2000 dilution), α-Synuclein 211 (mouse monoclonal; 1:500 dilution), transferrin (Tf, rabbit polyclonal; 1:500 dilution), caspase-3 (rabbit polyclonal; 1:1000 dilution), cytochrome c (rabbit polyclonal; 1:2000

dilution), COX-IV (mouse monoclonal; 1:2000 dilution) or DMT-1 (rabbit polyclonal; 1:2000 dilution). The primary antibody treatments were followed by treatment with IR800-conjugated anti-rabbit or Alexa Fluor 680-conjugated anti-mouse secondary antibody for 1 h at room temperature. To confirm equal protein loading, blots were reprobed with β-actin antibody (1:15000 dilution). Western blot images were captured with the Odyssey IR Imaging system (LI-COR) and data were analyzed using Odyssey 2.0 software.

Slot blot analysis

After manganese exposure, protein aggregation and accumulation were evaluated with anti-oligomeric antibody (A11) via slot blot analysis. Cell lysates were prepared as described for Western blot analysis, and equal amounts of protein were loaded to each well and adsorbed onto the nitrocellulose membrane using a slot blot apparatus (Bio-Dot and Bio-Dot SF Microfiltration apparatus, Bio-Rad). Following adsorption, the membranes were pre-incubated with LI-COR blocking buffer and incubated overnight at 4°C with anti-A11 (1:1000 dilution, Invitrogen). After incubation with primary antibody, membranes were incubated with an IR800-conjugated anti-rabbit secondary antibody. Slot blot images were captured with the Odyssey IR Imaging system (LI-COR) and data were analyzed using Odyssey 2.0 software.

Assessments of aggresomes and inclusion body formation

Assessment of aggresome formation was performed using a ProteoStat aggresome detection kit according to the manufacturer's instructions (Enzo Life Sciences). Briefly, 1.5×10^4 α-Syn cells were plated on poly-D-lysine-coated glass coverslips and treated with 300 μM manganese for 36-48 h. After treatment, cells were fixed with 4% PFA,

permeabilized with 0.5% Triton X-100 and incubated with ProteoStat aggresome dye and Hoechst 33342 nuclear stain as directed by the manufacturer. Analysis was done with a NIKON TE2000 fluorescence microscope using a Texas Red filter for imaging the cell aggresome signal and a UV filter for imaging the nuclear signal. Following prolonged manganese exposure, cytoplasmic protein aggregation or inclusion body formation was analyzed by a newly developed microplate-based ProteoStat inclusion body cytotoxicity kit (Enzo Life Sciences) following the procedure recommended by the manufacturer. Briefly, 2.5×10^3 α-Syn and Vec cells were plated in 96-well plates, treated with 300 μM manganese for 36-48 h, and then fixed with 4% PFA for 15 min. At the end of fixation, cells were washed with PBS and incubated at room temperature for 15 min with permeabilization buffer. Cells were then incubated in dual-color detection buffer for 30 min, and fluorescence was measured using the Synergy 2 fluorescence plate reader with 500 nm excitation and 600 nm emission filters for aggresome readings and 350 nm excitation and 450 nm emission filters for Hoechst nuclear readings. Increases in the ratio of the ProteoStat aggresome signal (500/600 nm), relative to the Hoechst signal (350/450 nm), indicate the formation of aggregated proteins within aggresomes and related inclusion bodies in response to manganese exposure.

Primary mesencephalic neuronal cultures

All procedures involving animal handling were approved by the Institutional Animal Care and Use Committee (IACUC) at Iowa State University. Primary mesencephalic neuronal cultures were prepared as described in our previous publications (Ghosh et al., 2013; Jin et al., 2011a). Briefly, 24-well plates containing coverslips were coated 2 h with 0.1 mg/ml of poly-D-lysine. Mesencephalon tissues were dissected from

gestational 14-day-old mouse embryos and kept in ice-cold DMEM. Cells were then dissociated in DMEM containing trypsin–0.25% EDTA for 30 min at 37°C. After incubation, 10% heat-inactivated fetal bovine serum in DMEM was added to inhibit trypsin digestion. The cells were triturated and suspended in neurobasal medium supplemented with 2% B27 supplement, 500 μM L-glutamine, 100 IU/ml penicillin, and 100 μg/ml streptomycin, plated at 7.5×10^5 cells/well and incubated in a humidified CO_2 incubator. Half of the culture medium was replaced every 2 days, and transfections of primary neuronal cultures were conducted on the fourth day.

Transfection of human α-Syn in primary mesencephalic neuronal cultures

Transfection of primary mesencephalic cultures was carried out on the fourth day of culture *ex vivo* using Lipofectamine LTX and PLUS Reagent per manufacturer's instructions. Briefly, 1.0 μg pmaxGFP-α-Syn or pmaxGFP control plasmid was diluted in 100 μL of Opti-MEM-I media and 2.5 μL of PLUS Reagent was added. This mixture was incubated for 5 min at room temperature. After incubation, 1.5 μL of Lipofectamine LTX reagent was added to the above diluted Opti-MEM:DNA solution, mixed gently and incubated for 30 min to form DNA-Lipofectamine LTX Reagent complexes. Then 100 μL of the DNA-Lipofectamine LTX complexes was added directly to each well and incubated in a humidified CO_2 incubator for 18-24 h before expose to manganese. GFP-α-Syn expression was confirmed through fluorescence microscopy.

Quantification of neurite processes

Primary mesencephalic neuronal cultures transfected with human wild-type α-Syn were treated with 50 μM manganese for 24 h, and coverslips were processed for GFP immunofluorescence staining as described above. MetaMorph image analysis software, version 5.0 (Molecular Devices, Sunnyvale, CA), was used to measure the neurite length of primary dopaminergic neurons from each coverslip in the control and treatment groups as described in our previous publications (Afeseh Ngwa et al., 2009; Ghosh et al., 2013). Data from at least six different cultures per experimental group were pooled and analyzed using Prism 4.0 software (Graphpad Software, San Diego, CA).

[^{3}H]-Dopamine uptake assays

The neuroprotective effect of human wild-type α-Syn on dopaminergic neurons in fetal mouse mesencephalic cultures exposed to manganese was quantified using the ^{3}H-DA uptake assay (Harischandra et al., 2014). This functional assay is more sensitive than TH-positive neuron counting (Afeseh Ngwa et al., 2009; McCoy et al., 2006) and overcomes difficulties in TH-positive cell counting associated with transfection studies. Briefly, human wild-type α-Syn-transfected primary mesencephalic neuronal cultures were treated with 50 μM manganese for 24 h. After washing the cells twice with Krebs Ringer buffer (5.6 mM glucose, 1.3 mM EDTA, 1.2 mM MgSO$_4$, 1.8 mM CaCl$_2$, 4.7 mM KCl, 120 mM NaCl, 16 mM Na$_3$PO$_4$), cells were incubated with 10 μM ^{3}H-DA (30 Ci/mol) for 30 min at 37°C in Krebs Ringer buffer. The dopamine reuptake blocker Mazindol (1 nM) served as a positive control to assess the efficiency of ^{3}H-DA uptake. The uptake was stopped by removing the reaction mixture followed by a triple wash with fresh ice-cold Krebs Ringer buffer. Cells were then lysed with 1 N sodium hydroxide,

and their radioactivity was measured by liquid scintillation counter (Tri-Carb 4000; Packard, Meriden, CT) after adding a 5-mL scintillation cocktail to each vial.

Statistical analysis

Prism 4.0 software was used to analyze data from two or more independent experiments, each with n ≥ 6. Bonferroni's multiple comparison testing was used to find significant differences between treatment and control groups. Differences with $p < 0.05$ were considered significantly different.

Results

Generation of N27 dopaminergic cells stably expressing wild-type human α-Syn

The α-Syn protein has three metal binding sites: one at N-terminus, one at central region and one at C-terminus of the protein (Fig. 1A). The metal binding sites near 49-52 and 110-140 are known to interact with divalent metals including manganese (Uversky et al., 2001). To understand the role of α-Syn in manganese neurotoxicity, we first established a rat mesencephalic N27 dopaminergic cell model stably expressing human wild-type α-Syn by transfecting them with the plasmid pCEP4-α-Syn or pCEP control vector. Stable expression of human α-Syn in N27 cells was determined by Western blot analysis (Fig. 1B) using an α-Syn antibody as described previously (Kaul et al., 2005a). Endogenous α-Syn levels were too low to detect in N27 Vec cells, whereas strong expression of a single 19-kDa human α-Syn band could readily be detected in α-Syn-expressing N27 cells comparable to that described in our previous publications (Jin et al., 2011b; Kaul et al., 2005a). Western blot analysis comparing α-Syn expression in N27 cells to rat brain lysates (Fig. 1B) showed that α-Syn was not overexpressed in N27 cells,

but was within physiologic relative to rat brain. Additional analysis through *immunocytochemistry* demonstrated brightly stained subcellular localization of α-Syn corresponding to its even distribution in α-Syn-expressing N27 cells, whereas no immunoreactivity was observed in Vec cells (Fig. 1C).

Human wild-type α-Syn expression attenuates Manganese-induced cytotoxicity

To evaluate the effect of wild-type α-Syn expression on manganese-induced neurotoxicity, α-Syn-expressing and Vec N27 cells were treated with 300 μM manganese and cell death was measured at various time points over a 24 h period. As revealed by the SYTOX Green cytotoxicity assay (Fig. 2A), α-Syn-expressing cells showed ~50% protection against manganese neurotoxicity (at 24 h) as compared to that of Vec cells. To confirm the results obtained with the fluorescence plate readings, SYTOX Green-positive cells were also imaged using fluorescence microscopy (Fig. 2B), where phase-contrast (bottom panels) and Sytox FITC fluorescence (top panels) images were captured from random fields to compare cell death between manganese-treated α-Syn and Vec cells. Vec cells treated with manganese experienced significantly higher cell death compared to manganese-treated α-Syn cells, as evidenced by the bright SYTOX positive cells.

Further analysis of α-Syn's neuroprotective effect at later time points (36 h and 48 h) indicates that its ability to withstand manganese-induced cytotoxicity is gradually reduced (Figs. 2A and 2C). As shown in Fig. 2C, determination of the percentage reduction in neuroprotection by subtracting the rate of cell death in α-Syn cells from that in Vec cells at 24, 36 and 48 h revealed a gradual loss of α-Syn's neuroprotective function over time. Together, we observed a novel observation that wild-type α-Syn

expression is neuroprotective against early stages of manganese cytotoxicity in a dopaminergic cell model but the proective effect declines during prolonged manganese exposure.

α-Syn expression attenuates manganese-induced cytochrome c release without augmenting manganese-induced oxidative stress in N27 dopaminergic cells

Several studies, including our previous work, have shown that various dopaminergic toxicants such as MPP^+, dieldrin, $MnCl_2$, V_2O_5 and Methylcyclopentadienyl manganese tricarbonyl (MMT), induce cell death through early oxidative events resulting in mitochondrial depolarization accompanied by cytochrome c release (Afeseh Ngwa et al., 2009; Kaul et al., 2005a; Latchoumycandane et al., 2005). Therefore, we examined by DCF-DA assay whether increased α-Syn expression modulates manganese-induced early ROS production in α-Syn and Vec cells. Quantitative analysis of ROS generation revealed that exposure of both α-Syn and Vec cells to manganese resulted in time-dependent early ROS generation (Fig. 3A). However, levels of manganese-induced ROS generation did not differ significantly between these two cells (Fig. 3A). This suggests that the neuroprotective effects induced by the cellular expression of wild-type human α-Syn in N27 dopaminergic cells may occur independently of manganese-induced early ROS production.

Increased intracellular ROS production is known to trigger mitochondrial depolarization and the release of cytochrome c very rapidly, thereby activating downstream apoptotic pathways. Therefore, we examined whether α-Syn expression can reduce manganese-induced cytochrome c release from the mitochondria, thereby rescuing

dopaminergic cells from apoptotic cell death. After 300 μM manganese exposure for 6 h, cytosolic and mitochondrial fractions were isolated and subject to Western blot analysis. Exposure to 300 μM manganese caused cytochrome c release from both Vec and α-Syn cells, however, the release was significantly less in α-Syn cells (Figs. 3B and C).Thus, these data indicate that α-Syn expression can indeed attenuate the release of the key mitochondrial proapoptotic molecule cytochrome c into the cytosol during early stages of manganese exposure.

α-Syn expression suppresses manganese-induced caspase cascade activation and DNA fragmentation and attenuates manganese-induced proteolytic activation of PKCδ

Cytochrome c is known to play a key regulatory role in activating apoptotic cell death during neurotoxic stress (Afeseh Ngwa et al., 2009; Kaul et al., 2003). Cytosolic cytochrome c first activates caspase-9, thereby initiating an intrinsic apoptotic caspase cascade, resulting further in the activation of caspase-3, the major effector caspase that is responsible for proteolytic cleavage of apoptotic cell signaling molecules. Previous studies in our laboratory have shown that dopaminergic neurotoxicants can activate the caspase cascade in dopaminergic cells (Afeseh Ngwa et al., 2009; Ghosh et al., 2013; Kaul et al., 2005b). Herein, we examined whether α-Syn expression blocks caspase cascade activation induced by manganese. For this study, we treated α-Syn-expressing and Vec control N27 cells with 300 μM manganese for 12 h, and then caspase-9 and -3 activities were determined using one of the fluorometric substrates Ac-LEHD-AFC or Ac-DEVD-AFC. Caspase-9 and caspase-3 were significantly activated (>2.5 fold) in Vec

cells after 12 h of exposure to 300 μM manganese, whereas their activation was suppressed in α-Syn-expressing cells (Figs. 4A-B). These results show that α-Syn expression attenuates manganese-induced sequential activation of caspase-9 and caspase-3.

DNA fragmentation is one of the hallmarks of apoptosis, resulting from endonuclease activation and the breakdown of chromatin. Therefore, we further characterized the neuroprotective effect of human α-Syn by quantifying DNA fragmentation. As shown in Fig. 4C, manganese exposure significantly increased DNA fragmentation in manganese-treated compared to untreated Vec cells, whereas α-Syn cells almost completely suppressed the manganese-induced DNA fragmentation at the 24-h time point. These results, together with caspase cascade activation, clearly indicate that α-synuclein protects dopaminergic cells against early stages of manganese toxicity.

Previously, we had reported that caspase-3-mediated proteolytic activation of PKCδ serves as a key proapoptotic effector in manganese-induced dopaminergic neurodegeneration (Latchoumycandane et al., 2005). In a more recent publication, we also showed that α-Syn downregulates PKCδ expression by negatively modulating p300- and NFκB-dependent transactivation in N27 dopaminergic cells (Jin et al., 2011b). Therefore, we next examined whether α-Syn expression attenuates manganese-induced proteolytic activation of PKCδ. For this, we treated α-Syn and Vec cells with 300 μM manganese for 6-24 h and examined PKCδ proteolytic cleavage by Western blot analysis. As shown in Fig. 4D, a significant proportion of the native PKCδ (72–74 kDa) protein in Vec cells was proteolytically cleaved to yield a 41-kDa catalytically active fragment. At 24 h, a significant amount of the native PKCδ protein had been cleaved as evidenced by a

less intense native 72–74-kDa band and a concomitant increase in the catalytically active 41-kDa cleaved fragment. In contrast, proteolytic cleavage of PKCδ in α-Syn cells was significantly attenuated compared to vector control cells (Fig. 4D). More importantly, the manganese-induced PKCδ proteolytic cleavage band observed in Vec cells at 24 h was almost completely absent in α-Syn-expressing cells, suggesting that α-Syn negatively regulates PKCδ signaling in N27 dopaminergic cells. This finding could explain the neuroprotective effect of α-Syn on manganese neurotoxicity.

We had previously demonstrated that phosphorylation of PKCδ at Tyr-311 precedes caspase-3-mediated PKCδ proteolytic activation (Kaul et al., 2005b). In examining whether α-Syn expression alters Tyr-311 phosphorylation of PKCδ in response to manganese exposure, we show that manganese significantly increased the phosphorylation of PKCδ Tyr-311 in Vec cells, while it was markedly attenuated in α-Syn cells (Fig. 4E). To further determine whether the attenuations, both of Tyr-311 phosphorylation and PKCδ proteolytic activation, in α-Syn cells are reflected in decreased kinase activity, we determined kinase activity by an *in vitro* kinase assay using [^{32}P]-ATP following PKCδ immunoprecipitation. In agreement with the observed effects on PKCδ proteolytic cleavage and Y311 phosphorylation, α-Syn overexpression also significantly reduced the Mn-induced PKCδ kinase activity (Fig. 4F-G). These findings suggest that α-Syn attenuates PKCδ tyrosine phosphorylation, kinase activity and its proteolytic cleavage during an acute manganese insult in dopaminergic cells.

α-Syn protects against manganese-induced dopaminergic degeneration in primary mesencephalic neuronal cultures

To understand the biological relevance of the study, we extended our studies to include primary neuronal cultures. For this, we transfected pmaxGFP-α-Syn, encoding human α-Syn fused to eGFP or pmaxGFP empty vector, into cultured primary nigral cells obtained from mesencephalic tissues of E14-16 mouse embryos. After 18-24 h post-transfection, cells were exposed to 50 μM manganese for 24 h and primary mesencephalic nigral cultures were processed for GFP immunocytochemistry. (Fig. 5A). A low dose of Mn (50 μM) was used because primary mesencephalic neuronal cultures are more sensitive to manganese than are clonal cell lines. Images were taken with a NIKON TE2000 microscope, and neurite lengths were analyzed using the Morphometry Analysis (IMA) function of MetaMorph image analysis software. Once threshold values were determined, at least 10 neurons were analyzed from different slides of both control and treatment groups of pmaxGFP-α-Syn or pmaxGFP empty vector transfected cells. The loss of neuronal processes was measured as an indication of manganese-induced neurotoxicity. Primary neurons transfected with pmaxGFP-α-Syn displayed significantly less manganese-induced loss of neuronal processes compared to pmaxGFP-transfected cells (Figs. 5A-B). Under control conditions, both transfected cells had comparable neuronal process lengths, suggesting that expression of α-Syn alone did not induce cytotoxicity in primary neuronal cells. We also assessed the functional neurotoxic response of dopaminergic neurons in primary dopaminergic neuronal cultures by dopamine uptake assay. The uptake of tritiated [^{3}H] dopamine was measured in empty vector- or pmaxGFP-α-Syn-transfected primary cultures after manganese treatment.

Compared to pmaxGFP-transfected neurons, pmaxGFP-α-Syn-transected neurons significantly attenuated the manganese-induced decrease in dopamine uptake (Fig. 5C). Collectively, these results demonstrate a significant protection by human α-Syn against acute manganese toxicity in primary neuronal cultures.

Effect of α-Syn expression on manganese uptake and metal transporters

Since expression of human α-Syn in N27 dopaminergic cells may interfere with metal uptake, we measured intracellular manganese uptake by ICP-MS (Fig. 6A). Exposure to 300 µM manganese for 24 h resulted in about an 80-fold increase in intracellular manganese levels in both α-Syn (408±64 ppb) and Vec (402±44 ppb) cells. Similarly, intracellular manganese levels did not differ significantly between untreated Vec (11±0.5 ppb) and untreated α-Syn (17±1.7) cells, suggesting that α-Syn expression does not interfere with manganese uptake. To further demonstrate that stable transfection of α-Syn did not interfere with the expression of major metal ion transporters, we assessed the endogenous expression of transferrin (Tf) and divalent metal ion transporter (DMT1) (Afeseh Ngwa et al., 2009; Aschner and Aschner, 2005) in Vec and α-Syn cells. Immunoblot results indicate that both of these cells expressed these transporters at comparable levels (Fig. 6B-C), suggesting that both cells have the same ability to transport manganese into the cells and that α-Syn expression did not interfere with manganese transport to the cells.

Prolonged exposure to manganese promotes α-synuclein protein aggregation

Interestingly, even though dopaminergic cells expressing human α-Syn are neuroprotective against acute (<24 h) manganese toxicity, we observed through immunocytochemistry that prolonged (>36 h) exposure induced α-Syn protein to aggregate in dopaminergic cells as evidenced by punctate aggregates of the protein (Fig. 7A). Slot blot analysis (Figs. 7B-C) with the oligomeric-specific antibody A11 indicated significant accumulation of misfolded oligomeric proteins after 36 h and 48 h exposures to manganese. We further validated these observations via fluorescence microscopy using the newly available aggresome-specific ProteoStat dye, which showed an enhanced fluorescence signal of aggregated protein accumulation following prolonged manganese exposure (Fig. 7D). Moreover, our ProteoStat inclusion body microplate assay showed that α-Syn cells accumulated significantly more aggregated protein compared to Vec cells after both cells were exposed to manganese for an extended time (>36 h) (Fig. 7D-E). Collectively, these results indicate that α-Syn protects against acute manganese neurotoxicity, but loses its protective ability during prolonged exposure to manganese due to misfolding.

Discussion

Alpha-synuclein is a primary component of Lewy bodies and Lewy neurites in Parkinson's pathology, but the exact physiological function of wild-type α-Syn remains unclear. Various hypotheses have been proposed to explain whether α-Syn is neuroprotective or cytotoxic. Furthermore, the role of α-Syn's multiple metal binding sites has not been well studied. In this context, protein aggregation has been recognized

as a major mechanism of neurotoxicity in many neurodegenerative diseases, including PD, but the role of manganese in α-Syn aggregation is not well established. To this end, we developed an α-Syn-expressing dopaminergic neuronal cell model for examining the role of α-Syn in both acute and prolonged manganese neurotoxicity. Our results demonstrate for the first time that human wild-type α-Syn plays a neuroprotective role against manganese neurotoxicity in its early stages, but the protein becomes increasingly susceptible to aggregation during prolonged metal exposure.

We provide direct evidence for the neuroprotective effect of human α-Syn in dopaminergic neurons during acute manganese toxicity. We observed this effect at 300 µM manganese, a dose consistent with previously published work (Exil et al., 2014; Latchoumycandane et al., 2005; Martin et al., 2011). Relatively higher doses of test compounds are needed to elicit responses in *in vitro* studies due to the acute nature of the treatments compared to long-term animal dosing experiments. However, we were able to elicit a neurotoxic response with 300 µM manganese in N27 dopaminergic cells, which is a low dose relative to the 0.5-1 mM manganese used in hippocampal and mesencephalic dopaminergic neuronal cells (Tamm et al., 2008; Yoon et al., 2011). Moreover, manganese dosimetry vastly depends on treatment conditions, and its toxicokinetics in biological systems depends on its absorption, distribution, metabolism, and elimination. Indeed, our current understanding of the health risks posed by manganese was dramatically improved by mechanistic studies of manganese-induced neurotoxicity conducted at different doses across an array of both *in vitro* and *in vivo* model systems exploring a phylogenetic range of alternative animal species such as *Caenorhabditi*s *elegans*. Depending upon the dose, duration, and route of exposure,

manganese concentrations can reach up to 350 µM in certain brain regions (Ingersoll et al., 1999), and thus the concentration used in our study was within the toxicologically relevant range. It is estimated that the adequate intake of manganese for adult men and women is 2.3-1.8 mg/day, and children aged between 1-3 and 4-8 years have intakes of 1.2-1.5 mg/day of manganese respectively (Aschner and Aschner, 2005). Manganese is essential for regulating some key enzymes (e.g. manganese superoxide dismutase) and many normal biological functions. A manganese deficiency could lead to severe health consequences such as impaired growth, skeletal abnormalities, reproductive deficits, ataxia in newborns and defects in lipid and carbohydrate metabolism (Aschner and Aschner, 2005). However, since adequate manganese is present in many common foods including leafy vegetables, nuts, grains and animal products, manganese deficiency is very rare in humans. In contrast, manganese over-exposure seems to be the major heath concern since it is used in the manufacture of iron and steel alloys, fertilizers, varnish, fungicides and livestock nutritional supplements. Human manganese exposure in well water, as a gasoline additive, and in welding fumes has been documented (Aschner et al., 2009; Bowman et al., 2011; Karki et al., 2013).

Several epidemiological studies report a significant correlation between manganese exposure and the risk of developing Parkinson-like symptoms (Cox, 2006; Goldman et al., 2005). Recent studies have shown that manganese exposure leads to the aggregation of α-Syn protein in cell free systems as well as in animal models (Uversky et al., 2001; Verina et al., 2013), providing direct experimental evidence for a close relationship between manganese and the proteins implicated in PD. In our current study, dopaminergic cells expressing human wild-type α-Syn exhibited significantly lower

apoptotic cell death compared to vector control N27 cells upon acute manganese toxicity. Our α-Syn-expressing N27 cells had roughly the same levels of α-Syn protein expression as found in rat midbrain tissues, suggesting that human α-Syn was being expressed in these cells at physiological expression levels. To further characterize the mechanism underlying the neuroprotective effect of α-Syn against manganese-induced apoptotic cell death, and because manganese is known to impair mitochondrial function (Gunter et al., 2009; Latchoumycandane et al., 2005), we systematically examined the mitochondria-dependent apoptotic signaling events. Interestingly, α-Syn does not hamper the cells' ability to produce ROS when exposed to manganese (Fig. 3A). Although α-Syn has been shown to act as an antioxidant in preventing lipid oxidation in membranes containing phospholipids with unsaturated fatty acids in cell-free systems (Zhu et al., 2006), in our study α-Syn does not possess antioxidant properties. Instead, we found a significant attenuation of cytochrome c release to cytosol from the mitochondrial inner-membrane in α-Syn-expressing cells, suggesting that α-Syn interferes with the process of cytochrome c release during early phases of manganese neurotoxicity. It is possible that a previously described (Elkon et al., 2002) protein-protein interaction between α-Syn and the mitochondrial complex IV enzyme, cytochrome c oxidase (COX), contributes to the neuroprotection of α-Syn at the mitochondrial level, attenuating the downstream apoptotic cascade involving initiator caspase-9 and effector caspase-3 activity, which are early and essential steps in the manganese-triggered apoptotic signaling pathway (Latchoumycandane et al., 2005).

As previously demonstrated, PKCδ is an oxidative stress-sensitive kinase that plays a causal role in apoptotic cell death in neuronal cells (Afeseh Ngwa et al., 2009;

Harischandra et al., 2014; Kaul et al., 2003). In our current study, we observed a time-dependent proteolytic cleavage of PKCδ in vector control cells but not in α-Syn-expressing cells, indicating that α-Syn interferes with PKCδ by reducing its proteolytic cleavage and kinase activity, thereby protecting cells from manganese-induced toxicity. Recently, we reported that α-Syn modulates PKCδ expression in dopaminergic neurons by reducing p300 histone acetyltransferase activity (Jin et al., 2011b). The observed downregulation of PKCδ in α-Syn cells (Fig. 4D) is consistent with our previously reported *in vitro* and *in vivo* data (Jin et al., 2011b) and may also contribute to the neuroprotective role of α-Syn. As shown in Figs. 2A, 2C and 7C, the neuroprotective response of α-Syn declined over prolonged manganese exposures. The observed neuroprotective effect in our study is not due to any possible interference with intracellular manganese transport by α-Syn because intracellular concentrations of manganese and the expression levels of the metal transporters DMT and Tf proteins did not differ significantly between vector control and α-Syn-expressing N27 cells.

In this study, the neuroprotective effect of wild-type human α-Syn protein was also evaluated by its ectopic expression in mouse primary mesencephalic cells. Manganese-induced neurotoxicity in α-Syn expressing cells was attenuated as evidenced by longer and healthier neurites compared to those of vector-transfected neurons. Since the cell bodies of neurons remained intact while neurites shrank in response to manganese exposure, our results show that α-Syn expression retained primary neuronal morphology after manganese-induced cytotoxicity. A functional dopamine uptake assay further validated that wild-type α-Syn rescues primary dopaminergic cells from manganese toxicity.

Alpha-Syn protein misfolding and accumulation have been recognized as major pathological features of PD. Our immunocytochemistry data indicate intracellular protein aggregates immunoreactive to α-Syn during prolonged manganese exposure in dopaminergic neuronal cells (Fig. 7A). The slot blot analysis indicates increased accumulation of misfolded protein in α-Syn cells at 36 and 48 h, but not at 24 h of manganese exposure (Fig. 7B). These observations were validated using the ProteoStat aggresome detection kit (Enzo) and the ProteoStat inclusion body kit (Enzo) to indicate the accumulation of aggregated proteins in α-Syn cells compared to Vec cells after prolonged manganese exposure. These protein aggregates may be relevant to Lewy body pathology seen in postmortem PD brains. Whether these aggregates are cytotoxic or cytoprotective to neuronal cells remains debatable. Nevertheless, the loss of α-Syn's neuroprotective effect clearly correlates with the rate of formation of protein aggregates in our study. Alpha-Synuclein has several metal binding sites (Fig. 1A) (Uversky et al., 2001), and binding to certain divalent metals, including manganese, causes α-Syn aggregation in cell-free *in vitro* experiments (Uversky et al., 2001). Moreover, the central hydrophobic domain (residues 66-95), also known as the non-amyloid-β component (NAC) domain, is highly amyloidogenic and appears to be essential for α-Syn aggregation (Auluck et al., 2010). Specifically, a GAV motif (residues 66-74) within this region has been identified as the critical core for fibrillization and cytotoxicity of α-Syn. Our results support the idea that α-Syn initially protects against manganese-induced neurotoxicity by reducing mitochondria-dependent apoptotic signaling, whereas prolonged exposure to manganese significantly alters the stability of α-Syn protein, increasing the amount of aggregated α-Syn protein.

In conclusion, we demonstrate that physiological levels of human wild-type α-Syn protein attenuate manganese-induced dopaminergic neuronal degeneration in cell culture models at early stages of manganese toxicity. However, prolonged manganese exposure promotes α-Syn aggregation and dampens its neuroprotective effect. These findings may have important implications in our understanding of the physiological functions of α-Syn protein as well as the pathogenesis of environmentally-linked Parkinson's disease.

Acknowledgments

References

Afeseh Ngwa, H., et al., 2009. Vanadium induces dopaminergic neurotoxicity via protein kinase Cdelta dependent oxidative signaling mechanisms: relevance to etiopathogenesis of Parkinson's disease. Toxicol Appl Pharmacol. 240, 273-85.

Aschner, J. L., Aschner, M., 2005. Nutritional aspects of manganese homeostasis. Mol Aspects Med. 26, 353-62.

Aschner, M., et al., 2009. Manganese and its role in Parkinson's disease: from transport to neuropathology. Neuromolecular Med. 11**,** 252-66.

Auluck, P. K., et al., 2010. alpha-Synuclein: membrane interactions and toxicity in Parkinson's disease. Annu Rev Cell Dev Biol. 26**,** 211-33.

Bates, C. A., Zheng, W., 2014. Brain disposition of alpha-Synuclein: roles of brain barrier systems and implications for Parkinson's disease. Fluids Barriers CNS. 11**,** 17.

Bowman, A. B., et al., 2011. Role of manganese in neurodegenerative diseases. J Trace Elem Med Biol.

Choong, C. J., Say, Y. H., 2011. Neuroprotection of alpha-synuclein under acute and chronic rotenone and maneb treatment is abolished by its familial Parkinson's disease mutations A30P, A53T and E46K. Neurotoxicology. 32**,** 857-63.

Cowan, D. M., et al., 2009. Manganese exposure among smelting workers: blood manganese-iron ratio as a novel tool for manganese exposure assessment. Biomarkers. 14**,** 3-16.

Cox, L. A., Jr., 2006. Prevalence of parkinsonism and relationship to exposure in a large sample of Alabama welders. Neurology. 66**,** 616-7; author reply 616-7.

Dawson, T. M., et al., 2010. Genetic animal models of Parkinson's disease. Neuron. 66**,** 646-61.

Dydak, U., et al., 2011. In vivo measurement of brain GABA concentrations by magnetic resonance spectroscopy in smelters occupationally exposed to manganese. Environ Health Perspect. 119**,** 219-24.

Elkon, H., et al., 2002. Mutant and wild-type alpha-synuclein interact with mitochondrial cytochrome C oxidase. J Mol Neurosci. 18**,** 229-38.

Exil, V., et al., 2014. Activation of MAPK and FoxO by manganese (Mn) in rat neonatal primary astrocyte cultures. PLoS One. 9**,** e94753.

Filipov, N. M., Dodd, C. A., 2012. Role of glial cells in manganese neurotoxicity. J Appl Toxicol. 32**,** 310-7.

Gasser, T., 2009. Molecular pathogenesis of Parkinson disease: insights from genetic studies. Expert Rev Mol Med. 11**,** e22.

Ghosh, A., et al., 2013. The Peptidyl-prolyl Isomerase Pin1 Upregulation and Proapoptotic Function in Dopaminergic Neurons: Relevance to the Pathogenesis of Parkinson Disease. J Biol Chem.

Goldman, S. M., et al., 2005. Occupation and parkinsonism in three movement disorders clinics. Neurology. 65**,** 1430-5.

Guilarte, T. R., 2013. Manganese neurotoxicity: new perspectives from behavioral, neuroimaging, and neuropathological studies in humans and non-human primates. Front Aging Neurosci. 5**,** 23.

Gunter, T. E., et al., 2009. The case for manganese interaction with mitochondria. Neurotoxicology. 30**,** 727-9.

Harischandra, D. S., et al., 2014. Role of proteolytic activation of protein kinase Cdelta in the pathogenesis of prion disease. Prion. 8.

Ingersoll, R. T., et al., 1999. Central nervous system toxicity of manganese. II: Cocaine or reserpine inhibit manganese concentration in the rat brain. Neurotoxicology. 20**,** 467-76.

Jellinger, K. A., 2004. Lewy body-related alpha-synucleinopathy in the aged human brain. J Neural Transm. 111**,** 1219-35.

Jin, H., et al., 2011a. Transcriptional regulation of pro-apoptotic protein kinase Cdelta: implications for oxidative stress-induced neuronal cell death. J Biol Chem. 286**,** 19840-59.

Jin, H., et al., 2011b. alpha-Synuclein negatively regulates protein kinase Cdelta expression to suppress apoptosis in dopaminergic neurons by reducing p300 histone acetyltransferase activity. J Neurosci. 31**,** 2035-51.

Kanthasamy, A. G., et al., 2012. Effect of divalent metals on the neuronal proteasomal system, prion protein ubiquitination and aggregation. Toxicol Lett. 214**,** 288-95.

Karki, P., et al., 2013. Manganese neurotoxicity: a focus on glutamate transporters. Ann Occup Environ Med. 25**,** 4.

Kaul, S., et al., 2005a. Wild-type alpha-synuclein interacts with pro-apoptotic proteins PKCdelta and BAD to protect dopaminergic neuronal cells against MPP+-induced apoptotic cell death. Brain Res Mol Brain Res. 139**,** 137-52.

Kaul, S., et al., 2005b. Tyrosine phosphorylation regulates the proteolytic activation of protein kinase Cdelta in dopaminergic neuronal cells. J Biol Chem. 280**,** 28721-30.

Kaul, S., et al., 2003. Caspase-3 dependent proteolytic activation of protein kinase C delta mediates and regulates 1-methyl-4-phenylpyridinium (MPP+)-induced apoptotic cell death in dopaminergic cells: relevance to oxidative stress in dopaminergic degeneration. Eur J Neurosci. 18**,** 1387-401.

Latchoumycandane, C., et al., 2005. Protein kinase Cdelta is a key downstream mediator of manganese-induced apoptosis in dopaminergic neuronal cells. J Pharmacol Exp Ther. 313**,** 46-55.

Lee, M., et al., 2001. Effect of the overexpression of wild-type or mutant alpha-synuclein on cell susceptibility to insult. J Neurochem. 76**,** 998-1009.

Madison, J. L., et al., 2012. Disease-toxicant interactions in manganese exposed Huntington disease mice: early changes in striatal neuron morphology and dopamine metabolism. PLoS One. 7**,** e31024.

Martin, D. P., et al., 2011. Infectious prion protein alters manganese transport and neurotoxicity in a cell culture model of prion disease. Neurotoxicology.

McCoy, M. K., et al., 2006. Blocking soluble tumor necrosis factor signaling with dominant-negative tumor necrosis factor inhibitor attenuates loss of dopaminergic neurons in models of Parkinson's disease. J Neurosci. 26**,** 9365-75.

Sidoryk-Wegrzynowicz, M., Aschner, M., 2013. Role of astrocytes in manganese mediated neurotoxicity. BMC Pharmacol Toxicol. 14**,** 23.

Tamm, C., et al., 2008. Mitochondrial-mediated apoptosis in neural stem cells exposed to manganese. Toxicol Sci. 101**,** 310-20.

Tanaka, M., et al., 2004. Aggresomes formed by alpha-synuclein and synphilin-1 are cytoprotective. J Biol Chem. 279**,** 4625-31.

Uversky, V. N., et al., 2001. Metal-triggered structural transformations, aggregation, and fibrillation of human alpha-synuclein. A possible molecular NK between Parkinson's disease and heavy metal exposure. J Biol Chem. 276**,** 44284-96.

Verina, T., et al., 2013. Manganese exposure induces alpha-synuclein aggregation in the frontal cortex of non-human primates. Toxicol Lett. 217**,** 177-83.

Yoon, H., et al., 2011. Apoptosis Induced by Manganese on Neuronal SK-N-MC Cell Line: Endoplasmic Reticulum (ER) Stress and Mitochondria Dysfunction. Environ Health Toxicol. 26**,** e2011017.

Zhu, M., et al., 2006. Alpha-synuclein can function as an antioxidant preventing oxidation of unsaturated lipid in vesicles. Biochemistry. 45**,** 8135-42.
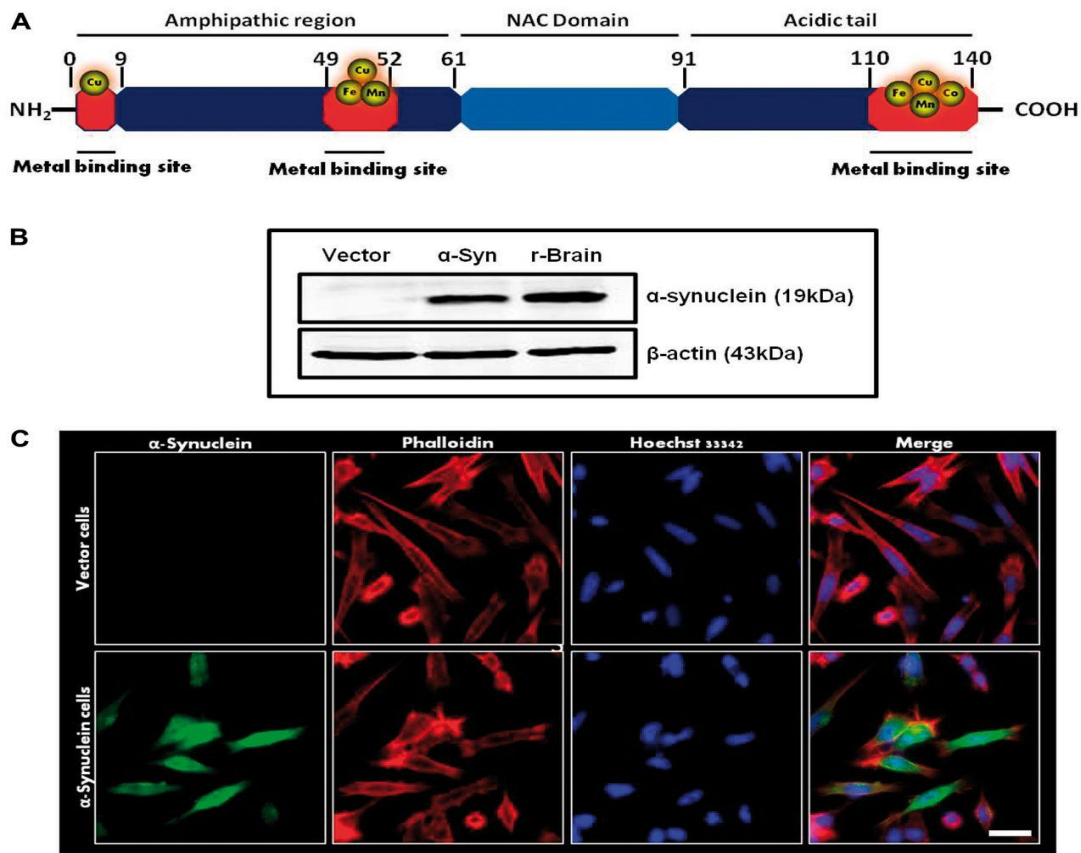
Figure 1. Generation of N27 cells stably expressing human wild-type α-synuclein protein. (A) Structure of α-Syn indicating metal binding sites. (B) Stable expression of α-Syn was determined by Western blot analysis. A 19-kDa band corresponding to the

molecular mass of human α-syn was detected in α-Syn-expressing cells, whereas no expression appeared in vector cells. (C) Immunocytochemical analysis depicting stable expression of wild-type human α-Syn protein in N27 dopaminergic cells. Alpha-Syn-expressing cells exhibit strong ubiquitous expression of α-Syn, whereas vector cells showed no detectable α-Syn immunoreactivity. Magnification, 40 X. Scale bar, 20 μm.
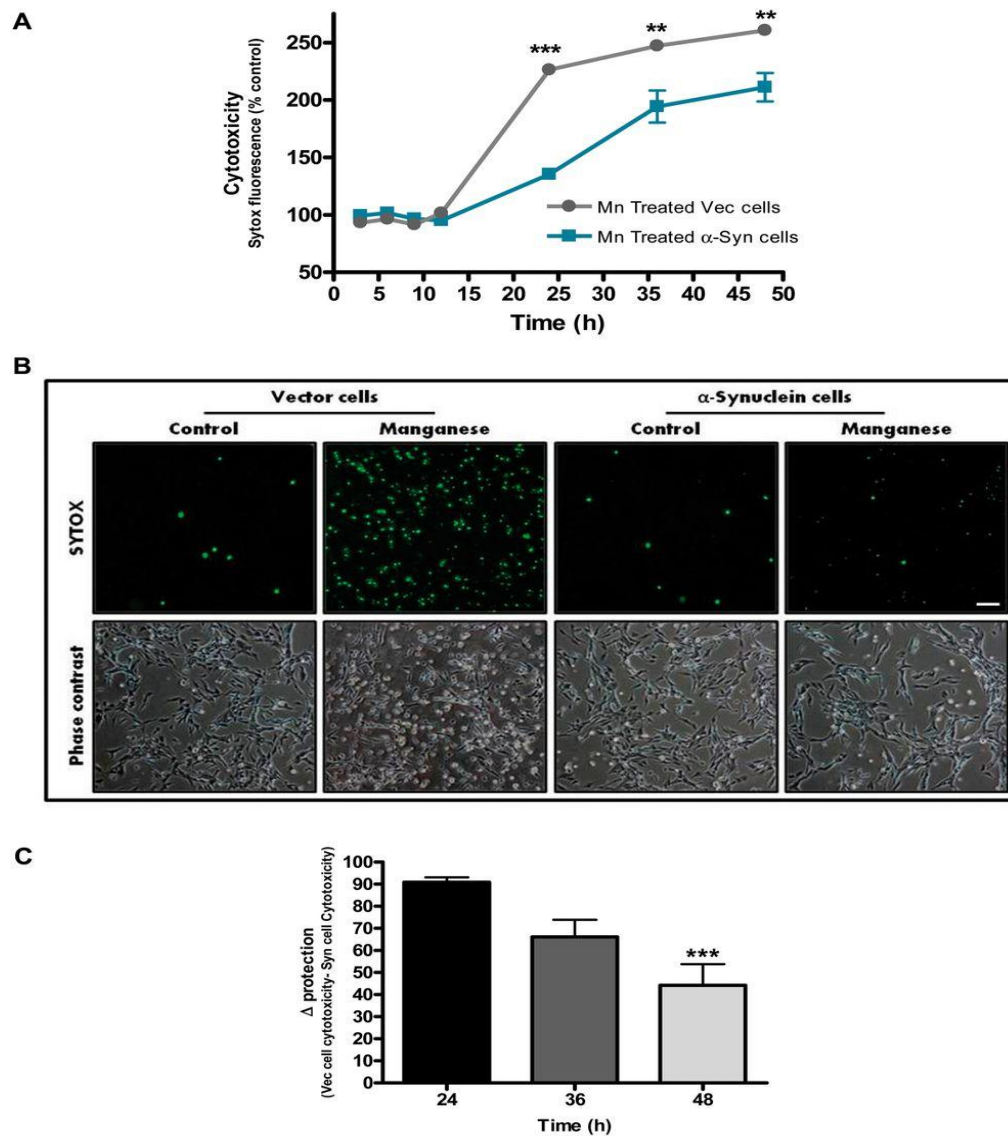
Figure 2. Human wild-type α-synuclein expression attenuates manganese-induced cytotoxicity. (A) α-Syn and Vector cells were treated with 300 μM manganese, and

neurotoxicity was assessed at various time points (3, 6, 9, 12, 24 and 36 h) using SYTOX Green cytotoxicity assays. Cell death was expressed as a percentage of the time-matched control groups. Results are represented by the mean ± SEM from at least six samples in each treatment group (**p<0.01, ***p<0.001). (B) *In situ* measurement of cell death by SYTOX Green dye during Mn exposure. Alpha-Syn and vector cells were treated with 300 μM manganese for 24 h. After treatment, SYTOX Green-positive cells were viewed via fluorescence microscopy. Phase-contrast (lower panels) and Sytox FITC fluorescence (upper panels) images were captured on random fields to compare cell death between manganese -treated α-Syn and vector cells. Magnification, 20 X. Scale bar, 50 μm. (C) Determination of change in percent protection (Δ protection) as determined by subtracting the percentage of cell death of α-Syn cells from the percentage of cell death of Vec cells at 24, 36 and 48-h time points (***p < 0.001 vs 24-h time point).
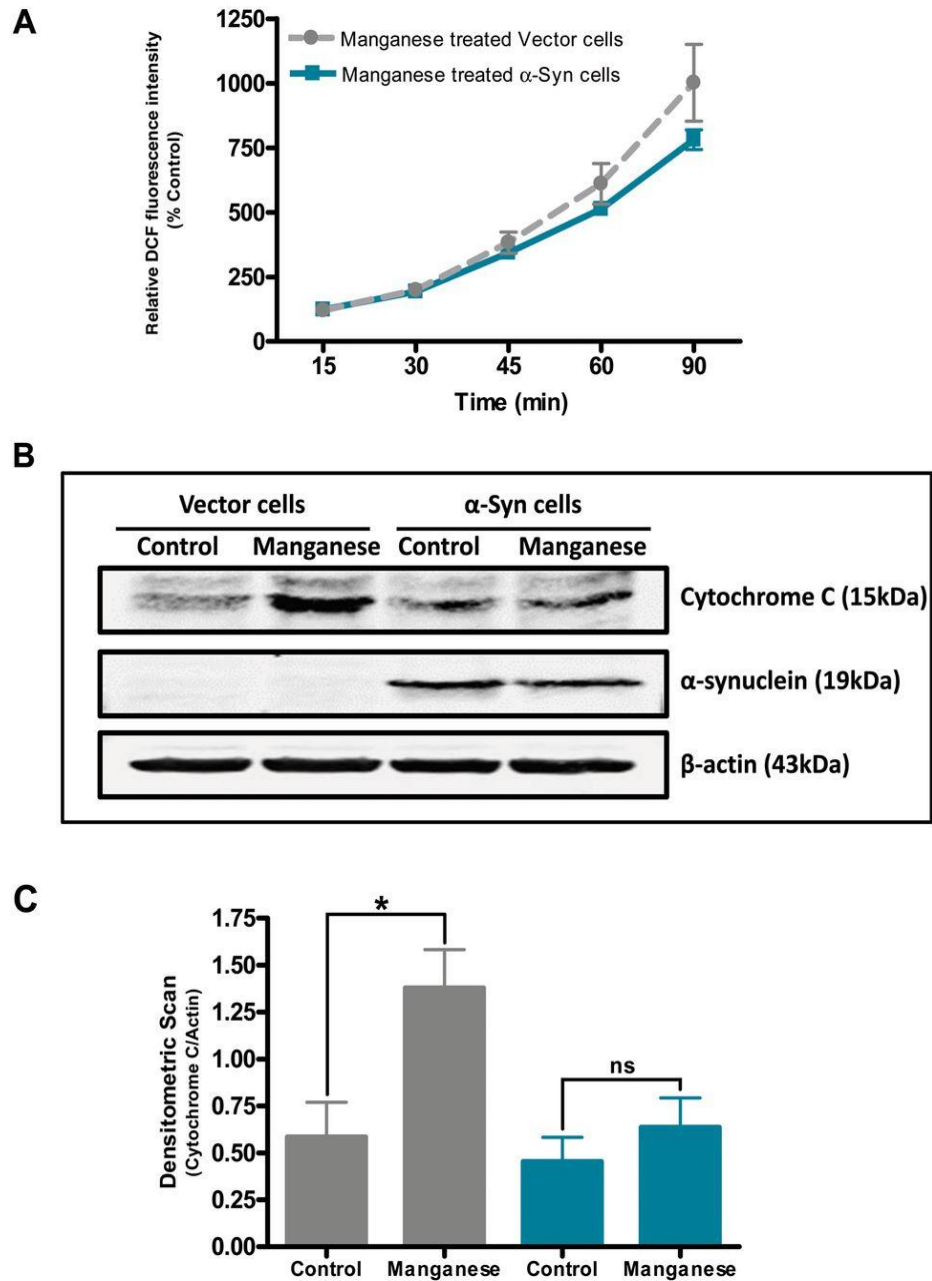
Figure 3. Effect of α-synuclein expression on oxidative stress induced by manganese exposure and attenuation of manganese-induced cytochrome c release. (A) Manganese induced a time-dependent ROS generation in α-Syn and vector cells. The measurements were conducted in a 96-well plate containing the α-Syn and Vec cells

exposed to 300 μM manganese for up to 90 min. ROS generation was measured at 15, 30, 45, 60 and 90-min time points during manganese treatment in HBSS, co-treated with 10 μM H2DCF-DA reagent. Both α-Syn and vector cells generated ROS in a time-dependent manner and ROS generation did not differ significantly between α-Syn and Vec cells. (B) Mitochondrial release of cytochrome c in manganese-treated α-Syn and Vec cells. The cells were treated with 300 μM manganese for 6 h, cytosolic fractions were isolated, and cytochrome c was measured by Western blot. To confirm equal protein-loading in each lane, the membranes were reprobed with β-actin antibody. (C) Quantification of cytosolic cytochrome c band intensities reveals a reduced release of mitochondrial cytochrome c in α-Syn-expressing cells when compared to vector-treated cells. Each group represented by the mean ± SEM from at least four separate measurements (*$p < 0.05$ vs control).
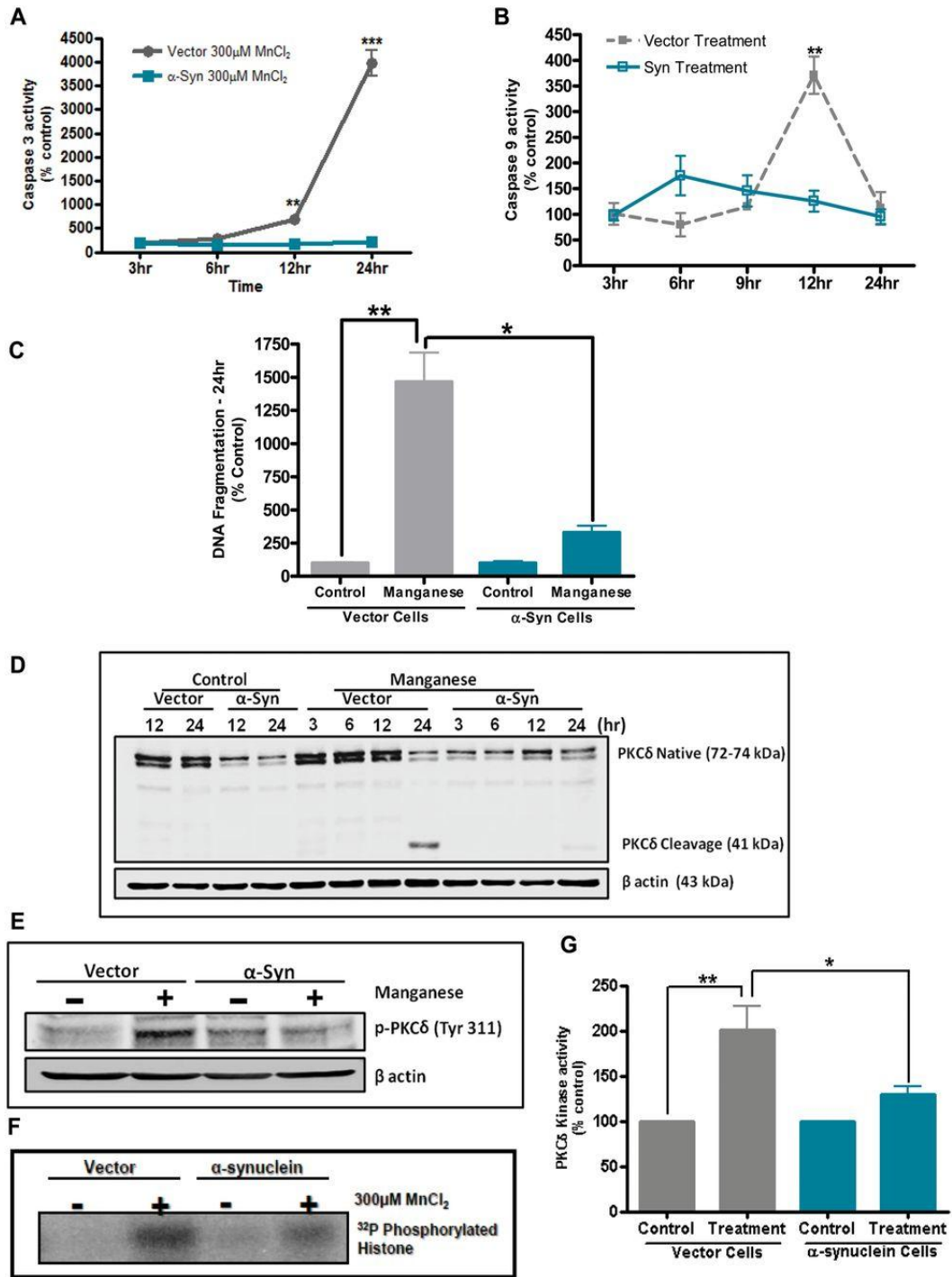
Figure 4. Suppression of manganese-induced caspase-9 and caspase-3 activations, PKCδ proteolytic activation and DNA fragmentation. Exposure to 300 μM manganese induced (A) caspase-3 and (B) caspase-9 enzyme activities up to 24 h in a

time-dependent manner in Vec cells compared to α-Syn cells. Caspase-9 activation precedes caspase-3 activation, peaking at 12 h or later. Results represented as mean ± SEM from at least six samples in each treatment group (** $p<0.01$, and *** $p<0.001$). (C) Quantitative analysis of DNA fragmentation by ELISA after treating α-Syn and Vec cells with 300 μM manganese for periods of 24 h. Data represented as mean ± SEM from three separate observations, and * $p < 0.05$ or ** $p < 0.01$ represents significant differences between the Vec and α-Syn cells treated with 300 μM manganese, or between Vec-treated and Vec-untreated control cells. (D) A time-dependent increase of PKCδ proteolytic cleavage was observed over 24 h in vector control cells treated with 300 μM manganese, whereas similarly treated α-Syn cells showed minimal amounts of PKCδ proteolytic cleavage. (E) Western blot analysis of PKCδ phosphorylation (Tyr311) after manganese insult. (F-G) PKCδ *in vitro* kinase activities 24 h after 300 μM manganese treatment. To confirm equal protein-loading in each lane, the membranes were reprobed with β-actin antibody. Results were compiled from at least three individual experiments.
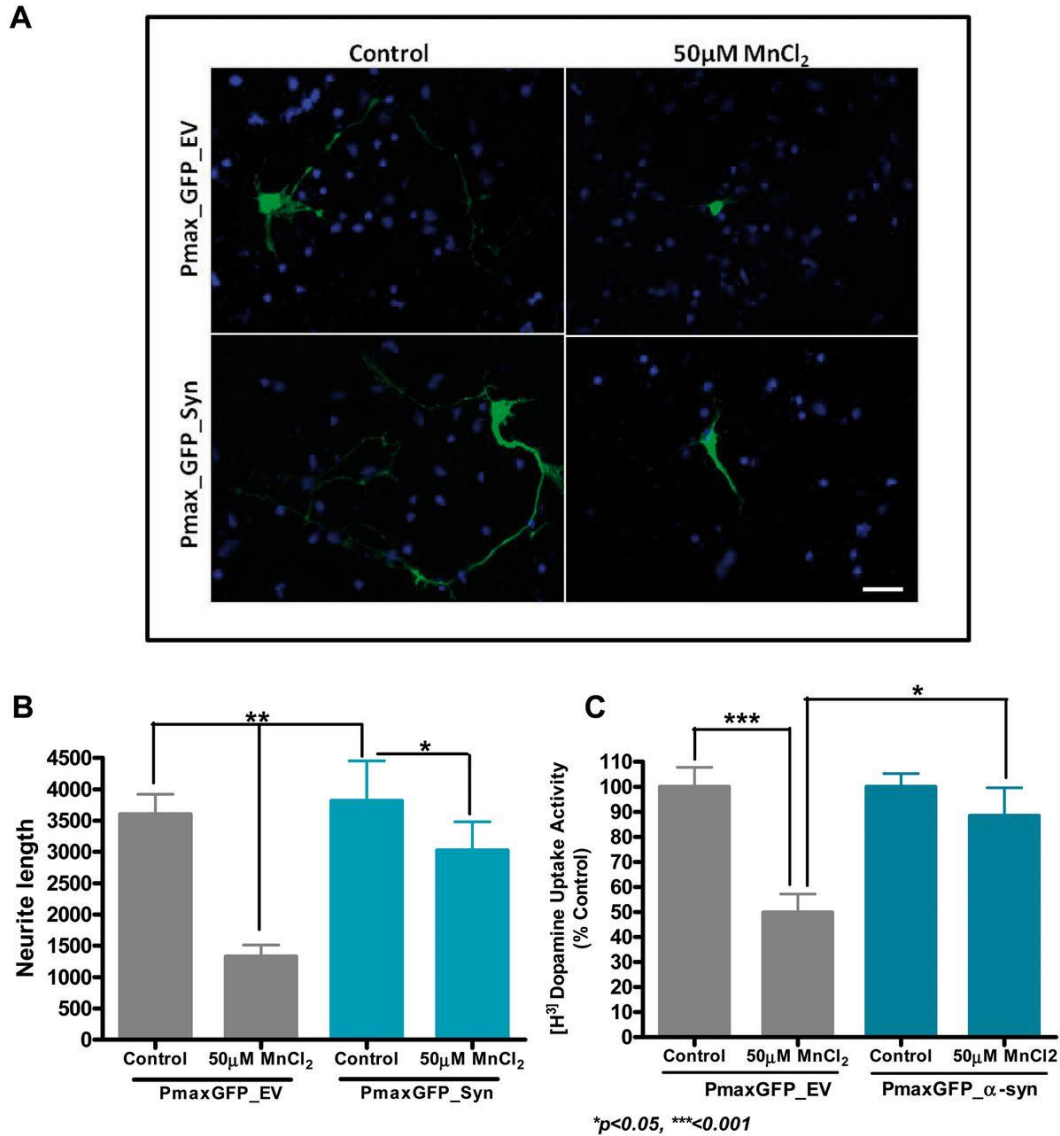
Figure 5. Neuroprotective effect of α-synuclein in manganese-induced dopaminergic degeneration in primary mesencephalic neuronal cultures. Mouse primary mesencephalic neuronal cultures were transfected with pmaxGFP_EV or pmaxGFP-α-Syn plasmids and treated with 50 μM manganese for 24 h. (A) GFP immunocytochemical analysis of neuronal morphology. Magnification, 60 X. Scale bar, 20 μm. (B) Measurements of neurite length as an indication of α-Syn neuroprotection. (C) Neuronal

CHAfunction after manganese treatment was assessed by dopamine uptake assay. Each group represented as mean ± SEM from at least 10 measurements from two separate experiments (* p < 0.05 ,** p < 0.01 and , *** p < 0.001).
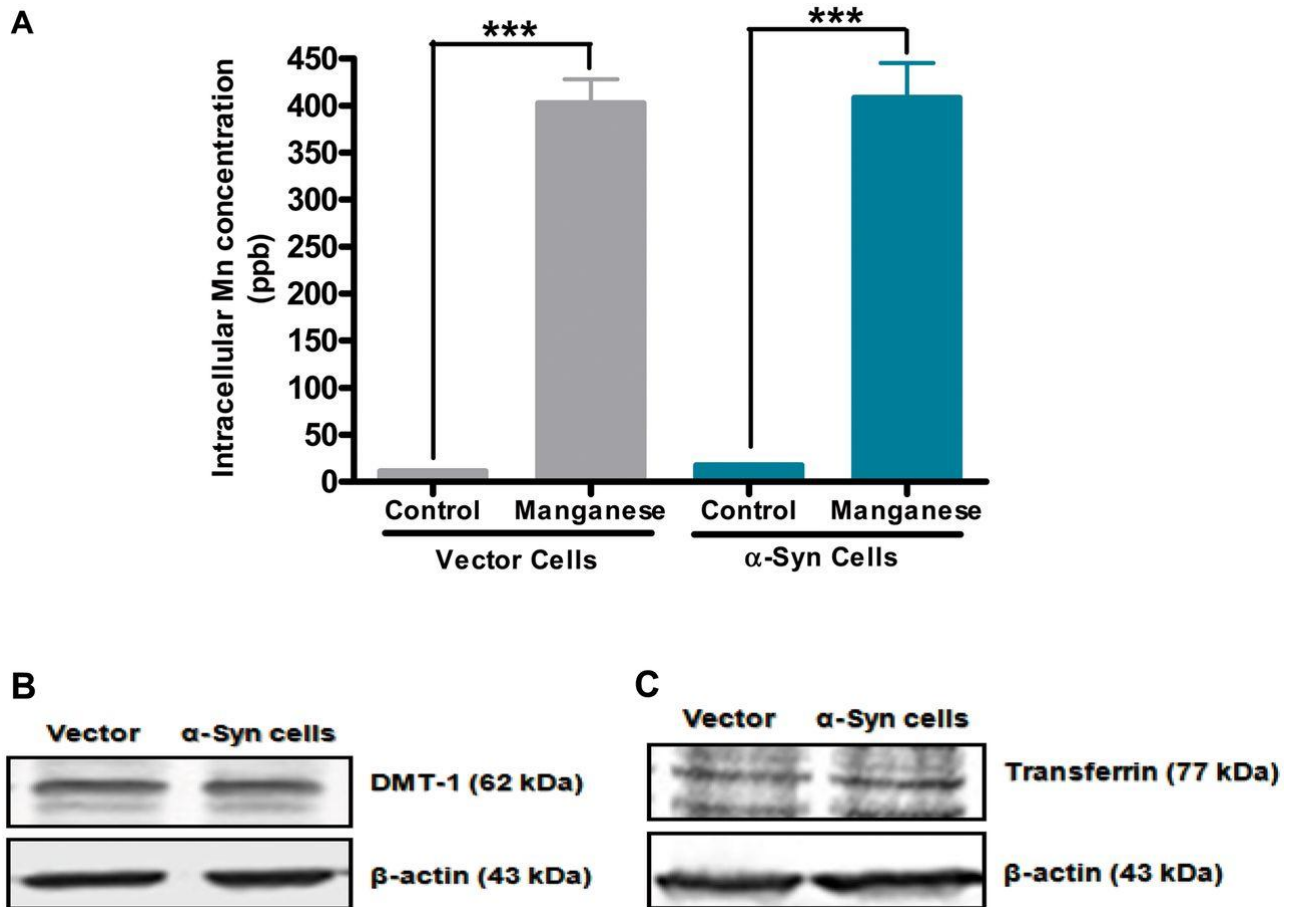
Figure 6. Determination of intracellular manganese concentration and expression of major ion regulatory transporters in the cells. (A) Cells were treated with 300 μM manganese for 24 h, and then intracellular manganese concentrations were measured using ICP-MS assays. Each group represented as mean ± SEM from at least three ICP-MS measurements. (B-C) Representative images of Western blot analysis of divalent metal ion transporter (DMT1) and Transferrin (Tf) protein expression.
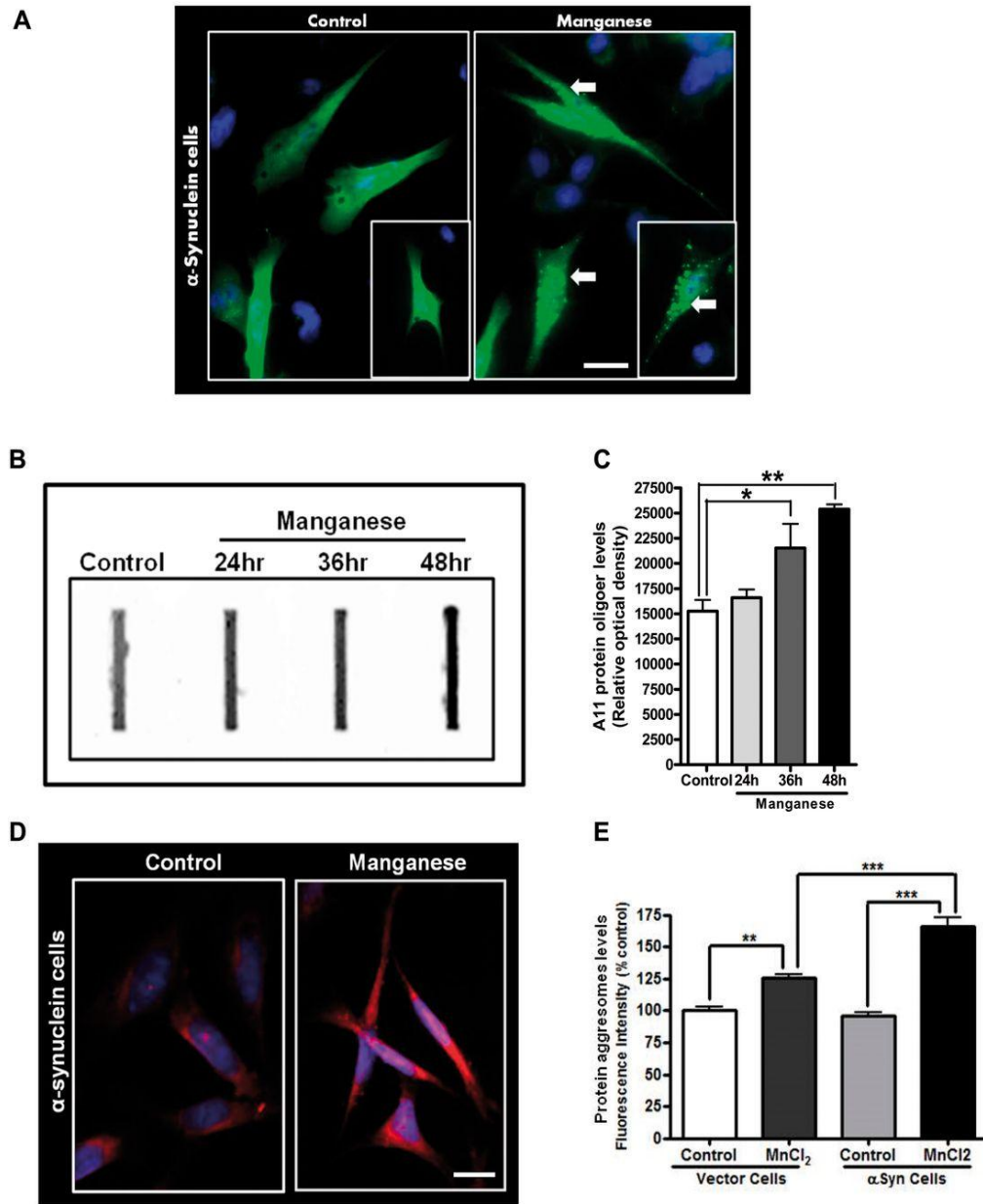
Figure 7. Prolonged manganese exposure induces α-synuclein aggregation.

(A) Immunocytochemical analysis of α-Syn immunoreactive aggregates after exposure to 300 μM manganese for 36 h or more. Magnification, 60 X. Scale bar, 20 μm. (B) Representative slot blot analysis with the oligomeric protein specific antibody (A11), indicating a time-dependent accumulation of the misfolded protein after manganese exposure. (C) Quantification of slot blot band intensities reveals a time-dependent

accumulation of aggregated protein in α-Syn-expressing cells. Each group represented by the mean ± SEM from at least four separate measurements (*p < 0.05 vs control, **p < 0.01 vs control). (D) Representative fluorescence images of aggresome dye after exposing α-Syn cells to manganese. (E) Quantification of fluorescence intensities after manganese exposure in α-Syn and Vec cells. Magnification, 60 X. Scale bar, 20 μm. Data obtained from the ProteoStat inclusion assay kit. Each group represented as mean ± SEM from at least eight measurements.

CHAPTER III

THE ENVIRONMENTAL NEUROTOXICANT MANGANESE PROMOTES PRION-LIKE CELL-TO-CELL TRANSMISSION OF α-SYNUCLEIN VIA EXOSOMES IN CELL CULTURE AND ANIMAL MODELS OF PARKINSONISM

A manuscript to be submitted to *Nature Communication*

Dilshan S. Harischandra[1], Matthew L. Neal[1#], Dharmin Rokad[1#], Shivani Ghaisas[1], Sireesha Manne[1], Nikhil Panicker[1], Gary Zenitsky[1], Huajun Jin[1], Mechelle Lewis[2], Xuemei Huang[2], Arthi Kanthasamy[1], Vellareddy Anantharam[1], Anumantha G. Kanthasamy[1‡]

[1]Parkinson Disorders Research Program, Iowa Center for Advanced Neurotoxicology, Department of Biomedical Sciences, Iowa State University, Ames, IA 50011.

[2]Departments of Neurology and Pharmacology, Pennsylvania State University-Milton S. Hershey Medical Center, Hershey, PA 17033

[#] These authors contributed equally to this work.

[‡] To whom correspondence should be addressed: Parkinson Disorders Research Laboratory, Department of Biomedical Sciences, 2062 Veterinary Medicine Building, Iowa State University, Ames, IA, 50011. Tel.: (515) 294-2516, Fax: (515) 294-2315, E-mail akanthas@iastate.edu

Abstract

The aggregation of α-synuclein (αSyn) is considered a key pathophysiological feature of a group of neurodegenerative disorders such as Parkinson's disease (PD), multiple system atrophy (MSA), and diffuse Lewy body disease, which collectively are termed synucleinopathies. Recent studies also suggest that a prion-like cell-to-cell transfer of misfolded αSyn contributes to the spreading of αSyn pathology in MSA. The biological mechanisms underlying the propagation of the disease with respect to environmental neurotoxic chemical exposures, however, are not well understood. Considering the role of the divalent metal manganese (Mn) in synucleinopathy-related neurological disorders, we characterized its effect on αSyn misfolding and transmission in experimental parkinsonian models. Using dopaminergic cell line stably expressing wild-type human αSyn, we have shown that αSyn secreted into extracellular media following Mn exposure through exosomes. In functional studies, we demonstrated that exosomes released during Mn treatment can e*ndocytosis via caveolae* to microglial cells and induce neuroinflammatory responses microglial cultures and neurodegeneration in differentiated human dopaminergic cells (LUHMES) through the activation of caspase-3 signaling. Furthermore, using the *BiFC* assay we have shown that Mn elevates α-syn cell-to-cell transmission and results in dopaminergic neurotoxicity in a mouse model of Mn neurotoxicity. Interestingly, we also reported that welders exposed to Mn have higher misfolded αSyn content in their serum exosomes and showed for the first time that stereotaxic delivery of αSyn-containing exosomes isolated from Mn-treated αSyn-expressing cells into the striatum can initiate parkinsonian-like pathological features in mice. Collectively, these results demonstrate that Mn exposure promotes αSyn secretion

via exosomal vesicles, which subsequently evoke pro-inflammatory and neurodegenerative responses in both cell culture and animal models.

Keywords: Manganese (Mn), α-synuclein, exosome, protein aggregation, prion-like

Introduction

There are a number of neurodegenerative diseases marked by the presence of cytoplasmic inclusions called Lewy bodies and neurites composed of α-synuclein (αSyn) and ubiquitin. Together, they constitute synucleinopathy-related disorders. Among them, Parkinson's disease is the most common, marked by motor dysfunction and progressive degeneration of dopaminergic neurons projecting from the substantia nigra pars compacta (SNpc) to the striatum and the presence of Lewy bodies in dopaminergic neurons. Multiple system atrophy (MSA) and diffuse Lewy body disease (DLB) also belong to this group of disorders, with Lewy bodies found primarily in glial cells of the basal ganglia in MSA and in more diffuse areas of the cortex in DLB. While the physiological functions of αSyn are poorly understood, evidence suggests that the accumulation of aberrant αSyn species exerts intracellular toxic effects in the central nervous system (CNS). The idea that αSyn can pathologically propagate throughout the CNS recently gained much attention with the finding of αSyn species in human plasma and CSF (El-Agnaf et al., 2003; Kordower et al., 2008) and host-to-graft propagation of αSyn-positive Lewy bodies in fetal ventral mesencephalic and embryonic nigral neurons transplanted in human PD patients (Kordower et al., 2008; Li et al., 2008). In agreement to this, recent studies have suggested that transcellular transmission of αSyn aggregates is associated with the

progression of PD (Bae et al., 2014; Danzer et al., 2012; Lee et al., 2010) and MSA (Prusiner et al., 2015).

Growing evidence indicates that extracellular αSyn induces pathogenic actions by activating neuroinflammatory and neurodegenerative responses *in vitro*(Emmanouilidou et al., 2010; Su et al., 2008). The nature of the secretory mechanisms of αSyn remains elusive; however, recent studies have shown that neurons can secrete αSyn into the extracellular milieu via a brefeldin A-insensitive pathway involving exosome vesicles (Danzer et al., 2012; Lee et al., 2005). Exosomes are nano-scale vesicles generated within the endosomal system and secreted upon fusion of multivesicular bodies with the plasma membrane. Originally exosomes were thought to be molecular "trash bags". However, it was recently discovered that exosomes contain miRNAs and proteins and mediate cell-to-cell communications, which could potentially lead to therapeutic and biomarker discoveries.

Moreover, emerging evidence from many neurodegenerative disorders including synucleinopathy-related disorders now has expanded the notion of cell-to-cell transmission of misfolded proteins as a common mechanism for the onset and progression of the disease (Luk et al., 2012a; Luk et al., 2009; Volpicelli-Daley et al., 2014; Volpicelli-Daley et al., 2011). Although the exact mechanisms for protein aggregate spreading in the CNS still largely remain unknown, several models including exocytosis, cell injury, receptor-mediated endocytosis, tunneling nanotubes, and exosomal transmission have been proposed(Lee et al., 2010). Although genetic

predisposition is an important risk factor in many familial cases of parkinsonian syndromes, environmental exposure to certain metals, herbicides, or insecticides augments the susceptibility to mitochondrial dysfunction and the progressive nature of these diseases. Specifically, divalent metal Mn is used widely in consumer and agricultural products. In trace amounts, Mn is essential for human health, but environmental exposure to high doses of Mn results in manganism, a neurodegenerative movement disorder sharing many parkinsonian features although it may not represent clinical PD because of the lack of the classic response to levodopa (Koller et al., 2004) . Yet, despite its prevalence and thus potential risk to human health and the development of neurodegenerative disorders, the mechanisms by which Mn exerts its neurotoxic effects and its role in the prion-like propagation of αSyn aggregates are not well studied thus far.

Hence, in this study we assess the effects of Mn as an environmental factor on αSyn aggregation, secretion, and cell-to-cell transmission. To elucidate the mechanism of Mn-induced αSyn release, we followed a systematic approach from *in vitro* to *ex vivo* to *in vivo* experimental models to better understand the role of exosomes in cell-to-cell transmission of misfolded αSyn protein. We show that Mn exposure promotes the extracellular secretion of αSyn via exosomal vesicles, which subsequently evoke pro-inflammatory and neurodegenerative responses in both cell culture and animal models.

Materials and Methods

Chemicals and Reagents

All chemicals were purchased from Sigma-Aldrich and reagents related to cell cultures were obtained from Invitrogen unless otherwise specified.

Cell cultures and stable expression of αSyn

For αSyn release and exosome isolation experiments, we created a GFP-tagged αSyn stably-expressing MN9D dopaminergic cell line. Expression plasmids encoding human full-length αSyn-pMAXGFP and control pMAXGFP (Lonza) were transfected into MN9D cells using Lipofectamine 2000 reagent and grown in DMEM (D5648; Sigma) supplemented with 50 IU/ml penicillin, 50 μg/ml streptomycin, and 10% fetal bovine serum (FBS). For stable transfection, MN9D cells were selected after culturing in 400 μg/ml of geneticin for one week post-transfection and then maintained in media supplemented with 200 μg/ml of geneticin. GFP-positive αSyn-expressing (MN9D_Syn$_{GFP}$) and vector control (MN9D_EV$_{GFP}$) cells were selected further by FACSAria III (BD Bioscience) high-speed sorting flow cytometer to obtain homogeneously transgene-expressing cell populations.

Primary murine microglial cells were isolated from primary mixed cultures prepared from C57BL/6 mouse pups, postnatal days P0 to P1, using a column-free magnetic separation method as previously described (Gordon et al., 2011). Exosome-induced neurodegeneration experiments were carried out with primary mesencephalic cultures and differentiated Lund human mesencephalic (LUHMES) cells. Primary mesencephalic

neuronal cultures and LUHMES cells were grown and differentiated as previously described (Ay et al., 2015; Jin et al., 2014; Scholz et al., 2011).

The immortalized wild-type (C57BL/6) murine microglial cell (WTMC) line with morphology and surface marker expression highly similar to primary murine microglia was a kind gift from Dr. Douglas Golenbock at the University of Massachusetts Medical School, Worcester, MA (Halle et al., 2008). These cells were grown in DMEM medium supplemented with 50 IU/ml penicillin, 50 μg/ml streptomycin, and 10% fetal bovine serum (FBS) and exosome stimulation done in 2% DMEM. WTMC used for exosome-induced neuroinflammation experiments and generation of Caveolin-1 and Clathrin knockdown cells using the CRISPR/Cas9 nuclease RNA-guided genome editing system. The lentivirus-based CRISPR/Cas9 KO plasmids, pLV-U6g-EPCG-Cav1 and pLV-U6g-EPCG-Cltc with the Caveolin-1 and Clathrin gRNA target sequences GTTGAGATGCTTGGGGTCGCGG and TACTGAAGCCAATGTTTGCTGG, respectively, were purchased from Sigma-Aldrich. To make lentivirus, the lenti-CRISPR/Cas9 Cav1 and C1tc KO plasmids and control plasmid were transfected into 293FT cells using the Mission Lentiviral Packaging Mix from Sigma-Aldrich according to manufacturer's instructions. The lentivirus was harvested 48 h post-transfection and added to the microglial cell line at an MOI of 100 to knockdown Caveolin-1 and Clathrin expression.

MTT assays

The 3-(4,5-dimethylthiazol-3-yl)-2,5-diphenyl tetrazolium bromide (MTT) assay has been widely used to assess the median lethal dose (LC_{50}) and cell viability by measuring

mitochondrial dehydrogenase enzymes that cleave the tetrazolium ring to produce formazan (Latchoumycandane et al., 2005). In this study, we used the MTT assay to determine the LC_{50} of Mn for MN9D cells. Briefly, 20,000 MN9D cells were seeded on a 96-well microplate, allowed to adhere for 16 h, and then treated for 24 h with Mn (0 to 10 mM) in serum-free DMEM media. Following the treatment, the cells were washed with warm PBS and then incubated with 200 μl 0.25% (w/v) MTT in serum-free DMEM for 2 h at 37 °C. The supernatant was removed and MTT crystals were solubilized in 200 μl dimethyl sulfoxide (DMSO). Mitochondrial activity was measured with the SpectraMax spectrophotometer (Molecular Devices Corporation) at 570 nm with the reference wavelength at 630 nm.

Western and Slot blotting

Whole cell lysates or exosome lysates were prepared using modified RIPA buffer containing protease and phosphatase inhibitor cocktail (Thermo Scientific, Waltham, MA), as described previously (Harischandra et al., 2015; Harischandra et al., 2014). For αSyn release experiments, MN9D_Syn$_{GFP}$ and MN9D_EV$_{GFP}$ cells were treated in serum-free medium and spiked with 10μg/ml BSA, and then the media was collected and centrifuged for 5 min at 3000 x g to remove any dislodged cells or cell debris. The conditioned media were concentrated using 5000 MWCO Vivaspin-20 spin columns (GE Lifescience), and then protein concentrations were determined with the Bradford protein assay kit (Bio-Rad). Cell lysates containing equal amounts of protein were separated on a 12-15% SDS-polyacrylamide gel. After separation, proteins were electro-blotted onto a nitrocellulose membrane and nonspecific binding sites were blocked by treating with LI-

COR blocking buffer. Primary antibodies for Syn-1 (BD Bioscience), Flotillin-1 (BD Bioscience), BSA (Invitrogen), LDHA (Cell Signalling), Aip1/Alix (Millipore), IBA-1 (Wako), iNOS (Santa Cruz), and β-actin (Sigma) were used to blot the membranes.

The formation of oligomeric proteins following Mn exposure was analyzed with a slot blot apparatus (Bio-Dot, Bio-Rad) using the antibody against protein Oligomers (A11) (Invitrogen). Following protein adsorption, membranes were blocked with 5% BSA and incubated overnight with the A11 antibody. Membranes then were developed with IR800-conjugated anti-rabbit or Alexa Fluor 680-conjugated anti-mouse secondary antibody for 1 h at room temperature. Western and slot blot images were captured with the Odyssey IR Imaging system (LI-COR) and data were analyzed using Odyssey 2.0 software.

Immunocytochemistry and Immunohistochemistry

For immunocytochemistry, MN9D cells and microglia cells were plated on 50 μg/mL poly-D-lysine-coated 12-mm glass coverslips and treatments were done as described. LUHMES cells were plated on coverslips pre-coated with 50 μg/mL poly-l-ornithine (Sigma-Aldrich) overnight, washed twice with cell culture grade water (Invitrogen) and then incubated with 1 μg/mL fibronectin (Sigma-Aldrich) overnight. After treatments, cells were washed with PBS and incubated in 4% paraformaldehyde for 30 min at room temperature. After fixing, the cells were washed with PBS and incubated in blocking agent (2% BSA, 0.05% Tween-20, and 0.5% Triton X-100 in PBS) for 45 min. Cells then were incubated with antibodies against human αSyn (Syn 211; Santa Cruz, 1:500), GFP (Abcam 1:2000), and IBA-1 (Wako, 1:500) overnight at 4°C or the cytoskeleton marker

Phalloidin (Alexa Fluor 647 phalloidin, Invitrogen) for 30 min at room temperature. After primary incubation, the cells were washed and incubated in the dark for 90 min with Alexa-488 and -555 dye-conjugated secondary antibodies (Invitrogen, 1:1000). Hoechst 44432 was used as a nuclear stain and the coverslips were then mounted on glass slides and viewed with $63\times$ and $43\times$ oil objectives using a Leica DMIRE2 confocal microscope. *Photomicrographs were further processed using* Imaris software to analyze the Z-stack images for exosome internalization. Using 3D surface reconstruction, we generated surface topology images using the maximum intensity projection (MIP) image.

For immunohistochemistry studies, fixed brains embedded in *optimal cutting temperature* (*OCT*) compound were sectioned at 30 μm using a Cryostat (CryoStar NX70, Thermo Scientific). Free-floating sections were processed for immunohistochemical analysis as described in our previous publications (Ghosh et al., 2013; Panicker et al., 2015) using antibodies against tyrosine hydroxylase (TH) (clone LNC1; Millipore, 1:1200). Diaminobenzidine (DAB) immunostaining was performed on substantia nigra sections as described previously (Ghosh et al., 2010; Ghosh et al., 2013; Panicker et al., 2015) for stereologically counting of TH+ neurons. Briefly, 30-μm sections were incubated with anti-TH antibody (clone LNC1; Millipore, 1:1200) overnight at 4°C. Then sections were incubated with biotinylated anti-rabbit secondary antibody (1:300, Vector Labs) for 1 h at room temperature followed by incubation with avidin peroxidase (Vectastain ABC Elite kit, Burlingame, CA). Immunolabeling was visualized by exposure to 0.5 mg/ml 3,3′ diaminobenzidine (DAB), 2.5 mg/ml nickel ammonium sulfate and 0.03% H_2O_2 followed by incubation with hematoxylin nuclear counterstain (Vector Hematoxylin QS, H-3404). Sections were mounted on charged glass slides, dehydrated to xylene and coverslipped

with DPX mounting medium (Sigma, Cat# 44581). Total numbers of TH-stained neurons in the SN were counted stereologically with Stereo Investigator software (MicroBrightField, Inc., Williston, VT) using an optical fractionator. For pS129 αSyn studies, 7-μm thick paraffin-embedded sections of mouse tissues were deparaffinized and subjected to antigen retrieval using formic acid treatment followed by 0.05% trypsin treatment. Sections were then incubated with blocking reagent (10% normal goat serum, 2% BSA, and 0.5% Triton X-100 in PBS) for 60 min before being incubated with mouse monoclonal antibody against S129-phosphorylated human αSyn (Clone No. pSyn #64, Wako, 1:2000).

Exosome isolation

Cell-produced exosomes were isolated using the ExoQuickTC (System Biosciences) exosome precipitation reagent or were purified by differential ultracentrifugation via slight modification of a process described by Emmanouilidou and collegues {Emmanouilidou, 2010 #7} . Briefly, MN9D_Syn$_{GFP}$ and MN9D_EV$_{GFP}$ cells at 70-80% confluency were treated with or without 300 μM Mn in exosome-depleted medium containing 10% FBS for 24 h. After treatment, cell culture supernatant was collected and spun at 300 x g for 10 min to remove cells and 10,000 x g for 15 min to exclude cell debris from the supernatant. The resulting media then was passed through a 0.2-μm syringe filter (Millipore) to remove any remaining particles or cell debris, and the filtrate was centrifuged at 100,000 x g for 90 min using a Beckman Optima L-100 XP ultracentrifuge. The pellet containing exosomes was washed once with cold PBS and centrifuged again at 100,000 x g for 90 min using a Beckman optima MAX

ultracentrifuge. Exosome pellets were resuspended in 50 μl of RIPA buffer for Western blot analysis, or when treating primary microglia cells, they were resuspended in 150 μl of DMEM-F12. Total serum exosomes from control and welder subjects were isolated using ExoQuick (System Biosciences) reagent following the manufactures' recommended protocol.

Nitric oxide and cytokine detection in microglia

Quantification of nitric oxide production by microglia cells upon exosome treatment was measured indirectly by quantification of nitrite in the supernatant using the Griess reagent (Sigma Aldrich). Microglia plated at 70,000 cells/well were treated for 24 h with exosomes (1:100) or pretreated with endocytosis inhibitors for one hour and co-treated with exosomes for 24 h. At the end of the treatment, equal volumes of cell media and Griess reagent were added to a 96-well plate along with a sodium nitrite standard curve, and absorbance at 540nm was measured on SpectraMax microplate reader. The supernatant was used to determine extracellular cytokine levels using the Luminex bead-based immunoassay system and recombinant standards for IL-6, IL-12, IL-10, TNF-α, and IL-1β (Gordon et al., 2011).

Nanoparticle tracking analysis (NTA)

Ultracentrifuged or ExoQuick/TC-precipitated exosome samples were used for NTA, as previously described (Soo et al., 2012). Briefly, isolated exosomes were resuspended in 500-1000 μL PBS, from which approximately 300 μL was loaded into the sample chamber of an LM10 unit (Nanosight, Amesbury, UK) using a disposable syringe. Sample durations of 30-60 sec per sample were analyzed with NTA 2.3 software

(Nanosight). Samples containing higher numbers of exosomes were diluted before the analysis and their relative concentrations then were calculated according to the dilution factor.

Transmission electron microscopy (TEM)

Purified exosomes were resuspended in 200 µl PBS, 20 µL of each sample was mixed with uranyl acetate 2% (w/v) and incubated for 5 min, and then 5 µl were applied to carbon-coated copper grids. Images were taken using a JEOL 2100 200 kV scanning and transmission electron microscope (STEM) with a Thermo Fisher Noran System 6 elemental analysis system. TEM was operated at 80 kV and images were obtained at 18000-20000 x magnification.

Quantification of αSyn in exosomes

Concentrations of αSyn in cell-derived exosomes and human exosomes isolated from serum were determined by using human αSyn ELISA kits (Invitrogen, Cat# KHB0061 and Covance, Cat# SIG-38974), as previously described (Wennstrom et al., 2012). Briefly, exosomes were isolated using ultracentrifugation or by ExoQuick reagent and lysed using RIPA buffer following manufacturer's instructions.

Small RNA isolation and characterization

For detection of RNA species in exosome samples isolated from Mn- and vehicle-stimulated MN9D_Syn$_{GFP}$ and MN9D_EV$_{GFP}$ cells, we used the mirVana (Invitrogen, Cat# KHB0061) miRNA and small RNA isolation kit according to the manufacturer's protocol. The quality, yield, and size of exosomal small RNAs were analyzed using the

Agilent 2100 Bioanalyzer (Agilent Technologies, Foster City, CA) with the Agilent RNA 6000 Nano kit as described previously (Zamanian et al., 2015).

Alpha-synuclein fibril formation assays

For the αSyn amyloid *fibrillization assay*, purified recombinant non-aggregated human αSyn was used as a substrate and exosomes isolated from welder and control serum samples were used as a seed. The assay also consisted of blank (PBS) wells as a negative control and exogenously produced recombinant αSyn fibrils as a positive control. Each sample was run in 4 replicates and the representative graph shown for welders and controls consists of average fluorescence from all the welders and controls with 4 replicates for each sample. The αSyn *fibrillization assay* was performed in a 100 μl reaction mixture consisting of 5 μl of 100-fold diluted serum exosomes in 0.05% SDS in PBS, 0.2 mg/ml recombinant αSyn, 300 mM NaCl, 10 μM EDTA, and 20 μM Thioflavin-T in a BMG Clariostar plate reader using Nunc™ MicroWell™ 96-well optical-bottom plates. The reaction was carried out at 37°C with alternate cycles of shake and rest every other minute and readings were taken every 30 minutes for a 60-hour period.

Animal studies

Male C57BL/6 mice (8- to 12-week-old) were purchased from Charles River Laboratories and used for all mouse experiments. Human αSyn A53T overexpressing rats (model number 10680) and non-carrier littermate control *Sprague Dawley* rats were obtained from Taconic Biosciences (Germantown, NY). Rodents were housed on a 12-h light/dark cycle with *ad libitum* access to food and water. Iowa State University's (ISU)

laboratory animal facility is fully accredited by the Association for Assessment and Accreditation of Laboratory Animal Care (AAALAC), and all procedures involving animal handling were approved by the Institutional Animal Care and Use Committee (IACUC) at ISU. For unilateral viral transduction experiments, we injected a total volume of 2 µl of virus at a rate of 0.2 µl/min using a 10-µl Hamilton syringe with a 30-gauge needle, which was guided using the Angle 2 stereotaxic apparatus (Leica Biosystems, St. Louis, MO) to target the SN with the use of the following coordinates: AP -3.30, ML -1.20 and DV -4.60 (mm from bregma). For co-transduction of AAV_V1S and AAV_SV2 viruses, 1 µl of pAAV-CBA-Venus1-Synuclein-WPRE (AAV_V1S) virus (titer 8.3 x 10^{12} viral genome/ml) and 1 µl of pAAV-CBA-Synuclein-Venus2-WPRE (AAV_SV2) virus (titer 8.7 x 10^{12} viral genome/ml) were injected. For the venusYFP transduction group, 2 µl of pAAV-CBA-Venus virus (titer 1 x 10^{12} viral genome/ml) was injected. Four weeks post-injection, the AAV_V1S/AAV_SV2 co-transduction group received either 15 mg/kg body weight/day Mn (as $MnCl_2$) for 30 days or an equal volume of vehicle (water) via oral gavage to assess the impact of environmental Mn exposure on αSyn cell-to-cell transmission. To control for the unintended effect of stereotaxic injections on animals, we also included a group of animals receiving 15 mg/kg Mn or an equal volume of vehicle similar to the AAV co-transduction group but without stereotaxic injection. To evaluate the effect of Mn on serum exosomes numbers, human αSyn A53T overexpressing and non-transgenic rats were exposed to a similar Mn treatment paradigm as in mice studies. This Mn dose regimen was chosen based on previous studies in humans and animals (Crossgrove and Zheng, 2004; Li et al., 2006; Zheng et al., 2000).

For stereotaxic delivery of exosomes to the striatum, we injected a total volume of 3 µl of exosomes (3.6 x 10^5 particle numbers) isolated from Mn- or vehicle-stimulated MN9D_SynGFP and MN9D_EVGFP cells. Twelve weeks post-injection, animals were subjected to a battery of behavior tests, including an open-field test and the amphetamine-induced rotational test. Mice then were sacrificed and their tissues collected for biochemical and neurochemical analyses, or they were transcardially perfused for histological procedures.

Behavioral measurements

The exploratory locomotor activity was measured using the VersaMax open-field apparatus (Accuscan Instruments, Columbus, OH) as described previously (Ghosh et al., 2010) and the following indices were monitored for 10 min: rearing activity (labeled as vertical activity), horizontal activity, total distance traveled and total movement time. Motor coordination and motor learning were tested by measuring the latency to fall from a 3-cm diameter rod rotating at a constant 20 rpm for 20 min (Rota-rod, Accuscan Instruments). Each mouse was subjected to 5 trials separated by 5- to 7-min intervals to eliminate stress and fatigue. The rotameter test was used to assess the effects of unilateral exosome injection-induced lesions. At 90 days post-exosome injection, mice received 5 mg/kg amphetamine (D-amphetamine sulphate, Sigma) intraperitoneally. Then after 20 min, each mouse was placed in a cylindrical bowl within which amphetamine-induced ipsilateral rotation was recorded via a video-camera coupled to automated tracking software (ANY-maze, Stoelting). Rotational scores were used as an estimate of

the extent of lesions with data expressed as the average numbers of ipsilateral rotation per 20-min period.

Human studies

Eighty-one subjects were recruited initially from unions in central PA, USA, and local communities. Welders were defined as subjects who had welded at any point in their lifetime, and controls as those without history of welding. All subjects were male, answered negatively for past Parkinson's diagnosis or other neurological disorders, and were free of any obvious neurological or movement deficits using the Unified Parkinson's Disease Rating Scale-motor scores (UPDRS-III) with a threshold score of <15 (Lee et al., 2015). Written informed consent was obtained in accordance with guidelines approved by the Penn State Hershey Internal Review Board. Welders represented several different trades and industry groups (e.g., boilermakers, pipefitters, railroad welders, and a variety of different manufacturing jobs). Controls were age-matched volunteers from the same regional community with various occupations. Seven subjects either failed to complete the DTI acquisition (3 welders and 1 control) or had poor image co-registration (2 welders and 1 control). Thus, their data were excluded from the analysis resulting in 31 controls and 43 welders (Table 1).

Exposure Assessment and Blood analysis

Exposure first was assessed by the work history (WH; Lee et al., 2015) questionnaire that collected job information over the individual's working lifetime, emphasizing welding and other jobs associated with welding exposure. Responses to the WH questionnaire enabled a cumulative lifetime years welding (YrsW = years spent welding during the

subjects' life) estimate (Lee et al., 2015). An additional supplementary exposure questionnaire (SEQ; Lee et al., 2015) focused on the 90-day period prior to the MRI and determined the time spent welding, type of metal welded, and various types of welding performed. The exposure metrics derived from the SEQ were: hours welding, brazing, or soldering [HrsW = (weeks worked) * (h/week) * (fraction of time worked related directly to welding)](Lee et al., 2015) in the 90 day period preceding the MRI.

Whole blood samples were obtained by venipuncture, Samples were allowed to sit at room temperature for ~15 min, after which they were centrifuged at 4° for 20 min. The serum supernatant then was pipetted in 1 mL aliquots into 2.5 mL cryovials (manufacturer) and stored at -80° C. When preparing samples for shipment to Iowa State, samples were thawed and 200 µL of serum was pipetted into another 2.5 mL cryovial. The samples then were frozen in a -80° C freezer and packaged with a sufficient supply of dry ice to maintain their frozen status during overnight shipment.

Statistical analysis:

Data analysis was performed using Prism 4.0 software (GraphPad). Normally distributed raw data were first analyzed using one-way ANOVA, and then Tukey's post-test was performed to compare all treatment groups. Raw data not follow Gaussian distribution were analyzed with Kruskal-Wallis test followed by Dunn's multiple comparison test to compare all treatment groups. Statistically significant differences were denoted as $*p<0.05$, $**p<0.01$, and $***p<0.001$.

Results

Manganese exposure upregulates the release of αSyn into the extracellular milieu.

Growing evidence indicates that misfolded αSyn is a transmissible pathological agent responsible for the initiation and spread of parkinsonian pathology(Desplats et al., 2009; Gallegos et al., 2015; Hansen et al., 2011; Jucker and Walker, 2013; Oueslati et al., 2014; Recasens and Dehay, 2014; Visanji et al., 2013). To further investigate the effect of exposure to the neurotoxic metal Mn on αSyn transmission and the underlying molecular mechanisms, we established a human αSyn expressing dopaminergic cell line (MN9D_Syn$_{GFP}$) by stably transfecting MN9D mouse dopaminergic cells with a construct encoding amino-terminal GFP-tagged human wild-type αSyn. A control cell line (MN9D_EV$_{GFP}$) also was generated by stably transfecting a pmaxFP-Green-N control vector. As shown in Fig. 1A, immunocytochemical analyses indicate that >90% of the MN9D_Syn$_{GFP}$ cells were positive for GFP-tagged human αSyn, and that all MN9D_EV$_{GFP}$ cells were positive for GFP. Further analysis through Western blot indicates a low-level expression of endogenous αSyn in both stable cells and a strong expression of the higher molecular weight GFP-tagged αSyn in MN9D_Syn$_{GFP}$ cells (Fig. 1B).

Next, we performed MTT assays to determine the sensitivity of naïve MN9D cells to Mn. As shown in Fig. 1C, an LC50 value of 1129 μM for Mn was obtained when exposing MN9D cells to Mn for 24 h under serum-free conditions. Based on this LC$_{50}$ and previously published doses for Mn in dopaminergic neuronal cell lines (Cai et al., 2010; Latchoumycandane et al., 2005), we chose to use a non-toxic dose of 300 μM Mn for our

subsequent studies. To evaluate whether αSyn was released from the cells, we analyzed the amount of secreted αSyn in the conditioned media following Mn treatment in serum-free DMEM. The medium was collected and concentrated using *centrifugal concentrators* together with 10ug/ml (final concentration) BSA as a loading control. Mn treatment at 300 μM markedly upregulated the release of GFP-tagged αSyn into the extracellular milieu when compared to time-matched untreated cells (Fig. 1D-F). We also immunoblotted the same membranes with an antibody against LDHA, a cytosolic enzyme indicative of cellular toxicity. Our results show that the cytotoxicity following 300 μM Mn exposure was minimal in both MN9D_Syn$_{GFP}$ and MN9D_EV$_{GFP}$ cell groups, further confirming that the αSyn protein detected in the culture media resulted from the actual release of αSyn and was not due to cytotoxicity.

Manganese induces oligomeric αSyn secretion via exosomes.

To further investigate the underlying molecular mechanisms of αSyn secretion and its relevance in the progression of neurodegenerative disorders, we looked into the possible mechanisms of cargo used in αSyn secretion. For this, we analyzed the conditioned media collected from Mn- or vehicle-treated cells through TEM followed by differential ultracentrifugation. Our results indicate the presence of nanoscale exosomal vesicles morphologically similar to previously reported exosomes (Emmanouilidou et al., 2010) in both vehicle- and Mn-treated samples (Fig. 2A). Since exosomes reportedly contain a unique RNA profile distinct from that of host cells(Valadi et al., 2007), we further analyzed the exosomes for small non-coding RNAs, such as microRNAs (Mongabadi et al.). Exosomal RNA was isolated using the mirVana^{TM} miRNA isolation kit, and small

RNAs were analyzed with the Agilent 2100 Bioanalyzer Lab-on-a-Chip instrument system (Agilent Technologies). Our data show that the isolated exosomes do indeed contain small RNAs with sizes ranging from 4-150 nucleotides, of which about 86% are positive for miRNAs (Fig. 2B), suggesting that these exosomes not only play an important role in cell signaling, but also impact biological processes in the recipient cells upon fusion.

In parallel experiments, we used the NanoSight LM10 instrument to visualize, count, and measure the size of exosomes isolated from MN9D_Syn$_{GFP}$ cells in the presence or absence of Mn. The average diameter of exosomes isolated from control cells, 150.8 $\pm$ 7.05 nm, was comparable to that of Mn-treated exosomes, 148.6 $\pm$ 12.42 nm (Fig. 2B) , indicating that Mn exposure does not alter the size distribution of exosomes. These calculated sizes are consistent with previously published observations(Danzer et al., 2012; Emmanouilidou et al., 2010). Interestingly, we were able to detect significantly more exosomes in the Mn-treated cells than in the vehicle-treated cells, indicating that Mn significantly upregulates the release of exosomes (Fig. 2C). To further characterize these cell-derived exosomes, we examined the presence of αSyn and exosomal surface proteins. Western blot analysis readily detected the exosomal surface membrane protein markers Alix and Flotillin-1 in all exosome samples (Fig. 2E). Surprisingly, we observed more GFP-tagged αSyn fusion protein in the exosomes isolated from Mn-exposed cells than from untreated cells (Fig. 2E), indicating Mn exposure increases the αSyn payload carried by exosomal cargos. Similar results were obtained by using quantitative ELISA analysis (Fig. 2F).

The existence of αSyn oligomers in biological fluids and exosomal fractions isolated from cultured cells(Danzer et al., 2012; Lee et al., 2005) has been well characterized. Therefore, using confirmation specific antibodies against peptide-independent prefibrillar oligomers(Glabe, 2008; Kordower et al., 2008) and prefibriller αSyn species, we sought to determine whether misfolded αSyn proteins are accumulated in exosomes isolated from Mn stimulated cells. As shown in Fig. 2G (upper panel), we have observed noticeably increased levels of prefibrillar oligomer accumulation in Mn-stimulated MN9D_EV$_{Syn}$ exosomes and to lesser extent in MN9D_EV$_{GFP}$ exosomes compare to exosomes isolated from vehicle treated cells. To further evaluate whether the observed differences in oligomeric protein accumulation due to Mn induced αSyn protein misfolding, we have extended our slot blot analysis with newly developed αSyn antibody against filament confirmation to evaluate prefibriller αSyn species accumulation in Mn stimulated exosomes isolated from MN9D_Syn$_{GFP}$ cells Fig. 2G (lower panel). Collectively, our data suggest that Mn exposure increases the amount of αSyn-containing exosomes released and also upregulates the aggregated protein cargos packaged into these exosomes.

Manganese-stimulated exosomes promote neuroinflammatory responses.

Although exosomes play an important role in many physiological and pathological processes, the exosome-cell interaction mode and the intracellular trafficking pathway of exosomes in their recipient cells remain unclear. Recently, Feng and colleagues have shown that exosomes are taken up more efficiently by phagocytic cells than non-phagocytic cells, which suggests that phagocytic capability is essential for exosome

uptake (Feng et al., 2010). This is particularly important *in microglia*, which are the brain and spinal cord's *resident* macrophages and whose phagocytic capability makes them the first and main form of active immune defense. Moreover, aberrant activation of glial cells and associated proinflammatory cytokines becomes elevated in neurodegenerative (Amor et al., 2010; Heppner et al., 2015; Kordower et al., 2008; Lindqvist et al., 2013; Wyss-Coray and Mucke, 2002) and in experimental models of PD(Gao et al., 2011). Therefore, we exposed primary murine microglia to either vehicle- or Mn-stimulated exosomes to study whether Mn-stimulated exosomes have any role in neuroinflammatory processes. We added purified exosomes to primary microglia and allowed their cellular internalization to occur for 24 h at 37°C. Immunocytochemical analysis with an anti-IBA-1 antibody revealed that microglia exposed to Mn-stimulated αSyn-containing exosomes exhibited an amoeboid morphology as a result of activation and formation of diverse forms of surface protrusions, such as blebs and filopodia, similar to that observed in other phagocytic cells (Fig. 3A). Furthermore, GFP-positive punctate structures were observed inside the microglia cells, indicating potent exosomal internalization in microglial cells. The expression of IBA-1 and iNOS, as revealed by Western blot analysis, increased significantly in cells treated with Mn-induced αSyn-containing exosomes in contrast to cells receiving vehicle-stimulated αSyn-containing exosomes, further confirming a pronounced activation of microglia and subsequent oxidative stress (Fig. 3B-D). Supporting these observations, we found a significantly elevated release of proinflammatory cytokines, such as TNFα, IL-12, IL-1β and IL-6, from microglia upon exposure to Mn-stimulated αSyn-containing exosomes, compared to vehicle-stimulated αSyn-containing exosomes or GFP control exosomes (Fig. 3E-H). We also measured the

anti-inflammatory cytokines IL-10 and IL-5 in our Luminex bead-based cytokine assays. Neither IL-5 nor IL-10 levels, however, were changed significantly in any treatment group (Supplementary Fig. 1A-B). These data collectively indicate that Mn-stimulated αSyn-containing exosomes are biologically active and capable of activating microglial cells and inducing the release of proinflammatory cytokines, which may further potentiate inflammatory process.

Microglia internalize manganese-stimulated αSyn exosomes through caveolin-1-mediated endocytosis

The process of endocytosis in mammalian cells involves multiple mechanisms depending on the host cell type as well as cargo type and fate. So far, different modes of endocytosis seem to be responsible for the uptake of exosomes by both phagocytic and non-phagocytic cells (Feng et al., 2010; Mulcahy et al., 2014; Tian et al., 2014). The previously described mechanisms of classical endocytosis include clathrin-dependent endocytosis, macropinocytosis and clathrin-independent endocytic pathways (e.g. caveolae-mediated uptake that is associated with lipid rafts in the plasma membrane). However, the mechanisms by which exosomes interact with recipient cells and how exosomes are sorted after entry into these cells remain unclear. Therefore, using immortalized microglial cells (WTMC) with morphology and surface marker expression highly similar to primary microglia (Halle et al., 2008) we have attempted to determine which endocytic pathway microglia use to take up exosomes. We treated WTMC with various pharmacological inhibitors of endocytosis, including dynasore, which binds dynamin to inhibit both caveolae- and clathrin-dependent endocytosis; (N-ethyl-N-

isopropyl)-amiloride (EIPA), an inhibitor of macropinocytosis; and chlorpromazine and genistein, which inhibit clathrin- and caveolin-mediated endocytosis, respectively (Mulcahy et al., 2014; Rejman et al., 2005). To better visualize exosomal vesicles, the cell-derived exosomes were pre-labeled with the green fluorescent dye *PKH67,* which is stably incorporated into lipid regions of the vesicle membrane, and then incubated with WTMC cells. Confocal microscopy revealed efficient internalization of the vehicle- and Mn-stimulated αSyn-containing exosomes by the WTMC cell line *(*Supplementary Fig. 2A). The 3D surface reconstruction images generated by Imaris software clearly indicate the homogeneous internalization of exosomes by the microglial cells and the activated microglial morphology upon internalization of Mn-stimulated, but not vehicle-stimulated, αSyn-containing exosomes *(*Supplementary Fig. 2A*).* Next, we pre-treated the WTMC with the endocytosis inhibitors, either chlorpromazine (5 μM) or genistein (50 μM) or EIPA (10 μM) or dynasore (50 μM), for 60 min at 37°C. Subsequently, Mn-stimulated PKH67-labeled αSyn-containing exosomes were added and incubation was continued for 24 h. Confocal microscopy indicated *(*Fig 4A*)* successful inhibition (80-90%) of exosome uptake by dynasore and genistein, whereas EIPA and chlorpromazine were unable to effectively inhibit (40-50%) exosome uptake. Therefore, given its clathrin independence and dynamin dependence during the internalization, exosome uptake in our microglial cell cultures were controlled through caveolae-dependent endocytosis. In a parallel experiment, we co-treated the microglial cells with Mn-stimulated αSyn-containing exosomes and the aforementioned inhibitors to further analyze the production of proinflammatory cytokines and nitrite. Similarly, treatment with dynasore and genistein significantly attenuated the production of the proinflammatory cytokines TNFα, IL-1β

and IL-6 in response to Mn-stimulated αSyn exosomes, whereas chlorpromazine and EIPA did so only marginally or not at all (Fig. 4B-D). Furthermore, we detected significantly reduced nitrite production upon treating cells with dynasore, genistein, and EIPA, but not with chlorpromazine (Fig. 4E). Therefore, these data indicate that the high capacity uptake of Mn-stimulated αSyn-containing exosomes by microglia involves multiple mechanisms, with the caveolae-dependent endocytosis playing a central role in regulating this process.

Next, using primary murine microglial cultures we confirmed the prominent role of caveolin-1-mediated endocytosis in microglial uptake of αSyn-containing exosomes. For this, we employed fluorescently labeled transferrin and the cholera toxin B subunit (ctxB), which are widely recognized as ligands exclusively internalized via clathrin-mediated endocytosis and caveolae-mediated endocytosis, respectively, in several cell types(Hansen et al., 1993; Orlandi and Fishman, 1998; Rejman et al., 2005; Singh et al., 2003). Primary microglia cells were pre-treated with chlorpromazine or genistein as described above for 60 min at 37°C. At the end of the incubation, cells were co-treated with either Alaxa-555-labeled transferrin and PKH67-labeled exosomes (Fig 4F) or Alaxa-555-labeled ctxB and PKH67-labeled exosomes (Fig 4G) for 24h at 37°C. As depicted in Fig. 4F-G, chlorpromazine treatment led to a significant inhibition of Alexa555-conjugated transferrin uptake, whereas only a moderate inhibition of the uptake of PKH67-labeled exosomes or Alexa555-conjugated ctxB was observed. Furthermore, cells treated with genistein exhibited 90-100% inhibition of both Alexa555-conjugated ctxB and PKH67-labeled exosome uptake. Genistein, however, did not inhibit

transferrin uptake by the microglial cells. Therefore, our data suggest that caveolin-mediated endocytosis primarily facilitate for the recognition and internalization of neuronal exosomes by microglia.

In an effort to rule out the possible non-specific effects of pharmacological/chemical inhibitors, we next employed the CRISPR/Cas9 nuclease RNA-guided genome editing technique to individually knockdown (KD) caveolin-1 or clathrin in the murine wide-type microglial cell line to validate our experimental results involving chemical inhibition of endocytosis. The inhibition of *αSyn-containing* exosome uptake in caveolin-1-KD cells was significantly greater than in clathrin-KD microglial cells as seen by confocal microscopy *(FIGURE)*. In parallel experiments involving Luminex magnetic bead-based cytokine analysis, the release of the proinflammatory cytokines IL-6, IL-12, TNFα, and IL-1β was reduced significantly by exposing clathrin--KD cells to *Mn-stimulated αSyn exosomes in* contrast to control microglial cells *(*Fig. 4I-K*)*. A further reduction in αSyn exosome-stimulated proinflammatory cytokine release occurred in caveolin-1-KD cells. Therefore, we report that microglial internalization of exosomes derived from *αSyn-overexpressing dopaminergic* cells depends on multiple mechanisms, in particular the involvement of caveolin-1-dependent endocytosis.

Manganese-stimulated αSyn exosomes induce neurodegeneration *in vitro*.

After establishing the role of Mn-stimulated *αSyn* exosomes in promoting neuroinflammation, we further extended our experiments to evaluate whether these exosomes mediate neurodegeneration. For this purpose, we established a neuron-glia mixed culture system using primary microglial cells and differentiated Lund human

mesencephalic (LUHMES) cells (Fig. 5A). By using a transwell cell culture system, we were able to mimic the biological environment where microglia and neurons reside in close proximity and to evaluate the extent of *αSyn* exosome-mediated neurodegeneration. Since LUHMES cells can be differentiated into morphologically and biochemically mature post-mitotic dopamine-like neurons, they are widely used as an *in vitro* model system for dopaminergic neurotoxicity. As shown in Fig. 5B, Mn-stimulated αSyn exosomes evoked apoptosis as indicated by increased caspase-3 activity in differentiated LUHMES cells. In contrast, we did not observe significantly increased caspase-3 activity in cells that received either GFP exosomes or vehicle-stimulated αSyn exosomes, indicating that this observed cell death may result from the combined effects of increased inflammation and prefibrillar oligomers packaged in Mn-stimulated αSyn exosomes.

Immunocytochemical analysis of the exosome-treated LUHMES cells readily detected exosome uptake as evidenced by GFP-immunoreactive punctate structures inside the neuronal cells (Fig. 5C). Immunolabeling of the LUHMES cells with neuron-specific class II β-tubulin (Tuj1) confirmed the fully differentiated post-mitotic nature of the LUHMES cells, as described previously (Scholz et al., 2011). Collectively, our data indicate that Mn-stimulated αSyn exosomes could initiate neuronal apoptosis *in vitro*.

Live cell model for αSyn oligomer transmission

To further clarify the role of Mn in cell-to-cell transmission of αSyn aggregates, we adopted an assay based on bimolecular fluorescence complementation (BiFC), which has been successfully applied to assess protein oligomerization, protein-protein interaction,

and cell-to-cell transmission in *in vitro* and *in vivo* models (Bae et al., 2014; Danzer et al., 2012; Dimant et al., 2013). For this assay, human wild type αSyn is fused to either the amino terminus (V1S) or carboxy terminus (SV2) fragment of the Venus protein, which is an improved variant of GFP (Fig. 6A). When V1S or SV2 constructs were individually transfected into MN9D cells, neither cells fluoresced (Fig. 6D). Once cells were co-transfected with V1S and SV2, however, αSyn-αSyn interactions brought together (Danzer et al., 2012) and reconstituted the Venus fluorescent protein as a result of cell-to-cell transmission of αSyn as visualized using BiFC (Fig. 6D). Utilizing this assay system, we have shown that Mn exposure increases αSyn-αSyn interactions in living cells and reconstitutes the Venus fluorophore which only occurs when each fragment is brought together and covalently linked.

To study the nature of αSyn species visualized by the BiFC assay, in parallel Western blot experiments we immunoblotted with anti-Ubiquitin, αSyn and GFP antibodies. As expected, cells transfected with V1S+SV2 followed by Mn treatment accumulated high molecular weight poly-ubiquitinated proteins and mono-ubiquitinated proteins, indicating that Mn enhanced protein oligomerization when compared with vehicle-treated cells (Fig. 6E). Under these experimental conditions, we also detected discrete bands corresponding to Venus-link-αSyn (V1S) and αSyn-Venus (SV2) protein expression and their N-terminal Venus fluorescent tag (Fig. 6E).

To ensure αSyn oligomerization and transmission were not driven by the Venus fluorescent moieties, we adopted another protein complementation assay based on a luciferase assay system consisting of the two fusion constructs αSyn-hGLuc1 (S1) and

αSyn-hGLuc2 (S2) as described elsewhere (Danzer et al., 2012; Outeiro et al., 2008). This assay works on the same principle as the BiFC assay, and *Gaussia princeps* luciferase only reconstitutes with S1 and S2 protein interaction, allowing direct monitoring of these protein interactions in their normal cellular environment. Transient transfection of S1 and S2 constructs showed about 5 times higher luciferase activity relative to the background signal from cells transfected with either S1 or S2 plasmids. Furthermore, cells transfected with S1+S2 followed by Mn exposure showed about 8 times higher luciferase activity relative to background and about 160% higher activity than vehicle-treated S1+S2 co-transfected cells (Fig. 6F). These data are consistent with our fluorescent-based BiFC assay results and support our finding that Mn exposure induces cell-to-cell transmission of misfolded αSyn species. Interestingly, the luciferase signal in cells co-transfected with S1+S2 and treated with magnesium (Mg), another divalent metal commonly found in biological systems, did not differ from that of vehicle-treated cells (Supplementary fig). These results suggest some specificity to Mn in misfolded αSyn formation and transmission.

We used flow cytometry to further confirm that Mn promotes cell-to-cell transmission of oligomeric αSyn. Since the Venus fluorescent protein in our plasmid constructs (V1S and SV2) used in the BiFC experiment matures at 37°C as a strong fluorescent signal, we used fluorescent-activated cell sorting (FACS) to contrast GFP-positive cell populations exposed to Mn or vehicle treatments (Fig. 6G). Cells co-transfected with V1S and SV2 and treated with either Mn or vehicle for 24 h were fixed and processed for flow cytometry analysis. Our FACS analysis shows significantly more GFP-positive cells in Mn-exposed cells than in the vehicle-treated control group (Fig. 6H). Consistent with our

BiFC assay, we did not detect GFP-positive cells when they were transfected with either V1S or SV2. Thus, using multiple experimental approaches, we have shown that Mn exposure promotes cell-to-cell transmission of oligomeric αSyn in our cell culture system.

Direct detection of manganese-induced cell-to-cell transmission of α-synuclein oligomers and associated neurotoxicity *in vivo*.

Once we established the effect of Mn in cell-to-cell transmission of oligomeric αSyn *in vitro*, we shifted to *in vivo* models of Mn toxicity. Using a novel *in vivo* protein complementation approach consisting of co-injecting AAVs encoding αSyn fused to the N- or C-terminal half of VenusYFP(Dimant et al., 2013), we showed elevated levels of αSyn oligomers *in vivo* in Mn-exposed animals. Thirty days after stereotaxically co-injecting AAV-V1S and AAV-SV2 into the SNpc of C57BL6 (Fig. 7A), animals were exposed to either vehicle or Mn (15 mg/kg/day) via oral gavage once daily for another 30 days (Fig. 7B). Two additional control groups were injected with either AAV-V1S or AAV-SV2 virus to exclude the possibility of non-specific fluorescence from one half of the VenusYFP protein, and another group was injected with AAV-CBA-VenusYFP as a positive control for the experiment. At 60 days post-viral injection, VenusYFP fluorescence was clearly visible in the substantia nigra pars compacta (SNpc) of animals injected with AAV-CBA-VenusYFP, confirming our injection target and the expression of VenusYFP epifluorescence (Fig. 7C).

To determine whether Mn exposure promotes αSyn oligomerization and pathogenesis *in vivo*, we used Kodak Image Station In-Vivo FX to image VenusYFP expression in

vehicle-treated and Mn-exposed mice. Whole brain images were captured using its fluorescence imaging capability and converted into heat-maps using MATLAB and superimposed on white-light reference images to show anatomical localization of VenusYFP fluorescence (Fig. 7D). Imaging clearly indicates that Mn exposure promotes αSyn oligomerization, which increased about 350% in Mn-exposed animals compared to vehicle-treated animals, based on ImageJ quantification of fluorescent intensities (Fig. 7D and E). Notably, control animals injected with either AAV-V1S or AAV-SV2 alone did not express any VenusYFP fluorescence on the injected side (data not shown), demonstrating that the fragmented Venus protein lacks background fluorescence.

To further characterize the effect of Mn in αSyn-mediated neurotoxicity, we compared the behavior deficits of viral-transduced and non-transduced mice exposed to Mn via oral gavage. Non-transduced and transduced mice were age-matched littermates and the Mn or vehicle exposures were conducted simultaneously. To assess Mn-induced motor deficits in mice after the 30-day Mn treatment paradigm, we measured various motor performance parameters using a computerized infrared activity monitoring system (VersaMax, Accuscan). Representative maps of the locomotor movements of vehicle-treated and Mn treated non-transduced (No injection) and transduced (AAV-V1S+AAV_SV2) mice suggest that Mn decreased movements in both experimental groups, and viral-transduced mice exhibited greater movement deficits upon Mn exposure (Fig. 7F). Quantitative analysis of infrared beam breaks confirmed that Mn exposure markedly decreased the total number of movements (Fig. 7I), total distance travelled (Fig. 7J), and the horizontal activity (Fig. 7K) in transduced mice compared to

vehicle-treated animals, further indicating that Mn exposure augments αSyn-mediated neurotoxicity in animals by enhancing αSyn oligomerization and pathogenesis.

To determine whether Mn-induced αSyn oligomerization promotes dopaminergic neurodegeneration in SN, we examined neuronal viability *in vivo* after a 30-day Mn exposure period in both AAV-V1S+AAV_SV2 virus-transduced and non-transduced animals. Coronal sections through the SN were immunostained for tyrosine hydroxylase (TH) and immunopositive cells visualized by DAB (Fig. 7G). Dopaminergic neuronal loss was evaluated using unbiased stereology of TH-immunoreactive neurons on both the ipsilateral and contralateral sides. TH DAB staining and stereological counts revealed severe loss of nigral dopaminergic neurons, especially TH-positive neurons in the SNpc and substantia nigra pars reticulata SNpr of Mn-treated AAV_V1S+AAV_SV2 virus-transduced animals relative to vehicle controls (Fig. 7H). These observations further support Mn-induced cell-to-cell transmission of αSyn promoting dopaminergic neurodegeneration *in vivo*. In contrast, Mn-exposed non-transduced animals showed no significant loss of TH+ neurons when compared to their age-matched vehicle control animals. Overall these results, together with the abovementioned whole brain imaging of the cell-to-cell transmission of αSyn, strongly demonstrate that exposure to environmental neurotoxicants such as Mn can augment the progression of αSyn misfolding *in vivo,* resulting in dopaminergic cell death.

Manganese exposure promotes exosome release in transgenic animals and αSyn oligomer transmission in humans

Having shown that exposing viral transduced mice to Mn induces αSyn oligomerization and dopaminergic neurodegeneration, we then evaluated total serum exosome release in

rats expressing the human αSyn-A53T mutation. Rats were dosed with Mn as described above and their blood was collected through cardiac puncture at study termination. Serum separation and exosome isolation were carried out as described above and total serum exosome numbers were counted using the Nanosight particle analyzer. Mn challenged αSyn-A53T transgenic rats produced significantly higher concentrations of exosome than did either vehicle-treated transgenic rats (p=0.0035) or non-transgenic rats (p value 0.0082) (Fig. 8A). Manganese exposure did not alter exosome size and it only increased the number of exosomes released during a neurotoxic insult (Fig. 8B). Therefore, exosomes may act as a means of cell-to-cell communication during increased intracellular stress conditions and use as a cargo for secretion and cell-to-cell transmission of harmful or unwanted cellular proteins.

It has been proposed that exogenously added misfolded αSyn serves as nucleation seeds for propagating aggregate-initiated polymerization of αSyn in *in vitro* and *in vivo* models of PD (Luk et al., 2012a; Luk et al., 2012b; Luk et al., 2009; Nonaka et al., 2010; Volpicelli-Daley et al., 2014). Since exosomes are well recognized as one of the potential mechanisms mediating cell-to-cell transmission of cytosolic protein aggregates (Guo and Lee, 2014), and given the strong interaction between heavy metals and neurodegenerative disease or parkinsonian syndromes (Fored et al., 2006; Racette et al., 2012; Willis et al., 2012; Wright Willis et al., 2010), we undertook an exploratory study to compare the αSyn content in 21 serum exosome samples from welders (aged 26-65 years; 46 ± 11.2 years) recently (within 90 days) exposed to Mn fumes to 27 healthy controls (aged 28-73 years; 49 ± 11.0 years with no history of welding (see details in Lee et, al 2015 for the first description of the

subjects, also see Lee 2016) . Serum exosomes were isolated as described above and total exosome numbers were counted using Nanosight particle analysis. Contrary to our previous observations with transgenic cells and rats, the exosome counts in welders and controls did not differ significantly (p=0.0993) (Fig. 8C). We also analyzed the total αSyn concentration in these exosomes using a commercially available, highly sensitive luciferase-based αSyn ELISA assay (BioLegend; 844101). Total αSyn cargo in the serum exosomes did not differ between welders and controls (p=0.6848; Fig. 8D), indicating that the level of Mn exposure experienced by the welders in this sample was not sufficient to alter exosome numbers or total αSyn cargo in humans.

Though the outcome we observed in humans did not directly support changes observed in transgenic cells and rats, it has been reported that varying αSyn expression levels in peripheral blood and CSF in PD patients and healthy controls (El-Agnaf et al., 2003; El-Agnaf et al., 2006; Foulds et al., 2011; Mollenhauer et al., 2013; Tinsley et al., 2010). Importantly, in the αSyn model of neuron injury, β-sheet-rich soluble oligomers are considered more toxic than monomers(Lashuel et al., 2013; Sharon et al., 2003; Winner et al., 2011). Therefore, we measured the αSyn oligomer levels in these exosomes using the highly sensitive, Thioflavin T (ThT)-based αSyn fibril formation assay. In this microplate-based cell-free seeding assay, exosomes isolated from welders and controls, serving as the seeds presumably with trace amounts of αSyn fibrils, are added to a recombinant human αSyn substrate (Supplementary Fig 4A) and repeatedly agitated. First we optimized the assay using different concentrations of synthetically aggregated αSyn as a seed, and we showed that the onset of fibril formation, which increases fluorescence

intensity when ThT binds to aggregates, directly correlates to αSyn fibril seed density (Supplementary Fig 4B). This correlation is predicted by theory and has been used previously to quantify the aggregation kinetics of two major forms of amyloid-beta peptides and TSE-associated forms of prion protein(Henderson et al., 2015; Meisl et al., 2014; Orru et al., 2015; Pedersen and Heegaard, 2013). Blank and baseline-corrected average kinetic traces for seeded fibrillar formation assays revealed a significant difference in the lag-phase of the averaged traces of welders and control exosome samples. The lag phase duration was determined from the point where the ThT fluorescence intensity first reached the threshold value for detecting the presence of amyloid (Fig. 8E). This threshold was defined as five standard deviations of the fluorescence intensity of the first 10 h from the blank (3.66) sample. Standard error of the mean lag phase was calculated via bootstrap with replacement protocol in MATLAB. The calculated lag phases for control and welders' exosomes were 23.5±1.2 h and 16.2±5.1 h, respectively. Furthermore, we calculated final fluorescence intensity for comparing two kinetic traces by averaging the raw ThT fluorescence of the last 10 data points of each trace (Fig. 8F). By averaging intensity values for controls (270 data points) and welders (210 data points), we observed a statistically significant difference in their final ThT fluorescence intensities, indicating that exosomes isolated from welders have higher seeding capacity and misfolded αSyn protein content compared to exosomes isolated from healthy controls.

Manganese-stimulated exosomes induce motor deficits in mouse models of PD

The accumulation of misfolded proteins and associated behavioral deficits are fundamental pathogenic processes in the progression of PD and number of other

synuclopathy-related disorders(Luk et al., 2012b). Furthermore, evidence from recent *in vitro* and *in vivo* studies suggests that misfolded proteins play a central role in a variety of neurodegenerative disorders by functioning as a "seed" for the protein misfolding and aggregation processes; much like prions (Sacino et al., 2013; Ubeda-Banon et al., 2013; Watts et al., 2013). Thus far, we have shown that Mn-stimulated exosomes contain prefibrillar αSyn oligomers could potentiate neuroinflammatory and degenerative response *in vitro*. Therefore, we further extended our study to evaluate the effects of these exosomes in mouse models, that mimic of the neurodegenerative process.

To investigate whether exosomes carry disease-associated prefibrillar αSyn oligomers that can seed and propagate pathology *in vivo*, we injected 2 to 3-month old wild-type C57BL/6 mice with exosomes isolated from Mn or vehicle-treated pMAXGFP and pMAXGFP_αSyn cells. Roughly 4-5 x 10^8 exosomal particles (5 µg total exosome proteins) from each treatment group were stereotaxically injected into one side of the striatum (Fig. 9A) and neurological behavioral deficits were monitored over time. Interestingly, we observed attenuated behavioral performance in animals injected with αSyn exosomes at 90 days post-inoculation (dpi). Specifically, mice receiving Mn-stimulated αSyn exosomes showed reduced exploratory locomotor activity as measured by stereotypy counts, movement time (Fig. 9 C-D) in an open field test. Some of these observed behavioral deficits, however, are not statistically significant, which may be attributable to the fact that the exosome injections were done unilaterally, lesioning only one side of the brain. Also, the amphetamine-induced rotation test indicates increased ipsilateral movements in the Mn-stimulated αSyn exosome injected mice, indicating

unilateral CNS damage in in these animals compared to mice receiving vehicle-stimulated αSyn exosomes or vehicle- and Mn-stimulated GFP exosomes (Fig 9B).

Lewy bodies and Lewy neurites are pathological hallmarks of synucleinopathy-related disorders. As a final step, we performed histological evaluations of brain sections to check for the presence of these proteinaceous inclusions. Interestingly, we detected αSyn(Ser(p)^{129})-immunoreactive cytoplasmic inclusions in mice injected with Mn-stimulated αSyn exosomes compared to vehicle-stimulated αSyn exosomes or vehicle- and Mn-stimulated GFP exosomes injected mice. These data suggest that αSyn exosomes are able to initiate synucleinopathy pathologies in experimental models of PD. Mice receiving GFP exosomes did not appear to have any protein inclusions or GFP immune-positive structures, suggesting that the GFP protein may have been cleaved-off and degraded. Collectively, our results clearly indicate that αSyn-containing exosomes could initiate parkinsonian symptoms and propagate αSyn misfolding and aggregation *in vivo*. These observations also may help further the understanding of prion-like, cell-to-cell transmission of aggregated proteins in progressive neurodegenerative disorders.

Discussion

The role of extracellular αSyn in the progression of PD gained much interest recently with the discovery of αSyn in human cerebrospinal fluid (CSF) and blood plasma (El-Agnaf et al., 2003). Recent reports support a pathogenic role for extracellular αSyn, showing that αSyn aggregates released from neurons unleash toxic effects in recipient neurons by forming Lewy body-like inclusions (Desplats et al., 2009; Emmanouilidou et al., 2010) or by activating inflammatory responses in microglia (Kim et al., 2013). Also,

adding exogenous fibrillar αSyn into αSyn-overexpressing cells and primary neurons actively recruits soluble endogenous αSyn, converting it into a detergent-insoluble misfolded state (Luk et al., 2009; Volpicelli-Daley et al., 2014; Volpicelli-Daley et al., 2011) much like the mechanism observed in prion disease (Aguzzi and Falsig, 2012). Furthermore, inoculation of pathological αSyn and recombinant αSyn amyloid (Luk et al., 2012b) were sufficient to transmit and initiate parkinsonian symptoms in animal models of neurodegenerative disorders, providing evidence that misfolded αSyn serves as a seed and template for endogenous αSyn to propagate αSyn aggregation in a prionic manner. However, given the strong synergistic environmental influence and multifactorial etiology in synucleinopathy-related pathogenesis, it is important to understand the role of environmental neurotoxicants and their interaction with genetic risk factors to further our understanding of neurodegenerative processes. Chronic exposure to heavy metals in occupational settings, especially exposure to Mn through mining, welding and smelting, has been reported as a putative risk factor for environmentally-linked neurodegenerative disorders (Fored et al., 2006; Gorell et al., 1997; Racette et al., 2012). However, despite the strong association with exposure to agro-chemicals and heavy metals, little is known about environmental influences on the cell-to-cell transmission of pathogenic proteins.

Though previous studies have shown that Mn neurotoxicity leads to neuronal apoptosis and the upregulation and aggregation of αSyn in experimental models of PD (Cai et al., 2010; Hirata, 2002; Kordower et al., 2008), its role in the release and transmission of pathogenic αSyn has not been studied. Therefore, to further understand the role of Mn in

the cellular release of αSyn, we systematically carried out experiments to show that Mn increases the release of αSyn amyloid containing exosomes, which could increase neuroinflammatory and neurodegenerative responses in experimental models of neurodegenerative disorders. We also show that low-dose chronic exposure to Mn increases the exosomal release of αSyn cargo resulting in αSyn oligomerization *in vitro* and *in vivo*. We show further that humans exposed to Mn through welding fumes contain higher misfolded αSyn in their serum exosomes than control subjects. These findings could improve our understanding of exosome-mediated cell-to-cell propagation of αSyn and its role in the progression of neurological disorders.

Our wild-type human αSyn-overexpressing cell culture model clearly demonstrates that Mn exposure significantly enhances the release and accumulation of extracellular αSyn (Fig 1D and E) providing direct evidence of an environmental influence of αSyn release. Since αSyn protein structure doesn't contain a signal recognition sequence, which would be required for the conventional ER/Golgi secretion pathway (Emmanouilidou et al., 2011; Vekrellis et al., 2011), several unconventional excretion mechanisms have been implicated in αSyn release, including an endosomal pathway, direct transfer across the membrane, and release through exosomes (Emmanouilidou et al., 2010; Lee et al., 2005). Therefore, to characterize the mode of αSyn release induced by Mn, we analyzed the conditioned media through TEM and Western blotting followed by differential ultracentrifugation. We readily detected micro-vesicles similar in size and morphology to exosomes (Fig. 2A). Our exosomes also contained Alix and Flotillin, which are common to these vesicles and serve as "markers" along with tetraspanin (CD63, CD81) and heat shock proteins (HSP70, 90) (Schneider and Simons, 2013). Mn exposure in αSyn cells

resulted in significantly higher αSyn amyloid-containing exosome release. This is particularly interesting because the regulation of exosome release previously was thought to be controlled by lysosomal dysfunction (Alvarez-Erviti et al., 2011) and a *calcium*-dependent mechanism (Emmanouilidou et al., 2010) but the role of environmental neurotoxicants remained ill-studied.

Extracellular αSyn reportedly interacts with CD36 (Su et al., 2008), toll-like receptor 4 (TLR4), (Fellner et al., 2013) and TLR2, (Kim et al., 2013) and thus activates microglial inflammatory processes and enhances ROS production. In this regard, we further characterized the capability of exosomal amyloid αSyn content to trigger neuroinflammatory responses by activating primary microglial cells and releasing pro-inflammatory cytokines. In line with recent observations indicating that neuroinflammation is a pivotal step in neurodegenerative disorders (Rocha et al., 2015), our experiments show that Mn-stimulated exosome treatments in primary microglial cells significantly elevated the release of IL1-β, IL-6, IL-12 and TNF-α (Fig. 3E-H). Our results further provide evidence that exosomes are biologically active entities that interact with recipient cells. The membrane transport mechanisms and the downstream signaling events involved in the uptake of these exosome vesicles, however, are inconclusive. Fate of the exosome cargo in recipient cells is often determined by which endocytic pathway is used to gain entry and often distinguished on the basis of their differential sensitivity to pharmacological/chemical inhibitors. The possibility of nonspecific effects of such inhibitors, however, frequently is overlooked. For example, the potent GTPase inhibitor dynasore, which prevents endocytosis by rapidly and reversibly inhibiting dynamin activity, was shown to reduce labile cholesterol in the plasma membrane and to disrupt

lipid raft organization in a dynamin-independent manner (Preta et al., 2015).Moreover, genistein is reported to be a general Src tyrosine protein kinase inhibitor (Kaul et al., 2005), a competitive inhibitor of ATP, (Versantvoort et al., 1994) and inhibits cancer metastasis, and these actions may or may not directly influence its inhibition of caveolin-mediated endocytosis. Therefore, in this study, using both selective inhibitors and CRISPR/Cas gene editing molecular tools, we shown that caveola-mediated endocytosis was primarily involved in the microglial uptake of neuronal cell-derived exosomes. These findings add insights into the endocytic pathway and the biological significance of exosome-mediated neuroinflammation. Having shown the capability of αSyn amyloid-containing exosomes to increase inflammation, we further characterized their ability to exert a neurodegenerative effect by using a neuron-glia mixed culture system. In concordance with previous observations by Emmanouilidou and colleagues (Emmanouilidou et al., 2010), we also have seen increased caspase-3 activity upon αSyn containing exosomes leading to neuronal apoptosis upon exposure to differentiated LUHMES cells (Fig. 4C); differentiated LUHMES cells show morphological and biochemical characteristics similar to mature post-mitotic dopamine-like neurons and primary neuronal cultures (Scholz et al., 2011).

The current study also provided direct evidence for enhanced αSyn transmission from Mn by increasing BiFC-positive cells in Mn exposed cells and greatly increasing extracellular V1S/SV2 exsosomal protein content. Thus, we have shown for the first time that Mn not only causes αSyn oligomerization but also cell-to-cell transmission. We extended these *in vitro* findings to animals, showing a significantly elevated BiFC-positive signal in animals exposed to Mn, supporting the notion that environmental neurotoxicants can

cause αSyn misfolding and cell-to-cell transmission. Previously, we showed that physiological levels of human wild-type αSyn protein attenuate acute Mn-induced dopaminergic neuronal degeneration in cell culture models, but prolonged Mn exposure promotes αSyn aggregation and neurotoxicity (Harischandra et al., 2015). Except for studies showing accumulation in the globus pallidus and striatum causing GABAergic and dopaminergic toxicity (Crossgrove and Zheng, 2004; Li et al., 2006; Zheng et al., 2000), few have addressed Mn's long-term effects in animal models or in humans. Moreover, the findings from neuroimaging and neurobehavior studies of humans exposed to Mn through mining or welding are inconclusive due to conflicting outcomes on the possibility of nigrostriatal dopamine neuron degeneration (Fored et al., 2006; Guilarte, 2010; Racette et al., 2012; Willis et al., 2012). In fact, it has been reported that Mn decreases dopamine turnover in the striatum of transgenic mice expressing human wild-type αSyn, but didn't result nigrostriatal degeneration (Peneder et al., 2011). Despite the discrepancies in the published literature on Mn-induced dopaminergic neurodegeneration, we clearly observed TH[+]-neuron loss and related behavior deficits in animals transduced with V1S/SV2 AAV and exposed to Mn. This may result from Mn-induced cell-to-cell transmission causing αSyn oligomerization *in vivo,* which in turn causes toxicity to dopaminergic cells. Therefore, these findings have important implications on our current understanding of gene-environment interactions in neurodegenerative disorders.

In this study, Mn also significantly elevated concentrations of serum exosomes in rats expressing the human A53T-αSyn mutation, a genetic risk factor for PD. A strong correlation existed between the effects of genetic risk factors and environmental

neurotoxicants on exosome release. Although, we did not see higher exosome numbers nor larger αSyn concentrations in exosomes isolated from humans exposed to Mn via welding fumes, our study of active welders was constrained by our inability to measure actual brain Mn levels and it was not a randomized controlled experiment. Nevertheless, we have reported that these welders do have higher misfolded αSyn content in their serum exosomes that may explain previous epidemiological studies on welding as a putative risk factor for developing parkinsonian neurological symptoms in later life (Gorell et al., 1997; Racette et al., 2012; Racette et al., 2005; Willis et al., 2012). Given the fact that these welder cohorts may have the potential for multiple etiologies and confounding variables (e.g., ergonomics, disease states, other exposures, age), however, clinical significance is uncertain and yet to be determined. Yet, the ability to detect amyloid αSyn species in serum exosomes can be studied further as a potential noninvasive biomarker, taking diagnosis of familial and *sporadic PD* to the next level.

We also evaluated whether exosomes function as a "seed" for the protein misfolding and aggregation process in experimental models of PD. Having shown that αSyn-overexpressing cells produce exosomes rich in αSyn amyloid upon Mn exposure, we unilaterally injected these Mn-stimulated exosomes into the mouse striatum to evaluate possible nucleation-dependent protein polymerization. Behaviorally, these mice displayed compromised locomotor activity, as measured by attenuated vertical activity, horizontal activity, and total distance travelled, whereas amphetamine-induced ipsilateral rotations were increased. Interestingly, we also detected $\alpha Syn(Ser(p)^{129})$ immuno-positive inclusion bodies, indicating that exosomal αSyn propagates *in vivo*, resulting in

inclusions similar to Lewy bodies and Lewy neurites, as reported elsewhere (Luk et al., 2012b; Luk et al., 2009; Watts et al., 2013).

In conclusion, we identified a possible mechanism for how the environmental neurotoxicant Mn contributes to exosome-mediated cell-to-cell transmission of αSyn and thus to the progression of neurodegenerative processes. Importantly, we showed that Mn exposure upregulates the release of αSyn-packed exosomes capable of propagating and accumulating in animal models of neurodegeneration. We also report that humans exposed to Mn through welding fumes contain higher αSyn amyloid content in their circulating exosomes. More well-designed, epidemiology studies, however, are needed that combine detailed histories of occupational exposure in welders with both behavioral and biochemical endpoints of neurotoxicity. Moreover, our findings might be relevant to other environmental toxicants implicated in protein misfolding disorders and possibly to the development of pharmacological interventions to block exosome-mediated disease progression.

Author contributions

D.S.H and A.G.K conceived and designed experiments. D.S.H., M.L.N., D.R., S.G., S.S., N.P. and G.Z. performed the experiments and analyzed the data. A.K, H.J. and V.A. provided intellectual input on experimental design, data analysis, interpretation and manuscript preparation. M.L. and X.H. provided key data regarding human samples (welder and controls) and assistance with the experimental design and interpretation, and review of the manuscript. D.S.H., H.J., G.Z. and A.G.K. wrote the manuscript and reviewed and edited the manuscript

Acknowledgements

Supplementary section

Alpha-Synuclein purification and aggregation: Expression and purification of recombinant human wild-type αSyn Expression protein was performed in E.coli Bl21(DE3) in a pT7-7 based expression system. After IPTG induction bacterial cell pellets were harvested by centrifugation and resuspended in 10 mM Tris-HCl, pH 8.0, 1 mM EDTA, and 1 mM PMSF, lysates were sonicated and centrifuged at 10,000 x g for 30 min. at 4°C. Streptomycin sulfate precipitated DNA was removed and ammonium sulfate precipitation step was performed to selectively precipitate the αSyn protein. Resulting lysates were filtered through 0.22-μm membranes and loaded onto a Bio-Rad UNO Q6 ion exchange column on BioLogic DuoFlow (Bio-Rad) chromatography system. Fractions collected during elution with a salt gradient were assayed for the presence of α-synuclein protein by SDS-PAGE followed by Coomassie staining. Fractions containing α-synuclein were pooled, dialyzed against 10 mM HEPES, 50 mM NaCl, pH 7.4, and protein concentration determined by Bradford assay.

172

References

Aguzzi, A., Falsig, J., 2012. Prion propagation, toxicity and degradation. Nat Neurosci. 15**,** 936-9.

Alvarez-Erviti, L., et al., 2011. Lysosomal dysfunction increases exosome-mediated alpha-synuclein release and transmission. Neurobiol Dis. 42**,** 360-7.

Amor, S., et al., 2010. Inflammation in neurodegenerative diseases. Immunology. 129**,** 154-69.

Ay, M., et al., 2015. Molecular cloning, epigenetic regulation, and functional characterization of Prkd1 gene promoter in dopaminergic cell culture models of Parkinson's disease. J Neurochem. 135**,** 402-15.

Bae, E. J., et al., 2014. Glucocerebrosidase depletion enhances cell-to-cell transmission of alpha-synuclein. Nat Commun. 5**,** 4755.

Cai, T., et al., 2010. Manganese induces the overexpression of alpha-synuclein in PC12 cells via ERK activation. Brain Res. 1359**,** 201-7.

Crossgrove, J., Zheng, W., 2004. Manganese toxicity upon overexposure. NMR Biomed. 17**,** 544-53.

Danzer, K. M., et al., 2012. Exosomal cell-to-cell transmission of alpha synuclein oligomers. Mol Neurodegener. 7**,** 42.

Desplats, P., et al., 2009. Inclusion formation and neuronal cell death through neuron-to-neuron transmission of alpha-synuclein. Proc Natl Acad Sci U S A. 106**,** 13010-5.

Dimant, H., et al., 2013. Direct detection of alpha synuclein oligomers in vivo. Acta Neuropathol Commun. 1**,** 6.

El-Agnaf, O. M., et al., 2003. Alpha-synuclein implicated in Parkinson's disease is present in extracellular biological fluids, including human plasma. FASEB J. 17**,** 1945-7.

El-Agnaf, O. M., et al., 2006. Detection of oligomeric forms of alpha-synuclein protein in human plasma as a potential biomarker for Parkinson's disease. FASEB J. 20**,** 419-25.

Emmanouilidou, E., et al., 2011. Assessment of alpha-synuclein secretion in mouse and human brain parenchyma. PLoS One. 6**,** e22225.

Emmanouilidou, E., et al., 2010. Cell-produced alpha-synuclein is secreted in a calcium-dependent manner by exosomes and impacts neuronal survival. J Neurosci. 30**,** 6838-51.

Fellner, L., et al., 2013. Toll-like receptor 4 is required for alpha-synuclein dependent activation of microglia and astroglia. Glia. 61**,** 349-60.

Feng, D., et al., 2010. Cellular internalization of exosomes occurs through phagocytosis. Traffic. 11**,** 675-87.

Fored, C. M., et al., 2006. Parkinson's disease and other basal ganglia or movement disorders in a large nationwide cohort of Swedish welders. Occup Environ Med. 63**,** 135-40.

Foulds, P. G., et al., 2011. Phosphorylated alpha-synuclein can be detected in blood plasma and is potentially a useful biomarker for Parkinson's disease. FASEB J. 25**,** 4127-37.

Gallegos, S., et al., 2015. Features of alpha-synuclein that could explain the progression and irreversibility of Parkinson's disease. Front Neurosci. 9**,** 59.

Gao, H. M., et al., 2011. Neuroinflammation and alpha-synuclein dysfunction potentiate each other, driving chronic progression of neurodegeneration in a mouse model of Parkinson's disease. Environ Health Perspect. 119**,** 807-14.

Ghosh, A., et al., 2010. Neuroprotection by a mitochondria-targeted drug in a Parkinson's disease model. Free Radic Biol Med. 49**,** 1674-84.

Ghosh, A., et al., 2013. The peptidyl-prolyl isomerase Pin1 up-regulation and proapoptotic function in dopaminergic neurons: relevance to the pathogenesis of Parkinson disease. J Biol Chem. 288**,** 21955-71.

Glabe, C. G., 2008. Structural classification of toxic amyloid oligomers. J Biol Chem. 283**,** 29639-43.

Gordon, R., et al., 2011. A simple magnetic separation method for high-yield isolation of pure primary microglia. J Neurosci Methods. 194**,** 287-96.

Gorell, J. M., et al., 1997. Occupational exposures to metals as risk factors for Parkinson's disease. Neurology. 48**,** 650-8.

Guilarte, T. R., 2010. Manganese and Parkinson's disease: a critical review and new findings. Environ Health Perspect. 118**,** 1071-80.

Guo, J. L., Lee, V. M., 2014. Cell-to-cell transmission of pathogenic proteins in neurodegenerative diseases. Nat Med. 20**,** 130-8.

Halle, A., et al., 2008. The NALP3 inflammasome is involved in the innate immune response to amyloid-beta. Nat Immunol. 9**,** 857-65.

Hansen, C., et al., 2011. alpha-Synuclein propagates from mouse brain to grafted dopaminergic neurons and seeds aggregation in cultured human cells. J Clin Invest. 121**,** 715-25.

Hansen, S. H., et al., 1993. Molecules internalized by clathrin-independent endocytosis are delivered to endosomes containing transferrin receptors. J Cell Biol. 123**,** 89-97.

Harischandra, D. S., et al., 2015. alpha-Synuclein protects against manganese neurotoxic insult during the early stages of exposure in a dopaminergic cell model of Parkinson's disease. Toxicol Sci. 143**,** 454-68.

Harischandra, D. S., et al., 2014. Role of proteolytic activation of protein kinase Cdelta in the pathogenesis of prion disease. Prion. 8**,** 143-53.

Henderson, D. M., et al., 2015. Quantitative assessment of prion infectivity in tissues and body fluids by real-time quaking-induced conversion. J Gen Virol. 96**,** 210-9.

Heppner, F. L., et al., 2015. Immune attack: the role of inflammation in Alzheimer disease. Nat Rev Neurosci. 16**,** 358-72.

Hirata, Y., 2002. Manganese-induced apoptosis in PC12 cells. Neurotoxicol Teratol. 24**,** 639-53.

Jin, H., et al., 2014. Histone Hyperacetylation Upregulates PKCdelta in Dopaminergic Neurons to Induce Cell Death: Relevance to Epigenetic Mechanisms of Neurodegeneration in Parkinson's Disease. J Biol Chem.

Jucker, M., Walker, L. C., 2013. Self-propagation of pathogenic protein aggregates in neurodegenerative diseases. Nature. 501**,** 45-51.

Kaul, S., et al., 2005. Tyrosine phosphorylation regulates the proteolytic activation of protein kinase Cdelta in dopaminergic neuronal cells. J Biol Chem. 280**,** 28721-30.

Kim, C., et al., 2013. Neuron-released oligomeric alpha-synuclein is an endogenous agonist of TLR2 for paracrine activation of microglia. Nat Commun. 4**,** 1562.

Koller, W. C., et al., 2004. Effect of levodopa treatment for parkinsonism in welders: A double-blind study. Neurology. 62**,** 730-3.

Kordower, J. H., et al., 2008. Lewy body-like pathology in long-term embryonic nigral transplants in Parkinson's disease. Nat Med. 14**,** 504-6.

Lashuel, H. A., et al., 2013. The many faces of alpha-synuclein: from structure and toxicity to therapeutic target. Nat Rev Neurosci. 14**,** 38-48.

Latchoumycandane, C., et al., 2005. Protein kinase Cdelta is a key downstream mediator of manganese-induced apoptosis in dopaminergic neuronal cells. J Pharmacol Exp Ther. 313**,** 46-55.

Lee, E.-Y., et al., 2015. T1 relaxation rate (R1) indicates non-linear Mn accumulation in brain tissue of welders with low-level exposure. Toxicological Sciences. kfv088.

Lee, H. J., et al., 2005. Intravesicular localization and exocytosis of alpha-synuclein and its aggregates. J Neurosci. 25**,** 6016-24.

Lee, S. J., et al., 2010. Cell-to-cell transmission of non-prion protein aggregates. Nat Rev Neurol. 6**,** 702-6.

Li, G. J., et al., 2006. Molecular mechanism of distorted iron regulation in the blood-CSF barrier and regional blood-brain barrier following in vivo subchronic manganese exposure. Neurotoxicology. 27**,** 737-44.

Li, J. Y., et al., 2008. Lewy bodies in grafted neurons in subjects with Parkinson's disease suggest host-to-graft disease propagation. Nat Med. 14**,** 501-3.

Lindqvist, D., et al., 2013. Cerebrospinal fluid inflammatory markers in Parkinson's disease--associations with depression, fatigue, and cognitive impairment. Brain Behav Immun. 33**,** 183-9.

Luk, K. C., et al., 2012a. Pathological alpha-synuclein transmission initiates Parkinson-like neurodegeneration in nontransgenic mice. Science. 338**,** 949-53.

Luk, K. C., et al., 2012b. Intracerebral inoculation of pathological alpha-synuclein initiates a rapidly progressive neurodegenerative alpha-synucleinopathy in mice. J Exp Med. 209**,** 975-86.

Luk, K. C., et al., 2009. Exogenous alpha-synuclein fibrils seed the formation of Lewy body-like intracellular inclusions in cultured cells. Proc Natl Acad Sci U S A. 106**,** 20051-6.

Meisl, G., et al., 2014. Differences in nucleation behavior underlie the contrasting aggregation kinetics of the Abeta40 and Abeta42 peptides. Proc Natl Acad Sci U S A. 111**,** 9384-9.

Mollenhauer, B., et al., 2013. Total CSF alpha-synuclein is lower in de novo Parkinson patients than in healthy subjects. Neurosci Lett. 532**,** 44-8.

Mongabadi, S., et al., 2013. Effect of different frequencies of repetitive transcranial magnetic stimulation on acquisition of chemical kindled seizures in rats. Neurol Sci. 34**,** 1897-903.

Mulcahy, L. A., et al., 2014. Routes and mechanisms of extracellular vesicle uptake. J Extracell Vesicles. 3.

Nonaka, T., et al., 2010. Seeded aggregation and toxicity of {alpha}-synuclein and tau: cellular models of neurodegenerative diseases. J Biol Chem. 285**,** 34885-98.

Orlandi, P. A., Fishman, P. H., 1998. Filipin-dependent inhibition of cholera toxin: evidence for toxin internalization and activation through caveolae-like domains. J Cell Biol. 141**,** 905-15.

Orru, C. D., et al., 2015. Rapid and sensitive RT-QuIC detection of human Creutzfeldt-Jakob disease using cerebrospinal fluid. MBio. 6.

Oueslati, A., et al., 2014. Protein Transmission, Seeding and Degradation: Key Steps for alpha-Synuclein Prion-Like Propagation. Exp Neurobiol. 23**,** 324-36.

Outeiro, T. F., et al., 2008. Formation of toxic oligomeric alpha-synuclein species in living cells. PLoS One. 3**,** e1867.

Panicker, N., et al., 2015. Fyn Kinase Regulates Microglial Neuroinflammatory Responses in Cell Culture and Animal Models of Parkinson's Disease. J Neurosci. 35**,** 10058-77.

Pedersen, J. T., Heegaard, N. H., 2013. Analysis of protein aggregation in neurodegenerative disease. Anal Chem. 85**,** 4215-27.

Peneder, T. M., et al., 2011. Chronic exposure to manganese decreases striatal dopamine turnover in human alpha-synuclein transgenic mice. Neuroscience. 180**,** 280-92.

Preta, G., et al., 2015. Dynasore - not just a dynamin inhibitor. Cell Commun Signal. 13**,** 24.

Prusiner, S. B., et al., 2015. Evidence for alpha-synuclein prions causing multiple system atrophy in humans with parkinsonism. Proc Natl Acad Sci U S A. 112**,** E5308-17.

Racette, B. A., et al., 2012. Increased risk of parkinsonism associated with welding exposure. Neurotoxicology. 33**,** 1356-61.

Racette, B. A., et al., 2005. Prevalence of parkinsonism and relationship to exposure in a large sample of Alabama welders. Neurology. 64**,** 230-5.

Recasens, A., Dehay, B., 2014. Alpha-synuclein spreading in Parkinson's disease. Front Neuroanat. 8**,** 159.

Rejman, J., et al., 2005. Role of clathrin- and caveolae-mediated endocytosis in gene transfer mediated by lipo- and polyplexes. Mol Ther. 12**,** 468-74.

Rocha, N. P., et al., 2015. Insights into Neuroinflammation in Parkinson's Disease: From Biomarkers to Anti-Inflammatory Based Therapies. Biomed Res Int. 2015**,** 628192.

Sacino, A. N., et al., 2013. Conformational templating of alpha-synuclein aggregates in neuronal-glial cultures. Mol Neurodegener. 8**,** 17.

Schneider, A., Simons, M., 2013. Exosomes: vesicular carriers for intercellular communication in neurodegenerative disorders. Cell Tissue Res. 352**,** 33-47.

Scholz, D., et al., 2011. Rapid, complete and large-scale generation of post-mitotic neurons from the human LUHMES cell line. J Neurochem. 119**,** 957-71.

Sharon, R., et al., 2003. The formation of highly soluble oligomers of alpha-synuclein is regulated by fatty acids and enhanced in Parkinson's disease. Neuron. 37**,** 583-95.

Singh, R. D., et al., 2003. Selective caveolin-1-dependent endocytosis of glycosphingolipids. Mol Biol Cell. 14**,** 3254-65.

Soo, C. Y., et al., 2012. Nanoparticle tracking analysis monitors microvesicle and exosome secretion from immune cells. Immunology. 136**,** 192-7.

Su, X., et al., 2008. Synuclein activates microglia in a model of Parkinson's disease. Neurobiol Aging. 29**,** 1690-701.

Tian, T., et al., 2014. Exosome uptake through clathrin-mediated endocytosis and macropinocytosis and mediating miR-21 delivery. J Biol Chem. 289**,** 22258-67.

Tinsley, R. B., et al., 2010. Sensitive and specific detection of alpha-synuclein in human plasma. J Neurosci Res. 88**,** 2693-700.

Ubeda-Banon, I., et al., 2013. alpha-Synuclein in the olfactory system in Parkinson's disease: role of neural connections on spreading pathology. Brain Struct Funct.

Valadi, H., et al., 2007. Exosome-mediated transfer of mRNAs and microRNAs is a novel mechanism of genetic exchange between cells. Nat Cell Biol. 9**,** 654-9.

Vekrellis, K., et al., 2011. Pathological roles of alpha-synuclein in neurological disorders. Lancet Neurol. 10**,** 1015-25.

Versantvoort, C. H., et al., 1994. Competitive inhibition by genistein and ATP dependence of daunorubicin transport in intact MRP overexpressing human small cell lung cancer cells. Biochem Pharmacol. 48**,** 1129-36.

Visanji, N. P., et al., 2013. The prion hypothesis in Parkinson's disease: Braak to the future. Acta Neuropathol Commun. 1**,** 2.

Volpicelli-Daley, L. A., et al., 2014. Addition of exogenous alpha-synuclein preformed fibrils to primary neuronal cultures to seed recruitment of endogenous alpha-synuclein to Lewy body and Lewy neurite-like aggregates. Nat Protoc. 9**,** 2135-46.

Volpicelli-Daley, L. A., et al., 2011. Exogenous alpha-synuclein fibrils induce Lewy body pathology leading to synaptic dysfunction and neuron death. Neuron. 72**,** 57-71.

Watts, J. C., et al., 2013. Transmission of multiple system atrophy prions to transgenic mice. Proc Natl Acad Sci U S A. 110**,** 19555-60.

Wennstrom, M., et al., 2012. Altered CSF orexin and alpha-synuclein levels in dementia patients. J Alzheimers Dis. 29**,** 125-32.

Willis, A. W., et al., 2012. Predictors of survival in patients with Parkinson disease. Arch Neurol. 69**,** 601-7.

Winner, B., et al., 2011. In vivo demonstration that alpha-synuclein oligomers are toxic. Proc Natl Acad Sci U S A. 108**,** 4194-9.

Wright Willis, A., et al., 2010. Geographic and ethnic variation in Parkinson disease: a population-based study of US Medicare beneficiaries. Neuroepidemiology. 34**,** 143-51.

Wyss-Coray, T., Mucke, L., 2002. Inflammation in neurodegenerative disease--a double-edged sword. Neuron. 35**,** 419-32.

Zamanian, M., et al., 2015. Release of Small RNA-containing Exosome-like Vesicles from the Human Filarial Parasite Brugia malayi. PLoS Negl Trop Dis. 9**,** e0004069.

Zheng, W., et al., 2000. Comparative toxicokinetics of manganese chloride and methylcyclopentadienyl manganese tricarbonyl (MMT) in Sprague-Dawley rats. Toxicol Sci. 54**,** 295-301.
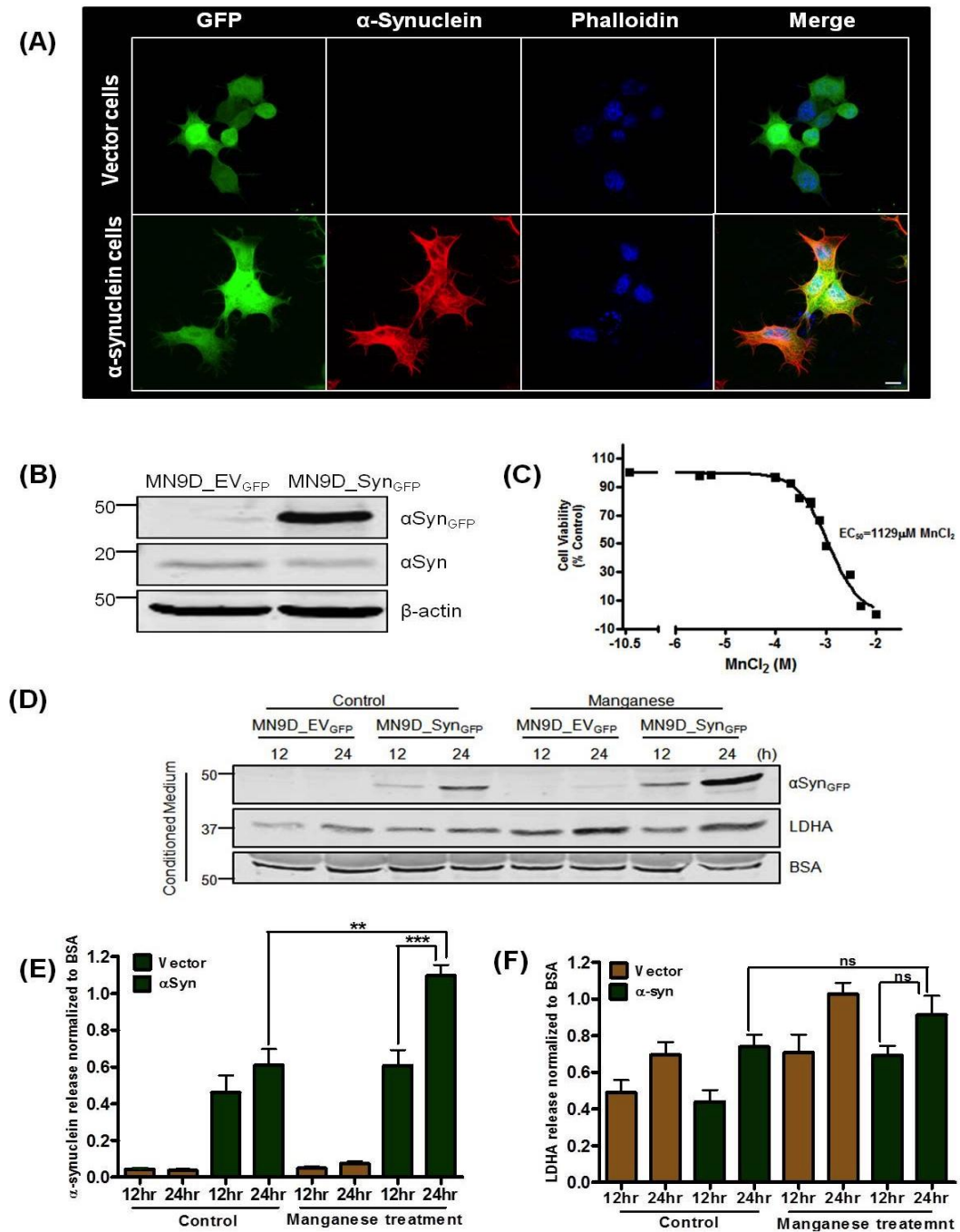
Figure 1: Generation of GFP-tagged stable α-synuclein expressing MN9D cells and manganese-induced α-synuclein secretion.

(A) Immunocytochemical analysis depicting stably expressed GFP-tagged wild-type αSyn protein in MN9D dopaminergic cells. αSyn-expressing cells exhibited strong

ubiquitous expression of αSyn, whereas vector cells showed no detectable αSyn immunoreactivity. (B) Stable expression of αSyn was determined by Western blot analysis. A 45-kDa band corresponding to the molecular mass of GFP-fused αSyn was detected in α-syn expressing cells, whereas no GFP-fused αSyn expression appeared in vector cells. However, both αSyn-expressing and control cells showed low levels of endogenous αSyn expression. (C) Manganese dose-dependent toxicity measured by MTS assay. (D) Increased α-syn release in extracellular media as measured by Western blot. (E-F) Densitometric analysis of a-syn and LDH respectively released in extracellular media normalized to BSA.
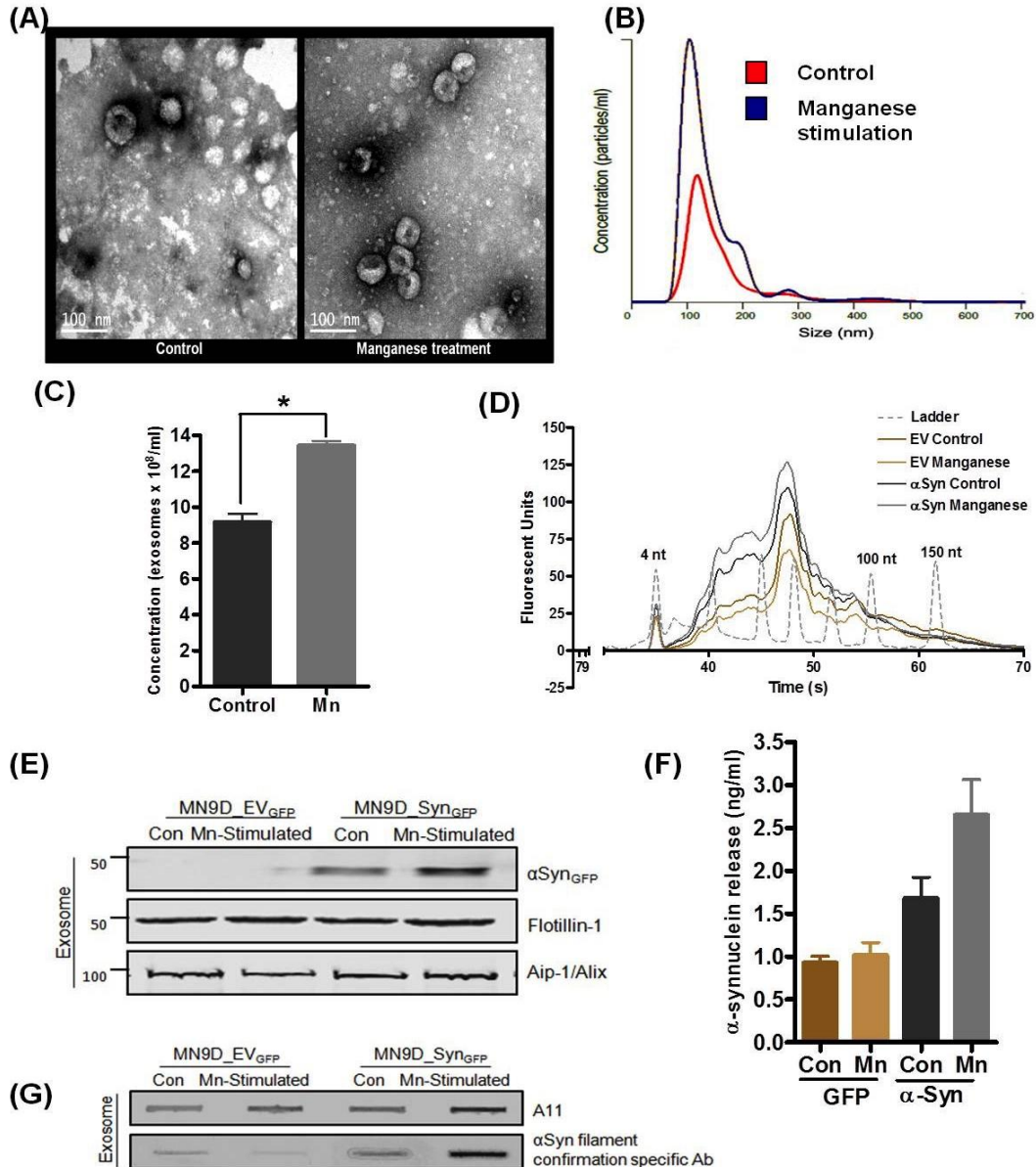
Figure 2: Manganese induces exosomes release from neuronal cells.

(A) Electron micrograph of isolated exosomes revealing that transmission electron microscopy of ultracentrifuged conditioned medium readily detected exosomes. (B) Nanosight-generated histogram of particle size and abundance of isolated exosomes. (C) Exosome concentrations showing that manganese exposure upregulated the release of exosomes into the extracellular micro-environment. (E) Western blot analysis shows

exosomal surface membrane protein markers alix and flotillin-1 in all exosomes samples and elevated αSyn in manganese stimulated αSyn-pmaxGFP exosomes.

(G) Slot blot analysis showing higher oligomeric protein accumulation in exosomes isolated from manganese-stimulated exosomes from both αSyn-pmaxGFP and control pmaxGFP cells relative to vehicle-treated αSyn-pmaxGFP and control pmaxGFP cells. However, exosomes from manganese-stimulated αSyn-pmaxGFP indicate greater accumulation of prefibrillar oligomeric protein.
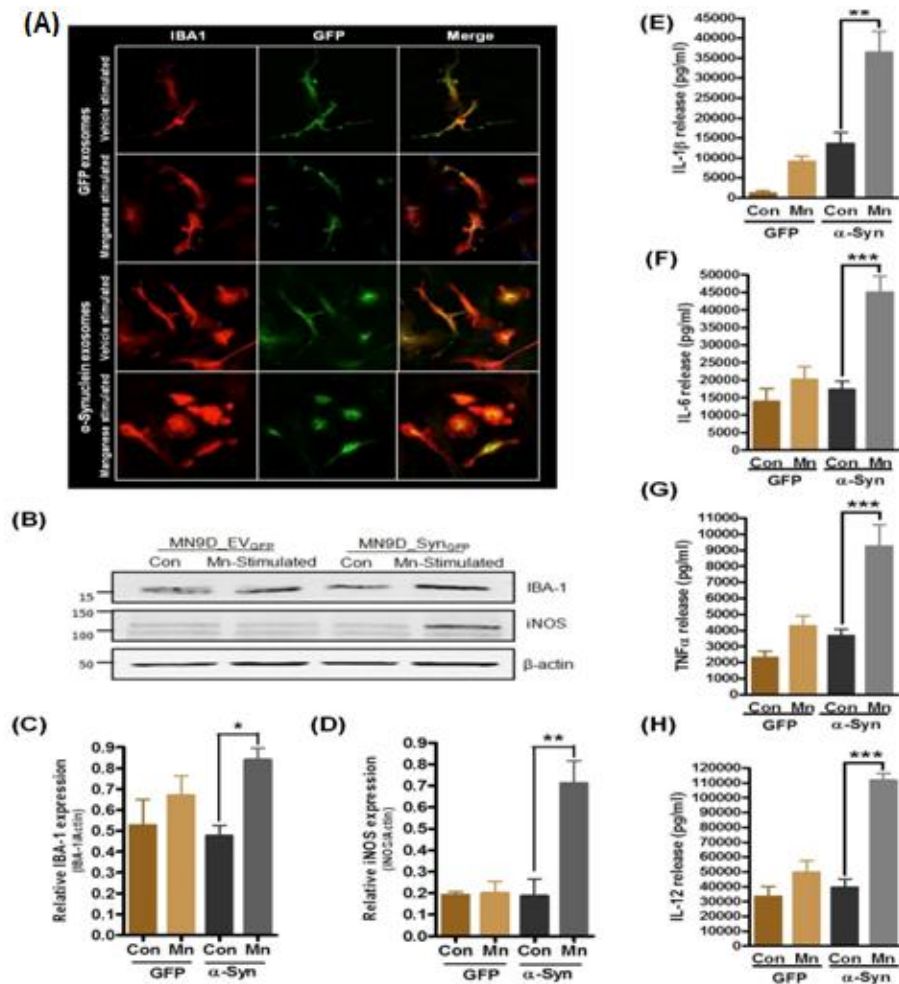
Figure 3: (A) Immunocytochemical analysis depicting activation of microglia upon Mn stimulation only in the presence of αSyn exosomes. (B-D) Increased protein expression

of IBA-1 and iNOS in Mn-stimulated MN9D_SynGFP cells compared to MN9D_EVGFP and control treated MN9D_SynGFP cells. (E-H) Increased cytokine release from Mn-stimulated MN9D_SynGFP cells compared to vehicle stimulated MN9D_SynGFP cells.
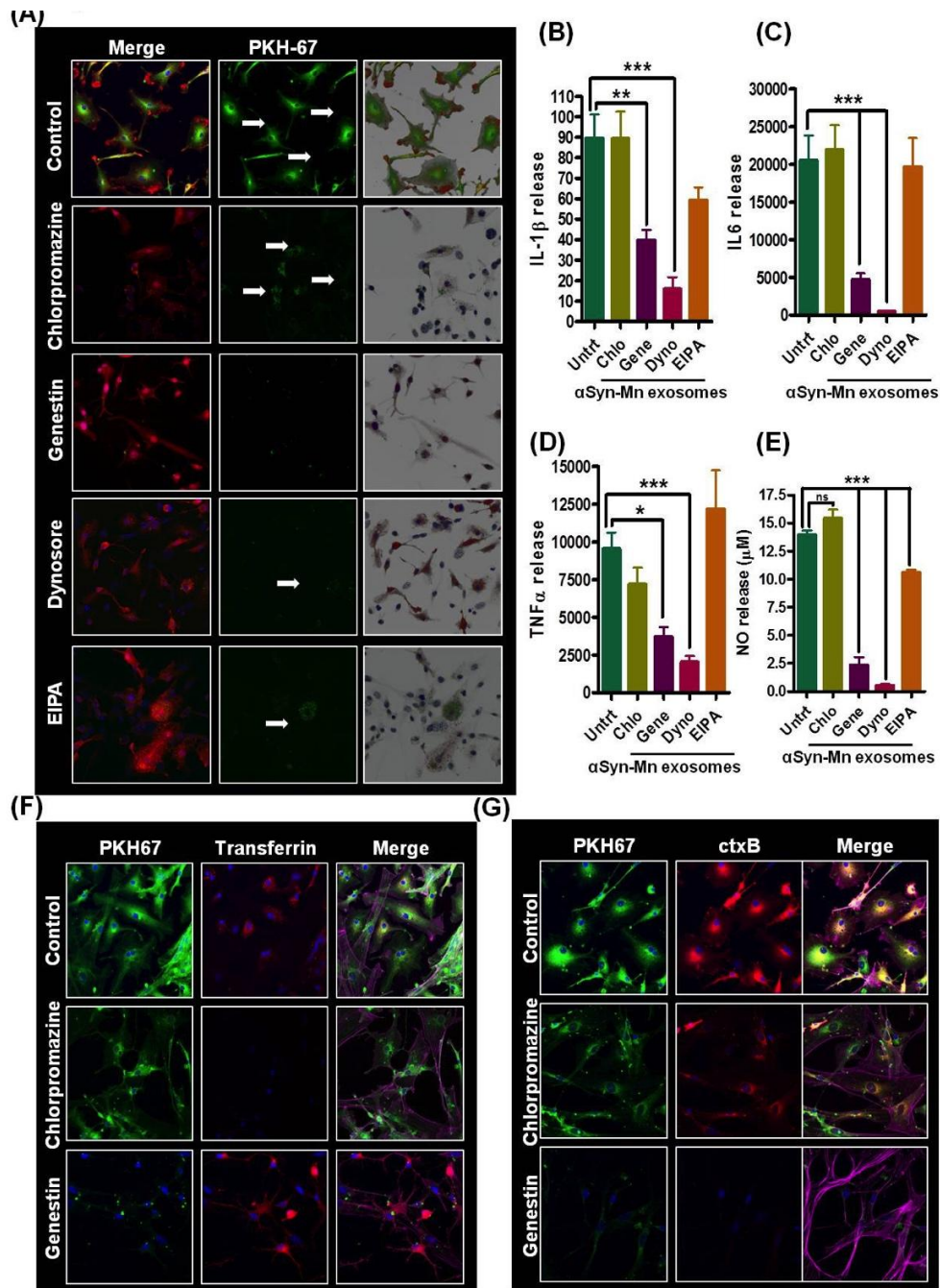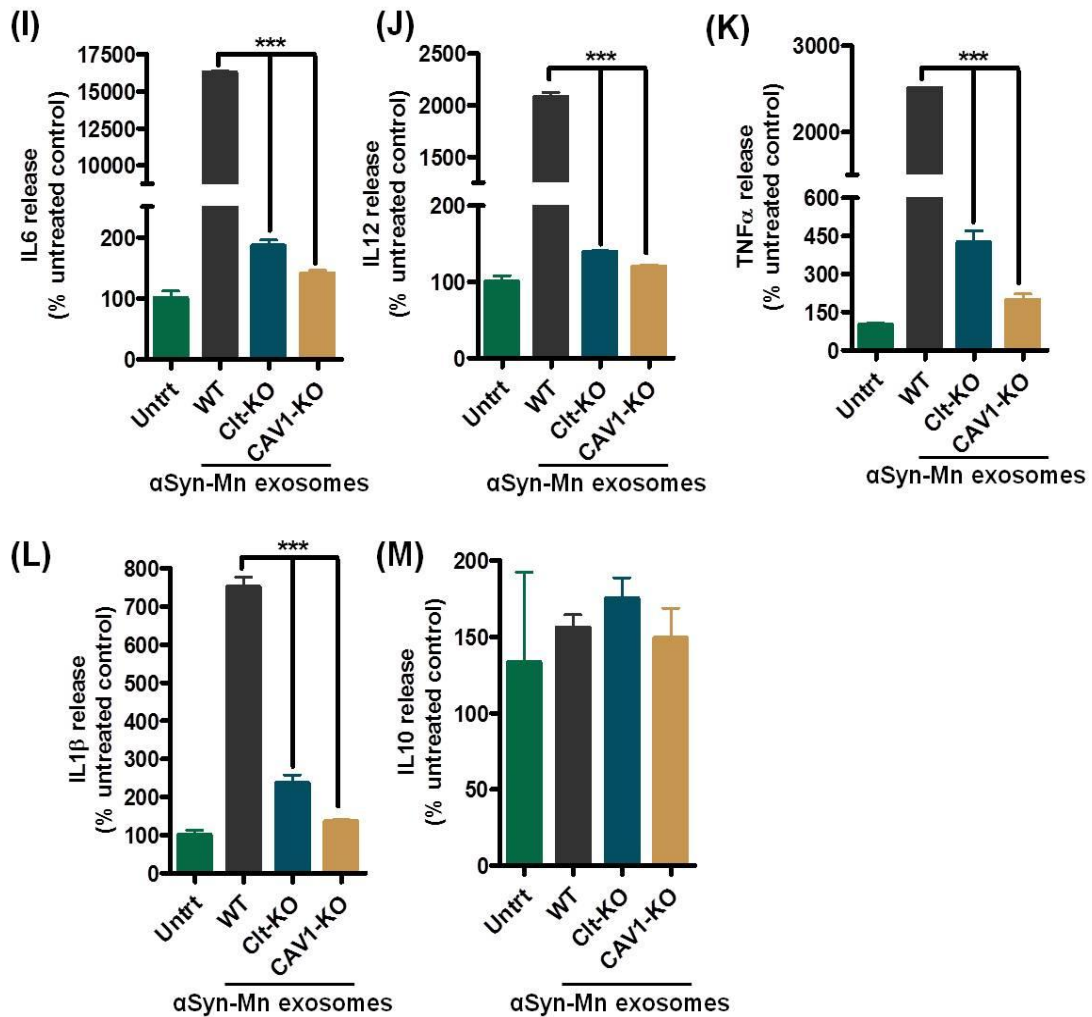
Figure 4: Exosome extry into neurons is primarily mediated by caveolin-mediated endocytotis. (A) Micorglia cell treatment with different endocytosis inhibitors. (B-E) Luminex cytokine analysis upon exosome treatment. (F-G) Selective inhibiton of Clathrin and caveolin1 endocytosis. (I-M) Decreased cytokine release from Clathirin and especially Caveolin knock-out MN9D cells exposed to exosomes collected from αSyn expressing MN9D cells exposed to Mn.
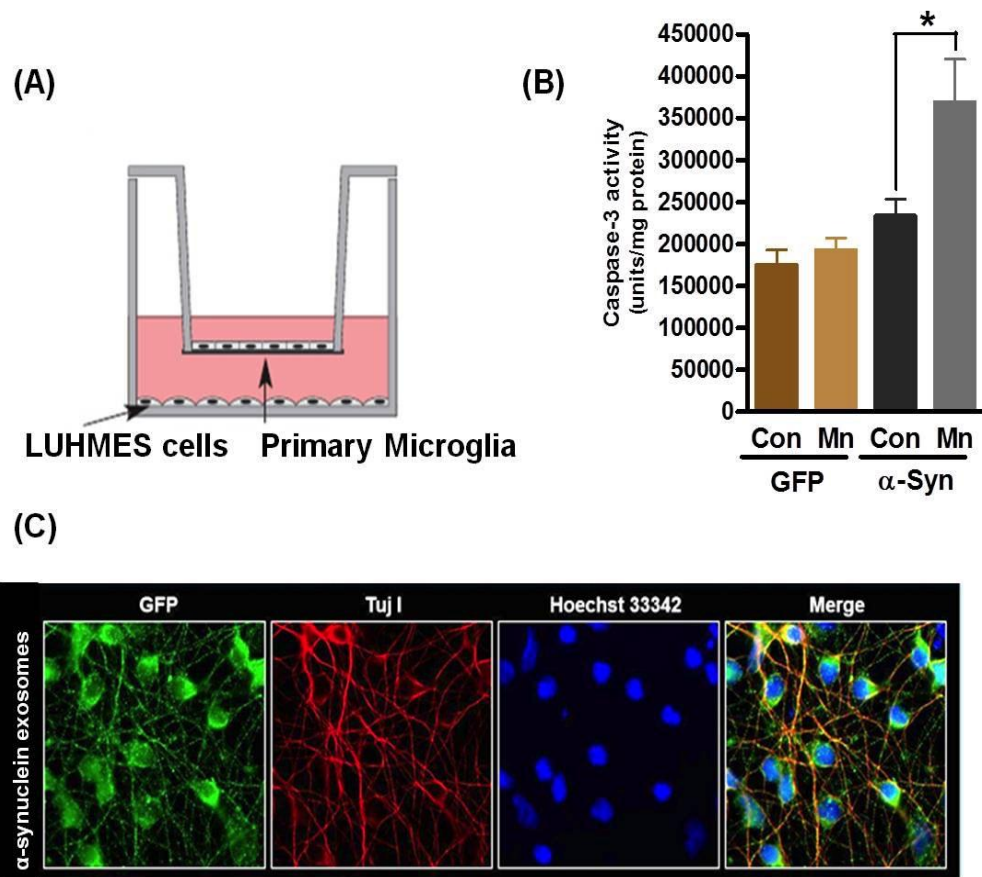
Figure 5: (A) Schematic representation of co-culture of LUHMES and primary microglia. (B) Increased caspase-3 activity in Mn-stimulated co-culture system pre-treated with αSyn exosomes. (C) Immunocytochemical analysis of LUHMES treated with GFP tagged exosomes.
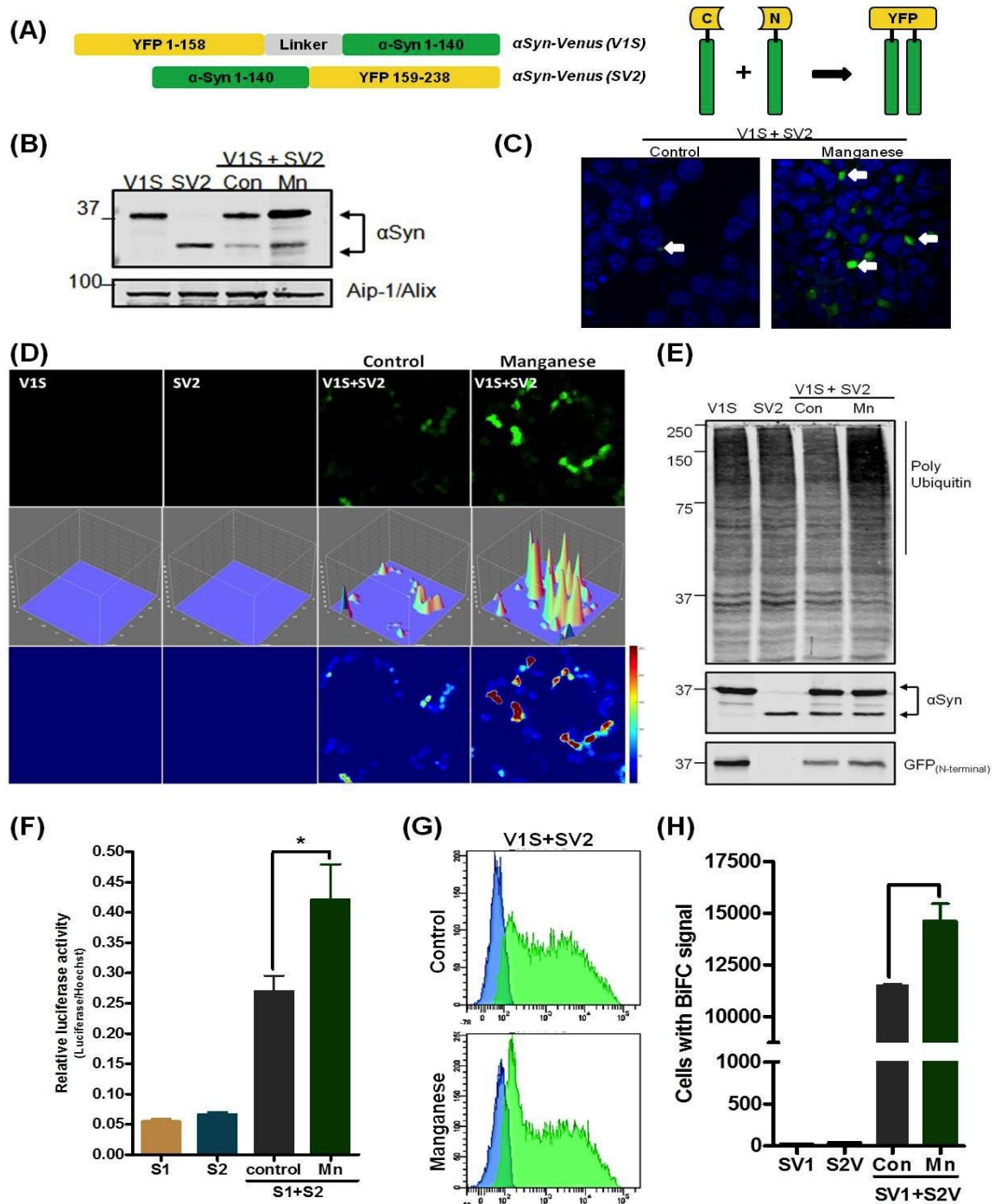
Figure 6: Increased cell to cell transmission of αSyn occurs upon Mn-stimulation

(A) Coordinates from bregma
AP -3.30
ML -1.20
DV -4.60

(B) Stereotaxic injection of AAV-V1S and AAV-SV2 — Manganese oral gavage — Study termination
Day 0 — Day 30 — Day 60
Mn (15mg/Kg/day)
Behavior analysis and tissue collection

(C) VenusYFP/ TH/ Hoechst

(D) Vehicle treatment / Manganese treatment

(E) Integrated fluorescence density — Control, Mn — AAV_V1S + AAV_SV2

(F) No injection (Control, Manganese) / AAV_V1S + AAV_SV2 (Control, Manganese)

(G) No injection (Control, Manganese) / AAV_V1S + AAV_SV2 (Control, Manganese)

(H) TH-positive neurons — Con, Mn, Con, Mn — V1S + SV2

190

www.manaraa.com

(I) **(J)** **(K)**

Figure 7: Direct detection of manganese-induced cell-to-cell transmission of α-synuclein oligomers and associated neurotoxicity *in vivo*. (A-B) Schematic representation of stereotaxic injection site and Mn-expoosure timeline. (C-D) 60 days post-viral injection, VenusYFP fluorescence is visible in the substantia nigra pars compacta (SNpc) of animals injected with AAV-CBA-VenusYFP. (F) Open-field test showing decreased locomotor activity of aSyn treated and Mn-exposed mice compared to vehicle exposed controls. (G-H) Loss of TH positive neurons in the substantia nigra assessed by DAB staining and stereological counts respectively. (I-K) Open field behavior of aSyn injected mice exposed to Mn shows decreased movement and motor behavior upon exposure to manganese.
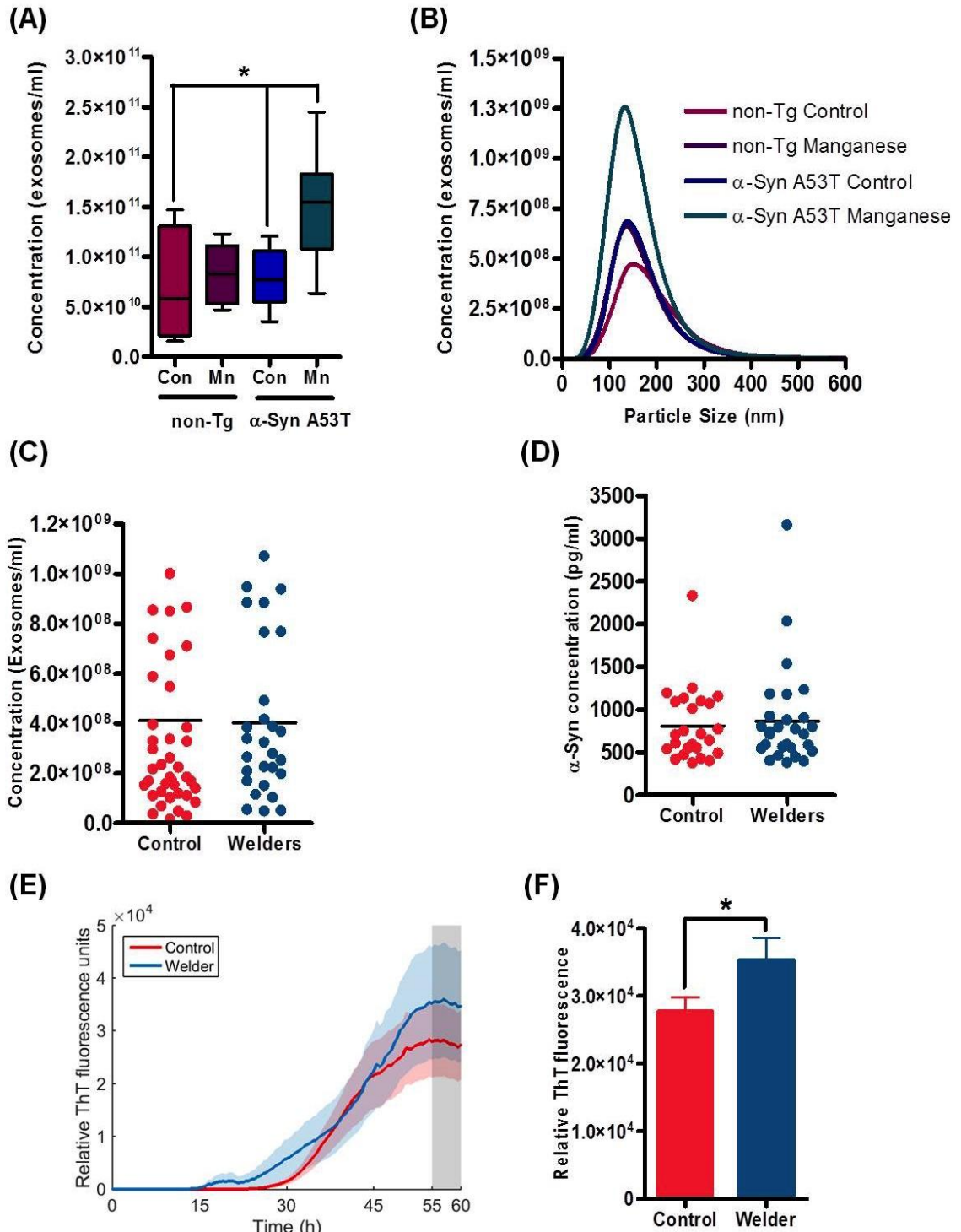
Figure 8: Manganese exposure promotes exosome release in transgenic animals and

αSyn oligomer transmission in humans: (A-B) Higher exosomes counts seen in Mn

challenged αSyn-A53T transgenic rats compared to either vehicle-treated transgenic rats

or non-transgenic rats. (C) Exosome counts of welders and age-matched controls by nanoparticle tracking analysis. No difference between either groups is seen. (D) No significant increase in the packaging of aSyn is seen between welders and controls. (E-F) ThT fluorescence measured by RTQuik of exosomes isolated from welders showing higher seeding capacity and misfolded αSyn protein content compared to exosomes isolated from healthy controls
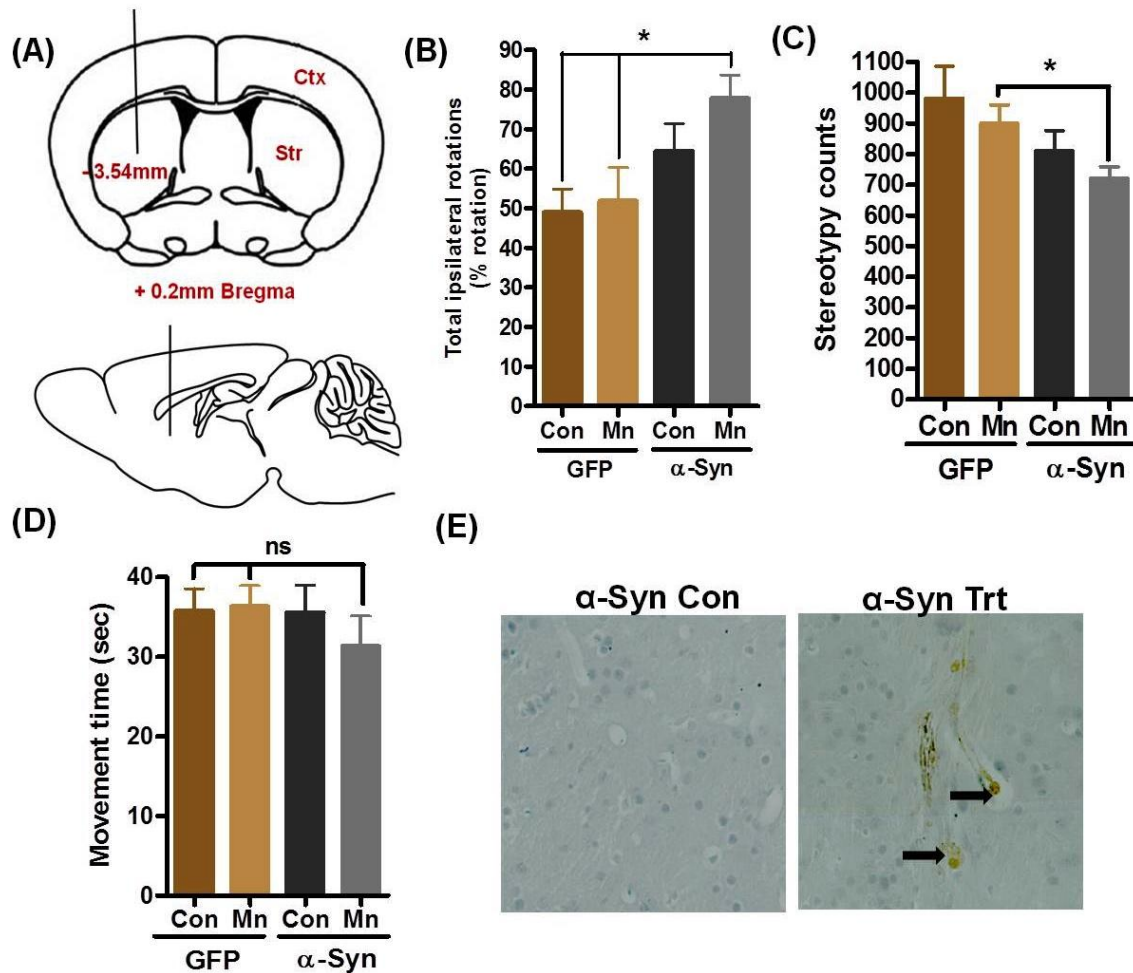
Figure 9: Manganese-stimulated exosomes induce motor deficits in mouse models of PD. (A) Pictoral representation of stereotaxy injection site in mice. (B) Rotameter readings showing greater ipsilateral rotations in amphetamine exposed mice denoting greater unilateral lesions in the brains of Mn-stimulated αSyn mice.(C-D) Reduced

exploratory locomotor activity seen in mice receiving Mn-stimulated αSyn exosomes as measured by stereotypy counts, movement time. (E) $αSyn(Ser(p)^{129})$-immunoreactive cytoplasmic inclusions detected in mice injected with Mn-stimulated αSyn exosomes compared to vehicle-stimulated αSyn exosomes or vehicle- and Mn-stimulated GFP exosomes injected mice.
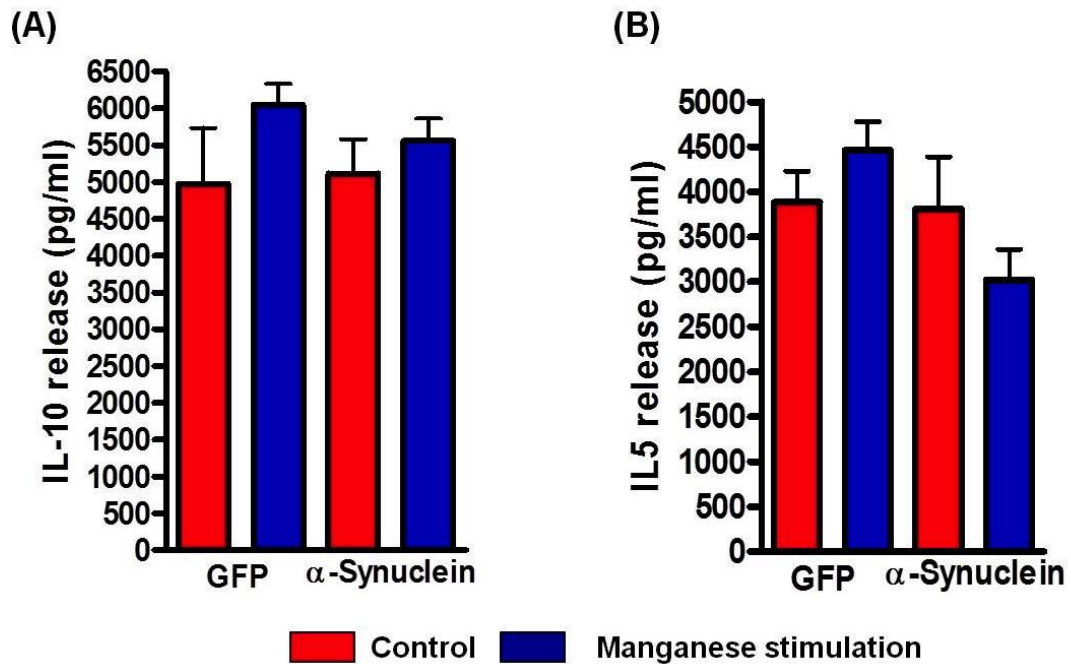
Supplementary figure 1: No change seen in serum IL-10 and IL-5 levels in vehicle or Mn-stimulated GFP/αSyn mice.

(A)

(B)
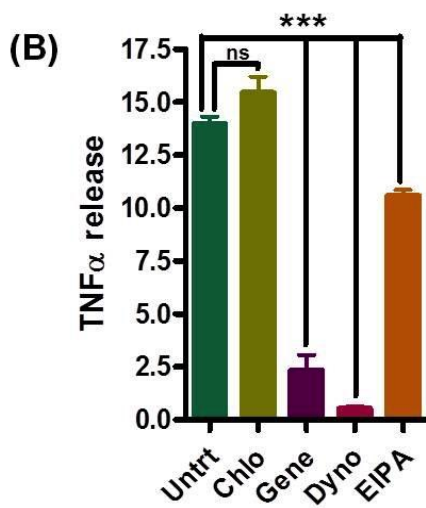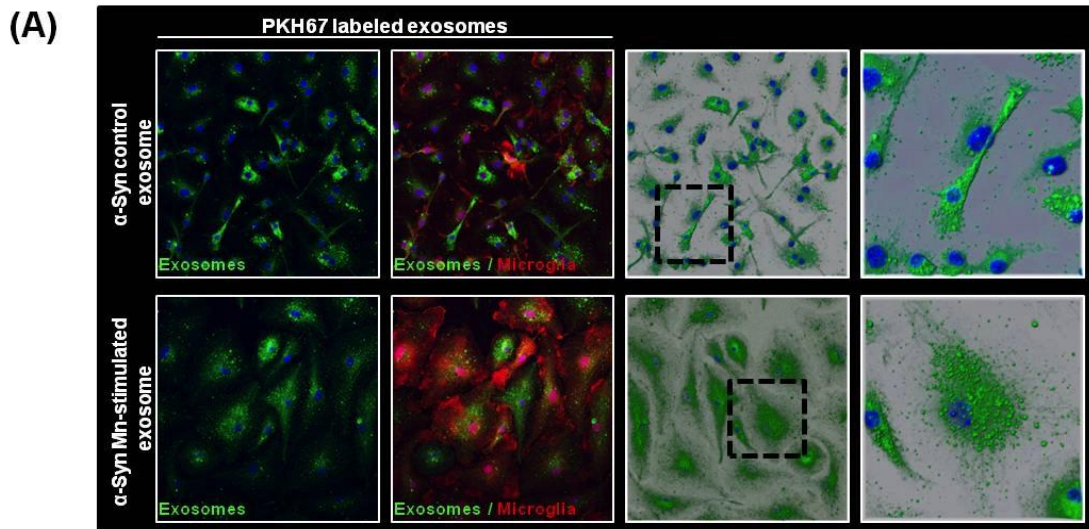
Supplementary figure 2: Confocal microscopy revealed efficient internalization of the vehicle- and Mn-stimulated αSyn-containing exosomes by the WTMC cell line.

CHAPTER IV

ENVIRONMENTAL NEUROTOXICANT MANGANESE INCREASES EXOSOME-MEDIATED MIRNA DELIVARY AND AUTOPHAGIC REGULATION IN CELL CULTURE MODEL OF PARKINSON'S DISEASE.

Dilshan S. Harischandra[1], Mostafa Zamanian[2], Dharmin Rokad[1], Shivani S. Ghaisas[1], Arthi Kanthasamy[1], Huajun Jin[1], Vellareddy Anantharam[1], Michael J Kimber[1], Anumantha Kanthasamy[1*]

[1]Department of Biomedical Sciences, Iowa Center for Advanced Neurotoxicology, Iowa State University, Ames, IA – 50011, [2]Department of Molecular Biosciences, Northwestern University Evanston, IL 60208

*Corresponding author:

Dr. Anumantha G. Kanthasamy, Distinguished Professor and Lloyd Chair,

Parkinson's Disorder Research Laboratory,

Iowa Center for Advanced Neurotoxicology,

Department of Biomedical Sciences,

2062 Veterinary Medicine Building,

 Iowa State University,

Ames, IA 50011, U.S.A.

 Phone: 1-515-294-2516;

Fax: 1-515-294-2315;

Email:akanthas@iastate.edu

Abstract

Many age-related neurodegenerative disorders share a common pathogenic mechanism involving the aggregation and deposition of misfolded proteins. In Parkinson's disease (PD), the accumulation of misfolded and aggregated α-synuclein (αSyn) is considered a key pathophysiological feature. Generally, these misfolded proteins can be degraded by autophagy via the lysosomal pathway. However, the lysosomal degradation pathway is impaired in the disease state, leading to a significant accumulation of autophagic vesicles in the neuronal body. Considering the role of the divalent metal manganese (Mn) in PD-like neurological disorders, we characterized the effect of Mn on misfolding as well as its role in autophagic/lysosomal dysfunction using a MN9D dopaminergic cell model of PD, which stably expresses wild-type human αSyn. Western blot analysis revealed that Mn increased the expression of the autophagosomal markers LC3-II and Beclin-1, whereas the lysosomal marker LAMP2 was downregulated in αSyn-expressing cells relative to vector control cells, suggesting that Mn treatment impairs the autophagic/lysosomal degradation pathway. Interestingly, Mn treatment also induced the release of αSyn-containing exosomes into the extracellular media, as determined by NanoSight particle analysis and electron microscopy. Furthermore, we found these αSyn-containing exosomes are bioactive and able to induce neuroinflammatory response and neurodegeneration in cell culture models of PD. To further elucidate the molecular mechanisms underlying Mn-induced autophagic/lysosomal dysregulation, we performed next-generation miRNA sequence analysis of manganese- and vehicle-stimulated exosomes. We identified 43 miRNAs differentially expressed in Mn-stimulated αSyn exosomes as compared to control exosomes. Among them, 12 mRNAs were associated

with regulation of autophagic/lysosomal degradation pathway. Three miRNAs (miRNAs124, 320a and 325) were previously reported to control autophagic regulation by targeting Bim, Hsc70 and E2F1 in experimental models of PD. Collectively, our results suggest a novel paradigm in which dysregulation of exosomal miRNA pertaining to autophagic degradative machinery may play a role in cell to cell transmission of misfolded αSyn protein.(NIH ES19267 ES10586, and NS088206, Lloyd Chair)

Introduction

Chronic exposure to high concentrations of metal manganese (Mn) can cause neurotoxicity and manganism, neurological syndrome consists of movement abnormalities that shares many parkinsonian features although it may not represent clinical Parkinson's disease (PD) because lack of nigrostriatal dopaminergic neuron damage and classic response to levedopa. Current evidence also indicate that primates exposed to manganese do not release dopamine, a key neurotransmitter necessary for normal motor function, when stimulated suggesting the dysfunctional dopamine system even though the neurons do not show the damage present with PD (El-Agnaf et al., 2003). Therefore, manganese-induced Parkinsonism predilection to accumulate in and damage the globus pallidus and striatum rather than the sunstancia nigra (SN) as does in PD. Therefore, given the Mn deposition in the globus pallidus and associated increased T1-weighted MRI signal in the extra-pallidal basal ganglia (caudate and putamen) has been studied as potential marker of neurotoxicity associated with manganese exposure. However, in clinical settings, differential diagnosis of manganese-induced Parkinsonism is primarily based on the Unified Parkinson Disease Rating Scale, motor subsection 3

(UPDRS3), a clinical rating scale associated with motor functions. Nevertheless, due to the fact UPDRS3 scale can only be applied when motor symptoms are present and MRI is expensive method yet not accessible throughout the world, and effectiveness of the current biomarker to detect Parkinsonism as early diagnosis criteria is not feasible.

Since there are no reliable quantitative diagnostic tests for these neurological disorders, molecular biomarker discoveries are important and potentially could be used to diagnose Parkinsonism in early stages. However, current candidate biomarkers are heavily based on individual proteins related to pathogenesis of PD in CSF and brain tissues, which often involve invasive techniques and surgeries. Therefore, the development and validation of noninvasive screening tests capable of detecting neurodegenerative diseases during early, presumably asymptomatic stage is important. Thus, blood based assays for diagnoses of neurodegenerative diseases are particularly interesting and informative to assay biomarkers such as proteins, antibodies and circulating miRNAs.

miRNA is a class of non-coding RNA, whose final product is an approximately 18-22 nucleotides long functional RNA molecule. miRNA repress translation and regulate degradation of their target mRNA by binding complementary regions of messenger transcripts. Research in various disease processes from cancer to cardiovascular disease has found that miRNAs play a role in disease pathogenesis and have potential as biomarkers and therapeutic agents. Recently, number of miRNA expression changes reported in different brain areas involved in AD development (Kordower et al., 2008) and comprehensive review by Tan et al 2013 (Kordower et al., 2008) identify the involvement of miRNA in the development of AD such as accumulation of amyloid-β,

tau toxicity, neuroinflammation and cell death. Identification of miRNA involvement in PD has been focused on miRNA expression in the midbrain and the role of miRNA for the functioning of doperminergic neurons. In late 2007 Kim and colleagues identified miR-133b that is specifically expressed in the midbrain doperminergic neurons in healthy adults were deficient in midbrain tissues isolated from PD patients (Li et al., 2008). Since then, several miRNAs controlling autophagy regulation (miR-124, miR-320a and miR-325) and α–synuclein synthesis (miR-7 and miR153) in experimental models of PD have been identified. Furthermore, a recent miRNA research looked at global miRNA expression patterns in circulating miRNAs in PD patients and age matched healthy individuals resulting in the identification of PD-predictive biomarkers k-TSP1 (miR-1826/miR-450b-3p), miR-626, and miR-505, with highest predictive power of 91% sensitivity and 100% specificity, bringing forth the ossiblity of diagnostic approach based on analysis of miRNAs in plasma (Bae et al., 2014). Importantly, studies have shown that circulating miRNA signatures discriminate PD from Multiple System Atrophy (MSA), patients and healthy controls providing further strengthening the idea of using miRNA differential diagnosis in diseases that have similar clinical and pathological resemblance (Danzer et al., 2012). Therefore, peripheral blood is important as a source of non-invasive biological sample to facilitate miRNA biomarker discoveires in humans, as well their future clinical applicability.

miRNAs are also found in blood,(Chen et al., 2008; Lawrie et al., 2008; Mitchell et al., 2008) and such circulating miRNAs are remarkably stable even under harsh conditions,(Chen et al., 2008; Mitchell et al., 2008) suggesting possible novel diagnostic potential of circulating miRNAs. Circulating miRNAs have been detected in plasma,

serum, urine, and saliva where they are protected from degradation by membranes of the exosomes and other microvesicles that contain them. Exosomes are nano-sized vesicles (50-250 nm) that are released from many cell types into the extracellular space. These vesicles are widely distributed in various body fluids and can easily cross the blood–brain and other barriers. Tremendous interest has emerged in recent years on exosome research because of its potential role in disease pathogenesis and biomarker discovery.(Alderton, 2015; Anastasiadou and Slack, 2014; Couzin, 2005; Minton, 2015; Thery et al., 2002) There are numerous examples of miRNA's as putative biomarkers of occupational and environmental exposures to polycyclic aromatic hydrocarbons,(Deng et al., 2014) dioxin,(Feitelson and Lee, 2007) metal rich particulate matter,(Volinia et al., 2006) arsenic,(Dai et al., 2009) and many others.(Vrijens et al., 2015) Growing evidence suggests that miRNAs play a significant role in the pathogenesis of many chronic diseases, including PD. For example, there are differences in miRNA expression in the midbrain and in circulating plasma miRNAs in PD patients compared to control subjects.(Cardo et al., 2013; Khoo et al., 2012; Kim et al., 2007) Circulating miRNA signatures can also discriminate PD patients from Multiple System Atrophy patients,(Vallelunga et al., 2014) demonstrating the feasibility of using circulating miRNAs as a biomarker to distinguish between diseases that share similar clinical and pathological features. Recently, several miRNAs regulating the synthesis of α-synuclein (αSyn), the hallmark protein of PD, as well as autophagy and apoptosis, were identified in experimental models of PD.(Alvarez-Erviti et al., 2013; Heman-Ackah et al., 2013; Kabaria et al., 2015; Wang et al., 2015) Yet, despite its prevalence, and thus potential risk

to human health, the mechanisms by which manganese exerts its neurotoxic factors effects by αSyn secretion and transmission is not well studied thus far.

Hence, in this study, we use manganese as environmental neurotoxicant to induce αSyn aggregation, secretion and cell-to-cell transmission miRNAs to manipulate recepeant cell gene expression via exosomes. To elucidate the molecular mechanisms of manganese-induced neurotoxicity, we used miRNA deep sequencing and custom miRNA PCR array technology to investigate role of exosomes in cell-to-cell transmission of miRNAs.

Materials and Methods

Chemical and Reagents

All chemicals were purchased from Sigma-Aldrich and reagents related to cell cultures were obtained from Invitrogen unless otherwise specified.

Cell culture and stable expression of αSyn

For αSyn release and exosome isolation experiments, we created a GFP-tagged αSyn stably-expressing MN9D cell line. Expression plasmids for human full-length αSyn-pMAXGFP and control pMAXGFP vectors (Lonza) were transfected into MN9D cells using Lipofectamine 2000 reagent (Invitrogen) and grown in DMEM (D5648; Sigma) supplemented with 50 IU/ml penicillin, 50 μg/ml streptomycin, and 10% FBS. For stable transfection, MN9D cells were selected after culturing in 400 μg/ml of geneticin for one week post-transfection, and then selected cells were cultured in media supplemented with 200 μg/ml of geneticin to maintain the stable transfection. GFP-positive αSyn-expressing (MN9D_Syn$_{GFP}$) and vector control (MN9D_EV$_{GFP}$) cells were further selected by

FACSAria III (BD Bioscience) high-speed sorting flow cytometer to obtain homogeneously transgene-expressing cell populations.

Western and slot blotting

Whole cell lysates or exosome lysates were prepared using modified RIPA buffer containing protease and phosphatase inhibitor cocktail (Thermo Scientific, Waltham, MA), as described previously (Emmanouilidou et al., 2010; Lee et al., 2010). For αSyn release experiments, cells were treated in serum-free medium spiked with 0.025 mg/ml BSA, and then at the end of their incubation, the media was collected and centrifuged for 5 min at 3000 x g to remove any dislodged cells or cell debris. The conditioned media was concentrated using 5000 MWCO Vivaspin-20 spin columns (GE Lifescience), and then protein concentrations were determined with the Bradford protein assay kit (Bio-Rad). Cell lysates containing equal amounts of protein were separated on a 12-15% SDS-polyacrylamide gel. After separation, proteins were electro-blotted onto a nitrocellulose membrane, and nonspecific binding sites were blocked by treating with LI-COR blocking buffer. Syn-1 (BD Bioscience), Flotillin (BD Bioscience), BSA (Invitrogen), LDHA (Cell Signalling), Aip1/Alix (Millipore), IBA-1 (Wako), iNOS (Santa Cruz) and β-actin (Sigma) primary antibodies were used to blot the membranes.

Oligomeric proteins treated with manganese were analyzed with a slot blot apparatus (Bio-Dot, Bio-Rad) using the antibody against protein Oligomers (A11) (Invitrogen). Following protein adsorption, membranes were blocked with 5% BSA and incubated overnight with the A11 antibody. Membranes were then developed with IR800-conjugated anti-rabbit or Alexa Fluor 680-conjugated anti-mouse secondary antibody for

1 h at room temperature. Western and slot blot images were captured with the Odyssey IR Imaging system (LI-COR) and data were analyzed using Odyssey 2.0 software.

Immunocytochemistry and Immunohistochemistry

For immunocytochemistry, MN9D cells and microglia cells were plated on 50 μg/mL PDL-coated 12-mm glass coverslips and treatments were done as described. LUHMES cells were plated on coverslips pre-coated with 50 μg/mL poly-l-ornithine (Sigma-Aldrich) overnight, washed twice with cell culture grade water (Invitrogen) at the end of the incubation and incubated with 1 μg/mL fibronectin (Sigma-Aldrich) overnight. After treatments, cells were washed with PBS and incubated in 4% paraformaldehyde for 30 min at room temperature. After fixing, the cells were washed with PBS and incubated in blocking agent (2% BSA, 0.05% Tween-20, and 0.5% Triton X-100 in PBS) for 45 min. Cells were then incubated with antibodies against human α-synuclein (Syn211; Santa Cruz, 1:500), GFP (Abcam 1:2000), IBA-1 (Wako, 1:500) overnight at 4°C or the cytoskeleton marker Phalloidin (Alexa Fluor 647 phalloidin, Invitrogen) for 30 min at room temperature. After primary incubation, the cells were washed and incubated in the dark for 90 min with Alexa-488 and -555 dye-conjugated secondary antibodies (Invitrogen, 1:1000). Hoechst 44432 was used as a nuclear stain and the coverslips were then mounted on glass slides and viewed with 63× and 43× oil objectives using a Leica DMIRE2 confocal microscope.

Exosome isolation

Cell-produced exosomes were isolated using ExoQuickTC (System Biosciences) reagent or were purified by differential ultracentrifugation via slight modification of a process

described by Emmanouilidou *et al.* (2010). Briefly, MN9D_Syn$_{GFP}$ and MN9D_EV$_{GFP}$ cells at 70-80% confluency were treated with or without 300 µM manganese in exosome-depleted medium containing 10% FBS for 24 h. After treatment, cell culture supernatant was collected and spun at 300 x g for 10 min to remove cells and 10,000 x g for 15 min to exclude cell debris from the supernatant. The resulting media was then passed through a 0.2-µm syringe filter (Millipore) to remove any remaining particles or cell debris, and the filtrate was centrifuged at 100,000 x g for 90 min using a Beckman Optima L-100 XP ultracentrifuge. The pellet containing exosomes was washed once with cold PBS and centrifuged again at 100,000 x *g* for 90 min using a Beckman optima MAX ultracentrifuge. Exosome pellets were resuspended in 50 µl of *Radioimmunoprecipitation assay* (RIPA) buffer for Western blot analysis, or when treating primary microglia cells, they were resuspended in 150 µl of DMEM-F12. Total serum exosomes were isolated using ExoQuick (System Biosciences) reagent following the manufactures' recommended protocol.

Nanoparticle tracking analysis (NTA)

Ultracentrifuged or ExoQuick/TC-precipitated exosome samples were used for NTA, as previously described (Su et al., 2008). Briefly, isolated exosomes were resuspended in 500-1000 µL PBS, from which approximately 300 µL was loaded into the sample chamber of an LM10 unit (Nanosight, Amesbury, UK) using a disposable syringe. Sample durations of 30-60 sec per sample were analyzed with NTA 2.3 software (Nanosight). Samples containing higher numbers of exosomes were diluted before the

analysis and their relative concentrations were then calculated according to the dilution factor.

Transmission electron microscopy (TEM)

Purified exosomes were resuspended in 200 μl PBS. We mixed 20 μl of each sample with uranyl acetate 2% (w/v), incubated them for 5 min, and then 5 μl were applied to carbon-coated copper grids. Images were taken using a JEOL 2100 200 kV scanning and transmission electron microscope (STEM) with a Thermo Fisher Noran System 6 elemental analysis system. TEM was operated at 80 kV and images were obtained at 18000-20000 x magnification.

Exosomal RNA extraction and characterization

For detection of RNA species in exosome samples isolated from manganese-stimulated αSyn-pMAXGFP and control pMAXGFP cells or vehicle-treated αSyn-pMAXGFP and control pMAXGFP cells, we used the miRCURY RNA isolation kit (Exiqon; 30010) according to the manufacturer's protocols. After extraction, a Nanodrop spectrophotometer used initially to determine the concentration and quality of the RNA preparation. Then RNA quality, yield, and size of exosomal small RNA were analyzed using the Agilent 2100 Bioanalyzer (Agilent Technologies, Foster City, CA) with the Agilent RNA 6000 Nano Kit as described previously (Danzer et al., 2012). Next generation sequencing of exosomal RNA

Upon manganese stimulation, whole conditioned media sent to SBI bioscience for exosome isolation, preparation of exoRNA libraries compatible with sequencing on

Illumina NGS platform. The amplified indexed libraries are then resolved in a polyacrylamide gel from which the desired bands are excised in a streamlined gel purification method. The recovered amplified libraries are then ready for analysis on the Illumina sequencing platforms (HiSeq, MiSeq, and Genome Analyzer II) with about 300M reads per sample in order to generate substantial sequencing depth. After sequencing, reads can be de-multiplexed based upon their unique index sequence and then assigned to their appropriate input samples identities. Using Maverix exoRNA analysis pipeline (Maverix Biomics; San Mateo, CA), sequences are mapped to a reference genome of choice to determine sequence identities and relative abundances of various RNA types such as ncRNAs, antisense transcripts, and miRNAs.

MicroRNA (miRNA) profiling and data validation

Total RNA that includes small non-coding miRNA was purified from exosomes isolated from untreated and manganese stimulated αSyn-pMAXGFP cells using miRCURY RNA isolation kit (Exiqon; 30010) following manufacturer's instructions. Post-isolation, RNA quality was determined using a Nanodrop 2000 instrument. For miRNA validation studies, SYBR green based custom miScript miRNA PCR Array (Qiagen, MD) was used. The custom miScript miRNA PCR Array allows the simultaneous detection of 41miRNAs previously identified in through our exosome miRNA NGS studies, as well as appropriate housekeeping assays and RNA quality controls. Diluted cDNA was mixed with universal primer and SYBR Green dye and added to the wells of 96-well plates containing lyophilized primer. The plates were run on a Stratagene Mx3005P instrument (Agilent technologies) and the expression of individual miRNAs was analyzed using the

obtained C_t values. As a normalizer, SNORD61 was used as a housekeeping miRNA. The plate assay was performed according to the manufacturer's protocol and fold changes in miRNA expression were calculated using the C_t value of the normalizer control

Statistical analysis

Prism 4.0 software was used to analyze data from two or more independent experiments, each with $n \geq 6$. Bonferroni's multiple comparison testing was used to find significant differences between treatment and control groups. Differences with $p < 0.05$ were considered significantly different

Results

Manganese exposure upregulates the release of αSyn into the extracellular milieu.

A transgenic cell line constitutively expressing GFP-tagged human wild-type αSyn was established by stably transfecting MN9D mouse dopaminergic cells with either plasmid pMAXGFP_αSyn or pMAXGFP_EV (empty vector). MN9D cell line is a widely used cell model in the area of PD research. Immunocytochemical analyses indicate that >90% of the pMAXGFP_αSyn cells were positive for the transgene human αSyn, and that all pMAXGFP cells were positive for GFP (Fig. 1A). Further analysis through Western blot indicates a low level expression of endogenous αSyn in both cell types and a strong expression of higher molecular weight GFP-tagged αSyn in pMAXGFP_αSyn (Fig. 1B).

Manganese induces exosomes release from neuronal cells.

To further investigate the underlying molecular mechanisms of αSyn secretion and its relevance in the progression of PD, we looked in to the possible mechanisms of cargo used in αSyn secretion. For this, we analyzed the conditioned media collected from

manganese-or vehicle treated cells through TEM followed by differential ultracentrifugation. Our results indicate the presence of nano-scale exosome vesicles morphologically similar to previously reported exosomes in both vehicle and manganese treated samples (Fig. 3A, Supplementary Fig 1A) (Emmanouilidou *et al*., 2010). Since exosomes reportedly contain a unique RNA profile distinct from that of host cells (Valadi *et al.*, 2007), we further analyzed the exosomes for small noncoding RNAs, such as microRNAs (miRNA). Exosomal RNA was isolated using the mirVanaTM miRNA isolation kit and small RNAs were analyzed with the Agilent 2100 Bioanalyzer Lab-ona-Chip instrument system (Agilent Technologies). Our data show that the isolated exosomes do indeed contain small RNAs, of which about 86% are positive for miRNAs (Supplementary FigB), suggesting that these exosomes not only play an important role in cell signaling, but also impact biological processes in the recipient cells upon fusion.

In parallel experiments, we carried out NanoSight analyses to visualize, count and measure the size of exosomes isolated from pMAXGFP_αSyn cells after manganese treatment. As illustrated in Fig 2B, the diameter of exosomes isolated from control cells, 150.8 ± 7.05 nm, was comparable to that of manganese-treated exosomes (148.6 ± 12.42 nm, data not shown), indicating that manganese exposure does not alter the average size of exosomes. These calculated sizes are consistent with previously published observations (Danzer *et al.*, 2012; Emmanouilidou *et al*., 2010). However, we were able to detect significantly more exosomes in the manganese-treated cells compared to the vehicle-treated cells, indicating that manganese highly upregulates the release of exosomes (Fig 2C).

Manganese induces oligomeric αSyn secretion via exosomes.

To further characterize these cell-derived exosomes, we examined the presence of αSyn and exosomal surface proteins. Western blot analysis readily detected the exosomal surface membrane protein markers alix and flotillin-1 in all exosomes samples (Fig. 3A). Surprisingly, we observed more GFP-tagged αSyn fusion protein in exosomes isolated from manganese-exposed cells than from untreated cells (Fig. 3A), indicating manganese exposure increases the αSyn payload carried by exosomal cargos.

Existence of αSyn oligomers in biological fluids and exosomal fractions isolated from cultured cells (Danzer et al., 2012; Lee et al., 2005) has been well characterized. Therefore, we sought to determine whether oligomeric αSyn proteins are present in the isolated exosomes by using slot blot analysis with the anti-oligomer antibody A11. This conformational-specific antibody detects peptide-independent prefibrillar oligomers (Glabe, 2008; Kordower et al., 2008). As shown in Fig.2F, the exosomes isolated from manganese-stimulated pMAXGFP-αSyn cells show a greater accumulation of the prefibrillar oligomers compared to manganese-treated pMAXGFP or untreated cells. Collectively, our data suggest that manganese exposure increases the amount of exosomes released and also upregulates the aggregated protein cargos packaged into these exosomes.

Manganese exposure leads to differential expression of small RNAs

To identity and abundance of small RNA changes upon manganese exposure, we have performed next-generation exosome RNA sequencing in exosomes. We isolate the exosomes from pMAXGFP-αSyn cells treated with manganese or vehicle, purify the

exoRNA and build the Illumina NGS libraries. These libraries are then sequenced using a 1x 50bp single end Illumina HiSeq NGS runs to provide enough depth of RNA sequence identification. Our small RNA subtype profiles (Fig 4.A) indicated gross changes in miRNA, rRNA, tRNA and ncRNAs expression indicating manganese exposure cause changes in small RNA profiles in exosomes. Then we have further analyzed the miRNA changes in manganese stimulated exosomes compare to vehicle treated exosomes. After filter out those with 0 expression in either sample, our analysis indicates (Fig 4.B) substantial changes in miRNA expression in manganese stimulated exosomes. The figure 4C shows log2 fold changes in normalized expression (positive/control) with green = miRNAs that are > 4-fold unregulated and red = miRNAs that are > 4-fold upregulated in the manganese stimulated sample.

Validation of miRNA targets through custom miScript PCR array technology.

After identification of differentially express miRNAs through RNA-sequencing, we have performed miRNA qPCR to validate out RNA Seq results. Our custom miRNA PCR array consist of 48 miRNA including 43 previously identified miRNAs and five internal controls for expression normalization. Our data indicated 12 miRNAs significantly increased in manganese stimulated exosomes compares to vehicle stimulated exosomes.

Discussion

In this study, we report that the environmental neurotoxicant manganese can enhance the release of miRNA containing exosomes into the extracellular milieu, inducing which may in-turn modulate host cell gene expression. Our results also identified 43 differentially

express miRNAs in manganese stimulated exosomes in manganese stimulated exosomes compare to vehicle treated exosomes. To the best of our knowledge, we are the first to demonstrate the ability of environmental neurotoxicants modulate miRNA expression in cell culture- derived exosomes in cell culture models of PD. These findings could improve our understanding of exosome-mediated cell-to-cell propagation of αSyn in the progression of neurological disorders.

Cell-to-cell transmission of αSyn and the role of extracellular αSyn in the progression of PD gained much interest recently with the discovery of αSyn in human cerebrospinal fluid (CSF) and blood plasma (El-Agnaf et al., 2003). In support of a pathogenic role for extracellular αSyn, recent reports showed that αSyn aggregates released from neurons unleash toxic effects in recipient neurons by forming Lewy body-like inclusions (Desplats et al., 2009; Emmanouilidou et al., 2010) or by activating inflammatory responses in microglia (Kim et al., 2013). Furthermore, recent studies have shown that adding exogenous fibrillar αSyn into αSyn-overexpressing cells actively recruits soluble endogenous αSyn, converting it into a detergent-insoluble misfolded state (Luk et al., 2009). Thus, much like the mechanism observed in prion disease (Aguzzi and Falsig, 2012), extracellular αSyn serves as a seed and template for endogenous αSyn to propagate αSyn aggregation.

In this study, we are evaluating the effect of the environmental neurotoxin manganese in modulating miRNA expression in exosomes. Although environmental toxicants accounts for most sporadic PD cases, its role in the release and regulation of gene expression is

poorly studied. Chronic occupational exposure to high levels of manganese by welding, mining, dry cell battery manufacturing and manganese rich agro-chemicals is known to cause manganism, a condition closely related to PD, as characterized by tremors, rigidity and psychosis (Gerber et al., 2002; Kordower et al.). Previous studies have shown that manganese neurotoxicity leads to neuronal apoptosis, αSyn upregulation and aggregation in experimental models of PD (Cai et al., 2010; Hirata, 2002; Kordower et al., 2008). To further understand the role of manganese in the cellular release of αSyn, we have created GFP-fused wild-type human αSyn constitutively expressing dopaminergic cells which we exposed to inorganic manganese. We subsequently collected and concentrated conditioned culture media to analyze possible αSyn release, and as our Western blot results indicate, we readily detected αSyn in the culture medium obtained from pMAXGFP-αSyn cells.

The αSyn protein structure doesn't contain a signal recognition sequence, hence the observed secretion could be independent of the ER/golgi secretion pathway (Emmanouilidou et al., 2011; Vekrellis et al., 2011). Moreover, several unconventional excretion mechanisms have been implicated in αSyn release, including an endosomal pathway, direct transfer across the membrane and release through exosomes (Emmanouilidou et al., 2010; Lee et al., 2005). Therefore, to understand the mode of the αSyn release induced by manganese, we analyzed the conditioned media through TEM followed by differential ultracentrifugation. As our results indicated, we readily detected exosomes (Fig. 2A). Further analysis through Western blot indicates significantly more αSyn in exosomes derived from manganese-exposed cells. Surprisingly, Nanosight

particle analysis showed a higher exosomal release upon manganese treatment (Fig. 2C), indicating that manganese increases the total exosome release and the αSyn cargo residing in the exosomes are higher too.

Furthermore, we have analyzed exosomal small RNA content through miRNA Seq analysis and identified 43 differentially express miRNA which among them, 12 miRNAs were previously reported to regulate cellular autophaic/lysosomal degradation pathway.

References

Aguzzi, A., Falsig, J., 2012. Prion propagation, toxicity and degradation. Nat Neurosci. 15**,** 936-9.

Alderton, G. K., 2015. Diagnosis: Fishing for exosomes. Nat Rev Cancer. 15**,** 453.

Alvarez-Erviti, L., et al., 2013. Influence of microRNA deregulation on chaperone-mediated autophagy and alpha-synuclein pathology in Parkinson's disease. Cell Death Dis. 4**,** e545.

Anastasiadou, E., Slack, F. J., 2014. Cancer. Malicious exosomes. Science. 346**,** 1459-60.

Bae, E. J., et al., 2014. Glucocerebrosidase depletion enhances cell-to-cell transmission of alpha-synuclein. Nat Commun. 5**,** 4755.

Cai, T., et al., 2010. Manganese induces the overexpression of alpha-synuclein in PC12 cells via ERK activation. Brain Res. 1359**,** 201-7.

Cardo, L. F., et al., 2013. Profile of microRNAs in the plasma of Parkinson's disease patients and healthy controls. J Neurol. 260**,** 1420-2.

Chen, X., et al., 2008. Characterization of microRNAs in serum: a novel class of biomarkers for diagnosis of cancer and other diseases. Cell Res. 18**,** 997-1006.

Couzin, J., 2005. Cell biology: The ins and outs of exosomes. Science. 308**,** 1862-3.

Dai, Y., et al., 2009. Comprehensive analysis of microRNA expression patterns in renal biopsies of lupus nephritis patients. Rheumatol Int. 29**,** 749-54.

Danzer, K. M., et al., 2012. Exosomal cell-to-cell transmission of alpha synuclein oligomers. Mol Neurodegener. 7**,** 42.

Deng, Q., et al., 2014. Plasma microRNA expression and micronuclei frequency in workers exposed to polycyclic aromatic hydrocarbons. Environ Health Perspect. 122**,** 719-25.

Desplats, P., et al., 2009. Inclusion formation and neuronal cell death through neuron-to-neuron transmission of alpha-synuclein. Proc Natl Acad Sci U S A. 106**,** 13010-5.

El-Agnaf, O. M., et al., 2003. Alpha-synuclein implicated in Parkinson's disease is present in extracellular biological fluids, including human plasma. FASEB J. 17**,** 1945-7.

Emmanouilidou, E., et al., 2011. Assessment of alpha-synuclein secretion in mouse and human brain parenchyma. PLoS One. 6**,** e22225.

Emmanouilidou, E., et al., 2010. Cell-produced alpha-synuclein is secreted in a calcium-dependent manner by exosomes and impacts neuronal survival. J Neurosci. 30**,** 6838-51.

Feitelson, M. A., Lee, J., 2007. Hepatitis B virus integration, fragile sites, and hepatocarcinogenesis. Cancer Lett. 252**,** 157-70.

Gerber, G. B., et al., 2002. Carcinogenicity, mutagenicity and teratogenicity of manganese compounds. Crit Rev Oncol Hematol. 42**,** 25-34.

Glabe, C. G., 2008. Structural classification of toxic amyloid oligomers. J Biol Chem. 283**,** 29639-43.

Heman-Ackah, S. M., et al., 2013. RISC in PD: the impact of microRNAs in Parkinson's disease cellular and molecular pathogenesis. Front Mol Neurosci. 6**,** 40.

Hirata, Y., 2002. Manganese-induced apoptosis in PC12 cells. Neurotoxicol Teratol. 24**,** 639-53.

Kabaria, S., et al., 2015. Inhibition of miR-34b and miR-34c enhances alpha-synuclein expression in Parkinson's disease. FEBS Lett. 589**,** 319-25.

Khoo, S. K., et al., 2012. Plasma-based circulating MicroRNA biomarkers for Parkinson's disease. J Parkinsons Dis. 2**,** 321-31.

Kim, C., et al., 2013. Neuron-released oligomeric alpha-synuclein is an endogenous agonist of TLR2 for paracrine activation of microglia. Nat Commun. 4**,** 1562.

Kim, J., et al., 2007. A MicroRNA feedback circuit in midbrain dopamine neurons. Science. 317**,** 1220-4.

Kordower, J. H., et al., 2008. Lewy body-like pathology in long-term embryonic nigral transplants in Parkinson's disease. Nat Med. 14**,** 504-6.

Lawrie, C. H., et al., 2008. Detection of elevated levels of tumour-associated microRNAs in serum of patients with diffuse large B-cell lymphoma. Br J Haematol. 141**,** 672-5.

Lee, H. J., et al., 2005. Intravesicular localization and exocytosis of alpha-synuclein and its aggregates. J Neurosci. 25**,** 6016-24.

Lee, S. J., et al., 2010. Cell-to-cell transmission of non-prion protein aggregates. Nat Rev Neurol. 6**,** 702-6.

Li, J. Y., et al., 2008. Lewy bodies in grafted neurons in subjects with Parkinson's disease suggest host-to-graft disease propagation. Nat Med. 14**,** 501-3.

Luk, K. C., et al., 2009. Exogenous alpha-synuclein fibrils seed the formation of Lewy body-like intracellular inclusions in cultured cells. Proc Natl Acad Sci U S A. 106**,** 20051-6.

Minton, K., 2015. Exosomes: Apoptotic beads on a string. Nat Rev Mol Cell Biol. 16**,** 453.

Mitchell, P. S., et al., 2008. Circulating microRNAs as stable blood-based markers for cancer detection. Proc Natl Acad Sci U S A. 105**,** 10513-8.

Su, X., et al., 2008. Synuclein activates microglia in a model of Parkinson's disease. Neurobiol Aging. 29**,** 1690-701.

Thery, C., et al., 2002. Exosomes: composition, biogenesis and function. Nat Rev Immunol. 2**,** 569-79.

Vallelunga, A., et al., 2014. Identification of circulating microRNAs for the differential diagnosis of Parkinson's disease and Multiple System Atrophy. Front Cell Neurosci. 8**,** 156.

Vekrellis, K., et al., 2011. Pathological roles of alpha-synuclein in neurological disorders. Lancet Neurol. 10**,** 1015-25.

Volinia, S., et al., 2006. A microRNA expression signature of human solid tumors defines cancer gene targets. Proc Natl Acad Sci U S A. 103**,** 2257-61.

Vrijens, K., et al., 2015. MicroRNAs as potential signatures of environmental exposure or effect: a systematic review. Environ Health Perspect. 123**,** 399-411.

Wang, H., et al., 2015. MiR-124 Regulates Apoptosis and Autophagy Process in MPTP Model of Parkinson's Disease by Targeting to Bim. Brain Pathol.
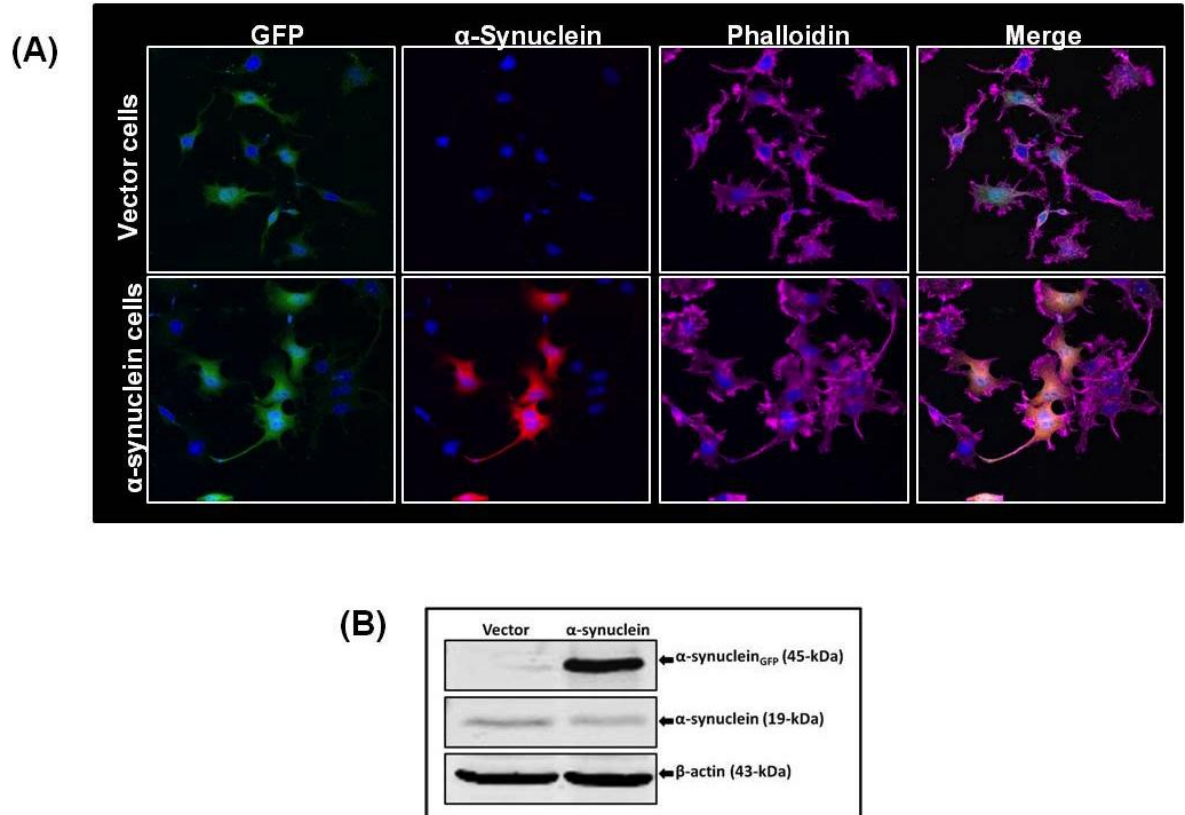
Figure 1. Generation of GFP-tagged stable human -α-synuclein expressing MN9D cells and manganese-induced α-synuclein secretion.

(A) Immunocytochemical analysis depicting stably expressed GFP-tagged wild-type human αSyn protein in MN9D dopaminergic cells. αSyn-expressing cells exhibited strong ubiquitous expression of αSyn, whereas vector cells showed no detectable αSyn immunoreactivity. (B) Stable expression of αSyn was determined by Western blot analysis. A 45-kDa band corresponding to the molecular mass of GFP-fused human αSyn was detected in α-synexpressing cells, whereas no human-specific αSyn expression

appeared in vector cells. However, both human αSyn-expressing and control cells showed

low levels of endogenous αSyn expression.

Figure 2. Manganese induces exosomes release from neuronal cells.

(A) Electron micrograph of isolated exosomes revealing that transmission electron

microscopy of ultracentrifuged conditioned medium readily detected exosomes. (B)

Nanosight-generated histogram of particle size and abundance of isolated exosomes. (C)

Exosome concentrations showing that manganese exposure upregulated the release of

exosomes into the extracellular micro-environment.
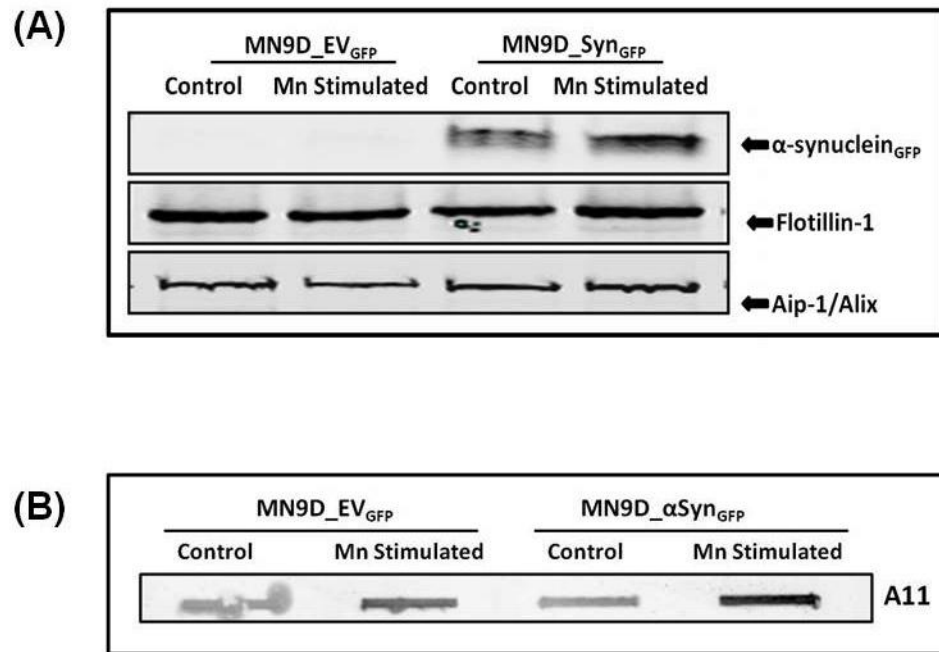
Figure 3. Manganese induces oligomeric αSyn secretion via exosomes.

Western blot analysis shows exosomal surface membrane protein markers alix and flotillin-1 in all exosomes samples and elevated αSyn in manganese stimulated αSyn-pmaxGFP exosomes.

Slot blot analysis showing higher oligomeric protein accumulation in exosomes isolated from manganese-stimulated exosomes from both αSyn-pmaxGFP and control pmaxGFP cells relative to vehicle-treated αSyn-pmaxGFP and control pmaxGFP cells. However, exosomes from manganese stimulated αSyn-pmaxGFP indicate greater accumulation of prefibrillar oligomeric protein
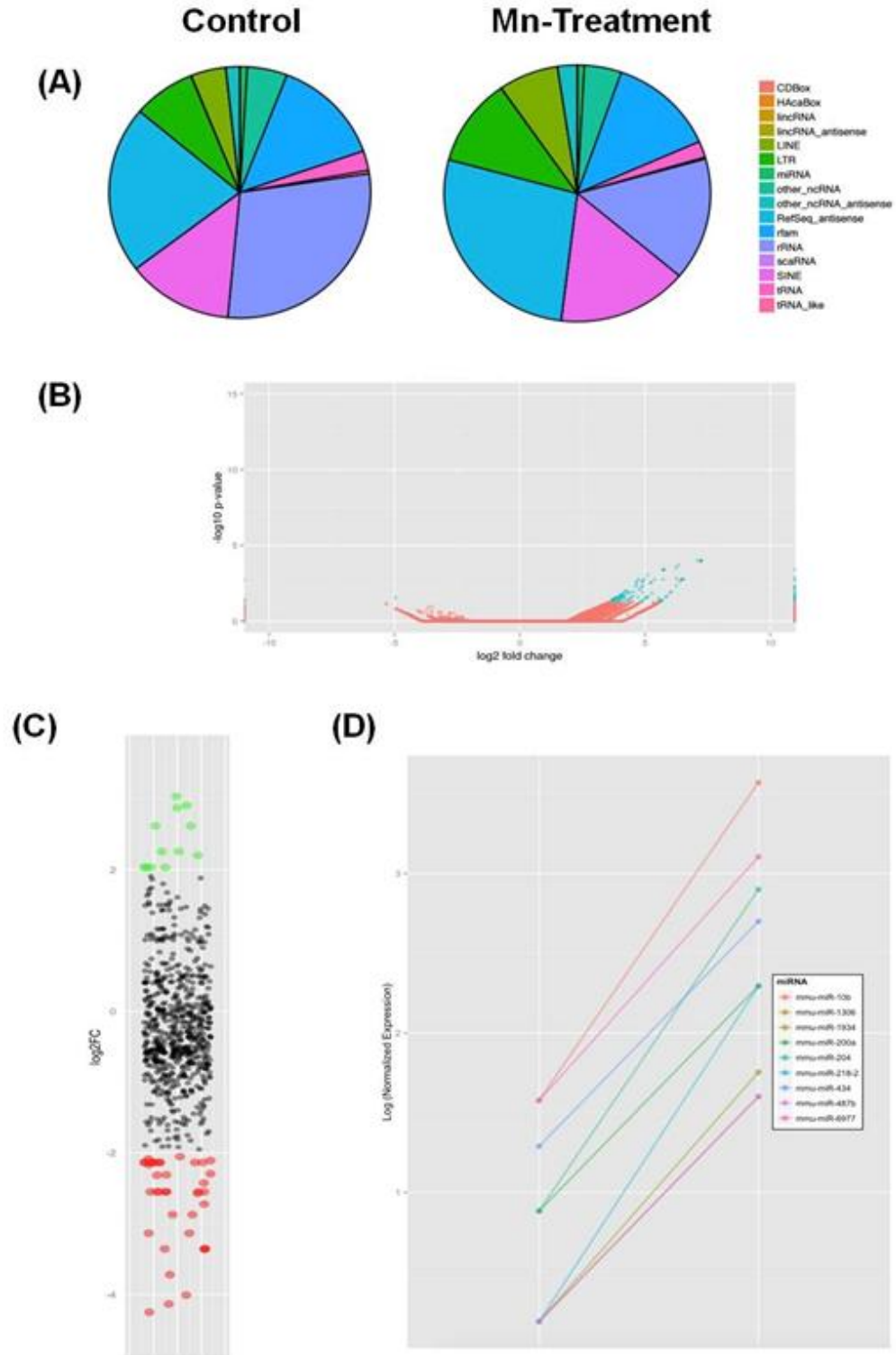
Figure 4: Top: Comparison of RNA profiles between Control (Left) and Positive (Right)

samples   reveals   different   abundances   of   small   RNA   subtypes.

Bottom: Differentially expressed miRNAs are highlighted in red (> 4-fold upregulation) and green (> 4-fold downregulation) (Left). The expression log-normalized expression profiles of specific upregulated (Middle) and downregulated (Right) miRNAs are plotted.
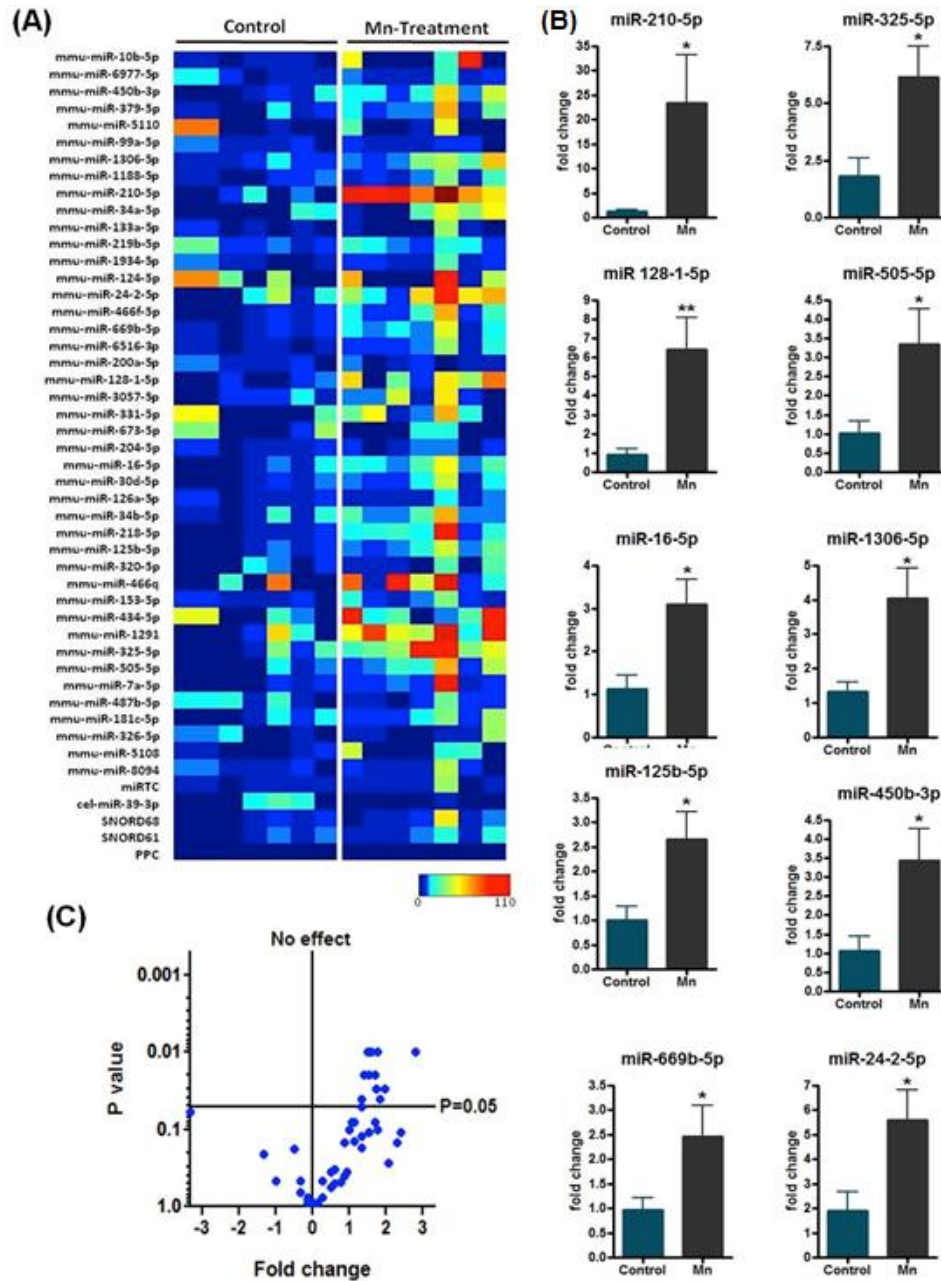
Figure 5: Validation of miRNA targets through custom miScript PCR array technology (A) Heat-map of miRNA expression between control and Mn-stimulated

exosomes. (B) Increased expression of miRNA's isolated from manganese stimulated exosomes compares to vehicle stimulated exosomes (C) Volcano-plot showing fold change and p-values of validated miRNA's. Data above p=0.05 show miRNA's with significantly different expression in Mn-stimulated exosomes compared to vehicle stimulated exosomes.

CHAPTER V: GENERAL CONCLUSIONS

This section presents an overview of the results and findings of this dissertation, with a special emphasis on overall implications of these findings for the roll of environmental neurotoxicants on cell-to-cell transmission of α-synuclein in Parkinson's disease. The major findings of each research chapter included in this dissertation are covered in the discussion section of the relevant chapter.

α-Synuclein Protects against Manganese Neurotoxic Insult during the Early Stages of Exposure in a Dopaminergic Cell Model of Parkinson's Disease

The primary finding from the chapter 2 of the thesis is that the human wild-type α-Syn plays a neuroprotective role against manganese neurotoxicity in its early stages, but the protein becomes increasingly susceptible to aggregation during prolonged metal exposure. In this study, we sought to understand possible the role of α-Syn's multiple metal binding sites and possible physiological function of wild-type α-Syn in manganese induce neurotoxicity. To this end, we developed an α-Syn-expressing dopaminergic neuronal cell model for examining the role of α-Syn in both acute and prolonged manganese neurotoxicity. Using this *in vitro* model, we provided direct evidence for the neuroprotective effect of human α-Syn in dopaminergic neurons during acute manganese toxicity. We observed this effect at 300 µM manganese, a dose consistent with previously published work (Exil et al., 2014; Latchoumycandane et al., 2005; Martin et al., 2011) and concentration within the toxicologically relevant range as its has been shown that

depending upon the dose, duration, and route of exposure, manganese concentrations can reach up to 350 µM in certain brain regions (Ingersoll et al., 1999).

In our current study, dopaminergic cells expressing human wild-type α-Syn exhibited significantly lower apoptotic cell death compared to vector control N27 cells upon acute manganese toxicity. Interestingly, α-Syn does not hamper the cells' ability to produce ROS when exposed to manganese. To further characterize the mechanism underlying the neuroprotective effect of α-Syn against manganese-induced apoptotic cell death, and because manganese is known to impair mitochondrial function (Gunter et al., 2009; Latchoumycandane et al., 2005), we systematically examined the mitochondria-dependent apoptotic signaling events. We found a significant attenuation of cytochrome c release to cytosol from the mitochondrial inner-membrane in α-Syn-expressing cells, suggesting that α-Syn interferes with the process of cytochrome c release during early phases of manganese neurotoxicity. However, our immunocytochemistry and slot blot analysis data indicate intracellular protein aggregate accumulation during prolonged manganese exposure in dopaminergic neuronal cells. These observations were validated using the ProteoStat aggresome detection kit (Enzo) and the ProteoStat inclusion body kit (Enzo) to indicate the accumulation of aggregated proteins in α-Syn cells compared to Vec cells after prolonged manganese exposure. Overall, our results support the idea that α-Syn initially protects against manganese-induced neurotoxicity by reducing mitochondria-dependent apoptotic signaling, whereas prolonged exposure to manganese significantly alters the stability of α-Syn protein, increasing the amount of aggregated α-Syn protein.

The Environmental Neurotoxicant Manganese Promotes Prion-like Cell-to-Cell Transmission of α-Synuclein via Exosomes in Cell Culture and Animal Models of Parkinson's Disease

Recent studies suggest that a prion-like cell-to-cell transfer of misfolded αSyn contributes to the spreading of αSyn pathology. However, the biological mechanisms underlying the propagation of the disease with respect to environmental neurotoxic chemical exposures are not well understood. Therefore, in chapter 3, we sought to understand possible manganese induced αSyn protein aggregation and extracellular secretion of αSyn via exosomal vesicles, which subsequently evokes pro-inflammatory and neurodegenerative responses in both cell culture and animal models. To elucidate the mechanism of manganese-induced release, we followed a systematic approach form *in vitro* to *ex vivo* to *in vivo* experimental models to better understand the role of exosomes in cell-to-cell transmission of misfolded αSyn protein. First, using wild-type human αSyn-overexpressing cell culture model, we provided direct evidence that manganese exposure significantly enhances the release and accumulation of extracellular αSyn providing direct evidence of an environmental influence of αSyn release.

Neuroinflammation is key to the pathogenesis of PD and other related α-synucleinopathies. To study whether manganese-stimulated exosomes have any role in neuroinflammatory processes, we exposed primary murine microglia to either vehicle or manganese-stimulated exosomes and quantified the neuroinflammatory effects. Our immunocytochemistry data and Luminex cytokine analysis indicate microglia cells treated with manganese-induced αSyn exosomes show enhanced levels of oxidative stress and proinflammatory cytokines, such as TNFα, IL12, IL1β and IL6, indicating that

exosomes can evoke inflammatory responses. Further characterization of exosomes through slot blot analysis with protein oligomer-specific antibodies indicated a greater accumulation of prefibrillar oligomers in manganese-stimulated αSyn exosomes. To further investigate whether exosomes carry disease-associated prefibrillar αSyn oligomers, which can seed and propagate pathology *in vivo*, we injected 2- to 3-month old wild-type C57BL/6 mice with exosomes isolated from manganese or vehicle-treated EV cells and αSyn cells. Interestingly, we detected human αSyn-immunoreactive cytoplasmic inclusions at 90 dpi in mice stereotaxically injected with either vehicle-stimulated or manganese-stimulated αSyn exosomes. However, mice injected with manganese-stimulated αSyn exosomes had more Lewy body/Lewy neurite structures compared to vehicle-stimulated αSyn exosome-injected mice. These data suggest that αSyn exosomes can initiate Parkinsonian neuro-pathologies in experimental models of PD.

Finally, we show further that humans exposed to manganese through welding fumes contain higher misfolded αSyn in their serum exosomes than control subjects. In conclusion, we identified a possible mechanism for how the environmental neurotoxicant manganese contributes to exosome-mediated cell-to-cell propagation of αSyn and its role in the progression of neurological disorders.

Environmental Neurotoxicant Manganese Increases Exosome-Mediated miRNA Delivery and Autophagic Regulation in Cell Culture Model of Parkinson's Disease.

miRNA is a class of small non-coding RNA, whose final product is an approximately 18-22 nucleotides long functional RNA molecule. miRNA repress translation and regulate degradation of their target mRNA by binding complementary regions of messenger

transcripts. Research in various disease processes from cancer to cardiovascular disease has found that miRNAs play a role in disease pathogenesis and have potential as biomarkers and therapeutic agents. Recently, number of miRNA expression changes reported in different brain areas involved in AD development (Kordower et al., 2008) and comprehensive review by Tan et al 2013 (Kordower et al., 2008) identify the involvement of miRNA in the development of AD such as accumulation of amyloid-β, tau toxicity, neuroinflammation and cell death. These miRNAs circulate through the body either by binding to certain proteins or as cargo packaged in exosomes, whereby it can modulate the recipient cell's gene expression upon endocytosis. Despites its importance, dysregulation of circulating miRNAs upon environmental neurotoxicant insults have rarely been studied. In chapter 4, we hypothesize that exposure to the environmental neurotoxicant manganese impairs the cellular protein degradation mechanism, causing a misfolded αSyn protein payload to accumulate in cells, and then induces secretion and transmission of aggregated αSyn via exosomes to its microenvironment.

In this study, we also analyzed and validated miRNA changes in exosomes collected from cells expressing human α-synuclein, a genetic risk factor for Parkinson's disease, upon manganese neurotoxic insult. Our study identified 43 differentially expressed miRNAs in manganese-stimulated αSyn exosomes as compared to control exosomes. Among them, majority of miRNAs were associated with regulation of autophagic/lysosomal degradation pathway by targeting important autophagic regulates such as Bim, Hsc70, E2F1 and etc in experimental models of PD. Our custom miRNA PCR array confirmed our NGS miRNA sequencing results and further validates and identified 12 miRNAs which significantly changes among control and manganese treated

group. In future studies, we will be validating the possible gene regulation by miRNA by feeding exosomes and synthetic miRNAs back to naïve differentiated dopaminergic cells and investigates its biological relevance. Hence, our in vitro assays demonstrate the exosome's capacity to deliver miRNAs and act as a cargo vessel that invades recipient cells much like a "Trojan horse mechanism," thereby exacerbating neuropathology.

With the recent clinical advancements with therapeutic siRNAs using liposomal and polymerbased delivery technologies, natural vesicular lipid transporters such as exosomes with the abundance of adhesive proteins that readily interact with cellular membranes, exosome-based drug delivery systems may have advantages in the treatment of neurodegenerative disorders. Therefore, we can further develop miRNA antagonists as novel therapeutics to inhibit endogenous miRNAs that show a gain-of-function in diseased state and fused in exosomes for effective delivery. Importantly, our research identified multiple miRNA targets potentially use as drug targets and address rather essential research questions related to protein misfolding and accumulation in neurodegenerative disorders.

References

Exil, V., et al., 2014. Activation of MAPK and FoxO by manganese (Mn) in rat neonatal primary astrocyte cultures. PLoS One. 9**,** e94753.

Gunter, T. E., et al., 2009. The case for manganese interaction with mitochondria. Neurotoxicology. 30**,** 727-9.

Ingersoll, R. T., et al., 1999. Central nervous system toxicity of manganese. II: Cocaine or reserpine inhibit manganese concentration in the rat brain. Neurotoxicology. 20**,** 467-76.

Kordower, J. H., et al., 2008. Lewy body-like pathology in long-term embryonic nigral transplants in Parkinson's disease. Nat Med. 14**,** 504-6.

Latchoumycandane, C., et al., 2005. Protein kinase Cdelta is a key downstream mediator of manganese-induced apoptosis in dopaminergic neuronal cells. J Pharmacol Exp Ther. 313**,** 46-55.

Martin, D. P., et al., 2011. Infectious prion protein alters manganese transport and neurotoxicity in a cell culture model of prion disease. Neurotoxicology.

APPENDIX I

MANGANESE AND PRION DISEASE

Huajun Jin[#], Dilshan S. Harischandra[#], Arthi Kanthasamy, Christopher Choi, Dustin Martin, Vellareddy Anantharam and Anumantha G. Kanthasamy*

Parkinson's Disorder Research Laboratory, Iowa Center for Advanced Neurotoxicology, Department of Biomedical Sciences, Iowa State University, Ames, Iowa 50011, USA

[#]The authors contributed equally to this chapter.

*Corresponding author. Email: akanthas@iastate.edu

Table of Contents

Abstract

Prion diseases are a class of fatal neurodegenerative diseases caused by misfolding of the endogenous prion protein (PrP^C) induced by exposure to the pathogenic conformational isomer of PrP (PrP^{Sc}) or by heritable mutation of PrP^C. Although the exact role of the protein has yet to be solved, considerable evidence reveals prion protein to be a metalloprotein harboring divalent metal-binding sites for various cations such as copper, manganese, zinc, and nickel. Despite low-affinity binding to prion protein, when manganese interacts with prion, it can alter the development and transmission of prion disease. In this chapter, the role of metals in the pathogenesis of prion disease will be discussed. Particular emphasis will be placed on the link between manganese and PrP^C.

Keywords: metals, manganese, copper, conformational change, protein aggregation and prion disease.

1. Introduction

Prion diseases, also termed transmissible spongiform encephalopathies (TSEs), describe a group of fatal neurodegenerative disorders affecting both humans and animals (Prusiner, 1991). Although the prevalence of prion disease is relatively low with about 300 cases reported annually in the United States, the potential for the disease to be transmitted between humans and animals raises strong concerns over its control. Prion disease occurs in many forms due to differences in pathology as well as modes of pathogenesis (Head, 2013). Their etiologies are also multi-fold in dimension with the possibility of iatrogenic routes from infected surgical materials, human grafts, and even

blood transfusions; or hereditary in nature. Typical clinical symptoms of prion diseases include rapidly developing dementia, difficulty walking, changes in gait, hallucinations, confusion, fatigue, muscle stiffness and difficulty speaking. Historically, prion diseases have been characterized neuropathologically by vacuolation of neutrophils, neuronal loss, gliosis, and by the deposition of amyloid plaques in the brain of diseased animals and humans (Belay and Schonberger, 2005; Wadsworth and Collinge, 2011). The neurodegeneration in prion disease primarily occurs in the brain regions that coordinate motor functions, such as the basal ganglia, cerebral cortex, thalamus and cerebellum (Jang et al., 2013; Mallucci, 2009). Reactive astrocytic gliosis, microglial activation and the deposition of amyloid plaques have been associated with the accumulation of the abnormal prion protein PrP^{Sc} (scrapie isoform) derived from the normal prion protein PrP^C (cellular isoform) (DeArmond et al., 1987). Thus far, neither effective treatment nor prevention methods have been developed for prion disease (Roettger et al., 2013; Wisniewski and Goni, 2012). Most confirmed cases have been identified post-mortem, so the development of ante-mortem tests are essential for effective detection. There are different methods of dealing with the prion disease (Forloni et al., 2013; Sim and Caughey, 2009). Since total eradication of the disease has not been possible, reducing its infectivity, reducing the substrate, and developing vaccinations have been explored.

Despite extensive research, the precise cause of prion disease remains unknown. However, it is generally believed that the diseased state of an organism occurs when the soluble α-helix-rich form of PrP^C has been converted to the insoluble β-sheet-rich pathogenic form of PrP^{Sc} (Collinge, 2005). The conversion steps required for the protein to become pathogenic remain unclear. Interestingly, different conformational isomers

with identical primary sequences can display widely varying pathology, indicating that the secondary and tertiary structures of PrP^{Sc} can encode different strains of TSE (Gambetti et al., 2011; Parchi et al., 2010; Weissmann et al., 2011). Though the absolute pathogenesis of prion disease remains obscure, several pathogenic mechanisms have been proposed, including synaptic damage, dendritic atrophy, autophagy, microglial activation, oxidative stress, protein misfolding, ER stress and apoptosis. Further complicating the effort to uncover the disease's etiology, a combination of multiple interlinking pathways, rather than a unifying mechanism, could contribute to the pathology of prion diseases.

Substantial evidence also highlights the prion protein to be a metalloprotein, and to have affinity to various cations such as copper, zinc, manganese, and nickel (Brown, 2004; Di Natale et al., 2005; Hornshaw et al., 1995). Many studies have reported significant differences in metal content in diseased humans and animals (Hesketh et al., 2007b; Wong et al., 2001a), suggesting the involvement of metal homeostasis in prion disease pathogenesis. The redox metals are essential trace element metals normally required for physiological process, and are precisely regulated by the cells. Interactions of these metal ions with prion protein may have a role in protein misfolding and the neurodegenerative progression of prion diseases. Therefore, a detailed understanding of metal-prion interactions would not only expand our understanding of the pathophysiological mechanisms of prion diseases, but may also enable the development of effective treatment strategies for these debilitating diseases.

2. Prion diseases

Although the biochemical process that converts PrP^C to PrP^{Sc} is not completely understood, according to a seeding-nucleation model, the pre-existing or acquired PrP^{Sc} oligomers catalyze the conversion of PrP^C molecules into PrP^{Sc} fibrils. The breakage of these fibrils provides more PrP^{Sc} templates for further seeding of the conversion process (Prusiner, 1982). This process results in more aberrant PrP^{Sc} proteins, which are extremely resistant to proteolysis or degradation by conventional means, thereby initiating the classical prion disease state.

The earliest description of TSE, dating back to the mid-18th century, was identified as scrapie, the prototypic prion disease affecting sheep and goat (Aguzzi, 2006). In the early 19th century, a critical experiment performed by Cuille and Chelle confirmed the transmissibility of scrapie to goats, turning a new page in prion biology (Cuille J., 1939). In 1920, the first human case of TSE, Creutzfeldt-Jakob disease (CJD), was reported (Aguzzi et al., 2008) and it remains the most common form of human prion disease. The number of identified human and animal prion diseases has increased steadily ever since and over fifteen different diseases have been described so far (Aguzzi, 2006; Imran and Mahmood, 2011). In the following section, we will review some of the prevalent human prion disease.

2.1 Creutzfeldt-Jakob disease

Initially CJD was described as a sporadic disease (sCJD) caused by the spontaneous transformation of PrP^C into PrP^{Sc}, resulting in rapid cognitive decline, involuntary movements, blindness, weakness of extremities and coma. Disease onset for

sCJD occurs at about age 60 and 90% of patients die within 1 year. Sporadic CJD accounts for 85% of all CJD cases with an annual incidence rate of approximately 0.6-1.2 cases/million worldwide (Ladogana et al., 2005). Epidemiologically, there are three other distinct types of CJD in addition to sCJD: familial (fCJD), iatrogenic (iCJD), and variant (vCJD). Familial CJD develops from a heritable mutation in the Prnp gene, which accounts for 5-10% of all CJD cases. Several point mutations have been identified as risk factors for fCJD, including E200K and V210I (Prusiner and DeArmond, 1994). A rather smaller number of cases (<5%) have been classified as acquired forms accounting for both iCJD and vCJD. These acquired CJD cases are mostly transmitted iatrogenically by accidental exposure to PrP^{Sc}-infected brain or nervous system tissues during medical procedures. The first reported iCJD case occurred in 1974 by corneal transplantation from a deceased patient with undiagnosed sCJD (Duffy et al., 1974). Pituitary growth hormones and dura matter graft-transplants obtained from CJD-infected individuals account for most iCJD cases (Gay et al., 1988), where the current worldwide total of growth hormone-associated cases of CJD is up to 226 (Gibbs et al., 1985). Variant CJD is a new subset of acquired CJD with its own distinct pathological and clinical phenotypes. The first confirmed case of vCJD was reported in 1996 in the United Kingdom (UK) (Will et al., 1996) and is suggested to be causally linked to the bovine spongiform encephalopathy (BSE) outbreak in Europe. By the end of 2013, 177 deaths in UK (http://www.cjd.ed.ac.uk/) have been attributed to vCJD. Unlike sCJD cases, vCJD patients are relatively young (median age of 28) and have relatively long incubation periods. Interestingly, unlike other CJD patients, vCJD patients lack the classic CJD electroencephalogram and they develop extensive fluoride plaques in the brain (Will et

al., 1996). Also, whereas epidemiological and experimental data suggest that sCJD doesn't transmit from person to person via blood transfusion, this might not apply to vCJD. For example, there is an incidence of one recipient developing symptoms of vCJD 6.5 years after receiving a transfusion of red blood cells donated by an individual later identified as a vCJD patient (Llewelyn et al., 2004). Such evidence continues to mount as there have been four more identified cases of vCJD resulting from blood transfusions in the UK. To prevent further transmission, since April 2004, anyone having received a blood transfusion in the UK after 1980 became ineligible to donate blood (http://www.hpa.org.uk/).

2.2 Kuru

Kuru is another acquired human prion disease seen exclusively in the Fore linguistic groups and neighboring tribes in the Okapa area of the Eastern Highlands of Papua New Guinea. The disease resulted from the practice of ritualistic cannibalism among the Fore, in which relatives prepared and consumed the tissues, including brain, of deceased family members. Kuru affected predominantly women and young children as they were exposed most to infectious brain and visceral tissues, while adult men primarily consumed muscles (Imran and Mahmood, 2011). Although the first case was observed ~1920, Kuru was not thoroughly documented until 1957, and since then over 2700 cases have been reported (Will, 2003). Dr. Gajdusek and colleagues have shown disease transmission in nonhuman primates by intracerebral introduction of brain homogenates from Kuru patients, proving that Kuru was caused by a transmissible agent

(Gajdusek et al., 1966), thus indicating for the first time the infectious nature of prion diseases.

Clinically, the prodrome stage of Kuru consists of headaches and joint pain in the legs followed by three clinical stages: an ambulatory stage, a sedentary stage and a tertiary stage (Kaufman et al., 1985). The symptoms seen in these clinical stages are characteristic of the term "Kuru", which means "to *shiver* from fever and cold" in Fore language. Additionally, Kuru is considered largely a cerebellar syndrome with ataxia, tremors, and choreiform and athetoid movements being the prominent clinical signs of the disease (Alpers, 1987); dementia is a late and less prominent symptom. Interestingly, recent genome-wide studies of Kuru confirmed a strong association with a single nucleotide polymorphism (SNP) localized within the codon 129 and also with two other SNPs localized within the genes retinoic acid receptor beta (RARB) and stathmin like 2 (STMN2; the gene encoding SCG10) (Lockwood, 1989; Thomson et al., 2012). Importantly, studies have shown that individuals with $129^{Val/Val}$ and $129^{Met/Met}$ genotypes are susceptible to Kuru (Cervenakova et al., 1998), whereas heterozygosity at codon 129 confers relative resistance to prion diseases (Mead et al., 2003). An evolutionarily strong balancing selection for these alleles had been imposed at this locus, not only in Fore, but also in those human populations practicing cannibalism (Liberski, 2013).

2.3 Gerstmann-Sträussler-Scheinker Syndrome

Gerstmann-Straussler-Scheinker disease (GSS) is a genetically determined adult prion disease associated with the autosomal dominant inheritance of *Prnp* mutations. GSS is also considered one of the rarest forms of prion disease with an incidence of 2-5

per 100 million people. However, this disorder may be underdiagnosed. Many of its key clinical symptoms, such as cerebellar ataxia, dysdiadochokinesia, speech disturbance, personality changes, and dementia, are also characteristic of other neurodegenerative diseases like Parkinson's disease (PD), amyotrophic lateral sclerosis (ALS or Lou Gherig's disease), Huntington's disease (HD), Alzheimer's disease (AD) and etc.

Neuropathologically, GSS is primarily characterized by prominent amyloid plaques and diffuse deposits resulting from the accumulation of PrP degradation products in the cerebellum (Masters et al., 1981). However, GSS shows great pathological heterogeneity, which often partly overlaps those found in AD, PD and Dementia with Lewy bodies (DLB). These phenotypic differences correlate to the haplotype-specific pattern. For instance, immunohistochemical analysis of the neocortex of GSS patients associates with F198S (Ghetti et al., 1989), Q227X (Liberski et al., 1998), D202N (Piccardo et al., 1998), etc, indicating the presence of neurofibrillary tangles normally found in AD. Patients with the F198S mutation have also been found with α-synuclein immunopositive Lewy bodies typical of PD (Piccardo P, 1998). Currently, at least 16 point mutations in the *Prnp* gene have been implicated as risk factors for GSS including P102L, P105L, A117V, Y145X, H187R, D178N, Q160X, Q217R, Y218N, Y226X, G131V, Q212P and S132I (Doh-ura et al., 1989; Hsiao et al., 1992; Imran and Mahmood, 2011; Jansen et al., 2010).

Biochemically, GSS is characterized by the presence of proteinase K (PK) resistant N- and C-terminal truncated and non-glycosylated PrP peptides ranging from ~7 to 15 kDa (Tagliavini et al., 1994). Interestingly, the transmissibility of GSS is widely studied and common GSS-associated mutations (P102L) seem to be more capable of

transmitting the disease than are less frequent GSS-associated mutations (Tateishi et al., 1988).

2.4 Fatal familial insomnia

Fatal familial insomnia (FFI) is an extremely rare genetic disorder arguably considered the deadliest form of insomnia which steals one's sleep, mind and eventually one's life. Clinically FFI is characterized by untreatable alterations of the sleep-wake cycle (loss of sleep spindles, slow-wave sleep, non-rapid eye movement and enacted dreams) (Brown, 2002; Huber et al., 1999), autonomic hyperactivation, and cognitive and motor impairments such as dysarthria, myoclonus, ataxia, tremor, pyramidal and extrapyramidal signs (Montagna et al., 2003). Thalamic atrophy is recognized as the histopathological hallmark of FFI, while pathological lesions in the neocortex and the limbic cortex are also observed. Since the importance of the thalamus in sleep physiology has been well characterized (Brown et al., 2012), observed sleep disturbance well accordance with the physiological changes. These clinical manifestations also result in dysautonomia (hyperhidrosis, hyperthermia, tachycardia, and hypertension) and endocrine disturbances (decreased adrenocorticotropic hormone secretion, increased cortisol secretion), and disturbances in growth hormone, melatonin, and prolactin secretion. In addition, FFI is the only known prion disease exhibiting these secondary heath complications (Engleberg, 2012).

Historically, FFI was first identified and characterized in 1986 by Lugaresi and colleagues, and to date, at least 40 unrelated kindred identified worldwide including families from Japan, China, Africa, as well as families with American and European

ancestry (Harder et al., 1999; Padovani et al., 1998; Zhang et al., 2010). Genetically, FFI is characterized as an autosomal dominant disease associated with a point mutation at codon 178 in the *Prnp* gene where asparagine has been substituted for aspartic acid (D178N) (Medori et al., 1992). However, the same D178N mutation is also linked to fCJD. What distinguishes the two diseases is the genotype at the polymorphic codon 129 where FFI is associated with methionine (M) (D178N-129M haplotype) and fCJD is associated with valine (V) (D178N-129V haplotype) (Taniwaki et al., 2000). Additionally the polymorphic codon 129 in the non-mutated allele determines the severity of the disease. In FFI, methionine at polymorphic codon 129 (Fig. 1A) is associated with a more severe insomnia and dysautonomia at onset and with thalamic damage and fewer cortical alterations, whereas heterozygotes (methionine/valine) (Fig. 1B) are associated with ataxia and dysarthria at onset, and after prolonged disease, with widespread neuropathological damage and cortical spongiosis (Medori and Tritschler, 1993; Tabernero et al., 2000).

Biochemically, FFI is quite distinct from other prion diseases. Where both fCJD and sCJD results in a ~21 kDa protein fragment after digestion with protease, in contrast, FFI results in a shorter ~19 kDa protein fragment (Prusiner, 1998). These results further confirm the "prion strain" hypothesis, allowing researchers to identify two different strains from their origin to their experimental transmission to laboratory animals. Further characterization of the glycosylation patterns helped to distinguish FFI from sporadic fatal insomnia (sFI), a rare sporadic form of the disease similar to FFI and its clinical symptoms. Biochemically, sFI is characterized by the predominant monoglycosylated

form, whereas FFI is characterized by an under-representation of the unglycosylated form (Broderick, 1977).

3. Prion protein (PrP^{C})

3.1 Structure of PrP^{C}

PrP^{C} is an N-linked glycoprotein tethered to extracellular membrane by a glycosylphosphatidylinositol (GPI) anchor and is ubiquitously expressed throughout the central nervous system, particularly in both neuronal and glial cells. In humans PrP^{C} is encoded by the PRNP gene located on the short arm of human chromosome 20 (20q13) as a 16-kb long single gene copy. The human PRNP gene encodes a 253-residue precursor prion protein, and upon translation, the first 22 N-terminal residues (signal peptide) post-translationally are cleaved during transport to the cell surface (Kretzschmar et al., 1986) (Fig. 2). The last 23 C-terminal amino acids are excised after the addition of the GPI anchor, resulting in mature PrP^{C} on the cell surface consisting of 208 amino acid residues (Stahl et al., 1987). Properly folded and GPI-anchored PrP^{C} becomes localized in detergent-resistant membranes, also known as lipid rafts (Aguzzi et al., 2008). This PrP^{C} is rapidly internalized from the cell membrane via caveolae-like (Marella et al., 2002; Peters et al., 2003) or clathrin-dependent (Prado et al., 2004; Taylor et al., 2005) endocytosis. Internalization is considered to be crucial for PrP^{C} function in regulating signal transduction pathways, neurite outgrowth, etc (Di Guglielmo et al., 2003; York et al., 2000). Experimentally this surface bound PrP^{C} can be removed *in vitro* by incubating with bacterial phosphatidylinositol-specific phospholipase C (PI-PLC), which liberates PrP^{C} from the cell membrane by cleaving the GPI anchor (Stahl et al., 1987; Weissmann,

2004). Structural modeling through nuclear magnetic resonance (NMR) studies on recombinant human PrP^C reveals the C-terminal globular domain to have three α helices ($α_1$, $α_2$ and $α_3$) and a short anti-parallel β-sheet ($β_1$ and $β_2$) (Zahn et al., 2000). The C-terminal domain of PrP^C also contains a single disulfide-bonded bridge linking the Cys residues of $α_2$ and $α_3$ at positions 179 and 214. This disulfide bridge is important for conformational stability of PrP^C and removal greatly destabilizes the native PrP^C structure, which could reversibly switch between α-helical conformation and a monomeric form rich in β-sheet structure (Maiti and Surewicz, 2001). The N-terminal moiety of the prion protein is an unstructured region that characteristically interacts with a broad range of partners having contrasting capabilities, including neuroprotection and neurotoxicity. One hallmark of this region is the highly conserved tandem repeats of an eight-residue sequence (PHGGSWGQ) referred to as an octapeptide repeat domain. The number of repeats differs from species to species (see Fig. 3 for PrP^C homology among mammalian species). For example, humans, mice, sheep, and deer each have five octapeptide repeats in the wild-type cellular protein while bovine PrP has six repeats (Mastrangelo and Westaway, 2001).

3.2 Physiological function of prion protein

Interestingly, octapeptide repeat regions have a high affinity for binding to divalent metals; their highest affinity is for copper, followed by nickel, zinc and manganese (Jackson et al., 2001). Metal binding has been suggested to play an important role in the biological function of prion protein and their pathogenesis. This protein also has been speculated to act as an antioxidant. Its role in antioxidant defense was

demonstrated by blocking toxic effect by treating cells with synthetic PrP^C 59-91 peptide in cells exposed to high levels of copper (Brown et al., 1998). Transmembrane signaling is another physiological function of prion proteins, which is regulated by different binding partners. Since most PrP^Cs are localized on plasma membranes, specifically on cholesterol- and glycosphingolipid-rich lipid raft domains serving as scaffolds for signal transduction (Taylor and Hooper, 2006), numerous studies have identified binding ligands of prion proteins. Indeed, PrP^C interacts with various macromolecules at the cell membrane to activate transmembrane signaling pathways involved in several different phenomena, including neuronal survival, neurite outgrowth and neurotoxicity. It has been demonstrated that both the laminin precursor protein (LRP), via the yeast two hybrid system (Rieger et al., 1997), and the neuronal cell adhesion molecule (N-CAM), via formaldehyde cross-linking studies (Schmitt-Ulms et al., 2001), interact with PrP^C on cell surfaces, promoting diverse transduction pathways involved in differentiation and neurite outgrowth (Colognato and Yurchenco, 2000; Maness and Schachner, 2007). Moreover, Santuccione and colleagues have shown that heterophilic *cis* and *trans* interactions between N-CAM and PrP at the neuronal surface promote N-CAM recruitment to lipid rafts for activation of $p59^{Fyn}$, a member of the Src family of non-receptor tyrosine protein kinases (Santuccione et al., 2005). Furthermore, studies carried out with the 1C11 neuronal differentiation model with antibody-mediated cross-linking have shown $p59^{Fyn}$ activation in a caveolin-1-dependent manner (Mouillet-Richard et al., 2000). In subsequent studies, as a downstream event, they also report NADPH oxidase-dependent ROS production and extracellularly regulated kinase 1/2 (ERK1/2) phosphorylation in

fully differentiated progenies, identifying NADPH oxidase and ERK1/2 as targets of PrP^C-mediated signaling in neuronal and non-neuronal cells (Schneider et al., 2003).

4. Metals and prion diseases

Our understanding of the role of metals in key neurobiological processes as well as in the pathogenesis of various neurodegenerative diseases has continued to expand over the last two decades. Although it is well known that elemental metals are required for cells to function normally, the degree to which the central nervous system (CNS) uses metals in synaptic signaling and the loss of metal homeostasis during neurodegenerative diseases was, until recently, unknown. Dyshomeostasis of transition metals such as manganese, iron, copper, and zinc have been implicated in major neurodegenerative conditions such as PD, AD, ALS, HD, and prion disease (Brown, 2009; Bush and Curtain, 2008; Kanthasamy et al., 2012; Molina-Holgado et al., 2007). Another common pathological feature of neurodegenerative diseases is the aggregation of proteins rich in β-sheets associated with each specific disease (Tyedmers et al., 2010). Alarmingly, exposing amyloidogenic proteins or their cleavage products to metals impacts the protein misfolding and progression of neurodegenerative processes (Brown, 2009). Specially, manganese has been shown to bind to the cellular form of prion protein, and this interaction has been implicated in the aggregation and misfolding of PrP^C. In this section, we will summarize the current evidence of manganese and prion interaction and its functional consequences in prion disease.

4.1 Manganese

Manganese (Mn) is one of the most abundant transitional metals on earth, comprising approximately 0.1% of the earth's crust. It may exist in both inorganic and organic forms, and has been heavily used in welding, mining, the manufacturing of batteries, glass, fireworks, chemicals, pesticides and fertilizers and in other industrial settings (Meeker et al., 2007). In nature, Mn exhibits 11 oxidation states ranging from -3 to +7, while in biological systems it occurs primarily as Mn^{2+}, Mn^{3+}, and Mn^{4+} (Su et al., 2013). In the human body, Mn is an essential trace element that functions as a key cofactor for numerous metalloenzymes, such as manganese superoxide dismutase, pyruvate carboxylase, arginase, and phosphoenolpyruvate decarboxylase and glutamine synthetase (Aschner and Aschner, 2005). As such, Mn is involved in various biochemical and cellular functions, including blood clotting, ATP production, immune responsiveness, digestion, and reproduction (Erikson et al., 2007). It also plays a key role in the development and normal functioning of the brain. Transport of Mn ions into the brain can be mediated through both the blood-brain and the blood-cerebrospinal fluid barriers (Crossgrove and Yokel, 2004; Yokel, 2002), and studies have documented various transporting mechanisms in this process (Aschner and Gannon, 1994; Aschner et al., 1999; Martinez-Finley et al., 2013). Recommended intake levels of Mn for men and women have been established at 2.3 mg/day and 1.8 mg/day, respectively (Trumbo et al., 2001). Although dietary Mn deficiencies are exceedingly rare in humans, diets low in Mn may cause many developmental defects. On the other hand, excess exposure to Mn results in a severe and degenerative neurologic condition, known as manganism or Mn-induced Parkinsonism. Early signs of manganism include a variety of psychiatric

disturbances, such as emotional liability, mania, and hallucinations, while motor symptoms including bradykinesia, rigidity, and dystonia are late manifestations of this disorder (Dobson et al., 2004). Unlike PD, manganism is pathologically characterized by the loss of neurons in the globus pallidus, cortex and hypothalamus and without the formation of Lewy bodies (Aschner et al., 2009; Verina et al., 2013). Although the pathogenic mechanisms underlying manganism are poorly understood, several lines of evidence suggest that Mn-induced neurotoxicity is associated with increased oxidative stress, impairment of energy metabolism and antioxidant systems, attenuation of astrocytic glutamate uptake, upregulation of binding sites for peripheral benzodiazepine receptor ligands, and alterations in various cell signaling pathways (Erikson and Aschner, 2003; Kitazawa et al., 2002; Roth and Garrick, 2003). We have previously reported that the proapoptotic kinase PKCδ plays a crucial role in mediating Mn-induced dopaminergic neurodegeneration (Anantharam et al., 2002; Kanthasamy et al., 2010; Kitazawa et al., 2005; Latchoumycandane et al., 2005). Interestingly, a role for Mn in the pathogenesis of prion disease has been emerging in recent years. Particularly, evidence has indicated that Mn-bound PrP^{Sc} can be isolated from both human and animal prion diseases (Wong et al., 2001b).

4.2 Manganese binding to PrP^C

As aforementioned, PrP^C is a putative metalloprotein since the octapeptide repeat sequences at the N-terminus of the protein have a high affinity for divalent cations including copper (Cu), Mn, and zinc (Zn). The possible complexation of Mn by PrP^C first came to light in 2000 when total reflection x-ray fluorescence spectrometry (TXRF) was applied (Brown et al., 2000). In this study, recombinant full-length PrP^C was discovered

to bind Mn *in vitro* followed by the refolding of this protein in the presence of high concentrations of Mn. However, deletion of the octapeptide repeat sequences completely abolished this Mn binding. The authors also documented that Mn can equivalently substitute for Cu in the octameric repeat region. These facts highlight the importance of the octameric repeat domain in mediating Mn and prion interactions. Later on, a few other studies on the affinity of Mn for prion were carried out using different amino acid sequences of recombinant prion protein; however, the results varied. Although evidence has indicated that Mn does have a binding affinity to the octameric repeat region, a spectroscopic study by Garnett and Viles showed that Mn does not bind to the PrP octameric repeat region (Garnett and Viles, 2003). Similarly, Treiber et al., using the surface plasmon resonance (SPR) technique, found that peptides covering the octameric repeat sequences of prion were not able to bind Mn and, on the contrary, full-length PrP and the mutant PrP lacking the octameric repeat region bound to Mn with a nanomolar dissociation constant (Treiber et al., 2007b). They concluded that the octameric repeat region is not involved in Mn binding and proposed a conformational binding site for Mn involving the PrP residues 91-230. In contrast, analysis involving NMR and circular dichroism (CD) spectroscopy in the presence of glycine, has confirmed the binding of Mn to the octameric repeat region despite an affinity at least three orders of magnitude less than Cu (Jackson et al., 2001). These divergent results might be due to variations in detection techniques and the use of different peptide sequences of PrP. Additional Mn-binding sites were identified at His 95 and 110 in the so-called "fifth site" (Jackson et al., 2001; Jones et al., 2004). However, a subsequent report from Dr. David Brown's laboratory revealed that His 95 is the preferential binding site for Mn in this region, and

249

to bind Mn *in vitro* followed by the refolding of this protein in the presence of high concentrations of Mn. However, deletion of the octapeptide repeat sequences completely abolished this Mn binding. The authors also documented that Mn can equivalently substitute for Cu in the octameric repeat region. These facts highlight the importance of the octameric repeat domain in mediating Mn and prion interactions. Later on, a few other studies on the affinity of Mn for prion were carried out using different amino acid sequences of recombinant prion protein; however, the results varied. Although evidence has indicated that Mn does have a binding affinity to the octameric repeat region, a spectroscopic study by Garnett and Viles showed that Mn does not bind to the PrP octameric repeat region (Garnett and Viles, 2003). Similarly, Treiber et al., using the surface plasmon resonance (SPR) technique, found that peptides covering the octameric repeat sequences of prion were not able to bind Mn and, on the contrary, full-length PrP and the mutant PrP lacking the octameric repeat region bound to Mn with a nanomolar dissociation constant (Treiber et al., 2007b). They concluded that the octameric repeat region is not involved in Mn binding and proposed a conformational binding site for Mn involving the PrP residues 91-230. In contrast, analysis involving NMR and circular dichroism (CD) spectroscopy in the presence of glycine, has confirmed the binding of Mn to the octameric repeat region despite an affinity at least three orders of magnitude less than Cu (Jackson et al., 2001). These divergent results might be due to variations in detection techniques and the use of different peptide sequences of PrP. Additional Mn-binding sites were identified at His 95 and 110 in the so-called "fifth site" (Jackson et al., 2001; Jones et al., 2004). However, a subsequent report from Dr. David Brown's laboratory revealed that His 95 is the preferential binding site for Mn in this region, and

www.manaraa.com

His 110 plays no role in Mn binding (Brown, 2009). Interestingly, further work by the same group suggests that the higher-affinity Mn binding site is not the octapeptide repeat motif, but the His 95 in the 5th site (Brazier et al., 2008). Using isothermal titration calorimetry, they identified two Mn binding sites for prion protein. The principle one is located at histidine residue 95 and the second low-affinity site is associated with the octameric repeat region, with dissociation constants of 63 µM and 200 µM, respectively (Brazier et al., 2008). This study also revealed an optimum pH of 5.5 for Mn binding at both sites. Additionally, the authors determined that PrP^C binds two molecules of Mn at these sites, while it was originally thought to bind up to four molecules of Mn at the octapeptide repeat region (Brown et al., 2000). This study went on to show that Mn is able to replace Cu in Cu-saturated prion, even though PrP has a higher affinity for Cu at both binding sites. It should be noted that the micromolar range of affinity values for Mn binding to prion is in the range of other known Mn-binding proteins (Brown, 2011). Although the research relating to PrP and Mn interaction has mostly been conducted *in vitro*, prion clearly is a Mn-binding protein. Given the important roles Mn and prion protein play in normal and disease states, it is logical to assume that the binding of Mn to prion protein has significant structural and functional consequences.

4.3 Role of manganese in the pathogenesis of prion disease

Over the past dozen or so years, evidence has been mounting suggesting a possible role for Mn binding to PrP in the pathogenesis of prion diseases. Limited proteolytic digestion experiments using proteinase K and recombinant prion protein have revealed that Mn-loaded PrP gains partial protease resistance *in vitro* (Brown et al.,

2000). Further cell-free studies involving the protein misfolding cyclic amplification (PMCA) technique supported the idea that Mn acts as a cofactor in the conversion of PrP^C into the protease-resistant PrP^{Sc}-like form PrP^{res}, and determined that this conversion ability was similar to but less profound than the diagnostic proteolytic resistance characteristic of PrP^{Sc} (Kim et al., 2005). Using a PrP-expressing yeast cell system, PrP^{res} formation was induced *in vivo* after the supplementation of Mn-containing media, suggesting that environmental Mn could be a risk factor for prion disease (Treiber et al., 2006). Similarly, *in vivo* PrP^{res} formation was detected in rat astrocytes when incubated with Mn for a prolonged period of time (Brown et al., 2000). These changes in protease resistance of PrP^C have been suggested to be related to an altered conformation of PrP when Mn is bound. Indeed, analysis of full-length recombinant PrP using CD indicated that Mn-bound PrP has increased β-sheet content (Brown et al., 2000; Giese et al., 2004). A near-infrared spectroscopy (NIRS) study on metal binding of prion protein in aqueous solutions documented that Mn-bound PrP undergoes highly different structural changes leading to fibril formation (Tsenkova et al., 2004). Interestingly, experiments using a method combining Raman optical activity (ROA) and ultraviolet circular dichroism (UV CD) demonstrated a very different impact of Cu and Mn on prion protein structure. Cu binding to prion protein destroyed its folded α-helical structure in the N-terminus; however, upon binding to Mn, the secondary structure became more organized, gaining more α-helices (Zhu et al., 2008). Another study with recombinant PrP further showed that Mn can replace Cu bound to PrP, resulting in an altered protein conformation with fewer helices (Brazier et al., 2008). In this study, cyclic voltammetric measurements indicated that the oxidation of Mn bound to PrP^C rendered the PrP^C

binding irreversible, which is not seen with Cu-bound PrP[C]. In addition to the resulting conformational changes in prion structure, Mn-bound PrP[C] has been shown to initiate PrP aggregation and seed polymerization of soluble PrP[C]. The protease-resistant PrP[res] with Mn was shown to propagate and form more PrP[res] in the presence of normal hamster brain homogenate by standard PMCA technique, whereas a treatment with the Mn chelator EDTA inhibited this process, indicating a reversible intermolecular Mn binding with PrP (Kim et al., 2005). Other studies confirmed that once bound to Mn, the β-sheet-rich PrP was able to seed polymerization of soluble metal-free PrP (Brazier et al., 2008; Lekishvili et al., 2004). Additionally, Hesketh et al. characterized the Mn-bound PrP seed in a non-denature polymerization assay (Hesketh et al., 2012). In this assay, a ~200 kDa oligomeric form of PrP seed capable of catalyzing PrP aggregation was generated by exposing recombinant prion protein to Mn. Using mutant recombinant PrP molecules, they further showed that Mn binding to PrP is essential for seed formation but not for polymerization. Another interesting finding from this report is that prion protein from chickens, in which no known prion disease is found, was able to generate PrP seed after treatment with Mn.

Despite extensive *in vitro* studies on prion-Mn interaction and its subsequent effects on prion aggregation, the *in vivo* consequences of Mn binding to prion in terms of neuronal loss have not yet been well studied. An earlier report showed that recombinant PrP refolding in the presence of Mn was toxic to PrP-expressing cell lines and primary neuronal cultures (Uppington and Brown, 2008). More recently, treatment with an effective and relatively selective chelator for Mn, cyclohexanediaminetetraacetic acid ($Na_2CaCDTA$), significantly extended survival time in an animal model of prion disease

where mice were infected with a low dose of prion disease (Brazier et al., 2010). In agreement with these findings, Hortells et al. demonstrated that that a Mn-rich diet in Scrapie prion-inoculated mice increased neuronal loss and the levels of PrP-containing plaques (Hortells et al., 2010), although this has not been replicated by other workers (Legleiter et al., 2007). Interestingly, elevated Mn levels in the brain and blood of humans and animals afflicted with TSE have been observed. In particular, altered Mn content has been observed in the blood and brains of humans infected with CJD (Hesketh et al., 2008; Wong et al., 2001b), mice infected with scrapie (Kim et al., 2005; Thackray et al., 2002), in cattle infected with BSE (Hesketh et al., 2007a), and in elk infected with chronic wasting disease (CWD) (White et al., 2010). What is more interesting is that the elevated blood Mn levels in scrapie and BSE were detected prior to the onset of disease symptoms, suggesting that altered metal levels might be a biomarker for diagnosis in the early stages of prion disease. Thus far, whether alteration in Mn levels in prion disease is a primary cause leading to infection or a secondary effect due to the infection itself remains unclear. Indeed, we lack clear evidence as to why Mn levels were elevated in these prion disease cases. At the cellular level, these increases may be linked to altered Mn homeostasis and signaling. Several cell culture studies including ours have shown that prion protein expression and infection can modulate the expression of Mn transporting proteins and cause ensuing Mn cellular retention (Kralovicova et al., 2009; Martin et al., 2011). On the other hand, as we have reported (Choi et al., 2010), increased Mn may in turn result in more PrP due to its inhibitory effects on proteasome degradation (Cai et al., 2007; Zhou et al., 2004). Therefore, a feed-forward mechanism may be involved in this process. One of the other consequences of increased Mn in prion disease

is likely the abnormalities in iron metabolism since both Mn and iron ions are generally complexed and transported to the brain through a transferrin-transferrin receptor pathway (Heilig et al., 2006). In fact, iron abnormalities have been found in the brains of humans and animals with prion diseases (Singh et al., 2013; Singh et al., 2009). Additionally, PrP^{Sc}-infected cells were more susceptible to oxidative stress (Fernaeus et al., 2005; Milhavet et al., 2000), suggesting that Mn toxicity might be responsible for TSE-related neuronal loss.

To date, the vast majority of work done to elucidate the mechanisms of TSE pathogenesis has focused on the genetic determinants and biophysical kinetics of protein aggregation. Despite the fact that essential trace minerals are not manufactured by the body and that foreign (ingested) PrP^{Sc} can propagate, their environmental contribution to TSE etiology has not received the same kind of attention. However, the evidence continues to build for an environmental role in the initiation or development of the disease. In particular, the environmental distribution of metals correlates with the incidence of TSE (Polano et al., 2008; Purdey, 2000). Likewise, a correlation between soil clay content and the incidence of chronic wasting disease in elk further indicates that soil constituents may affect the persistence of PrP^{Sc} in the environment (Johnson et al., 2007). A pair of monozygotic twins with a pathogenic hereditary mutation to PrP developed TSE pathology seven years apart from each other (Bowman et al., 2011), providing more evidence for an environmental trigger. The recurrence of TSE in livestock despite multiple governmental programs designed to eradicate the disease argues for the persistence of a pathogen or trigger in the environment. Interestingly, a recent study strongly argues in favor of the notion that environmental Mn levels could be

relevant to prion disease transmission. In this study, they found that infectious PrP^{Sc} can persist in soils for at least two years (Davies and Brown, 2009). Additionally, the presence of high levels of Mn in soils not only protects the protein from degradation, but may actually increase infectivity by up to 100-fold. These findings provide a route whereby PrP^{Sc} derived from carcasses or farm runoff can enter and persist in the environment. Thus, oral inoculation can occur in ruminants ingesting soil microparticles while grazing. The retention of infectivity in the environment seems to depend highly on the presence of Mn in the soil. However, it should be noted that soil is a very complex matrix comprising many other components that could influence the incidence of prion disease. A greater understanding of environmental determinants would greatly help in assessing the risk factors of TSE.

4.4 Role of manganese in the physiological function and expression of PrP^{C}

Current evidence suggests a role for prion protein in modulating metal homeostasis as well as antioxidant levels (Brown et al., 2002; Wong et al., 2001c). Previously, we examined the role of PrP^{C} in regulating Mn-induced neurotoxicity (Choi et al., 2007). Using mouse neuronal cell lines, we demonstrated that cells expressing prion protein (PrP^{C}) were more protected against Mn-induced neurotoxicity than were prion-knockout cells (PrP^{KO}). Inductively-coupled plasma mass spectrometry (ICP-MS) revealed that lacking prion protein expression caused significantly lower basal Mn levels in PrP^{KO} cells, and upon Mn treatment, PrP^{C} cells internalized significantly less Mn than did PrP^{KO} cells. Examination of reactive oxygen species (ROS) formation, caspase activation, and cell death all revealed that the mouse neuronal cell line lacking prion

protein expression was more susceptible to Mn neurotoxicity. This increased susceptibility likely resulted from the homeostatic imbalance of Mn, as evidenced by the significantly higher amount of cellular Mn in these cells following treatment. Similar findings were achieved with hydrogen peroxide, which also increased the susceptibility of PrP^{KO} cells (unpublished data). Our findings suggest that prion might act as a metal sink, thereby preventing Mn from entering the cells and exerting its neurotoxic effect. In another recent study (Choi et al., 2010), we further examined the fate of cellular prion protein in a Mn-treated PrP^{C}-expressing mouse neuronal cell line. Interestingly, our results indicated that with Mn treatment, prion protein levels significantly increased over time. A previous study showed increased prion protein expression in a particular cell line treated with Cu, which elevated the activity of the reporter vector with Prnp (Varela-Nallar et al., 2005). Surprisingly, this was not the case for the Mn-mediated upregulation of cellular prion protein. We eliminated the possibility that Mn increased the transcription or inhibition of the ubiquitin proteasomal system (UPS), and further verified that in our system, Mn treatment significantly altered the turnover of PrP^{C}. Pulse chase experiments confirmed that the half-life of PrP^{C} in Mn-treated cells was significantly increased. Together, these findings suggest that prion-mediated alterations in cellular Mn uptake and Mn-induced upregulation of PrP^{C} levels through increasing global protein stability may contribute to neurodegeneration in prion and other neurodegenerative diseases.

4.5 Role of other metals in prion disease

Additional metals such as Cu, Zn, and nickel (Ni) may have the potential to bind to prion protein. A reduced Zn content in brains with prion disease has been revealed

(Wong et al., 2001a; Wong et al., 2001b) and a few other studies suggest that Zn binds to the octapeptide repeats in PrP^C, albeit at an apparently lower affinity (Kenward et al., 2007; Stellato et al., 2011; Walter et al., 2007). Evidence also exists showing that the interaction promotes the endocytosis of PrP^c (Pauly and Harris, 1998; Perera and Hooper, 2001). Although Spevacek et al. showed that Zn binding changes the structure of murine PrP^c (Spevacek et al., 2013), the structural and functional consequences of Zn-prion interaction are still largely unknown. Interestingly, a recent study pointed out a role for cellular prion protein in facilitating the uptake of Zn into neurons, which was not observed in prion disease (Watt et al., 2013; Watt et al., 2012). The mechanism of prion-mediated metal uptake seems to be metal-specific since our study showed that prion protein reduced Mn uptake in neurons (Choi et al., 2007). Ni has been used to isolate PrP in affinity columns (Choi et al., 2006), but its potential interaction with PrP has been neglected since Ni binds to PrP^c with quite low affinity (Brown et al., 2000). In contrast, it is widely accepted that PrP binds Cu. Many lines of *in vitro* evidence indicate that the interaction between Cu and PrP^C primarily occurs within the octapeptide repeat region or a second site at the His 95 and 110 residues in the fifth site with a dissociation constant in the nanomolar range (Aronoff-Spencer et al., 2000; Jackson et al., 2001; Jones et al., 2004). Further studies on Cu coordination with the octapeptide repeat domain have shown that there are three distinct modes at physiological pH (Chattopadhyay et al., 2005). Similar to Zn, Cu binding governs PrP^c endocytosis, and this requires the octapeptide repeat region (Haigh et al., 2005; Pauly and Harris, 1998; Perera and Hooper, 2001). The binding of Cu to PrP^c appears to be crucial to the normal function of the protein. For instance, the antioxidant activity of PrP^C requires Cu bound within the

octapeptide repeat domain (Brown et al., 2001; Brown et al., 1999; Gaggelli et al., 2008; Treiber et al., 2007a). Cu bound by the octapeptide repeat domain of PrP[C] undergoes full and reversible redox chemistry and can detoxify superoxide and reduce hydroxyl radicals (Nadal et al., 2007). However, the concept that Cu-PrP complex acts as an antioxidant is controversial based on conflicting results of several studies (Hutter et al., 2003; Jones et al., 2005). Loss of Cu accompanied with increased Mn levels has been described in prion-infected brains (Thackray et al., 2002; Wong et al., 2001a; Wong et al., 2001b), suggesting that a Cu deficiency or Cu displacement from the PrP[C] might contribute to the pathology of prion disease. Unfortunately, experiments on the role of Cu in the pathology of prion disease have generated contradictory viewpoints. Some studies reported that Cu-bound PrP[c] undergoes conformational changes and increases protease resistance (Qin et al., 2000; Quaglio et al., 2001; Stockel et al., 1998), while others showed that when refolded in the presence of Cu, PrP[c] decreases its protease resistance and its level of aggregation (Bocharova et al., 2005; Wong et al., 2000). In addition, reduced Cu levels in the brain and blood using a Cu chelator extended the incubation period of the diseases (Sigurdsson et al., 2003), whereas another report indicated that increased Cu in the diet delayed the onset of prion disease (Hijazi et al., 2003). Overall, these findings and those of others suggest the contributions of Cu in the pathogenesis of prion disease tend to be far more complex than originally expected.

5. Conclusion

Prion protein readily binds Mn despite an apparent lower affinity. Once bound to Mn, it adopts a conformational change and converts into the protease-resistant PrP[Sc]-like

form that is essential for seed formation. Chelation of Mn in a prion animal model extended the incubation time for the disease, indicating that Mn could be a significant risk factor for prion disease. The discovery that Mn increased during the course of TSE in both humans and animals and that it could stabilize prions in the soil, thereby increasing PrP^{Sc} availability, further implicated Mn in the pathogenesis of the disease. However, many questions remain unanswered, like what's the impact of Mn binding on the normal functioning of PrP^C? What's the molecular basis behind the Mn-induced conformational conversion of prion protein? Furthermore, why are Mn levels altered in prion diseases?

Although Mn could be an important component in the pathogenesis of the disease, by no means is it the only causative factor in prion disease development and progression. Most likely, developing a prion disease results from the culmination of various environmental, genetic, and even sporadic conditions. Therefore, approaching cures to prion disease may require multifaceted strategies to effectively combat its progression and even development.

References

Aguzzi, A., 2006. Prion diseases of humans and farm animals: epidemiology, genetics, and pathogenesis. J Neurochem. 97**,** 1726-39.

Aguzzi, A., et al., 2008. The prion's elusive reason for being. Annu Rev Neurosci. 31**,** 439-77.

Alpers, M., Epidemiology and clinical aspects of kuru. In: M. M. Prusiner SB, (Ed.), Prions. Academic Press, New York, 1987.

Anantharam, V., et al., 2002. Caspase-3-dependent proteolytic cleavage of protein kinase Cdelta is essential for oxidative stress-mediated dopaminergic cell death after exposure to methylcyclopentadienyl manganese tricarbonyl. J Neurosci. 22**,** 1738-51.

Aronoff-Spencer, E., et al., 2000. Identification of the Cu^{2+} binding sites in the N-terminal domain of the prion protein by EPR and CD spectroscopy. Biochemistry. 39**,** 13760-71.

Aschner, J. L., Aschner, M., 2005. Nutritional aspects of manganese homeostasis. Mol Aspects Med. 26**,** 353-62.

Aschner, M., et al., 2009. Manganese and its role in Parkinson's disease: from transport to neuropathology. Neuromolecular Med. 11**,** 252-66.

Aschner, M., Gannon, M., 1994. Manganese (Mn) transport across the rat blood-brain barrier: saturable and transferrin-dependent transport mechanisms. Brain Res Bull. 33**,** 345-9.

Aschner, M., et al., 1999. Manganese uptake and distribution in the central nervous system (CNS). Neurotoxicology. 20**,** 173-80.

Belay, E. D., Schonberger, L. B., 2005. The public health impact of prion diseases. Annu Rev Public Health. 26, 191-212.

Bocharova, O. V., et al., 2005. Copper(II) inhibits in vitro conversion of prion protein into amyloid fibrils. Biochemistry. 44, 6776-87.

Bowman, A. B., et al., 2011. Role of manganese in neurodegenerative diseases. J Trace Elem Med Biol. 25, 191-203.

Brazier, M. W., et al., 2008. Manganese binding to the prion protein. J Biol Chem. 283, 12831-9.

Brazier, M. W., et al., 2010. Manganese chelation therapy extends survival in a mouse model of M1000 prion disease. J Neurochem. 114, 440-51.

Broderick, G. A., 1977. Effect of processing on protein utilization by ruminants. Adv Exp Med Biol. 86B, 531-44.

Brown, D. R., 2002. Don't lose sleep over prions: role of prion protein in sleep regulation. Neuroreport. 13, A1.

Brown, D. R., 2004. Metallic prions. Biochem Soc Symp. 193-202.

Brown, D. R., 2009. Brain proteins that mind metals: a neurodegenerative perspective. Dalton Trans. 4069-76.

Brown, D. R., 2011. Prions and manganese: A maddening beast. Metallomics. 3, 229-38.

Brown, D. R., et al., 2001. Antioxidant activity related to copper binding of native prion protein. J Neurochem. 76, 69-76.

Brown, D. R., et al., 2000. Consequences of manganese replacement of copper for prion protein function and proteinase resistance. EMBO J. 19, 1180-6.

Brown, D. R., et al., 2002. Lack of prion protein expression results in a neuronal phenotype sensitive to stress. J Neurosci Res. 67**,** 211-24.

Brown, D. R., et al., 1998. Effects of copper on survival of prion protein knockout neurons and glia. J Neurochem. 70**,** 1686-93.

Brown, D. R., et al., 1999. Normal prion protein has an activity like that of superoxide dismutase. Biochem J. 344 Pt 1**,** 1-5.

Brown, R. E., et al., 2012. Control of sleep and wakefulness. Physiol Rev. 92**,** 1087-187.

Bush, A. I., Curtain, C. C., 2008. Twenty years of metallo-neurobiology: where to now? Eur Biophys J. 37**,** 241-5.

Cai, T., et al., 2007. Proteasome inhibition is associated with manganese-induced oxidative injury in PC12 cells. Brain Res. 1185**,** 359-65.

Cervenakova, L., et al., 1998. Phenotype-genotype studies in kuru: implications for new variant Creutzfeldt-Jakob disease. Proc Natl Acad Sci U S A. 95**,** 13239-41.

Chattopadhyay, M., et al., 2005. The octarepeat domain of the prion protein binds Cu(II) with three distinct coordination modes at pH 7.4. J Am Chem Soc. 127**,** 12647-56.

Choi, C. J., et al., 2010. Manganese upregulates cellular prion protein and contributes to altered stabilization and proteolysis: relevance to role of metals in pathogenesis of prion disease. Toxicol Sci. 115**,** 535-46.

Choi, C. J., et al., 2007. Normal cellular prion protein protects against manganese-induced oxidative stress and apoptotic cell death. Toxicol Sci. 98**,** 495-509.

Choi, C. J., et al., 2006. Interaction of metals with prion protein: possible role of divalent cations in the pathogenesis of prion diseases. Neurotoxicology. 27**,** 777-87.

Collinge, J., 2005. Molecular neurology of prion disease. J Neurol Neurosurg Psychiatry. 76, 906-19.

Colognato, H., Yurchenco, P. D., 2000. Form and function: the laminin family of heterotrimers. Dev Dyn. 218, 213-34.

Crossgrove, J. S., Yokel, R. A., 2004. Manganese distribution across the blood-brain barrier III. The divalent metal transporter-1 is not the major mechanism mediating brain manganese uptake. Neurotoxicology. 25, 451-60.

Cuille J., C. P. L., 1939. Experimental transmission of trembling to the goat. C.R. Seances Acad. Sci. 1058-1160.

Davies, P., Brown, D. R., 2009. Manganese enhances prion protein survival in model soils and increases prion infectivity to cells. PLoS One. 4, e7518.

DeArmond, S. J., et al., 1987. Changes in the localization of brain prion proteins during scrapie infection. Neurology. 37, 1271-80.

Di Guglielmo, G. M., et al., 2003. Distinct endocytic pathways regulate TGF-beta receptor signalling and turnover. Nat Cell Biol. 5, 410-21.

Di Natale, G., et al., 2005. Copper(II) interaction with unstructured prion domain outside the octarepeat region: speciation, stability, and binding details of copper(II) complexes with PrP106-126 peptides. Inorg Chem. 44, 7214-25.

Dobson, A. W., et al., 2004. Manganese neurotoxicity. Ann N Y Acad Sci. 1012, 115-28.

Doh-ura, K., et al., 1989. Pro----leu change at position 102 of prion protein is the most common but not the sole mutation related to Gerstmann-Straussler syndrome. Biochem Biophys Res Commun. 163, 974-9.

Duffy, P., et al., 1974. Letter: Possible person-to-person transmission of Creutzfeldt-Jakob disease. N Engl J Med. 290**,** 692-3.

Engleberg, C. D., Victor J. Dermody, Terence S. , 2012. Schaechter's Mechanisms of Microbial Disease. Lippincott Williams & Wilkins.

Erikson, K. M., Aschner, M., 2003. Manganese neurotoxicity and glutamate-GABA interaction. Neurochem Int. 43**,** 475-80.

Erikson, K. M., et al., 2007. Manganese neurotoxicity: a focus on the neonate. Pharmacol Ther. 113**,** 369-77.

Fernaeus, S., et al., 2005. Increased susceptibility to oxidative stress in scrapie-infected neuroblastoma cells is associated with intracellular iron status. Neurosci Lett. 389**,** 133-6.

Forloni, G., et al., 2013. Therapy in prion diseases. Curr Top Med Chem. 13**,** 2465-76.

Gaggelli, E., et al., 2008. Structural characterization of the intra- and inter-repeat copper binding modes within the N-terminal region of "prion related protein" (PrP-rel-2) of zebrafish. J Phys Chem B. 112**,** 15140-50.

Gajdusek, D. C., et al., 1966. Experimental transmission of a Kuru-like syndrome to chimpanzees. Nature. 209**,** 794-6.

Gambetti, P., et al., 2011. Molecular biology and pathology of prion strains in sporadic human prion diseases. Acta Neuropathol. 121**,** 79-90.

Garnett, A. P., Viles, J. H., 2003. Copper binding to the octarepeats of the prion protein. Affinity, specificity, folding, and cooperativity: insights from circular dichroism. J Biol Chem. 278**,** 6795-802.

Gay, C. T., et al., 1988. Infantile botulism. South Med J. 81**,** 457-60.

Ghetti, B., et al., 1989. Gerstmann-Straussler-Scheinker disease. II. Neurofibrillary tangles and plaques with PrP-amyloid coexist in an affected family. Neurology. 39, 1453-61.

Gibbs, C. J., Jr., et al., 1985. Clinical and pathological features and laboratory confirmation of Creutzfeldt-Jakob disease in a recipient of pituitary-derived human growth hormone. N Engl J Med. 313, 734-8.

Giese, A., et al., 2004. Effect of metal ions on de novo aggregation of full-length prion protein. Biochem Biophys Res Commun. 320, 1240-6.

Haigh, C. L., et al., 2005. Copper binding is the governing determinant of prion protein turnover. Mol Cell Neurosci. 30, 186-96.

Harder, A., et al., 1999. Novel twelve-generation kindred of fatal familial insomnia from germany representing the entire spectrum of disease expression. Am J Med Genet. 87, 311-6.

Head, M. W., 2013. Human prion diseases: molecular, cellular and population biology. Neuropathology. 33, 221-36.

Heilig, E. A., et al., 2006. Manganese and iron transport across pulmonary epithelium. Am J Physiol Lung Cell Mol Physiol. 290, L1247-59.

Hesketh, S., et al., 2008. Elevated manganese levels in blood and CNS in human prion disease. Mol Cell Neurosci. 37, 590-8.

Hesketh, S., et al., 2007a. Elevated manganese levels in blood and central nervous system occur before onset of clinical signs in scrapie and bovine spongiform encephalopathy. J Anim Sci. 85, 1596-609.

Hesketh, S., et al., 2007b. Elevated Manganese Levels in Blood and CNS Occur Prior to Onset of Clinical Signs in Scrapie and BSE. J Anim Sci.

Hesketh, S., et al., 2012. Prion protein polymerisation triggered by manganese-generated prion protein seeds. J Neurochem. 120**,** 177-89.

Hijazi, N., et al., 2003. Copper binding to PrPC may inhibit prion disease propagation. Brain Res. 993**,** 192-200.

Hornshaw, M. P., et al., 1995. Copper binding to the N-terminal tandem repeat regions of mammalian and avian prion protein. Biochem Biophys Res Commun. 207**,** 621-9.

Hortells, P., et al., 2010. The effect of metal imbalances on scrapie neurodegeneration. Zoonoses Public Health. 57**,** 358-66.

Hsiao, K., et al., 1992. Mutant prion proteins in Gerstmann-Straussler-Scheinker disease with neurofibrillary tangles. Nat Genet. 1**,** 68-71.

Huber, R., et al., 1999. Prion protein: a role in sleep regulation? J Sleep Res. 8 Suppl 1**,** 30-6.

Hutter, G., et al., 2003. No superoxide dismutase activity of cellular prion protein in vivo. Biol Chem. 384**,** 1279-85.

Imran, M., Mahmood, S., 2011. An overview of human prion diseases. Virol J. 8**,** 559.

Jackson, G. S., et al., 2001. Location and properties of metal-binding sites on the human prion protein. Proc Natl Acad Sci U S A. 98**,** 8531-5.

Jang, B., et al., 2013. Peptidylarginine deiminase and protein citrullination in prion diseases: strong evidence of neurodegeneration. Prion. 7**,** 42-6.

Jansen, C., et al., 2010. Prion protein amyloidosis with divergent phenotype associated with two novel nonsense mutations in PRNP. Acta Neuropathol. 119**,** 189-97.

Johnson, C. J., et al., 2007. Oral transmissibility of prion disease is enhanced by binding to soil particles. PLoS Pathog. 3**,** e93.

Jones, C. E., et al., 2004. Preferential Cu2+ coordination by His96 and His111 induces beta-sheet formation in the unstructured amyloidogenic region of the prion protein. J Biol Chem. 279**,** 32018-27.

Jones, S., et al., 2005. Recombinant prion protein does not possess SOD-1 activity. Biochem J. 392**,** 309-12.

Kanthasamy, A., et al., 2010. Novel cell death signaling pathways in neurotoxicity models of dopaminergic degeneration: relevance to oxidative stress and neuroinflammation in Parkinson's disease. Neurotoxicology. 31**,** 555-61.

Kanthasamy, A. G., et al., 2012. Effect of divalent metals on the neuronal proteasomal system, prion protein ubiquitination and aggregation. Toxicol Lett. 214**,** 288-95.

Kaufman, M. P., et al., 1985. Attenuation of the reflex pressor response to muscular contraction by a substance P antagonist. Brain Res. 333**,** 182-4.

Kenward, A. G., et al., 2007. Copper and zinc promote interactions between membrane-anchored peptides of the metal binding domain of the prion protein. Biochemistry. 46**,** 4261-71.

Kim, N. H., et al., 2005. Effect of transition metals (Mn, Cu, Fe) and deoxycholic acid (DA) on the conversion of PrPC to PrPres. FASEB J. 19**,** 783-5.

Kitazawa, M., et al., 2005. Activation of protein kinase C delta by proteolytic cleavage contributes to manganese-induced apoptosis in dopaminergic cells: protective role of Bcl-2. Biochem Pharmacol. 69**,** 133-46.

Kitazawa, M., et al., 2002. Oxidative stress and mitochondrial-mediated apoptosis in dopaminergic cells exposed to methylcyclopentadienyl manganese tricarbonyl. J Pharmacol Exp Ther. 302**,** 26-35.

Kralovicova, S., et al., 2009. The effects of prion protein expression on metal metabolism. Mol Cell Neurosci. 41**,** 135-47.

Kretzschmar, H. A., et al., 1986. Molecular cloning of a human prion protein cDNA. DNA. 5**,** 315-24.

Ladogana, A., et al., 2005. Mortality from Creutzfeldt-Jakob disease and related disorders in Europe, Australia, and Canada. Neurology. 64**,** 1586-91.

Latchoumycandane, C., et al., 2005. Protein kinase Cdelta is a key downstream mediator of manganese-induced apoptosis in dopaminergic neuronal cells. J Pharmacol Exp Ther. 313**,** 46-55.

Legleiter, L. R., et al., 2007. Exposure to low dietary copper or low copper coupled with high dietary manganese for one year does not alter brain prion protein characteristics in the mature cow. J Anim Sci. 85**,** 2895-903.

Lekishvili, T., et al., 2004. BSE and vCJD cause disturbance to uric acid levels. Exp Neurol. 190**,** 233-44.

Liberski, P. P., 2013. Kuru: A Journey Back in Time from Papua New Guinea to the Neanderthals' Extinction. Pathogens 472-505.

Liberski, P. P., et al., 1998. A case of sporadic Creutzfeldt-Jakob disease with a Gerstmann-Straussler-Scheinker phenotype but no alterations in the PRNP gene. Acta Neuropathol. 96**,** 425-30.

Llewelyn, C. A., et al., 2004. Possible transmission of variant Creutzfeldt-Jakob disease by blood transfusion. Lancet. 363**,** 417-21.

Lockwood, A. H., 1989. Medical problems of musicians. N Engl J Med. 320**,** 221-7.

Maiti, N. R., Surewicz, W. K., 2001. The role of disulfide bridge in the folding and stability of the recombinant human prion protein. J Biol Chem. 276**,** 2427-31.

Mallucci, G. R., 2009. Prion neurodegeneration: starts and stops at the synapse. Prion. 3**,** 195-201.

Maness, P. F., Schachner, M., 2007. Neural recognition molecules of the immunoglobulin superfamily: signaling transducers of axon guidance and neuronal migration. Nat Neurosci. 10**,** 19-26.

Marella, M., et al., 2002. Filipin prevents pathological prion protein accumulation by reducing endocytosis and inducing cellular PrP release. J Biol Chem. 277**,** 25457-64.

Martin, D. P., et al., 2011. Infectious prion protein alters manganese transport and neurotoxicity in a cell culture model of prion disease. Neurotoxicology. 32**,** 554-62.

Martinez-Finley, E. J., et al., 2013. Manganese neurotoxicity and the role of reactive oxygen species. Free Radic Biol Med. 62**,** 65-75.

Masters, C. L., et al., 1981. Creutzfeldt-Jakob disease virus isolations from the Gerstmann-Straussler syndrome with an analysis of the various forms of amyloid plaque deposition in the virus-induced spongiform encephalopathies. Brain. 104**,** 559-88.

Mastrangelo, P., Westaway, D., 2001. Biology of the prion gene complex. Biochem Cell Biol. 79**,** 613-28.

Mead, S., et al., 2003. Balancing selection at the prion protein gene consistent with prehistoric kurulike epidemics. Science. 300**,** 640-3.

Medori, R., Tritschler, H. J., 1993. Prion protein gene analysis in three kindreds with fatal familial insomnia (FFI): codon 178 mutation and codon 129 polymorphism. Am J Hum Genet. 53**,** 822-7.

Medori, R., et al., 1992. Fatal familial insomnia, a prion disease with a mutation at codon 178 of the prion protein gene. N Engl J Med. 326**,** 444-9.

Meeker, J. D., et al., 2007. Manganese and welding fume exposure and control in construction. J Occup Environ Hyg. 4**,** 943-51.

Milhavet, O., et al., 2000. Prion infection impairs the cellular response to oxidative stress. Proc Natl Acad Sci U S A. 97**,** 13937-42.

Molina-Holgado, F., et al., 2007. Metals ions and neurodegeneration. Biometals. 20**,** 639-54.

Montagna, P., et al., 2003. Familial and sporadic fatal insomnia. Lancet Neurol. 2**,** 167-76.

Mouillet-Richard, S., et al., 2000. Signal transduction through prion protein. Science. 289**,** 1925-8.

Nadal, R. C., et al., 2007. Prion protein does not redox-silence Cu2+, but is a sacrificial quencher of hydroxyl radicals. Free Radic Biol Med. 42**,** 79-89.

Padovani, A., et al., 1998. Fatal familial insomnia in a new Italian kindred. Neurology. 51**,** 1491-4.

Parchi, P., et al., 2010. Agent strain variation in human prion disease: insights from a molecular and pathological review of the National Institutes of Health series of experimentally transmitted disease. Brain. 133, 3030-42.

Pauly, P. C., Harris, D. A., 1998. Copper stimulates endocytosis of the prion protein. J Biol Chem. 273, 33107-10.

Perera, W. S., Hooper, N. M., 2001. Ablation of the metal ion-induced endocytosis of the prion protein by disease-associated mutation of the octarepeat region. Curr Biol. 11, 519-23.

Peters, P. J., et al., 2003. Trafficking of prion proteins through a caveolae-mediated endosomal pathway. J Cell Biol. 162, 703-17.

Piccardo, P., et al., 1998. Phenotypic variability of Gerstmann-Straussler-Scheinker disease is associated with prion protein heterogeneity. J Neuropathol Exp Neurol. 57, 979-88.

Piccardo P, M. S., Young K, Gearing M, Dlouhy SR, Ghetti B, 1998. α-Synuclein accumulation in Gerstmann–Straussler–Schenker disease (GSS) with prion protein gene (PRNP) F198S. Neurobiol Aging. S724.

Polano, M., et al., 2008. Organic polyanions act as complexants of prion protein in soil. Biochem Biophys Res Commun. 367, 323-9.

Prado, M. A., et al., 2004. PrPc on the road: trafficking of the cellular prion protein. J Neurochem. 88, 769-81.

Prusiner, S. B., 1982. Novel proteinaceous infectious particles cause scrapie. Science. 216, 136-44.

Prusiner, S. B., 1991. Novel properties and biology of scrapie prions. Curr Top Microbiol Immunol. 172**,** 233-57.

Prusiner, S. B., 1998. Prions and Brain Diseases in Animals and Humans. Springer.

Prusiner, S. B., DeArmond, S. J., 1994. Prion diseases and neurodegeneration. Annu Rev Neurosci. 17**,** 311-39.

Purdey, M., 2000. Ecosystems supporting clusters of sporadic TSEs demonstrate excesses of the radical-generating divalent cation manganese and deficiencies of antioxidant co factors Cu, Se, Fe, Zn. Does a foreign cation substitution at prion protein's Cu domain initiate TSE? Med Hypotheses. 54**,** 278-306.

Qin, K., et al., 2000. Copper(II)-induced conformational changes and protease resistance in recombinant and cellular PrP. Effect of protein age and deamidation. J Biol Chem. 275**,** 19121-31.

Quaglio, E., et al., 2001. Copper converts the cellular prion protein into a protease-resistant species that is distinct from the scrapie isoform. J Biol Chem. 276**,** 11432-8.

Rieger, R., et al., 1997. The human 37-kDa laminin receptor precursor interacts with the prion protein in eukaryotic cells. Nat Med. 3**,** 1383-8.

Roettger, Y., et al., 2013. Immunotherapy in prion disease. Nat Rev Neurol. 9**,** 98-105.

Roth, J. A., Garrick, M. D., 2003. Iron interactions and other biological reactions mediating the physiological and toxic actions of manganese. Biochem Pharmacol. 66**,** 1-13.

Santuccione, A., et al., 2005. Prion protein recruits its neuronal receptor NCAM to lipid rafts to activate p59fyn and to enhance neurite outgrowth. J Cell Biol. 169**,** 341-54.

Schmitt-Ulms, G., et al., 2001. Binding of neural cell adhesion molecules (N-CAMs) to the cellular prion protein. J Mol Biol. 314**,** 1209-25.

Schneider, B., et al., 2003. NADPH oxidase and extracellular regulated kinases 1/2 are targets of prion protein signaling in neuronal and nonneuronal cells. Proc Natl Acad Sci U S A. 100**,** 13326-31.

Sigurdsson, E. M., et al., 2003. Copper chelation delays the onset of prion disease. J Biol Chem. 278**,** 46199-202.

Sim, V. L., Caughey, B., 2009. Recent advances in prion chemotherapeutics. Infect Disord Drug Targets. 9**,** 81-91.

Singh, A., et al., 2013. Prion protein regulates iron transport by functioning as a ferrireductase. J Alzheimers Dis. 35**,** 541-52.

Singh, A., et al., 2009. Abnormal brain iron homeostasis in human and animal prion disorders. PLoS Pathog. 5**,** e1000336.

Spevacek, A. R., et al., 2013. Zinc drives a tertiary fold in the prion protein with familial disease mutation sites at the interface. Structure. 21**,** 236-46.

Stahl, N., et al., 1987. Scrapie prion protein contains a phosphatidylinositol glycolipid. Cell. 51**,** 229-40.

Stellato, F., et al., 2011. Zinc modulates copper coordination mode in prion protein octa-repeat subdomains. Eur Biophys J. 40**,** 1259-70.

Stockel, J., et al., 1998. Prion protein selectively binds copper(II) ions. Biochemistry. 37, 7185-93.

Su, J., et al., 2013. CotA, a multicopper oxidase from Bacillus pumilus WH4, exhibits manganese-oxidase activity. PLoS One. 8, e60573.

Tabernero, C., et al., 2000. Fatal familial insomnia: clinical, neuropathological, and genetic description of a Spanish family. J Neurol Neurosurg Psychiatry. 68, 774-7.

Tagliavini, F., et al., 1994. Amyloid fibrils in Gerstmann-Straussler-Scheinker disease (Indiana and Swedish kindreds) express only PrP peptides encoded by the mutant allele. Cell. 79, 695-703.

Taniwaki, Y., et al., 2000. Familial Creutzfeldt-Jakob disease with D178N-129M mutation of PRNP presenting as cerebellar ataxia without insomnia. J Neurol Neurosurg Psychiatry. 68, 388.

Tateishi, J., et al., 1988. Gerstmann-Straussler-Scheinker disease: immunohistological and experimental studies. Ann Neurol. 24, 35-40.

Taylor, D. R., Hooper, N. M., 2006. The prion protein and lipid rafts. Mol Membr Biol. 23, 89-99.

Taylor, D. R., et al., 2005. Assigning functions to distinct regions of the N-terminus of the prion protein that are involved in its copper-stimulated, clathrin-dependent endocytosis. J Cell Sci. 118, 5141-53.

Thackray, A. M., et al., 2002. Metal imbalance and compromised antioxidant function are early changes in prion disease. Biochem J. 362, 253-8.

Thomson, J. M., et al., 2012. The identification of candidate genes and SNP markers for classical bovine spongiform encephalopathy susceptibility. Prion. 6**,** 461-9.

Treiber, C., et al., 2007a. Copper is required for prion protein-associated superoxide dismutase-I activity in Pichia pastoris. Febs J. 274**,** 1304-11.

Treiber, C., et al., 2006. Effect of copper and manganese on the de novo generation of protease-resistant prion protein in yeast cells. Biochemistry. 45**,** 6674-80.

Treiber, C., et al., 2007b. Real-time kinetics of discontinuous and highly conformational metal-ion binding sites of prion protein. J Biol Inorg Chem. 12**,** 711-20.

Trumbo, P., et al., 2001. Dietary reference intakes: vitamin A, vitamin K, arsenic, boron, chromium, copper, iodine, iron, manganese, molybdenum, nickel, silicon, vanadium, and zinc. J Am Diet Assoc. 101**,** 294-301.

Tsenkova, R. N., et al., 2004. Prion protein fate governed by metal binding. Biochem Biophys Res Commun. 325**,** 1005-12.

Tyedmers, J., et al., 2010. Cellular strategies for controlling protein aggregation. Nat Rev Mol Cell Biol. 11**,** 777-88.

Uppington, K. M., Brown, D. R., 2008. Resistance of cell lines to prion toxicity aided by phospho-ERK expression. J Neurochem. 105**,** 842-52.

Varela-Nallar, L., et al., 2005. Induction of cellular prion protein (PrPC) gene expression by copper in neurons. Am J Physiol Cell Physiol.

Verina, T., et al., 2013. Manganese exposure induces alpha-synuclein aggregation in the frontal cortex of non-human primates. Toxicol Lett. 217**,** 177-83.

Wadsworth, J. D., Collinge, J., 2011. Molecular pathology of human prion disease. Acta Neuropathol. 121**,** 69-77.

Walter, E. D., et al., 2007. The prion protein is a combined zinc and copper binding protein: Zn2+ alters the distribution of Cu2+ coordination modes. J Am Chem Soc. 129**,** 15440-1.

Watt, N. T., et al., 2013. Neuronal zinc regulation and the prion protein. Prion. 7**,** 203-8.

Watt, N. T., et al., 2012. Prion protein facilitates uptake of zinc into neuronal cells. Nat Commun. 3**,** 1134.

Weissmann, C., 2004. The state of the prion. Nat Rev Microbiol. 2**,** 861-71.

Weissmann, C., et al., 2011. Prions on the move. EMBO Rep. 12**,** 1109-17.

White, S. N., et al., 2010. Increased risk of chronic wasting disease in Rocky Mountain elk associated with decreased magnesium and increased manganese in brain tissue. Can J Vet Res. 74**,** 50-3.

Will, R. G., 2003. Acquired prion disease: iatrogenic CJD, variant CJD, kuru. Br Med Bull. 66**,** 255-65.

Will, R. G., et al., 1996. A new variant of Creutzfeldt-Jakob disease in the UK. Lancet. 347**,** 921-5.

Wisniewski, T., Goni, F., 2012. Could immunomodulation be used to prevent prion diseases? Expert Rev Anti Infect Ther. 10**,** 307-17.

Wong, B. S., et al., 2001a. Oxidative impairment in scrapie-infected mice is associated with brain metals perturbations and altered antioxidant activities. J Neurochem. 79**,** 689-98.

Wong, B. S., et al., 2001b. Aberrant metal binding by prion protein in human prion disease. J Neurochem. 78**,** 1400-8.

Wong, B. S., et al., 2001c. Increased levels of oxidative stress markers detected in the brains of mice devoid of prion protein. J Neurochem. 76**,** 565-72.

Wong, B. S., et al., 2000. Copper refolding of prion protein. Biochem Biophys Res Commun. 276**,** 1217-24.

Yokel, R. A., 2002. Brain uptake, retention, and efflux of aluminum and manganese. Environ Health Perspect. 110 Suppl 5**,** 699-704.

York, R. D., et al., 2000. Role of phosphoinositide 3-kinase and endocytosis in nerve growth factor-induced extracellular signal-regulated kinase activation via Ras and Rap1. Mol Cell Biol. 20**,** 8069-83.

Zahn, R., et al., 2000. NMR solution structure of the human prion protein. Proc Natl Acad Sci U S A. 97**,** 145-50.

Zhang, B., et al., 2010. Fatal familial insomnia: a middle-age-onset Chinese family kindred. Sleep Med. 11**,** 498-9.

Zhou, Y., et al., 2004. Proteasomal inhibition induced by manganese ethylene-bis-dithiocarbamate: relevance to Parkinson's disease. Neuroscience. 128**,** 281-91.

Zhu, F., et al., 2008. Raman optical activity and circular dichroism reveal dramatic differences in the influence of divalent copper and manganese ions on prion protein folding. Biochemistry. 47**,** 2510-7.
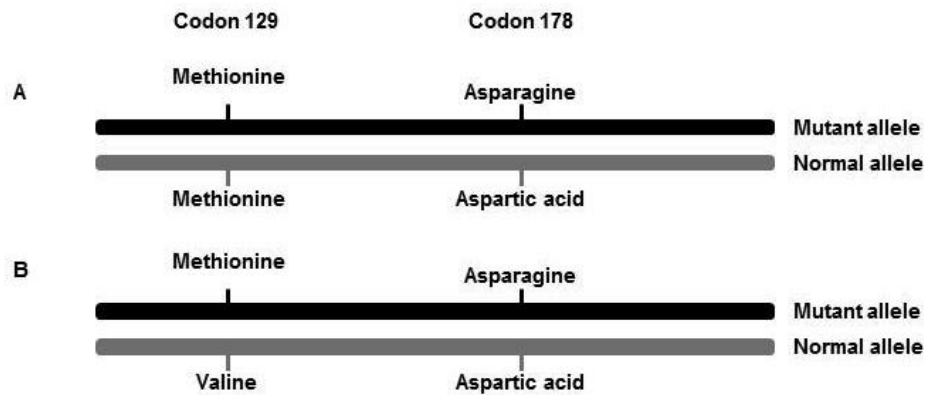
Figure 1: The haplotypes in fatal familial insomnia (FFI). (A) Methionine at polymorphic codon 129 is associated with thalamic damage and fewer cortical alterations, whereas (B) Valine at polymorphic codon 129 is associated with prolonged disease and widespread neuropathological damage with cortical spongiosis.
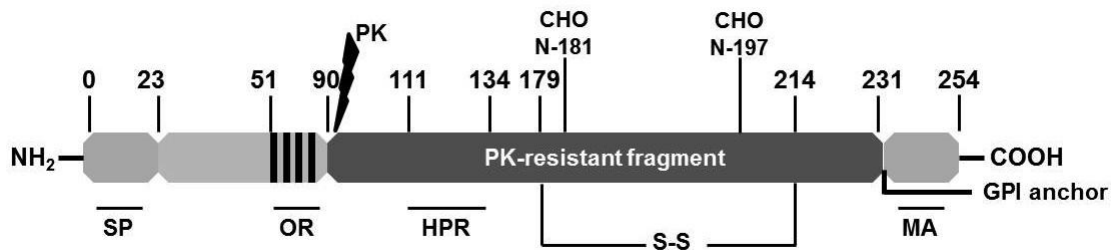
Figure 2: Structure of the prion protein. Mouse PrP^C molecule has 254 amino acids in length, with N-terminal signal peptide (SP) and C-terminal sequences that are cleaved shortly after translation. MA denotes the C-terminal membrane anchor region and HPR denotes the central hydrophobic domain (111-134) of the prion protein. Toward the N-terminus is the octapeptide repeat region (OR), which is suggested to play a role in metal binding. S-S indicates the single disulfide bridge between residues 179-214. Approximate

cutting site of PK within PrP^{Sc} is indicated by lightening symbol and a PK resistant fragment is in between residue 90 and 231.

Figure 3: Prion protein (PrP^C) sequence homology among various mammalian species. Peptide sequence was obtained from NCBI Entrez protein database and aligned using CLC DNA workbench 6 software.

APPENDIX II

ROLE OF PROTEOLYTIC ACTIVATION OF PROTEIN

KINASE Cδ IN THE PATHOGENESIS OF PRION DISEASE

Dilshan S. Harischandra[#], Naveen Kondru[#], Dustin P. Martin[#], Arthi Kanthasamy,

Huajun Jin, Vellareddy Anantharam, Anumantha G. Kanthasamy*

Department of Biomedical Sciences, Iowa Center for Advanced Neurotoxicology, Iowa
State University, Ames, Iowa, USA

[#]These authors contributed equally to this work.

Keywords: protein kinase Cδ, RML scrapie, phosphorylation, proteolytic activation, neurodegeneration

Abbreviations: RML, Rockey Mountain Laboratories; NBH, Normal brain homogenate; PKCδ, Protein kinase Cδ; COSC, Cerebellar organotypic slice cultures; TSE, transmissible spongiform encephalopathies; Thr, threonine; Tyr, Tyrosine; POSCA, prion organotypic slice culture assay.

Abstract

Prion diseases are infectious and inevitably fatal neurodegenerative diseases characterized by prion replication, widespread protein aggregation and spongiform degeneration of major brain regions controlling motor function. Oxidative stress has been implicated in prion-related neuronal degeneration but the molecular mechanisms underlying prion-induced oxidative damage are not well understood. In this study, we evaluated the role of oxidative stress-sensitive, pro-apoptotic protein kinase Cδ (PKCδ) in prion-induced neuronal cell death using cerebellar organotypic slice cultures (COSC) and mouse models of prion diseases. We found a significant upregulation of PKCδ in RML scrapie infected COSC as evidenced by increased levels of both PKCδ protein and its mRNA. We also found an enhanced regulatory phosphorylation of PKCδ at its two regulatory sites, Thr505 in the activation loop and Tyr311 at the caspase-3 cleavage site. The prion infection also induced proteolytic activation of PKCδ in our COSC model. Immunohistochemical analysis of scrapie-infected COSC revealed loss of PKCδ positive Purkinje cells and enhanced astrocyte proliferation. Further examination of PKCδ signaling in the RML scrapie adopted *in vivo* mouse model showed increased proteolytic cleavage and Tyr 311 phosphorylation of the kinase. Notably, we observed a delayed onset of scrapie-induced motor symptoms in PKCδ knockout (PKCδ-/-) mice as compared to wild type (PKCδ+/+) mice, further substantiating the role of PKCδ in prion disease. Collectively, these data suggest that PKCδ signaling likely plays a role in the neurodegenerative processes associated with prion diseases.

Introduction

Prion diseases, or transmissible spongiform encephalopathies (TSEs), are a group of fatal neurodegenerative diseases of humans and animals. Human prion diseases include Creutzfeldt-Jakob disease (CJD), Kuru, Gerstmann-Sträussler-Scheinker disease (GSS) and Fatal familial insomnia. Examples of TSEs found in animals include bovine spongiform encephalopathy (BSE), scrapie in sheep, chronic wasting disease (CWD) in deer and elk, and transmissible mink encephalopathy (TME)(Aguzzi et al., 2008; Martin et al., 2011; Prusiner, 1996). All these diseases share common neuropathological and clinical signs. Prion diseases are mainly characterized by misfolding of the normal cellular prion protein (PrP^C) into the pathological isoform PrP^{Sc} through unknown pathogenic mechanisms. Abnormally folded PrP^{Sc} is insoluble in non-denaturing detergents and partially resistant to protease digestion. Prion diseases generally involve long incubation periods, characteristic spongiform changes associated with protein aggregation and neuronal loss, and widespread gliosis.

PrP^C is a glycosylphosphatidylinositol (GPI)-linked extracellular membrane protein, which is ubiquitously expressed in the central nervous system, in both neuronal and glial cells(Aguzzi et al., 2008). The biological function of PrP^C is poorly understood, but evidence suggests that this protein functions as an antioxidant and metal-binding protein with a role in several cellular processes in the nervous system, including neurite outgrowth, synapse formation, and maintenance of myelinated axons(Aguzzi et al., 2008; Anantharam et al., 2008; Collinge et al., 1994; Kanthasamy et al., 2012; Martin et al.,

2011). During disease progression, abnormal conformational changes in PrP^C result in pathogenic PrP^{Sc} molecules, yet the mechanism by which this change occurs is unknown(Choi et al., 2006). Studies have shown that propagation of the infectious prion protein cannot occur in the absence of host prion proteins(Prusiner et al., 1993), indicating a causal role for prion proteins in pathogenesis.

Prion diseases cause severe neuronal damage mainly in brain regions that coordinate motor function, including the basal ganglia, cerebral cortex, thalamus, and cerebellum. Current knowledge about the molecular mechanisms underlying neurodegeneration in prion disease and related prionopathies is limited. However, growing evidence indicates that oxidative stress and apoptosis contribute to the neurodegenerative process in prion disease pathogenesis(Brown, 2005; Guentchev et al., 2000; Kim et al., 2001). Therefore, furthering our understanding of molecular signaling mechanisms involving early pathologic changes in prion disease is important for developing intervention strategies. We have previously shown that Protein kinase C-δ (PKC δ) is an oxidative stress-sensitive, pro-apoptotic kinase, which plays a causal role in apoptotic neuronal cell death(Kanthasamy et al., 2010; Kaul et al., 2005; Lin et al., 2012; Saminathan et al., 2011). We demonstrated that phosphorylation of tyrosine residue 311 and caspase-3-dependent proteolytic cleavage result in a persistent increase in the kinase activity, which promotes neuronal apoptosis(Kaul et al., 2005). Herein, we evaluate the role of PKCδ in prion neurotoxicity in *ex vivo* brain slice culture and *in vivo* experimental models of infectious prion disease. Our results reveal that PKCδ proteolytic signaling plays an important role in the neuronal damage and neurological deficits of prion disease.

Thus, our findings provide further mechanistic insight into pathogenesis of prion diseases.

Materials and Methods

Prion organotypic slice culture assay (POSCA)

Iowa State University's (ISU) College of Veterinary Medicine is accredited by the Association for Assessment and Accreditation of Laboratory Animal Care (AAALAC), and all procedures involving animal handling were approved by the Institutional Animal Care and Use Committee (IACUC) at ISU. Organotypic slice cultures were prepared as previously described with some modifications(Falsig and Aguzzi, 2008; Falsig et al., 2012). Briefly, brain blocks were prepared in 2% (w/v) low-melting-point agarose (Invitrogen 15517-022), and 350-µm thick cerebellar slices were prepared from 9-12 day-old C57BL/6 pups using a Compresstome™ Vf-300 microtome (Precisionary Instruments Inc). Slices were inoculated with 100 ug µg of 1% normal brain homogenate (NBH) or Rocky Mountain Laboratory (RML)-infected brain homogenate per 10 slices in Gey's balanced salt solution (GBSS: 137 mM NaCl, 5 mM KCl, 0.845 mM Na_2HPO_4, 1.5 mM $CaCl_2.2H_2O$, 0.66 mM KH_2PO_4, 0.28 mM $MgSO_4.7H2O$, 1.0 mM $MgCl_2.6H_20$, 2.7 mM $NaHCO_3$ and pH-adjusted to 7.4) supplemented with 1 mM of the glutamate receptor antagonist kynurenic acid. Free-floating slices were incubated for 1 h in the brain homogenate at 4°C and transferred to Millicell-CM Biopore PTFE membrane inserts (Millipore PICM03050) and maintained in slice culture medium (50% MEM, 25% Basal Eagle medium, 25% horse serum, 0.65% glucose supplemented with penicillin/streptomycin and glutamax). Organotypic slice cultures were maintained in a

humidified 37°C incubator with 5% CO_2 and 95% air for 14 days, and 90% of the media was exchanged every other day.

Immunohistochemistry

For immunohistochemistry, the organotypic slices were washed with PBS and fixed with 4% paraformaldehyde (PFA) for 1-2 h at room temperature. After fixing, the membrane inserts containing cerebellar slice cultures were washed with PBS and incubated with the blocking agent (2% goat serum, and 0.1% Triton X-100 in PBS) for 1 h. Membrane inserts were then incubated with the following combinations of primary antibodies: anti-GFAP (1:1000, Millipore) and anti-PKCδ (1:1000, Santa Cruz), or anti-beta III tubulin (Tuj1) (1:1000, Millipore) and anti-PKCδ (1:1000, Santa Cruz) for 2-3 days at 4°C. At the end of the incubation, membranes were washed with PBS and incubated with Alexa Fluor 555-conjugated anti-mouse secondary antibody (1:2000) or Alexa Fluor 488-conjugated anti-rabbit secondary antibody (1:2000) for 90 min in the dark. Hoechst 44432 was used as a nuclear stain. The culture membranes were removed from the inserts and mounted directly on microscope slides using Fluoromount mounting medium (Sigma) and viewed using a Nikon TE2000 microscope (Tokyo, Japan). Images were captured with a SPOT color digital camera (Diagnostic Instruments, Sterling Heights, MI).

Western blot

Slice cultures were washed twice in ice-cold PBS and lysed with Tissue extraction reagent (Invitrogen FNN0071) containing protease and phosphatase inhibitor cocktail

(Thermo Scientific). Whole tissue lysates were prepared as described(Jin et al., 2011b). Protein concentrations were determined with the Bradford protein assay kit (Bio-Rad). Immunoblot analysis was performed as previously described(Ghosh et al., 2013; Kanthasamy et al., 2006). Briefly, the indicated protein lysates containing equal amounts of protein were separated on a 12-15% SDS-polyacrylamide gel. After separation, proteins were transferred to a nitrocellulose membrane, and nonspecific binding sites were blocked by treating with LI-COR blocking buffer. The membranes were then incubated overnight with primary antibody directed against PKCδ (1:1000, Santa Cruz), pPKCδ-Thr505 (1:1000, Santa Cruz), pPKCδ-Tyr311 (1:1000, Santa Cruz), or PrP (POM-1, 1:5000, Prionatis AG). The primary antibody treatments were followed by treatment with IR800-conjugated anti-rabbit, Alexa Fluor 680-conjugated anti-mouse or Alexa Fluor 680-conjugated anti-rat secondary antibody for 1 h at room temperature. To confirm equal protein loadings, blots were reprobed with β-actin antibody (1:15000 dilutions). Western blot images were captured with the Odyssey IR Imaging system (LI-COR) and data were analyzed using Odyssey 2.0 software.

Limited proteolysis of prion protein resistance to proteinase-K digestion was measured as previously described with few modifications(Falsig and Aguzzi, 2008; Falsig et al., 2012). RML-infected and NBH-inoculated slice cultures were homogenized 35 days after infection in lysis buffer (50 mM Tris-HCl, pH 7.4, 0.5% Triton X, and 0.5% sodium deoxycholate). Protein concentration was determined by Bradford assay. Next, 40 μG of protein was digested with 25 μG/ml of proteinase-K and incubated for 30 min. The reaction was stopped by boiling the samples at 95°C for 7 minutes prior to analysis by Western blot as described above.

qRT-PCR

Organotypic slice cultures were washed once with PBS, and total RNA was isolated using the Absolutely RNA Miniprep kit from Agilent. Next, 500 ng of total RNA was converted to cDNA using the High Capacity cDNA Archive kit (Applied Biosystems). Quantitative real-time RT-PCR was performed using the Brilliant SYBER Green QPCR Master Mix kit (Qiagen) in an Mx3000P QPCR system (Agilent), as described previously(Jin et al., 2011a). The PKCδ primer set (Qiagen; QT00107513) was used to analyze relative gene expression with the 18s primer set (Qiagen; QT02448075) as the internal control for RNA quantity. The PCR reaction mixture included 2 μl of cDNA, 10 μl of 2x master mix, and 0.2 μM of each primer. A negative control lacking cDNA (no template control) was included in each assay. The PCR cycle conditions were as follows: 95°C for 10 min, then 40 cycles of 95°C for 15 s and 60°C for 1 min. The cycle threshold (Ct) values corresponding to the PCR cycle number at which fluorescence emission in real time reaches a threshold above the baseline emission were determined. The relative PKCδ expression was calculated after adjusting for 18s using $2^{-\Delta\Delta Ct}$, where ΔC_t is the PKCδ gene C_t -18s C_t.

PKCδ immunoprecipitation (IP)-kinase assays

The PKCδ enzymatic kinase activity assay was performed as described previously(Latchoumycandane et al., 2011). Briefly, RML scrapie- or NBH-infected slices were lysed with the lysis buffer (25mM HEPES, 20mM β-Glycerophosphate, 0.1mM Na3VO4, 0.1% Triton-X, 300mM NaCl, 1.5mM MgCl2, 0.2mM EDTA, 0.5mM

DTT and 10mM NaF) containing protease and phosphatase inhibitor cocktail (Thermo Scientific). The lysates were placed on ice for 20 min, sonicated gently and centrifuged at 12000 g for 45 min. After collecting the supernatant, protein concentration was determined using the Bradford assay. Next, 500 µg of total protein in a 250-µl volume was immunoprecipitated overnight at 4°C using 10 µg of the PKCδ antibody. After adding protein A-agarose beads (Sigma-Aldrich) the next day, the samples were incubated for 2 h at room temperature. The protein A-bound antibody complexes were then washed three times in $2 \times$ kinase assay buffer (40 mM Tris, pH 7.4, 20 mM MgCl$_2$, 20 µM ATP, and 2.5 mM CaCl$_2$), and then resuspended in 100 µl of the same buffer. The kinase reaction was started by adding 100 µl of the reaction buffer containing 0.4 mg of histone H1, 50 µg/ml phosphatidylserine, 4 µM dioleoylglycerol, and 10 µCi of [γ-^{32}P] ATP at 3,000 Ci/mM to the immunoprecipitated samples. The samples were incubated for 10 min at 30°C. The kinase reaction was stopped by adding $2 \times$ SDS-loading buffer and boiling the samples for 5 min. The proteins were separated on a 15 % SDS-PAGE gel and the phosphorylated histone H1 bands were scanned using a Fujifilm FLA 5000 imager. Image analysis and band quantification were performed using the Fujifilm Multigauge software package (Fujifilm USA, Stamford, CT).

Mouse models of murine scrapie

Mouse models are a popular and versatile in vivo method for studying the effects of prion proteins and for providing insights into the neurodegenerative mechanisms of prion disease. All work with prion-infected strains and animals was performed under the licensure granted by a United States Department of Agriculture (USDA) permit for

importation and exportation of controlled materials and it conformed to guidelines of the IACUC at ISU. Wild type (PKCδ (+/+) and PKCδ (-/-) C57 black mice at postnatal week 6-8 were arranged by weight and randomized into RML and mock NBH inoculation groups. PKCδ knockout animals were originally obtained from Dr. Keiichi Nakayama at the Medical Institute of Bioregulation, Fukuoka, Japan(Miyamoto et al., 2002). RML and NBH infections were performed by intracerebrally inoculating 30 μl of 1% w/v RML brain homogenate into deeply anesthetized mice using a 27 gauge needle. Mice were monitored for 48 h post-inoculation for adverse effects and euthanized if they displayed unequivocal neurological signs. At 60, 90, 120 and 150 days post inoculation (DPI), all animals were subjected to behavioral evaluations described below, then following euthanasia, brain tissues were extracted for biochemical evaluations.

Behavioral evaluations

Extensive neuronal loss during the course of transmissible spongiform encephalopathy (TSE) produces progressive motor deficits in humans and animals including ataxia, tremor, and postural instability. Grip stamina and motor control were evaluated using the horizontal bar test(Guenther et al., 2001; Mallucci et al., 2007). Each mouse was held by the tail and allowed to grip a 0.2 cm diameter brass rod 50 cm above a padded cage with its forelimbs. The padded Innovive (San Francisco, CA, USA) mouse cage was placed below the bar to protect the mice from injury by falling. The mouse was quickly released and the time it took for the mouse to fall was recorded. Scores were given based on the following paradigm: 0-5s = 1; 6-10s = 2; 11-20s = 3; 21-29s = 4; and 30s or reaching the side support = 5.

The Columbus Instrument (Columbus, OH, USA) grip strength meter was used to determine the maximal amount of force that each animal applied with its forelimbs to a specially designed bar (LaMonte et al., 2002; Lepore et al., 2008). For all measurements, the gauge was measured in PEAK mode and units were set to kgF. Animals were gripped firmly but gently at the base of the tail and the animal's forelimbs were placed on the grip bar. Once the animal gripped the bar with both forelimbs, it was steadily pulled directly away from the digital strength meter. This process was repeated 2-3 times to get the peak strength reading.

Behavioral evaluations were done by trained personnel in cooperation with ISU Laboratory Animal Resources. We evaluated uninfected and RML scrapie-infected C57BL/6 and PKCδ (-/-) mice once-weekly for differences in motor signs that reflected difficulty initiating ambulatory activities and changes in ambulatory activity patterns. Motor performance was scored on a scale from 0 to 4 with 0 = normal movement, 1 = slight alteration in ambulation, 2 = obvious intermittent motor signs, 3 = continuous pronounced motor signs, and 4 = almost complete lethargy. Test animals were monitored for changes in behavioral motor deficits over a period of several minutes. Mice were also evaluated for clasping of limbs when held aloft by the tail.

Statistical analysis:

Data analysis was performed using Prism 4.0 software (GraphPad). Raw data were first analyzed using one-way ANOVA, and then Tukey's post-test was performed to compare

all treatment groups. Differences with *p< 0.05, **p< 0.01, and ***p< 0.001 were considered significantly different.

RESULTS

Upregulation of PKCδ in RML infected cerebellar organotypic slice culture model of prion disease

Brain slice models preserve the tissue architecture and neural connectivity of the brain regions, making them ideal platforms to model the neuropathology of brain atrophy(Cho et al., 2007; Mewes et al., 2012). Cerebellar organotypic slice cultures (COSC) have recently been shown to retain and replicate prion infection and thereby serve as an excellent *ex vivo* model to study the pathogenesis of prion disease(Falsig et al., 2008; Falsig et al., 2012). Evidence has indicated that prion titers in COSC peaked at 4 weeks, while at 5 weeks of infection, the PrP^{Sc} titers correspond to terminal infection in mice 5 months post-infection (Falsig et al., 2012). In this study, we first investigated whether COSCs from wild-type C57BL/6 mice reproduce pathological changes of prion diseases. Since gliosis is a well-established integral part of prion infections, we evaluated the glial cell proliferation following RML infection by immunocytochemistry after two weeks of infection. Astrogliosis was enhanced in RML-infected COSCs, as evidenced by an enhanced GFAP immunofluorescence signal (Fig.1A), indicating that the slice cultures undergo the neurotoxic stress at the early stages of prion infection. Next, we examined whether PKCδ expression was altered during two weeks of prion infection by immunocytochemical analysis of PKCδ. As shown in Fig. 1A, PKCδ immunoreactivity in RML-infected COSCs was significantly higher than in the slices inoculated with

normal brain homogenate (NBH). These data suggest that PKCδ upregulation may have a role in prion pathogenesis.

We also evaluated whether COSCs retain PrP^{sc} infection for five weeks following RML brain homogenate inoculation. For this purpose, RML-infected or NBH-inoculated slices were subjected to limited proteolysis. This process completely digests PrP^{C}, whereas the C-terminal region of truncated PrP^{Sc} remains intact (these fragments are referred to as PrPcore), which is a disease-specific marker of prion infection(Bolton et al., 1982). Following PK digestion, protein lysates were separated by Western blot and membrane probed with the prion antibody POM-1, which specifically recognizes amino acid 121-230 at the globular domain of PrP(Polymenidou et al., 2008; Sigurdson et al., 2011). As shown in Fig.1B, after PK digestion, characteristic di-, mono- and unglycosylated forms of PK-resistant bands were observed only in RML scrapie-exposed slices, while they were completely digested in slices exposed to uninfected NBH, confirming that COSCs retain the prion infection over five weeks.

PKCδ activation during RML infection in organotypic slice cultures

We have previously shown that proteolytic activation of PKCδ plays an important role in the oxidative stress-induced apoptotic cell death in dopaminergic neurons (Gordon et al., 2012; Jin et al., 2011a; Kanthasamy et al., 2010; Kanthasamy et al., 2003b). It has also been reported that oxidative stress (Freixes et al., 2006; Pamplona et al., 2008), mitochondrial dysfunction (Yuan et al., 2013), and endoplasmic reticular (ER) stress (Anantharam et al., 2008) are involved in the pathogenesis of neurodegenerative diseases,

including prion diseases. In this study, we evaluated PKCδ activation in the early stages of RML infection in COSC exposed to NBH or RML for 14 days. Western blot analysis using the antibody that recognizes both native (72-74kDa) and cleaved PKCδ proteins (38-41kDa) showed a significant upregulation of native PKCδ as well as cleaved PKCδ protein fragments in RML-infected cultures (Fig. 2A). We previously demonstrated that phosphorylation of tyrosine 311 is required for caspase-3-mediated proteolytic activation of PKCδ (Kaul et al., 2005) and its pro-apoptotic function (Jin et al., 2011a; Latchoumycandane et al., 2011; Li et al., 1994; Saminathan et al., 2011) (Anantharam et al., 2008). In addition to tyrosine 311 phosphorylation, PKCδ-thr505 activation-loop phosphorylation is required for full kinase activity of PKCδ, and thus serves as a marker of PKCδ activation(Le Good et al., 1998). Therefore, we determined the phosphorylation of tyr311 and thr505 in prion-infected COSCs by Western blot using phospho-specific antibodies. As shown in Fig 2 A, 2 D-E, RML infection significantly increased tyr311 and thr505 phosphorylation compared to control NBH-inoculated slice cultures.

Next, we employed the ^{32}p IP-kinase assay to determine if RML-induced proteolytic activation of PKCδ is associated with a sustained activation of its kinase activity in organotypic slice cultures. PKCδ kinase assays performed in the absence of lipid cofactors showed a robust increase in PKCδ kinase activity in RML-infected samples compared to NBH-inoculated samples, indicating that proteolytic activation increases the kinase activity. To further confirm the PKCδ upregulation, we quantified PKCδ mRNA levels upon exposure to either NBH or RML scrapie infection by quantitative-RT-PCR analysis. Interestingly, our results show that RML infection leads to increased levels of

PKCδ mRNA, suggesting the RML infection-meditated upregulation of PKCδ is through transcriptional induction. Collectively, our results in the COSC model demonstrate that prion infection activates PKCδ kinase activity by proteolytic cleavage and upregulation of the kinase.

Cerebellar atrophy during RML infection

To evaluate the effect of RML infection on the cerebellum, we infected organotypic cerebellar cultures with either NBH or RML for two weeks, as described above. At the end of the incubation, cerebellar slices were analyzed for cerebellar atrophy induced by prion infection. As shown in Fig. 3, compared to slices inoculated with NBH, cultures infected by RML have more diffuse staining for TujI, a neuronal marker for neuron-specific class III β-tubulin, indicating that RML infection induces discernible cerebellar degeneration. Additionally, immunostaining for PKCδ indicates an intense PKCδ immunoreactivity in the RML-infected cerebellar brain slices, predominantly in the Purkinje cells lining the molecular layer. Histological evaluation of the RML-infected COSCs indicates a marked cerebellar atrophy compared to NBH-inoculated slices. In RML-infected cerebella slices, extensive degeneration was observed in the molecular layer, similar to previous reports evaluating neuropathological changes in human CJD and GSS incidents (Yang et al., 1999).

In vivo Proteolytic activation of PKCδ in murine-adapted RML scrapie-infected mice

Apoptosis has been characterized as a major mode of neuronal cell death associated with spongiform degeneration(Bourteele et al., 2007; Carimalo et al., 2005), and PKCδ has

been identified as a key pro-apoptotic molecule involved in neuronal apoptosis (Kanthasamy et al., 2010). To evaluate whether PKCδ activation occurs *in vivo* during TSE-induced neurodegeneration, we examined RML scrapie- and mock NBH-inoculated wild-type mice at 60, 90, 120 and 150 DPI for changes in native and proteolytically cleaved PKCδ fragments in cerebellar tissues. As shown in Fig. 4A, increased levels of cleaved PKCδ in RML-infected animals were observed at preclinical stages (90 and 120 DPI) of TSE, compared to mock-infected animals. Quantified immunoblots for the cleaved PKCδ protein fragment (Fig. 4C) show 75-80% induction of proteolytic activation in RML-infected animals beyond that expressed in NBH-inoculated animals at these preclinical stages, suggesting the induction of apoptotic stimuli leading to cerebellar atrophy-related behavioral deficits. However, we did not find increased native PKCδ protein levels, as observed in the RML-infected slice cultures (Fig. 2A and 2B). Furthermore, PKCδ protein level was slightly reduced at the time point (150 DPI) marking the terminal stages of TSE.

Next, we examined the phosphorylation of PKCδ at two regulatory sites: Tyr311 flanking the caspase-3 cleavage site of PKCδ and Thr505 within the activation loop. Analysis of Tyr311 phosphorylation upon RML infection (Fig. 4C) indicates a slight reduction at 60 DPI and then a significant increase in the phosphorylation signal at 90 and 120 DPI. It is noteworthy that the time-course pattern for this PKCδ cleavage-specific phosphorylation event is also reflected in the increase in cleaved PKCδ fragments at 90 and 120 DPI. This positive correlation indicates the potential significance of these events at these preclinical TSE stages. Additional quantitation of immunoblots for phosphorylated PKCδ at Thr505

(Fig. 4D) indicated about a 75% increase at 60 DPI and about a 25% increase of phosphorylation events at 90 and 120 DPI when normalized to Thr505 phosphorylation signals in NBH-inoculated samples at the respective time points. Together, our results in an animal model of prion disease revealed time-dependent alterations in PKCδ signaling.

TSE-related behavioral abnormalities are delayed in PKCδ (-/-) mice

The neurological symptoms of mice infected with mouse-adapted scrapie include kyphosis, tremor, cachexia, and ataxia(Aguzzi and Heikenwalder, 2006; Bessen et al., 2011; Castilla et al., 2008; Collins et al., 2001). Additionally, infected mice display clasping of limbs when held aloft by the tail(O'Shea et al., 2008). If PKCδ signaling contributes significantly to the neurodegeneration and neurological deficits associated with TSE, inhibition of PKCδ function would delay the onset of the disease. To further validate the role of PKCδ signaling in TSE, we utilized PKCδ knockout (PKCδ-/-) C57 black mice, as described in our previous publication(Zhang et al., 2007). Specifically, we evaluated the motor function in PKCδ (-/-) C57 black mice following inoculation with murine-adapted RML scrapie and compared with that of wild-type C57 black mice. After inoculation with either NBH or RML, mice were subjected to weekly behavioral analysis using the horizontal bar test and grip strength meter to assess grip strength, stamina, and coordination.

Beginning at week 14, wild-type RML-infected animals displayed significantly reduced forelimb strength, which continued until the end of the study (Fig. 4A). Conversely, RML-infected PKCδ (-/-) animals retained forelimb strength until sacrifice at 150 DPI.

For the horizontal bar test (Fig. 5B), mice were scored from 0 to 5, reflecting increasing hang durations while suspended from the metal bar. Infected wild-type animals began showing difficulty hanging on the bar at week 18, and the score significantly decreased at week 21 (Fig. 5A). PKCδ (-/-) mice showed no significant reduction during the course of infection. In addition to grip strength and horizontal bar measurements, general clinical evaluation of all mice was done weekly in order to identify behavioral signs of RML scrapie-induced motor deficits. We evaluated both wild-type and PKCδ (-/-) mice for differences in motor signs that reflect difficulty initiating ambulatory activities and changes in ambulatory activity patterns. We scored their pathology on a scale from 0 to 4, with 0 indicating normal movement and 4 indicating almost complete lethargy and ataxia (Fig. 5C). Test animals were monitored over a period of several minutes for changes in behavioral motor deficits reflecting postural instability and difficulty in open field ambulation. Symptoms began appearing in wild-type mice at week 17 and became progressively more pronounced over the course of monitoring. By contrast, PKCδ (-/-) mice showed a delayed onset of TSE-related ataxia, and their observable motor signs were scored as less severe. Additionally, mice were tested for the clasping of limbs when held aloft by the tail. PKCδ (-/-) mice likewise showed a delay in the onset of clasping, as well as reduced severity scores (Fig. 5D). Taken together, these results indicate that PKCδ knockdown delays the onset of neurological signs associated with mouse-adapted scrapie in animal models.

Discussion

In this study, we report that PKCδ is proteolytically activated during the preclinical stages of TSE in our experimental models of prion disease. Our results also demonstrate that phosphorylation of PKCδ at its activation loop and its catalytic domain is important for disease progression and neuronal cell death during the course of prion infection. To the best of our knowledge, we are the first to demonstrate that PKCδ (-/-) mice exhibit delayed onset of the behavioral symptoms associated with the prion disease. These findings could contribute to the development of interventional strategies for TSE-related motor deficits.

One of the main limitations for characterizing the molecular mechanisms of TSE is the lack of suitable *in vitro* experimental models of infectious prion disease. Indeed, several *in vitro* experimental models, such as neuronal cell lines infected with mouse-adapted scrapie, have been used to investigate the biochemical properties of PrP^{Sc} with some success at expanding the horizons of prion biology. However, due to several limitations associated with cell culture systems, they are not amenable for studying in-depth molecular mechanisms underlying infectious prion disease. Recently, Falsig and his colleagues successfully developed and validated(Falsig and Aguzzi, 2008; Falsig et al., 2008; Falsig et al., 2012) an *ex vivo* transmission model for prion disease using organotypic cerebellar slice cultures. In this study, we successfully adopted this organotypic cerebellar slice culture to study PKCδ-mediated neuronal cell death during TSE. First, we were able to reproduce the RML-infected organotypic cerebellar slice cultures in our laboratory with slight modifications. We observed an improved viability of cerebellar slices with use of Compresstome™ Vf-300 microtome, because this

procedure significantly reduced the cutting time and mechanical stress associated with slice preparation. Our slice cultures were able to retain infection, as seen by widespread gliosis during early stages of the infection (2 weeks, Fig. 1A) and by the presence of PK-resistant prion proteins after 5 weeks of RML incubation (Fig. 1B). Following establishment of COSCs with prion infection, we systematically studied the role of proteolytically activated pro-apoptotic kinase PKCδ in prion-induced neurodegeneration by comparing the kinase signaling in RML-infected and mock NBH-inoculated slice cultures.

We have previously shown that PKCδ is a key oxidative stress-sensitive kinase that can be activated by caspase-3 dependent proteolytic cleavage, by tyrosine and threonine phosphorylation(Gordon et al., 2012; Jin et al., 2011a; Jin et al., 2011b; Kanthasamy et al., 2003a). Also, oxidative stress has been identified as integral to prion-induced neurodegeneration(Brown, 2005; Guentchev et al., 2000; Kim et al., 2001; Sinclair et al., 2013; Sonati et al., 2013)Therefore, herein, we have evaluated PKCδ-mediated neuronal apoptosis in *ex vivo* cerebellar slice cultures and in RML-infected *in vivo* mice. Our data support the idea of PKCδ proteolytic activation during prion infection, as noted by the significantly increased native and cleaved PKCδ upon RML infection in COSCs. We also observed increased phosphorylation of PKCδ Tyr311 and Thr505 levels in RML-infected COSCs, compared to mock-infected tissues. Phosphorylation of Tyr311 at the hinge region of PKCδ, which reportedly causes conformational changes in the structure that opens the catalytic domain (Kikkawa et al., 2002), mediates caspase-3-dependent cleavage, thereby separating the catalytic and regulatory domains (Kanthasamy et al., 2003b; Kaul et al., 2005). This proteolytic activation of PKCδ promotes apoptosis by

activating downstream apoptotic cascades(Anantharam et al., 2002; Kanthasamy et al., 2003a). In addition, the cleaved catalytically active PKCδ fragment activates upstream caspase signaling, constituting a positive feedback mechanism leading to a further amplified apoptotic pathway (Anantharam et al., 2002; Kitazawa et al., 2003; Reyland, 2007). Furthermore, analysis of the PKCδ activation loop-specific site Thr505 indicates that RML infection could induce phosphorylation of Thr505 to further enhance the kinase activation. These observations were further validated by the upregulation of PKCδ kinase activity, as seen by PKCδ IP-kinase assays. We also analyzed the PKCδ mRNA and the native protein levels upon RML infection. Surprisingly, we observed increased PKCδ mRNA expression and protein levels in infected slices, indicating transcriptional upregulation of native PKCδ expression. Next, we performed immunohistochemical analysis of the extent of neurodegeneration in RML-infected cerebellar slices. We observed widespread neuronal cell death (Fig.3), as seen by diffused staining for the neuronal marker Tuj1 and increased PKCδ staining in RML-infected tissues compared to mock NBH-inoculated tissues. Also, we morphologically discerned cerebellar atrophy in the RML-infected slices, which can be extrapolated to cerebellar dysfunction and locomotor deficits involved with TSE.

Following the evaluation of PKCδ in organotypic slice cultures, we further characterized the role of PKCδ in *in vivo* experimental models of prion disease by intracerebrally inoculating mouse-adapted RML scrapie or NBH to wild-type C57BL/6 mice and analyzing PKCδ signals 60, 90, 120 and 150 days post-infection. Biochemical analysis of cerebellar tissues in these mice revealed significantly increased levels of cleaved PKCδ protein during preclinical stages, indicating the possible involvement of neuronal cell

death. These findings corroborate with previous reports indicating that oxidative stress is induced during early prion invasion, thus predisposing the brain to neurodegeneration(Yun et al., 2006). We also observed increased phosphorylation of PKCδ Tyr311 levels, via immunoblotting, which in combination with the proteolytic activation of PKCδ, makes neurons susceptible to downstream apoptotic cascades. Since PKCδ is abundantly expressed in the cerebellum(Merchenthaler et al., 1993), especially in Purkinje cells and the posterior cerebellar cortex (Barmack et al., 2000), these neurons may be more susceptible to TSE-induced neurotoxic stress and more likely to undergo degeneration resulting from the disease. Increased PKCδ cleavage without any significant change in the native kinase at 90 and 120 DPI suggests that PKCδ upregulation may have been compensated by increased proteolysis of the kinase at the early stages of the infection. The observed decrease in native PKCδ as well as the cleaved fragment at the terminal stage of the disease may be due to the loss of neurons normally expressing higher levels of PKCδ.

 Since TSE is a fatal neurodegenerative disease often involving motor and postural abnormalities associated with cerebellar dysfunction(Collins et al., 2001; Cooper et al., 2006; Glatzel et al., 2005), we performed several behavioral tests in RML-infected mice throughout the study. For our behavior testing, we included the transgenic PKCδ (-/-) mice to evaluate whether abolition of PKCδ would alter TSE-associated neurobehavioral deficits. We evaluated ataxia, hind limb clasping phenotype, forelimb grip strength and horizontal bar performance to assess neurological damage, particularly cerebellar ataxia and other motor deficits(Chou et al., 2008; Deacon, 2013; Guyenet et al., 2010). For most of the behavioral tests, wild-type animals infected with RML started showing

302

behavioral deficits around 14-17 weeks post-infection, whereas mice receiving the mock NBH inoculation did not show any behavior deficits throughout the study. Interestingly, PKCδ (-/-) showed a delayed onset of the motor deficits associated with TSE, suggesting that PKCδ signaling plays as a major role in the pathogenesis of prion disease. We have previously shown that the PKCδ inhibitor rottlerin effectively protected against locomotor deficits in an animal model of dopaminergic neurodegeneration(Zhang et al., 2007). Therefore, successful attenuation of scrapie-induced neurodegeneration by pharmacological inhibition of PKCδ could provide a basis for developing therapies effective prior to the onset of widespread spongiform neurodegeneration and motor deficits in TSE.

In conclusion, we have demonstrated an enhanced regulatory phosphorylation and proteolytic activation of PKCδ during the progression of mouse-adapted scrapie cerebellar slice cultures and a delayed onset of scrapie-induced motor symptoms in PKCδ knockout mice, suggesting a possible role of PKCδ in the neurotoxicity of prion disease. These findings may help to further elucidate the PKCδ dependent cell signaling mechanism in TSE pathogenesis and to develop potential pharmacological interventions for TSE.

References

Aguzzi, A., et al., 2008. The prion's elusive reason for being. Annu Rev Neurosci. 31**,** 439-77.

Aguzzi, A., Heikenwalder, M., 2006. Pathogenesis of prion diseases: current status and future outlook. Nat Rev Microbiol. 4**,** 765-75.

Anantharam, V., et al., 2008. Opposing roles of prion protein in oxidative stress- and ER stress-induced apoptotic signaling. Free Radic Biol Med. 45**,** 1530-41.

Anantharam, V., et al., 2002. Caspase-3-dependent proteolytic cleavage of protein kinase Cdelta is essential for oxidative stress-mediated dopaminergic cell death after exposure to methylcyclopentadienyl manganese tricarbonyl. J Neurosci. 22**,** 1738-51.

Barmack, N. H., et al., 2000. Regional and cellular distribution of protein kinase C in rat cerebellar Purkinje cells. J Comp Neurol. 427**,** 235-54.

Bessen, R. A., et al., 2011. Transmission of chronic wasting disease identifies a prion strain causing cachexia and heart infection in hamsters. PLoS One. 6**,** e28026.

Bolton, D. C., et al., 1982. Identification of a protein that purifies with the scrapie prion. Science. 218**,** 1309-11.

Bourteele, S., et al., 2007. Alteration of NF-kappaB activity leads to mitochondrial apoptosis after infection with pathological prion protein. Cell Microbiol. 9**,** 2202-17.

Brown, D. R., 2005. Neurodegeneration and oxidative stress: prion disease results from loss of antioxidant defence. Folia Neuropathol. 43**,** 229-43.

Carimalo, J., et al., 2005. Activation of the JNK-c-Jun pathway during the early phase of neuronal apoptosis induced by PrP106-126 and prion infection. Eur J Neurosci. 21, 2311-9.

Castilla, J., et al., 2008. Cell-free propagation of prion strains. EMBO J. 27, 2557-66.

Cho, S., et al., 2007. Brain slices as models for neurodegenerative disease and screening platforms to identify novel therapeutics. Curr Neuropharmacol. 5, 19-33.

Choi, C. J., et al., 2006. Interaction of metals with prion protein: possible role of divalent cations in the pathogenesis of prion diseases. Neurotoxicology. 27, 777-87.

Chou, A. H., et al., 2008. Polyglutamine-expanded ataxin-3 causes cerebellar dysfunction of SCA3 transgenic mice by inducing transcriptional dysregulation. Neurobiol Dis. 31, 89-101.

Collinge, J., et al., 1994. Prion protein is necessary for normal synaptic function. Nature. 370, 295-7.

Collins, S., et al., 2001. Gerstmann-Straussler-Scheinker syndrome,fatal familial insomnia, and kuru: a review of these less common human transmissible spongiform encephalopathies. J Clin Neurosci. 8, 387-97.

Cooper, S. A., et al., 2006. Sporadic Creutzfeldt-Jakob disease with cerebellar ataxia at onset in the UK. J Neurol Neurosurg Psychiatry. 77, 1273-5.

Deacon, R. M., 2013. Measuring the strength of mice. J Vis Exp.

Falsig, J., Aguzzi, A., 2008. The prion organotypic slice culture assay--POSCA. Nat Protoc. 3, 555-62.

Falsig, J., et al., 2008. A versatile prion replication assay in organotypic brain slices. Nat Neurosci. 11, 109-17.

Falsig, J., et al., 2012. Prion pathogenesis is faithfully reproduced in cerebellar organotypic slice cultures. PLoS Pathog. 8, e1002985.

Freixes, M., et al., 2006. Oxidation, glycoxidation, lipoxidation, nitration, and responses to oxidative stress in the cerebral cortex in Creutzfeldt-Jakob disease. Neurobiol Aging. 27, 1807-15.

Ghosh, A., et al., 2013. The peptidyl-prolyl isomerase Pin1 up-regulation and proapoptotic function in dopaminergic neurons: relevance to the pathogenesis of Parkinson disease. J Biol Chem. 288, 21955-71.

Glatzel, M., et al., 2005. Human prion diseases: molecular and clinical aspects. Arch Neurol. 62, 545-52.

Gordon, R., et al., 2012. Proteolytic activation of proapoptotic kinase protein kinase Cdelta by tumor necrosis factor alpha death receptor signaling in dopaminergic neurons during neuroinflammation. J Neuroinflammation. 9, 82.

Guentchev, M., et al., 2000. Evidence for oxidative stress in experimental prion disease. Neurobiol Dis. 7, 270-3.

Guenther, K., et al., 2001. Early behavioural changes in scrapie-affected mice and the influence of dapsone. Eur J Neurosci. 14, 401-9.

Guyenet, S. J., et al., 2010. A simple composite phenotype scoring system for evaluating mouse models of cerebellar ataxia. J Vis Exp.

Jin, H., et al., 2011a. Transcriptional regulation of pro-apoptotic protein kinase Cdelta: implications for oxidative stress-induced neuronal cell death. J Biol Chem. 286, 19840-59.

Jin, H., et al., 2011b. alpha-Synuclein negatively regulates protein kinase Cdelta expression to suppress apoptosis in dopaminergic neurons by reducing p300 histone acetyltransferase activity. J Neurosci. 31**,** 2035-51.

Kanthasamy, A., et al., 2010. Novel cell death signaling pathways in neurotoxicity models of dopaminergic degeneration: relevance to oxidative stress and neuroinflammation in Parkinson's disease. Neurotoxicology. 31**,** 555-61.

Kanthasamy, A. G., et al., 2006. A novel peptide inhibitor targeted to caspase-3 cleavage site of a proapoptotic kinase protein kinase C delta (PKCdelta) protects against dopaminergic neuronal degeneration in Parkinson's disease models. Free Radic Biol Med. 41**,** 1578-89.

Kanthasamy, A. G., et al., 2012. Effect of divalent metals on the neuronal proteasomal system, prion protein ubiquitination and aggregation. Toxicol Lett. 214**,** 288-95.

Kanthasamy, A. G., et al., 2003a. Role of proteolytic activation of protein kinase Cdelta in oxidative stress-induced apoptosis. Antioxid Redox Signal. 5**,** 609-20.

Kanthasamy, A. G., et al., 2003b. Proteolytic activation of proapoptotic kinase PKCdelta is regulated by overexpression of Bcl-2: implications for oxidative stress and environmental factors in Parkinson's disease. Ann N Y Acad Sci. 1010**,** 683-6.

Kaul, S., et al., 2005. Tyrosine phosphorylation regulates the proteolytic activation of protein kinase Cdelta in dopaminergic neuronal cells. J Biol Chem. 280**,** 28721-30.

Kikkawa, U., et al., 2002. Protein kinase C delta (PKC delta): activation mechanisms and functions. J Biochem. 132**,** 831-9.

Kim, J. I., et al., 2001. Oxidative stress and neurodegeneration in prion diseases. Ann N Y Acad Sci. 928, 182-6.

Kitazawa, M., et al., 2003. Dieldrin induces apoptosis by promoting caspase-3-dependent proteolytic cleavage of protein kinase Cdelta in dopaminergic cells: relevance to oxidative stress and dopaminergic degeneration. Neuroscience. 119, 945-64.

Latchoumycandane, C., et al., 2011. Dopaminergic neurotoxicant 6-OHDA induces oxidative damage through proteolytic activation of PKCdelta in cell culture and animal models of Parkinson's disease. Toxicol Appl Pharmacol. 256, 314-23.

Le Good, J. A., et al., 1998. Protein kinase C isotypes controlled by phosphoinositide 3-kinase through the protein kinase PDK1. Science. 281, 2042-5.

Li, W., et al., 1994. Tyrosine phosphorylation of protein kinase C-delta in response to its activation. J Biol Chem. 269, 2349-52.

Lin, M., et al., 2012. Methamphetamine-induced neurotoxicity linked to ubiquitin-proteasome system dysfunction and autophagy-related changes that can be modulated by protein kinase C delta in dopaminergic neuronal cells. Neuroscience. 210, 308-32.

Mallucci, G. R., et al., 2007. Targeting cellular prion protein reverses early cognitive deficits and neurophysiological dysfunction in prion-infected mice. Neuron. 53, 325-35.

Martin, D. P., et al., 2011. Infectious prion protein alters manganese transport and neurotoxicity in a cell culture model of prion disease. Neurotoxicology. 32, 554-62.

Merchenthaler, I., et al., 1993. Light and electron microscopic immunocytochemical localization of PKC delta immunoreactivity in the rat central nervous system. J Comp Neurol. 336**,** 378-99.

Mewes, A., et al., 2012. Organotypic brain slice cultures of adult transgenic P301S mice--a model for tauopathy studies. PLoS One. 7**,** e45017.

Miyamoto, A., et al., 2002. Increased proliferation of B cells and auto-immunity in mice lacking protein kinase Cdelta. Nature. 416**,** 865-9.

O'Shea, M., et al., 2008. Investigation of mcp1 as a quantitative trait gene for prion disease incubation time in mouse. Genetics. 180**,** 559-66.

Pamplona, R., et al., 2008. Increased oxidation, glycoxidation, and lipoxidation of brain proteins in prion disease. Free Radic Biol Med. 45**,** 1159-66.

Polymenidou, M., et al., 2008. The POM monoclonals: a comprehensive set of antibodies to non-overlapping prion protein epitopes. PLoS One. 3**,** e3872.

Prusiner, S. B., 1996. Molecular biology and pathogenesis of prion diseases. Trends Biochem Sci. 21**,** 482-7.

Prusiner, S. B., et al., 1993. Ablation of the prion protein (PrP) gene in mice prevents scrapie and facilitates production of anti-PrP antibodies. Proc Natl Acad Sci U S A. 90**,** 10608-12.

Reyland, M. E., 2007. Protein kinase Cdelta and apoptosis. Biochem Soc Trans. 35**,** 1001-4.

Saminathan, H., et al., 2011. Environmental neurotoxic pesticide dieldrin activates a non receptor tyrosine kinase to promote PKCdelta-mediated dopaminergic apoptosis in a dopaminergic neuronal cell model. Neurotoxicology. 32**,** 567-77.

Sigurdson, C. J., et al., 2011. Spongiform encephalopathy in transgenic mice expressing a point mutation in the beta2-alpha2 loop of the prion protein. J Neurosci. 31**,** 13840-7.

Sinclair, L., et al., 2013. Cytosolic caspases mediate mislocalised SOD2 depletion in an in vitro model of chronic prion infection. Dis Model Mech. 6**,** 952-63.

Sonati, T., et al., 2013. The toxicity of antiprion antibodies is mediated by the flexible tail of the prion protein. Nature. 501**,** 102-6.

Yang, Q., et al., 1999. Neuropathological study of cerebellar degeneration in prion disease. Neuropathology. 19**,** 33-9.

Yuan, F., et al., 2013. Cellular prion protein (PrPC) of the neuron cell transformed to a PK-resistant protein under oxidative stress, comprising main mitochondrial damage in prion diseases. J Mol Neurosci. 51**,** 219-24.

Yun, S. W., et al., 2006. Oxidative stress in the brain at early preclinical stages of mouse scrapie. Exp Neurol. 201**,** 90-8.

Zhang, D., et al., 2007. Neuroprotective effect of protein kinase C delta inhibitor rottlerin in cell culture and animal models of Parkinson's disease. J Pharmacol Exp Ther. 322**,** 913-22.
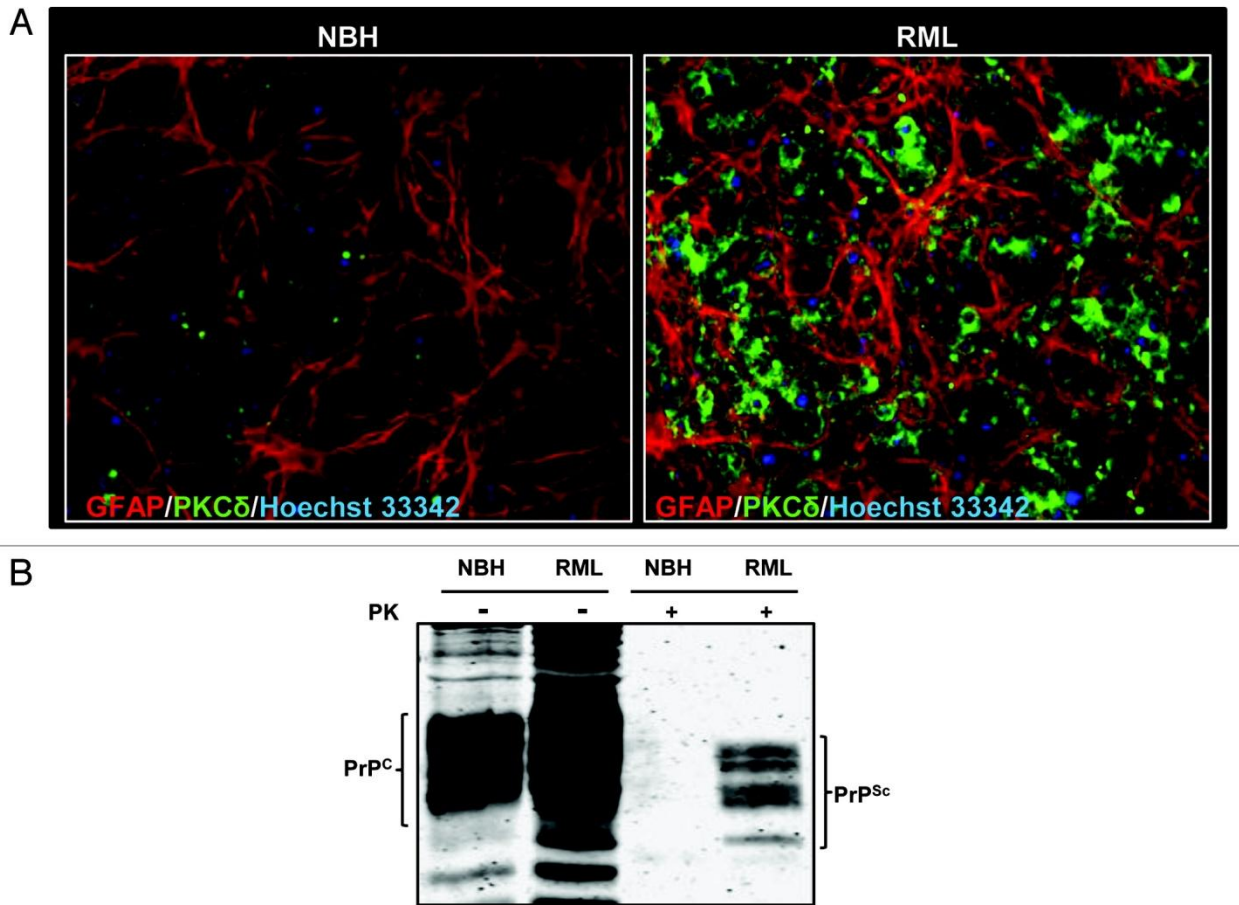
Figure 1:Prion replication and PKCδ upregulation in RML-scrapie infected organotypic cerebellar slice culture. (A) Immunohistochemical analysis of widespread astrogliosis and PKCδ upregulation in RML-scrapie infected cerebellar slice culture (right panel) as compared to control NBH inoculated cerebellar slice culture (left panel). (B) Western blot analysis of the proteinase-K resistant PrP^Sc isoform after five weeks of RML infection in cerebellar slice cultures.
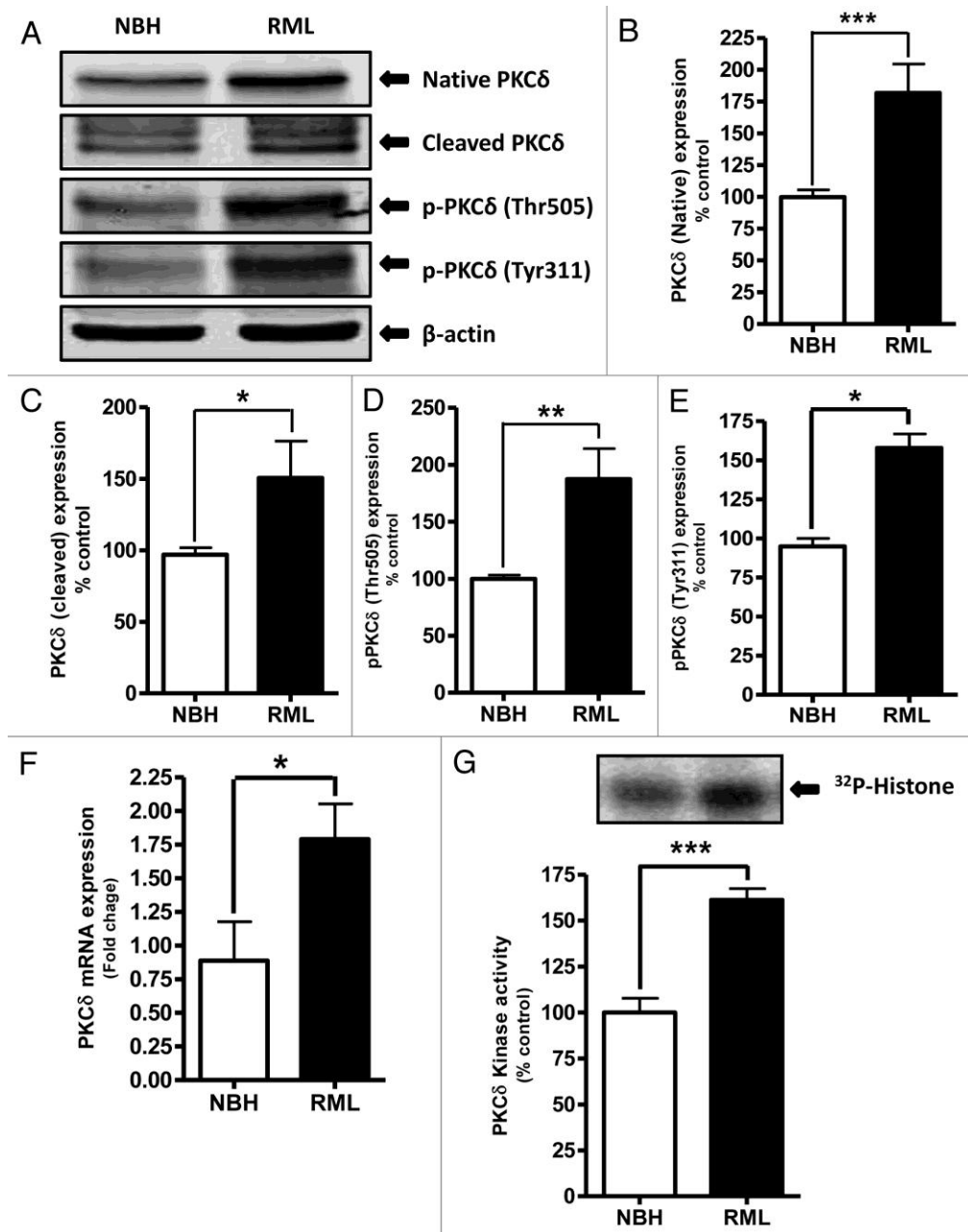
Figure 2: Proteolytic activation of PKCδ in RML-scrapie infected organotypic cerebellar slice culture. (A) Representative Western blots for PKCδ upregulation, cleavage and phosphorylation upon RML-scrapie infection in cerebellar slice cultures. Densitometric analysis of Western blots for (B) Native PKCδ (C) Cleaved PKCδ (D) p-PKCδ (Thr505) and (E) p-PKCδ (Tyr311) upregulation upon RML-scrapie infection.

Each group represented as mean $\pm$ S.E.M. from at least five separate measurements. (F) qRT-PCR analysis for PKCδ mRNA expression following RML-scrapie infection. Each group represented as mean $\pm$ S.E.M. from at least six measurements from three separate experiments. (G) PKCδ immunoprecipitation (IP)-kinase assay for augmented kinase activity upon RML-scrapie infection in organotypic slice cultures. Each group represented as mean $\pm$ S.E.M. from at least four measurements from two separate experiments ([*]$p < 0.05$ vs NBH, [**]$p < 0.01$ vs NBH, ***$p<0.001$ vs NBH).
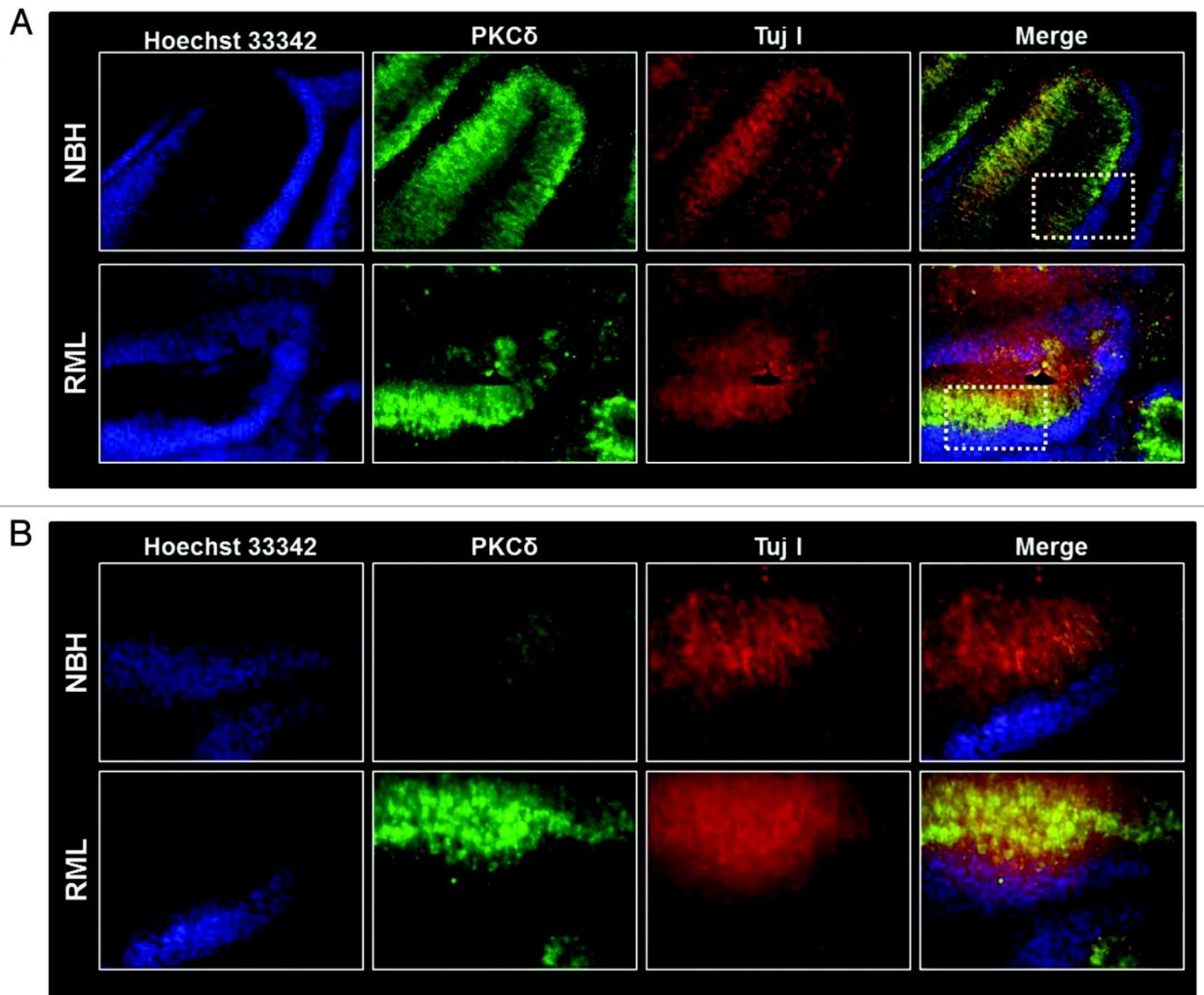
Figure 3: Cerebellar degeneration during RML infection in organotypic cerebellar slice culture. (A) Immunohistochemical analysis of pronounced cerebellar atrophy during RML infection (lower panel) and intact healthy histological morphology in control NHB-inoculated (upper panel) cerebellar slices. White dotted boxes represent regions magnified in slices described below. (B) Representative high magnification (20X) images indicating possible neuronal damage (as seen by diffuse Tuj1 staining) and PKCδ upregulation during RML infection (lower panel).
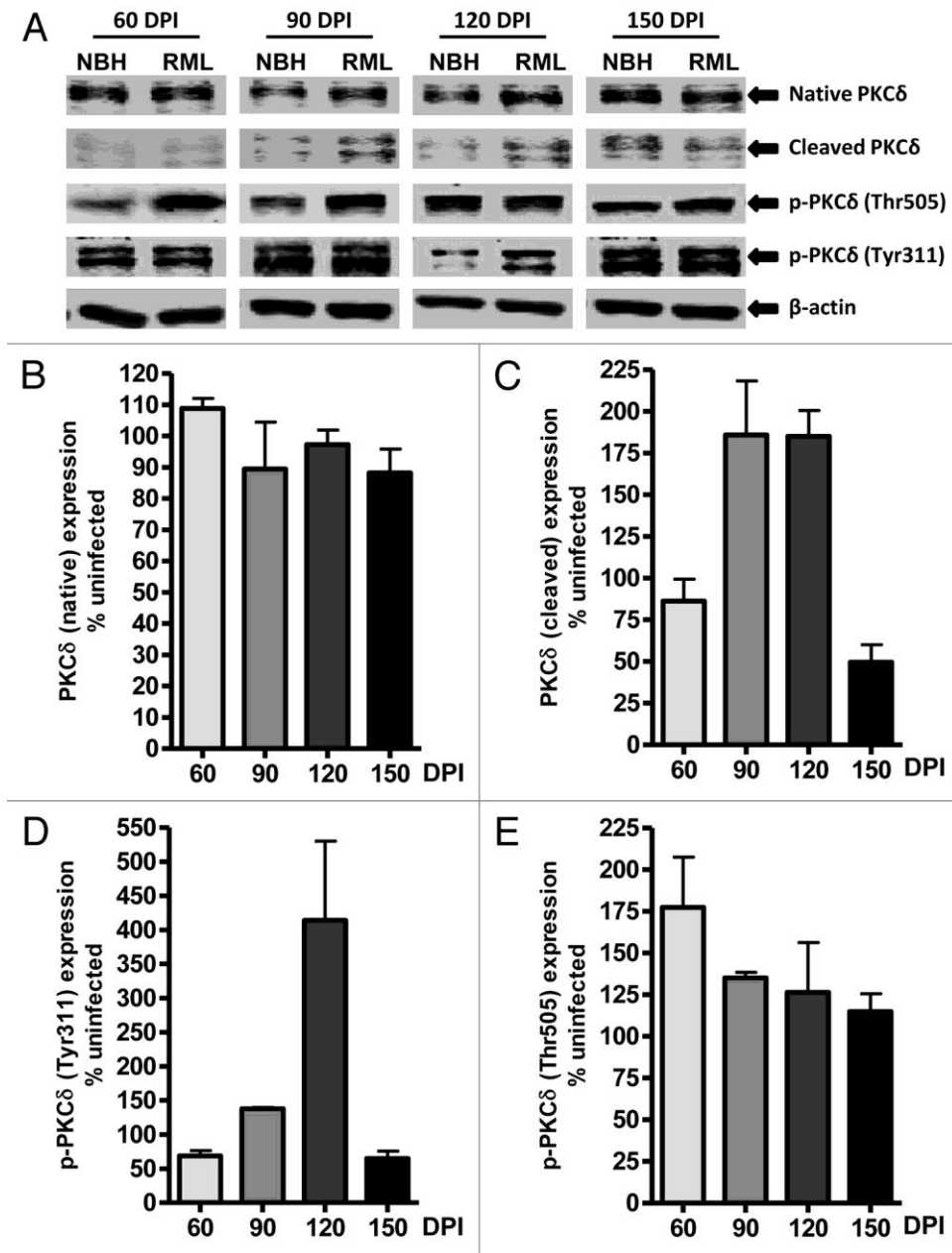
Figure 4: **PKCδ activation in RML scrapie-infected mice**. (A) Representative Western blots for native, cleaved and phosphorylated PKCδ at 60, 90, 120 and 150 days post-infection (DPI). Densitometric analysis of Western blots for changes in (B) Native PKCδ (C) Cleaved PKCδ (D) p-PKCδ (Tyr311) and (E) p-PKCδ (Thr505) upon RML infection at various time points. All data were normalized to NBH expression levels and are

represented as mean percentage (± S.E.M.) of uninfected protein expression from at least

three separate animals.
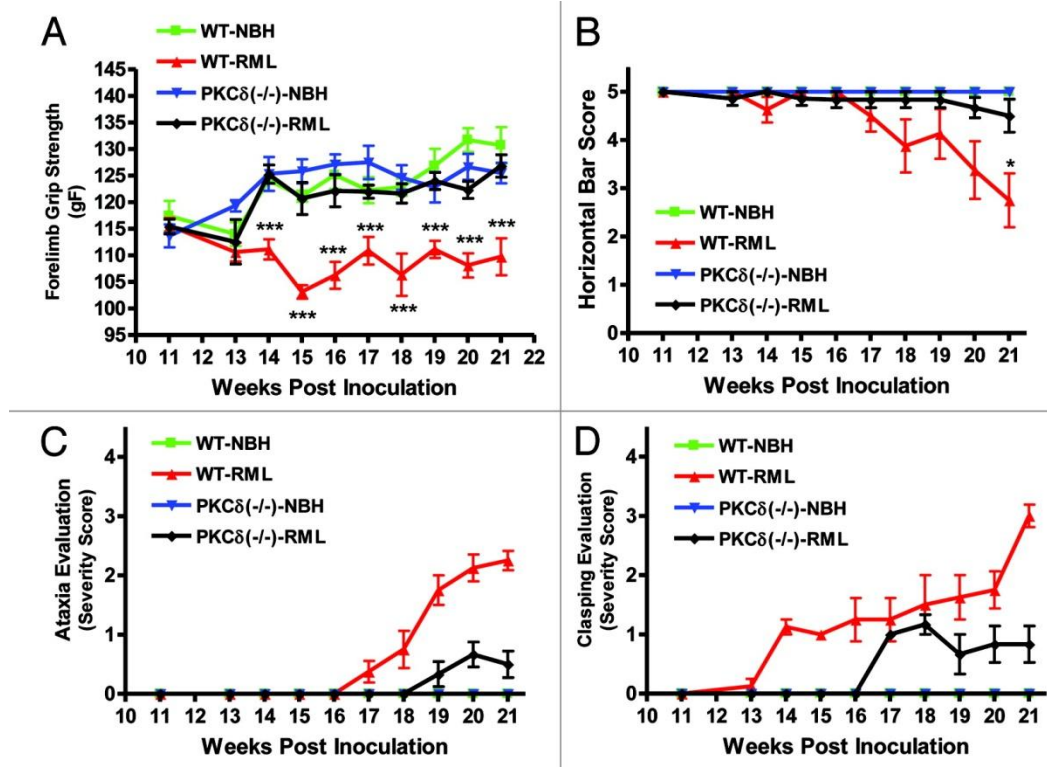
Figure 5:PKCδ knockout mice are resistant to RML scrapie induced motor deficits.
RML scrapie-infected WT and PKCδ (-/-) mice were evaluated weekly for motor changes

after inoculation. A) Forelimb grip strength was significantly reduced beginning at 14

weeks in wild type mice, whereas PKC (-/-) animals did not differ significantly from

mock-infected wild type animals throughout the course of infection. B) Motor function

was evaluated using the horizontal bar test. Wild type RML scrapie-infected mice began

to show deficits at 17 weeks, and changes became significant at 21 weeks. RML scrapie-

infected PKCδ (-/-) mice and mock-infected mice showed no significant changes. C)

Mice were evaluated for open-field ambulation and their ability to initiate movement over

the course of several minutes. Slight changes in motor function were observed in infected WT mice beginning at 18 weeks, progressing to significant ataxia by 21 weeks. Conversely, PKCδ (-/-) mice displayed a delayed onset in motor signs, and changes remained mild throughout the monitoring period. D) The clasping of limbs when held aloft by the tail was evaluated in WT and PKCδ (-/-) mice. Clasping symptoms began in WT mice at 14 weeks and steadily progressed to severe over the course of monitoring. PKCδ (-/-) animals did not begin clasping limbs until 17 weeks, and symptoms were mild over the course of monitoring. Data represented as mean ± SEM for each group.

APPENDIX III

ANTIOXIDANTS AND REDOX-BASED THERAPEUTICS IN PARKINSON'S DISEASE

*(**In press**) Inflammation, Oxidative Stress and Age-Related Disease*, edited by Stephen C. Bondy and Arezoo Campbell. Springer press (2016).

Dilshan S. Harischandra, Huajun Jin, Anamitra Ghosh, Vellareddy Anantharam, Arthi Kanthasamy and Anumantha G. Kanthasamy[‡]

Parkinson's Disorder Research Laboratory, Iowa Center for Advanced Neurotoxicology, Department of Biomedical Sciences, Iowa State University, Ames, Iowa 50011, USA

[‡]To whom correspondence should be addressed: Dept. of Biomedical Sciences, Iowa State University, 2062 College of Veterinary Medicine Building, Ames, IA 50011. Tel: 515-294-2516; Fax: 515-294-2315; Email: akanthas@iastate.edu

Dilshan S. Harischandra: dilshan@iastate.edu

Huajun Jin: egb761@iastate.edu

Anamitra Ghosh: Anamitra.Ghosh@vai.org

Vellareddy Anantharam: anantram@iastate.edu

Arthi Kanthasamy: arthik@iastate.edu

Anumantha G. Kanthasamy: akanthas@iastate.edu

318

Abstract

Parkinson's disease (PD) is a progressing neurodegenerative disorder of the central nervous system (CNS) characterized by a progressive loss of dopaminergic neurons in the substantia nigra and their axon terminals in the striatum. Although the etiology of PD is not completely understood and is believed to be multifactorial, oxidative stress and mitochondrial dysfunction are widely considered major contributors offering important clues about disease mechanisms. Given the relevance of oxidative stress in PD, a new class of antioxidant therapeutics, including mitochondria-targeted antioxidants, has been receiving attention as a possible treatment for PD. Here we summarize the recent discoveries of potential antioxidant compounds for modulating oxidative damage in PD.

Parkinson's disease

Parkinson's disease (PD) is a progressive neurodegenerative disorder affecting more than one million individuals over the age of 60 within the United States (Jankovic and Stacy, 2007). According to one recent article, the number of new cases increased by about 50,000 annually (Dauer and Przedborski, 2003). Although PD is an age-related disorder affecting nearly 3% of people over 60 years and 4-5% of those over age 85, nearly 10% of PD patients are under 40 years of age (Mizuno et al., 2001). Epidemiological studies suggest that sporadic PD cases (90%) are predominantly late onset, whereas the remainder (10%) is characterized by early onset occurring mainly in familial clusters (Mizuno et al., 2001; Tanner, 2003). Familial or early onset PD has been linked with mutations in several genes such as *parkin*, *ubiquitin C-terminal*

hydrolase L1, α-synuclein, leucine-rich repeat kinase 2 (LRRK2), PINK-1 or DJ1 (Bonifati et al., 2008; Gwinn-Hardy, 2002; Tang et al., 2006; Weng et al., 2007). The cause of sporadic or non-familial PD is not known, but several reports suggest environmental toxins, genetic factors, mitochondrial dysfunction, apoptosis, oxidative stress and neuroinflammation to be among the possible factors behind PD's neurodegeneration (Ben-Shachar et al., 1995; Hoehn and Yahr, 1998; McGeer et al., 2001; Schapira, 1994). Among the environmental toxins implicated in the pathogenesis and progression of the disease, the list includes infectious agents, pesticides, herbicides and heavy metals (Mizuno et al., 2001). Recent investigations have focused on inflammation and oxidative stress as the central players in the pathogenesis of PD.

In both idiopathic and genetic cases of PD, oxidative stress appears to be the common underlying mechanism contributing to the cascade leading to selective neurodegeneration in substantia nigra (SN) neurons and their terminals in the striatum. An imbalance between reactive oxygen species (ROS) generation and elimination mechanisms, such as impaired cellular antioxidant machinery, contributes to the pathogenesis of PD and other neurodegenerative disorders. The resulting oxidative stress is intimately linked to the other aspects of the degenerative process such as mitochondrial dysfunction, inflammation, protein misfolding and DNA damage.

Oxidative stress in PD

Oxidative stress in PD is supported by post-mortem studies on the SN of PD patients showing increased levels of oxidized lipids (Bosco et al., 2006), proteins, nucleic acids (Nakabeppu et al., 2007; Zhang et al., 1999) and impaired antioxidant mechanisms

such as a reduced glutathione (GSH) and oxidized glutathione (GSSG) ratio (Sian et al.,
1994). Therefore, oxidative stress appears to play a major role in the cascade of
biological changes culminating in dopaminergic cell death even though the precise
mechanisms involving oxidative stress-mediated nigral cell degeneration in PD are not
clear. However, accumulating evidence indicates that dopamine (DA), a neurotransmitter
under physiological conditions, may also serve as a neurotoxin and thereby participate in
the neurodegenerative process. The mechanism of dopamine neurotoxicity is strongly
linked to oxidative metabolism. Under physiological conditions, dopamine can be
oxidized enzymatically through monoamine oxidases (MAO) to dihydroxyphenylacetic
acid (DOPAC) and subsequently methylated by catechol-O-methyltransferase (COMT) to
homovanillic acid (HVA), or from dopamine to 3-methoxytyramine (3-MT) via COMT
and further oxidized to HVA through MOA. During this MAO-mediated DA turnover
process, hydrogen peroxide (H_2O_2) is produced as a byproduct of DA deamination, a
process serving as an inherent source of oxidative stress in the nigrostriatal system.
Dopamine can also be non-enzymatically oxidized by O_2 yielding quinones and H_2O_2.
These quinones also undergo intramolecular cyclization immediately followed by
cascading oxidative reactions ending in the formation of a black, insoluble polymeric
pigment known as neuromelanin (Graham, 1978; Hermida-Ameijeiras et al., 2004).
Neuromelanin renders dopaminergic neurons more susceptible to auto-oxidation through
quinone modification of dopamine, which increases basal levels of oxidative stress in SN
(Graham, 1978). What is becoming clear is that degrading dopamine either enzymatically
or non-enzymatically generates H_2O_2, which is easily converted through the Fenton's

reaction to highly toxic hydroxyl radicals (•OH) when in the presence of the high levels of ferrous iron (Fe^{2+}) normally found in the SN (Nappi and Vass, 1997).

Hydroxyl Radicals, Superoxide and Hydrogen peroxide in PD

As mentioned above, DA oxidation plays an important role in generating hydroxyl radical in the central nervous system, including the degeneration of dopaminergic neurons. Dopamine, like many catecholamines (dihydroquinones, QH2), can easily be oxidized by O_2 under physiological conditions. During this oxidation process, both semiquinones (•QH) and quinones (Q) are generated, resulting in •OH (via Fenton's reaction), the most toxic free radical in living cells (Klegeris et al., 1995). The resulting DA quinones also exert further neurotoxicity by covalently binding to cellular nucleophiles such as GSH and protein cysteinyl residues, which normally function as antioxidants important for cell survival (Levine et al., 1996; Requejo et al., 2010). Moreover, DA quinones bind and modify several proteins implicated in PD pathophysiology such as α-synuclein, DJ-1 and parkin (Conway et al., 2001; Girotto et al., 2012; LaVoie et al., 2005). However, among the various types of oxidative damage in cellular macromolecules, damage to nucleic acids is particularly hazardous as it could alter the genetic information. Among the five nucleobases - uracil, thymine, cytosine, adenine and guanine - guanine is most susceptible to nucleic acid oxidation through hydroxyl radicals (Cerchiaro et al., 2009; Cooke et al., 2003). Hydroxyl radical-mediated lesioning of the DNA strand produces 8-hydroxyguanosine (8OHG), the most studied oxidized DNA product. Moreover, DNA damage in PD also appears to be at the level of

8OHG and 8-hydroxyl-2-deoxyguanosine (8-OHdG) as elevated 8OHG and reduced 8-OHdG have been observed in the SN and cerebrospinal fluid (CSF) of PD patients (Isobe et al., 2010; Zhang et al., 1999).

Although the human brain comprises only 2% of the total body weight, it is especially prone to oxidative stress as it receives 15% of the cardiac output and 20% of total O_2 consumption of the body, making it highly metabolically active tissue that critically relies on oxidative phosphorylation to meet energy demands. Oxidative phosphorylation also produces potentially damaging radicals such as the superoxide anion O_2^- as a result of a one-electron reduction of O_2. Superoxide occurs widely in nature through a variety of enzymatic processes including xanthine oxidase and NADPH oxidase, a multimeric enzyme that generates both O^{2-} and H_2O_2 (Qureshi et al., 1995). Superoxide has the capacity to damage components of the electron transport chain and other cellular constituents. Superoxides are also produced at microsomal membranes, with electron transport systems dependent on NADH or NADPH, via detoxification of toxic compounds and the catalyzed oxidation of fatty acids (Berg et al., 2004). NADPH oxidase (also known as PHOX) is a membrane-bound enzyme that contributes to the production of O_2^- from O_2 in microglial cells leading to dopaminergic neuron damage (Gao et al., 2003; Wu et al., 2005). NADPH oxidase is a multimeric enzyme composed of plasma membrane bound gp91phox and p22phox subunits and cytosolic p40phox, p47phox and p67phox subunits. Upon activation, the cytosolic subunits undergo phosphorylation and translocate to the membrane, where together with small G proteins they associate with the membrane-bound subunits. The assembled and active enzyme complex then catalyzes the transfer of a single electron from NADPH to O_2 to release

superoxide. Moreover, O_2^- is generated as a normal byproduct of the mitochondrial electron transfer chain. Depending on the availability of substrates and cofactors, O_2^- can react as a one-electron oxidant, oxidizing hydroquinones to semiquinone radicals, ascorbate, or epinephrine with the concomitant production of H_2O_2 or a one-electron reductant, e.g., quinones or peroxides in the presence of transition metals (Berg et al., 2004). The flux of O_2^- is a function of the concentration of potential electron donors, the local concentration of O_2 and the second-order rate constants for the reactions between them. Two modes of operation by isolated mitochondria result in significant O_2^- production, predominantly from complex I, when 1) the mitochondria are not making ATP and consequently have a high Δp (proton motive force) and a reduced CoQ (coenzyme Q) pool, and when 2) a high $NADH/NAD^+$ ratio exists in the mitochondrial matrix. For mitochondria that are actively making ATP, and consequently have a lower Δp and $NADH/NAD^+$ ratio, the extent of O_2^- production is far lower.

Given the ability of mitochondria to produce superoxides and hamper a neuron's ability to produce ATP, which subsequently lead to apoptosis, several toxin-based models are employed to study PD and related molecular mechanisms. For instance, to mimic oxidative stress mechanisms in PD, researchers use rotenone, a complex I inhibitor, as well as other chemical inhibitors of electron flow that act further downstream in the electron transport chain because they increase ROS production and subsequent mitochondria-dependent apoptosis. Rotenone binds to the ubiquinone binding site of complex I and disrupts the electron transfer between the terminal iron-sulfur (FeS) cluster N2 and ubiquinone (Scatena et al., 2012). This process interferes with NADH's ability to produce ATP and pass electrons to CoQ, creating excess electrons within the

mitochondrial matrix (Hayes and Laws, 1991). This complex I inhibition causes electrons to react with O_2 prematurely, incompletely reducing it to superoxide radicals instead of water. Therefore, rotenone-induced oxidative stress activates a downstream apoptotic cascade in dopaminergic cells, which helps explain the observed systemic reduction in complex I activity and oxidative stress in PD brains (Greenamyre et al., 2001; Mizuno et al., 1989; Parker et al., 1989). Another highly lipophilic, selective neurotoxicant similar to rotenone is 1-methyl-4-phenyl-1,2,3,6-tetrahydropyridine (MPTP), which induces clinical features very similar to human PD (Jin et al., 2015). In the brain, MPTP is quickly metabolized to 1-methyl-4-phenyl-2,3-dihydropyridinium ($MPDP^+$) via monoamine oxidase B (MAO-B) in astroglial cells and serotonergic cells (Chiba et al., 1984; Kitahama et al., 1991). $MPDP^+$ is an unstable molecule that undergoes spontaneous oxidation to its active metabolite 1-methyl-4-phenylpyridinium (MPP^+). MPP^+ is selectively taken up by dopaminergic neurons via dopaminergic transporter (DAT) where it exerts its neurotoxicity by inhibiting mitochondrial complex I, thereby leading to ATP reduction and superoxide generation (Ghosh et al., 2013). Oxidopamine or 6-hydroxydopamine (6-OHDA) is another synthetic neurotoxicant that selectively destroys dopaminergic neurons by generating ROS such as superoxide radicals (Jin et al., 2014b; Latchoumycandane et al., 2011). Like MPP^+, 6-OHDA enters neurons via DAT (Bove et al., 2005). It activates cell death pathways by generating intracellular free radicals and mitochondrial inhibition (Blum et al., 2001). Therefore, 6-OHDA, like DA, could generate hydroxyl radicals and superoxide radicals by the deamination process via MAO or auto-oxidation, and iron-catalyzed via the Fenton reaction, thus further strengthening

the free radical hypothesis of PD. However, 6-OHDA's exact mechanism of ROS production and neurotoxicity remains unclear.

Alkoxy radicals (RO$^\bullet$) and peroxy radicals (ROO$^\bullet$) in PD

The most favorable biological substrates for peroxidation are the polyunsaturated fatty acid (PUFA) components of cell and subcellular membranes. Lipid peroxides result from the addition of double bonds or hydrogen abstraction in the presence of oxygen. Since PUFA are more sensitive than saturated fatty acids, it is apparent that the activated methylene (RH) bridge represents a critical target site. The double bond adjacent to a methylene group weakens the methylene C-H bond, thereby rendering the hydrogen more susceptible to abstraction (Catala, 2014). Like many radical reactions, lipid peroxidation is a multi-step process with initiation, propagation and termination. At the initiation step, ROS such as hydroperoxyl radicals or hydroxyl radicals react with PUFA to produce unstable fatty acid radicals that continue reacting with O_2 to produce unstable, intermediate fatty acid peroxy radicals. These fatty acid peroxy radicals and fatty acid radicals undergo chain reactions that produce organic hydroperoxides, which in turn can remove hydrogen from another PUFA (Halliwell and Gutteridge, 1984). This chain reaction is termed propagation, implying that one initiating hit can result in the conversion of numerous PUFA to lipid hydroperoxides. Since most biological membranes are composed of PUFA, lipid peroxidation is considered the main molecular mechanism underlying oxidative damage to cell structures and in toxicity-induced cell death. The end products of lipid peroxidation are reactive aldehydes such as 4-hydroxy-trans-2-nonenal (4-HNE), 4-oxo-trans-2-nonenal (4-ONE), malondialdehyde (MDA),

acrolein, isoprostanes, and isofurans (Aluru et al., 2015; Esterbauer et al., 1991). These markers are derived from arachidonic acid (ARA), which is released from neural membrane glycerophospholipids through the activation of cytosolic phospholipase A_2 (cPLA$_2$), an enzyme coupled with NMDA receptors through a G protein-independent mechanism (Farooqui and Horrocks, 2007; Farooqui and Farooqui, 2011).

The primary end product of lipid peroxidation, 4-HNE, is a highly reactive lipophilic α,β-alkenal that forms stable adducts with nucleophilic groups on proteins such as thiols and amines (Ullery and Marnett, 2012), and it chemically modifies cellular macromolecules and DNA. Moreover, 4-HNE shows time- and dose-dependent activation of caspase-8, caspase-9 and caspase-3 as well as apoptotic cell death accompanied by DNA fragmentation (Liu et al., 2000). Mechanistically, 4-HNE reduces glutathione (GSH) inhibition (Ahmed et al., 2002) of the NFκB signaling pathway (Yin et al., 2015), disinhibits mitochondrial complexes I and II, and it deactivates p53 (Cao et al., 2014) and poly-(ADP-ribose) polymerase (PARP) (Raza and John, 2006). The increased levels of 4-HNE immunopositive neurons in the brain tissue and cerebrospinal fluid of PD patients indicate not only a pathophysiological role for oxidative stress in these diseases, but also a role for 4-HNE in neuronal apoptosis (Liu et al., 2000; Yoritaka et al., 1996; Zarkovic, 2003).

Nitric oxide (NO) in PD

Nitric oxide (NO) is another potential source of oxidative stress. NO is produced by nitric oxide synthase (NOS) through converting L-arginine to L-citrulline utilizing NADPH oxidase and O_2 as cofactors (Day et al., 1999; Duval et al., 1996). There are 3

isoforms of NOS: neuronal NOS (nNOS), inducible NOS (iNOS) and endothelial NOS (eNOS), of which nNOS is expressed in several neuronal subtypes except dopaminergic neurons. In contrast to nNOS, iNOS is not normally expressed in the brain; however, under pathological conditions, iNOS can be induced. Activated glial cells produce iNOS, which leads to increased production of NO. Indeed, elevated iNOS levels mediated by CD23 have been reported in the SN of patients with PD (Hunot et al., 1996). MPTP administration in mice also produces glial cell-mediated increases in iNOS expression and NO production (Liberatore et al., 1999). Consequently, mice lacking the iNOS gene are less susceptible to MPTP-induced losses of SN DA neurons (Itzhak et al., 1998). The MPTP-induced striatal dopamine depletion, however, remains intact in iNOS null mice, as does MPTP-induced microglial activation (Dehmer et al., 2000; Liberatore et al., 1999). Although poorly reactive, NO and O_2^- free radicals can combine to form the highly reactive nitrogen species peroxynitrite ($ONOO^-$), which can cause oxidative damage to various proteins such as tyrosine hydroxylase (TH) and α-synuclein (Ara et al., 1998; Przedborski and Vila, 2001). Iron content increases in the SN of PD patients and in animal models of the disease (Hirsch, 2006). Through a superoxide-driven Fenton's reaction between hydrogen peroxide and the free ferrous iron catalyst, a substantial amount of highly reactive hydroxyl radicals (OH) can be produced. Reactive astrocytes produce myeloperoxidase (MPO), which oxidizes non-reactive nitrites (NO_2^-) that contribute to protein nitrosylation (van der Vliet et al., 1997). MPO is also implicated in the production of the non-radical oxidant hypochlorous acid (HOCl), which can damage macromolecules directly (Hampton et al., 1998). Altogether, an inflammatory, oxidative environment can be produced by activated glial cells in the SN region.

Antioxidants as therapeutics for PD

PD is a multifactorial disease wherein glial activation, inflammation, oxidative stress and mitochondrial dysfunction play central roles in dopaminergic neurodegeneration, specifically in the nigrostriatum. Increasing efforts are being devoted to searching for neuroprotective agents that will protect against the irreversible loss of neurons. Administration of a dopamine agonist or levodopa has been widely used to treat PD symptoms, but does not alter disease pathogenesis. Dopaminergic neuroprotection in animal models of PD has been demonstrated with various substances including glial cell line-derived neurotrophic factor (GDNF), brain-derived neurotrophic factor (BDNF) and TGF-β. Additionally, various anti-inflammatory agents, such as NSAIDs, COX inhibitors, statins, pioglitazone and minocycline, have been used in different animal models of PD. However, most of these compounds failed in either preclinical trials or in human phase I trials due to their inability to cross the blood-brain barrier or to limited bioavailability. Moreover, they also cause side effects and toxicity in animals. Hence, developing successful neuroprotective therapeutic approaches to halt progression of PD requires a better understanding of the disease mechanism.

Vitamin antioxidant therapy

Oxidative stress is closely linked to other components of the degenerative process, such as mitochondrial dysfunction, excitotoxicity, nitric oxide toxicity and inflammation. That is, neuronal injury and cell death in both acute and chronic pathological conditions can result from oxidative damage, for example, through superoxide (O_2^-), hydroxyl (OH^-), peroxyl (RO_2^-), hydrogen peroxide (H_2O_2), and peroxynitrite ($ONOO^-$). Therefore,

various vitamin antioxidants have been tested for their efficacy as scavengers of oxygen radicals and their potential as neuroprotective agents. Naturally, dietary sources supply many antioxidants. Vitamins C and E, β-carotene and coenzyme Q are the best known dietary antioxidants, of which Vitamin E is present in vegetable oils and found abundantly in wheat germ (Uttara et al., 2009). This fat soluble vitamin is absorbed in the gut and carried in the plasma by lipoproteins. Of eight natural isomeric forms of vitamin E, α-tocopherol is the most common and potent isomer. Being lipid soluble, vitamin E can effectively prevent lipid peroxidation of plasma membranes (Uttara et al., 2009). In the MPTP mouse model of PD, vitamin E inhibited the iron accumulation and thus reversed the MPTP-induced increase in oxidized glutathione (GSSG) and lipid peroxidation levels in brain tissues (Lan and Jiang, 1997). Moreover, in the 6-OHDA-induced rat model of PD, vitamin E significantly attenuated the effects of 6-OHDA on GSH and SOD in most brain regions (Perumal et al., 1992), indicating that vitamin antioxidants may serve as potential therapeutic agents in retarding the progression of neurodegeneration. However, epidemiological evidence regarding the associations between antioxidant vitamin intake and PD is limited and inconsistent. Observational data from humans suggest that the combined administration of high-dose α-tocopherol (vitamin E) and ascorbate (vitamin C) supplementation slows the progression of PD (Fahn, 1992) and that the dietary intake of vitamin E and β-carotene lowers the risk of developing PD (Miyake et al., 2011). In contrast, results from double-blind, randomized controlled trials found vitamin E to have no benefits in PD patients (Parkinson Study, 1993; Scheider et al., 1997).

Other plant-based antioxidants

Plants contain a wide variety of endogenous, free radical-scavenging antioxidants such as phenolic compounds (e.g., phenolic acids, flavonoids, quinones, coumarins, lignans, stilbenes, tannins), nitrogen compounds (e.g., alkaloids, amines, betalains), terpenoids (including carotenoids) and some other endogenous metabolites rich in antioxidant activity. Many of these have shown protective effects against oxidative-induced neuronal death (Uttara et al., 2009). Although consumer demand for phytotherapeutic agents is growing, they need scientific validation before plant-derived extracts gain wider acceptance and use.

Apocynin (4-hydroxy-3-methoxyacetophenone) is a non-toxic plant-derived molecule that has been well-studied in cell culture and animals models of PD in our lab and elsewhere (Anantharam et al., 2007; Philippens et al., 2013). Apocynin can effectively block NADPH oxidase and reduce ROS generation during neuronal injury or stress. Recently, we demonstrated that the apocynin dimer diapocynin is also neuroprotective and anti-neuroinflammatory in the MPTP animal model as well as in the progressively degenerative $LRRK2_{R1441G}$ transgenic mouse model (Dranka et al., 2013; Ghosh et al., 2012). Importantly, we were able to demonstrate that diapocynin crosses the blood brain barrier, which is one of the main limitations for antioxidant therapies. Upon reaching the midbrain of MPTP-treated mice, it attenuates the nigral activation of microglial and astroglial cells, inhibits the proinflammatory molecule iNOS and the production of NADPH oxidase-mediated superoxide formation and decreases oxidative stress, thereby protecting the nigrostriatum and improving neurobehavioral performance, suggesting it's potential as a therapeutic candidate for clinical trials of human PD

patients. In these studies, both apocynin and diapocynin were orally administered at 300 mg/kg body weight. Although these high doses were not toxic to animals, there is a need for more efficacious apocynin analogs that will translate into human clinical trials.

In recent years resveratrol has gained much attention as a therapeutic for prevention and treatment of neurodegeneration disorders. Resveratrol is present in a variety of vegetables, fruits, grains, teas, and wines. It is protective against a number of cardiovascular and neurodegenerative diseases and cancer. Although the mechanisms behind resveratrol's health benefits have not yet been clearly elucidated, a number of studies have reported on its antioxidant, anti-inflammatory, and metal-chelating properties (Ndiaye et al., 2005; Sun et al., 2008), as well as its ability to activate Sirtuin 1 (SIRT1) and vitagenes, which can prevent the deleterious effects triggered by oxidative stress (Sun et al., 2010). In fact, SIRT1 activation by resveratrol is gaining importance in the development of innovative treatment strategies for stroke and other neurodegenerative disorders (Sun et al., 2010).

Quercetin, found abundantly in vegetables and fruits, is another natural antioxidant flavonoid capable of protecting cells against oxidative damage, and thus has therapeutic potential for the prevention and treatment of cardiovascular disease, cancer, and neurodegenerative disease. Importantly, there is now compelling evidence of its neuroprotective role in various neurodegenerative diseases (Ansari et al., 2009; Haleagrahara et al., 2013; Karuppagounder et al., 2013; Sabogal-Guaqueta et al., 2015). In nature, quercetin mainly occurs as glycosides, ethers, and to a lesser extent, sulfates. When tested in PC12 cells in a cell culture model of AD, a glycoside form of quercetin, quercetin-3'-glucoside, reduced H_2O_2-induced ROS generation and also protected against

Aβ-induced cell death (Zhu et al., 2007). Isoquercitrin, another glycoside form of quercetin, was neuroprotective against 6-OHDA-induced neurotoxicity in a PC12 cell model of PD (Magalingam et al., 2014). When the 6-OHDA-treated PC12 cells were pre-treated with isoquercitrin, the levels of ROS-scavenging enzymes (SOD, catalase, and GPx) increased and lipid peroxidation decreased. Similarly, quercetin treatment reduced protein carbonyl content and lipid hydroperoxide (LPO) levels in the striatum of 6-OHDA-treated rats (Haleagrahara et al., 2011).

Mitochondria-targeted antioxidant therapy

Mitochondrial oxidative stress, mitochondrial DNA deletions, altered mitochondrial morphology and mitochondrial interactions with pathogenic proteins increase oxidative damage leading to dopaminergic neurodegeneration in PD. Therefore, therapeutic approaches targeting mitochondrial dysfunction and related oxidative stress hold great promise as potential cures for PD. MPTP and other complex-I inhibitors such as rotenone, maneb, paraquat, fenzaquin and trichloroethylene result in the loss of nigral dopaminergic neurons in mouse models of PD, implicating mitochondrial dysfunction in PD pathogenesis. Moreover, reduced complex-I activity and an increased susceptibility to MPP$^+$, the toxic metabolite of MPTP, were also observed in mitochondrial DNA from PD patients, clearly demonstrating the mtDNA-encoded defects in PD. Based on all the evidence, it could be inferred that intervening in one or more of these processes could alleviate the harmful effects of mitochondrial dysfunction. During the past decade, numerous antioxidant analogs have been developed to specifically target mitochondria and have been shown to improve mitochondrial function in experimental models of PD.

333

To target small-molecule antioxidants to mitochondria, two general strategies have so far been shown to be safe and effective in pre-clinical studies: conjugations to lipophilic cations or incorporation into mitochondria-targeted peptides. Since lipophilic cations can easily pass through the lipid bilayers of plasma membranes and the mitochondrial inner membrane, they accumulate in the mitochondrial matrix in response to the large mitochondrial membrane potential (from outer positive to inner negative) (Ross et al., 2005). The best characterized and most widely used lipophilic cation for conjugating small molecules is triphenylphosphonium (TPP), which has traditionally been used to determine mitochondrial inner membrane potential. Using TPP chemistry, Murphy and colleagues (Ross et al., 2005) developed a series of orally bioavailable mitochondria-targeted antioxidants, including $MitoQ_{10}$, MitoVitE and MitoTEMPOL (Jin et al., 2014a).

Mito-Q_{10} (Mito-quinone), the most studied mitochondria-targeted antioxidant, protects dopaminergic neurons from 6-OHDA in a cell model (Solesio et al., 2013) and from MPTP-induced toxicity in a mouse model of PD (Ghosh et al., 2010). Mito-Q_{10} consists of TPP covalently attached to the ubiquinone moiety of Coenzyme Q (CoQ_{10}) through a ten-carbon alkyl chain. CoQ_{10} is a component of the electron transport chain enabling cellular respiration and it works as a strong endogenous antioxidant. Like its parent CoQ_{10}, MitoQ continually scavenges peroxyl, peroxynitrite and superoxide, thereby protecting mitochondria against lipid peroxidation. MitoVitE is a TPP-conjugated mitochondria-targeted antioxidant, which by coupling the antioxidant phenolic moiety of α-tocopherol, gets taken up by mitochondria about 80 times more effectively than vitamin E itself and thus affords better protection against oxidative damage (Smith et al., 1999). MitoVitE also reduces H_2O_2-induced caspase activity and can prevent cell death in

fibroblasts in patients with Friedrich ataxia, an inherited nervous system disease associated with decreased frataxin and increased iron-catalyzed oxidative damage (Jauslin et al., 2003). In a study targeting cerebellar granule cells, MitoVitE diminished the ethanol-induced accumulation of intracellular oxidants and counteracted the suppression of not only glutathione peroxidase/glutathione reductase functions, but also the protein expression of γ-glutamylcysteine synthetase and total cellular glutathione levels (Siler-Marsiglio et al., 2005). MitoTEMPOL is another TPP derivative, but one with the stable piperidine nitroxide radical TEMPOL (4-hydroxy-2,2,6,6-tetramethylpiperidine-1-oxy). MitoTEMPOL also acts as a cytosolic SOD mimetic, converting superoxide molecules into water, and is able to detoxify ferrous iron by oxidizing it to ferric iron. Although MitoTEMPOL has not yet been tested in experimental models of PD, it reduced protein oxidation and mitochondrial and cytosolic ROS production in rat models of breast cancer (Dickey et al., 2013) and diabetes (Pung et al., 2012), respectively. In an LRRK2^{R1441G} mouse model of PD, the novel mitochondria-targeted antioxidant MitoApo developed with apocynin, a plant-derived antioxidant and NADPH oxidase inhibitor, markedly improved coordinated motor skills and olfactory function (Dranka et al., 2014). The authors also showed that the presence of a highly lipophilic and delocalized cationic moiety in MitoApo-C$_{11}$ makes it more cell-permeable and bioavailable (Dranka et al., 2014). In our own MitoApo studies, we have observed significant neuroprotection against MPP$^+$-induced loss of dopaminergic neurons in primary mesencephalic culture wherein MitoApo reduced glial cell-mediated inflammatory reactions. Moreover, administration of MitoApo in mice protects dopaminergic neurons and terminals from MPTP toxicity by reducing inflammatory

reactions and oxidative stress (unpublished data). MitoPBN is a TPP derivative of phenoxy-butyl-nitrone. The spin trap PBN was chosen based on PBN's well-known reactivity with carbon-centered radicals (Murphy et al., 2003). MitoPBN is rapidly taken up by mitochondria and can block the oxygen-induced activation of uncoupled proteins (Murphy et al., 2003).

Another major alternative approach to targeting antioxidants to mitochondria is through the use of small positively charged peptides call Szeto-Schiller (SS)-peptides (Zhao et al., 2004). SS-peptides contain an aromatic cationic sequence that facilitates the delivery of small molecules directly to mitochondria where they localize in the inner mitochondrial membrane with an approximately 1000-5000 fold accumulation (Zhao et al., 2003; Zhao et al., 2004). These SS-peptides can scavenge H_2O_2 and peroxynitrite and inhibit lipid peroxidation. Their antioxidant action can be attributed to the tyrosine or dimethyltyrosine residue (Szeto, 2006). By reducing mitochondrial ROS, these peptides inhibit mitochondrial permeability transition and cytochrome *c* release, thus preventing oxidant-induced neuronal apoptosis. Among the SS-peptides recently developed, SS-31 (D-Arg-(2'6'-dimethyltyrosine)-Lys-Phe-NH$_2$) and SS-20 (Phe-D-Arg-Phe-Lys-NH$_2$) have been studied most and both comprise a dimethyltyrosine residue, which reacts with a variety of free radicals and inhibits lipid peroxidation (Szeto, 2008). Studies with isolated mitochondria showed that both SS-31 and SS-20 prevented MPP$^+$-induced inhibition of oxygen consumption and ATP production and mitochondrial swelling, indicating their protective effect in cell culture models of PD (Yang et al., 2009). Furthermore, SS-31 exhibited complete dose-dependent protection against the MPTP-induced loss of dopamine and its metabolites in the striatum, as well as against the loss of

tyrosine hydroxylase immunoreactive neurons in the SN. These findings provide strong evidence that these neuroprotective peptides, which target both mitochondrial dysfunction and oxidative damage, are a promising approach for the treatment of PD (Yang et al., 2009).

Conclusions

PD is a complex, multifactorial disease condition strongly influenced by environmental factors. Exposure to different environmental conditions including pesticides, heavy metals, solvents (trichloroethylene), polychlorinated biphenols (PCBs) and repeated head injury increases the risk of developing sporadic PD later in life. Although the exact mechanisms underlying neurodegeneration in PD is not well understood, substantial evidence has implicated mitochondrial dysfunction and oxidative damage as important components of PD pathogenesis. Since the brain is particularly vulnerable to the effects of ROS due to its high demand for oxygen and its abundance of highly peroxidisable substrates, mitochondria-targeted interventions have emerged as a tool for modulating oxidative stress in the prevention and treatment of PD. As described above, a series of mitochondria-targeted antioxidants have been developed over the past few years showing great results in *in vitro* and *in vivo* models of PD. Despite their efficacy in animal studies, similar outcomes for these novel antioxidant therapies have not been borne out in clinical studies of neurodegenerative diseases. Therefore, research on effective strategies targeting mitochondria with bioactive molecules capable of penetrating the blood brain barrier is essential. Moreover, increasing the innate cellular antioxidant defense through other mitochondrial drug targets may be as important. PGC-

1α, a master regulator of mitochondrial biogenesis, and Nrf2, a natural antioxidant and inflammation fighter, are possible therapeutic targets for PD, with important roles in the function and survival of dopaminergic neurons in the SN. However, at present, antioxidants and mitochondria-targeted therapeutics have seen very limited success in the prevention or treatment of PD, and randomized clinical trials in humans, as well as animal studies, are urgently needed to identify and understand the effects of mitochondria-targeted therapeutics in the treatment of PD.

References

Ahmed, I., et al., 2002. Differential modulation of growth and glutathione metabolism in cultured rat astrocytes by 4-hydroxynonenal and green tea polyphenol, epigallocatechin-3-gallate. Neurotoxicology. 23**,** 289-300.

Aluru, N., et al., 2015. Targeted mutagenesis of aryl hydrocarbon receptor 2a and 2b genes in Atlantic killifish (Fundulus heteroclitus). Aquat Toxicol. 158**,** 192-201.

Anantharam, V., et al., 2007. Pharmacological inhibition of neuronal NADPH oxidase protects against 1-methyl-4-phenylpyridinium (MPP+)-induced oxidative stress and apoptosis in mesencephalic dopaminergic neuronal cells. Neurotoxicology. 28**,** 988-97.

Ansari, M. A., et al., 2009. Protective effect of quercetin in primary neurons against Abeta(1-42): relevance to Alzheimer's disease. J Nutr Biochem. 20**,** 269-75.

Ara, J., et al., 1998. Inactivation of tyrosine hydroxylase by nitration following exposure to peroxynitrite and 1-methyl-4-phenyl-1,2,3,6-tetrahydropyridine (MPTP). Proc Natl Acad Sci U S A. 95**,** 7659-63.

Ben-Shachar, D., et al., 1995. Dopamine neurotoxicity: inhibition of mitochondrial respiration. J Neurochem. 64**,** 718-23.

Berg, D., et al., 2004. Redox imbalance. Cell Tissue Res. 318**,** 201-13.

Blum, D., et al., 2001. Molecular pathways involved in the neurotoxicity of 6-OHDA, dopamine and MPTP: contribution to the apoptotic theory in Parkinson's disease. Prog Neurobiol. 65**,** 135-72.

Bonifati, V., et al., 2008. Re: LRRK2 mutation analysis in Parkinson disease families with evidence of linkage to PARK8. Neurology. 70**,** 2348; author reply 2348-9.

Bosco, D. A., et al., 2006. Elevated levels of oxidized cholesterol metabolites in Lewy body disease brains accelerate alpha-synuclein fibrilization. Nat Chem Biol. 2**,** 249-53.

Bove, J., et al., 2005. Toxin-induced models of Parkinson's disease. NeuroRx. 2**,** 484-94.

Cao, Z. G., et al., 2014. Comparison of 4-hydroxynonenal-induced p53-mediated apoptosis in prostate cancer cells LNCaP and DU145. Contemp Oncol (Pozn). 18**,** 22-8.

Catala, A., 2014. Reactive oxygen species, lipid peroxidation, and protein oxidation. Nova Science Publishers, Inc., Hauppauge, New York.

Cerchiaro, G., et al., 2009. Hydroxyl radical oxidation of guanosine 5'-triphosphate (GTP): requirement for a GTP-Cu(II) complex. Redox Rep. 14**,** 82-92.

Chiba, K., et al., 1984. Metabolism of the neurotoxic tertiary amine, MPTP, by brain monoamine oxidase. Biochem Biophys Res Commun. 120**,** 574-8.

Conway, K. A., et al., 2001. Kinetic stabilization of the alpha-synuclein protofibril by a dopamine-alpha-synuclein adduct. Science. 294**,** 1346-9.

Cooke, M. S., et al., 2003. Oxidative DNA damage: mechanisms, mutation, and disease. FASEB J. 17**,** 1195-214.

Dauer, W., Przedborski, S., 2003. Parkinson's disease: mechanisms and models. Neuron. 39**,** 889-909.

Day, B. J., et al., 1999. A mechanism of paraquat toxicity involving nitric oxide synthase. Proc Natl Acad Sci U S A. 96**,** 12760-5.

Dehmer, T., et al., 2000. Deficiency of inducible nitric oxide synthase protects against MPTP toxicity in vivo. J Neurochem. 74**,** 2213-6.

Dickey, J. S., et al., 2013. Mito-tempol and dexrazoxane exhibit cardioprotective and chemotherapeutic effects through specific protein oxidation and autophagy in a syngeneic breast tumor preclinical model. PLoS One. 8, e70575.

Dranka, B. P., et al., 2013. Diapocynin prevents early Parkinson's disease symptoms in the leucine-rich repeat kinase 2 (LRRK2R(1)(4)(4)(1)G) transgenic mouse. Neurosci Lett. 549, 57-62.

Dranka, B. P., et al., 2014. A novel mitochondrially-targeted apocynin derivative prevents hyposmia and loss of motor function in the leucine-rich repeat kinase 2 (LRRK2(R1441G)) transgenic mouse model of Parkinson's disease. Neurosci Lett. 583, 159-64.

Duval, D. L., et al., 1996. Characterization of hepatic nitric oxide synthase: identification as the cytokine-inducible form primarily regulated by oxidants. Mol Pharmacol. 50, 277-84.

Esterbauer, H., et al., 1991. Chemistry and biochemistry of 4-hydroxynonenal, malonaldehyde and related aldehydes. Free Radic Biol Med. 11, 81-128.

Fahn, S., 1992. A pilot trial of high-dose alpha-tocopherol and ascorbate in early Parkinson's disease. Ann Neurol. 32 Suppl, S128-32.

Farooqui, A. A., Horrocks, L. A., 2007. Glycerophospholipids in brain : phospholipase A2 in neurological disorders. Springer, New York, N.Y.

Farooqui, T., Farooqui, A. A., 2011. Lipid-mediated oxidative stress and inflammation in the pathogenesis of Parkinson's disease. Parkinsons Dis. 2011, 247467.

Gao, H. M., et al., 2003. Critical role for microglial NADPH oxidase in rotenone-induced degeneration of dopaminergic neurons. J Neurosci. 23, 6181-7.

Ghosh, A., et al., 2010. Neuroprotection by a mitochondria-targeted drug in a Parkinson's disease model. Free Radic Biol Med. 49, 1674-84.

Ghosh, A., et al., 2012. Anti-inflammatory and neuroprotective effects of an orally active apocynin derivative in pre-clinical models of Parkinson's disease. J Neuroinflammation. 9, 241.

Ghosh, A., et al., 2013. The peptidyl-prolyl isomerase Pin1 up-regulation and proapoptotic function in dopaminergic neurons: relevance to the pathogenesis of Parkinson disease. J Biol Chem. 288, 21955-71.

Girotto, S., et al., 2012. Dopamine-derived quinones affect the structure of the redox sensor DJ-1 through modifications at Cys-106 and Cys-53. J Biol Chem. 287, 18738-49.

Graham, D. G., 1978. Oxidative pathways for catecholamines in the genesis of neuromelanin and cytotoxic quinones. Mol Pharmacol. 14, 633-43.

Greenamyre, J. T., et al., 2001. Complex I and Parkinson's disease. IUBMB Life. 52, 135-41.

Gwinn-Hardy, K., 2002. Genetics of parkinsonism. Mov Disord. 17, 645-56.

Haleagrahara, N., et al., 2011. Neuroprotective effect of bioflavonoid quercetin in 6-hydroxydopamine-induced oxidative stress biomarkers in the rat striatum. Neurosci Lett. 500, 139-43.

Haleagrahara, N., et al., 2013. Effect of quercetin and desferrioxamine on 6-hydroxydopamine (6-OHDA) induced neurotoxicity in striatum of rats. J Toxicol Sci. 38, 25-33.

Halliwell, B., Gutteridge, J. M., 1984. Oxygen toxicity, oxygen radicals, transition metals and disease. Biochem J. 219**,** 1-14.

Hampton, M. B., et al., 1998. Inside the neutrophil phagosome: oxidants, myeloperoxidase, and bacterial killing. Blood. 92**,** 3007-17.

Hayes, W. J., Laws, E. R., 1991. Handbook of pesticide toxicology. Academic Press, San Diego.

Hermida-Ameijeiras, A., et al., 2004. Autoxidation and MAO-mediated metabolism of dopamine as a potential cause of oxidative stress: role of ferrous and ferric ions. Neurochem Int. 45**,** 103-16.

Hirsch, E. C., 2006. Altered regulation of iron transport and storage in Parkinson's disease. J Neural Transm Suppl. 201-4.

Hoehn, M. M., Yahr, M. D., 1998. Parkinsonism: onset, progression, and mortality. 1967. Neurology. 50**,** 318 and 16 pages following.

Hunot, S., et al., 1996. Nitric oxide synthase and neuronal vulnerability in Parkinson's disease. Neuroscience. 72**,** 355-63.

Isobe, C., et al., 2010. Levels of reduced and oxidized coenzyme Q-10 and 8-hydroxy-2'-deoxyguanosine in the cerebrospinal fluid of patients with living Parkinson's disease demonstrate that mitochondrial oxidative damage and/or oxidative DNA damage contributes to the neurodegenerative process. Neurosci Lett. 469**,** 159-63.

Itzhak, Y., et al., 1998. Resistance of neuronal nitric oxide synthase-deficient mice to cocaine-induced locomotor sensitization. Psychopharmacology (Berl). 140**,** 378-86.

Jankovic, J., Stacy, M., 2007. Medical management of levodopa-associated motor complications in patients with Parkinson's disease. CNS Drugs. 21**,** 677-92.

Jauslin, M. L., et al., 2003. Mitochondria-targeted antioxidants protect Friedreich Ataxia fibroblasts from endogenous oxidative stress more effectively than untargeted antioxidants. FASEB J. 17**,** 1972-4.

Jin, H., et al., 2014a. Mitochondria-targeted antioxidants for treatment of Parkinson's disease: preclinical and clinical outcomes. Biochim Biophys Acta. 1842**,** 1282-94.

Jin, H., et al., 2015. Targeted toxicants to dopaminergic neuronal cell death. Methods Mol Biol. 1254**,** 239-52.

Jin, H., et al., 2014b. Histone hyperacetylation up-regulates protein kinase Cdelta in dopaminergic neurons to induce cell death: relevance to epigenetic mechanisms of neurodegeneration in Parkinson disease. J Biol Chem. 289**,** 34743-67.

Karuppagounder, S. S., et al., 2013. Quercetin up-regulates mitochondrial complex-I activity to protect against programmed cell death in rotenone model of Parkinson's disease in rats. Neuroscience. 236**,** 136-48.

Kitahama, K., et al., 1991. Distribution of type B monoamine oxidase immunoreactivity in the cat brain with reference to enzyme histochemistry. Neuroscience. 44**,** 185-204.

Klegeris, A., et al., 1995. Autoxidation of dopamine: a comparison of luminescent and spectrophotometric detection in basic solutions. Free Radic Biol Med. 18**,** 215-22.

Lan, J., Jiang, D. H., 1997. Desferrioxamine and vitamin E protect against iron and MPTP-induced neurodegeneration in mice. J Neural Transm. 104**,** 469-81.

Latchoumycandane, C., et al., 2011. Dopaminergic neurotoxicant 6-OHDA induces oxidative damage through proteolytic activation of PKCdelta in cell culture and animal models of Parkinson's disease. Toxicol Appl Pharmacol. 256**,** 314-23.

LaVoie, M. J., et al., 2005. Dopamine covalently modifies and functionally inactivates parkin. Nat Med. 11**,** 1214-21.

Levine, R. L., et al., 1996. Methionine residues as endogenous antioxidants in proteins. Proc Natl Acad Sci U S A. 93**,** 15036-40.

Liberatore, G. T., et al., 1999. Inducible nitric oxide synthase stimulates dopaminergic neurodegeneration in the MPTP model of Parkinson disease. Nat Med. 5**,** 1403-9.

Liu, W., et al., 2000. 4-hydroxynonenal induces a cellular redox status-related activation of the caspase cascade for apoptotic cell death. J Cell Sci. 113 (Pt 4)**,** 635-41.

Magalingam, K. B., et al., 2014. Protective effects of flavonol isoquercitrin, against 6-hydroxy dopamine (6-OHDA)-induced toxicity in PC12 cells. BMC Res Notes. 7**,** 49.

McGeer, P. L., et al., 2001. Inflammation in Parkinson's disease. Adv Neurol. 86**,** 83-9.

Miyake, Y., et al., 2011. Dietary intake of antioxidant vitamins and risk of Parkinson's disease: a case-control study in Japan. Eur J Neurol. 18**,** 106-13.

Mizuno, Y., et al., 2001. Parkin and Parkinson's disease. Curr Opin Neurol. 14**,** 477-82.

Mizuno, Y., et al., 1989. Deficiencies in complex I subunits of the respiratory chain in Parkinson's disease. Biochem Biophys Res Commun. 163**,** 1450-5.

Murphy, M. P., et al., 2003. Superoxide activates uncoupling proteins by generating carbon-centered radicals and initiating lipid peroxidation: studies using a

mitochondria-targeted spin trap derived from alpha-phenyl-N-tert-butylnitrone. J Biol Chem. 278**,** 48534-45.

Nakabeppu, Y., et al., 2007. Oxidative damage in nucleic acids and Parkinson's disease. J Neurosci Res. 85**,** 919-34.

Nappi, A. J., Vass, E., 1997. Comparative studies of enhanced iron-mediated production of hydroxyl radical by glutathione, cysteine, ascorbic acid, and selected catechols. Biochim Biophys Acta. 1336**,** 295-302.

Ndiaye, M., et al., 2005. Red wine polyphenol-induced, endothelium-dependent NO-mediated relaxation is due to the redox-sensitive PI3-kinase/Akt-dependent phosphorylation of endothelial NO-synthase in the isolated porcine coronary artery. FASEB J. 19**,** 455-7.

Parker, W. D., Jr., et al., 1989. Abnormalities of the electron transport chain in idiopathic Parkinson's disease. Ann Neurol. 26**,** 719-23.

Parkinson Study, G., 1993. Effects of tocopherol and deprenyl on the progression of disability in early Parkinson's disease. N Engl J Med. 328**,** 176-83.

Perumal, A. S., et al., 1992. Vitamin E attenuates the toxic effects of 6-hydroxydopamine on free radical scavenging systems in rat brain. Brain Res Bull. 29**,** 699-701.

Philippens, I. H., et al., 2013. Oral treatment with the NADPH oxidase antagonist apocynin mitigates clinical and pathological features of parkinsonism in the MPTP marmoset model. J Neuroimmune Pharmacol. 8**,** 715-26.

Przedborski, S., Vila, M., 2001. The last decade in Parkinson's disease research. Basic sciences. Adv Neurol. 86**,** 177-86.

Pung, Y. F., et al., 2012. Resolution of mitochondrial oxidative stress rescues coronary collateral growth in Zucker obese fatty rats. Arterioscler Thromb Vasc Biol. 32**,** 325-34.

Qureshi, G. A., et al., 1995. Increased cerebrospinal fluid concentration of nitrite in Parkinson's disease. Neuroreport. 6**,** 1642-4.

Raza, H., John, A., 2006. 4-hydroxynonenal induces mitochondrial oxidative stress, apoptosis and expression of glutathione S-transferase A4-4 and cytochrome P450 2E1 in PC12 cells. Toxicol Appl Pharmacol. 216**,** 309-18.

Requejo, R., et al., 2010. Cysteine residues exposed on protein surfaces are the dominant intramitochondrial thiol and may protect against oxidative damage. FEBS J. 277**,** 1465-80.

Ross, M. F., et al., 2005. Lipophilic triphenylphosphonium cations as tools in mitochondrial bioenergetics and free radical biology. Biochemistry (Mosc). 70**,** 222-30.

Sabogal-Guaqueta, A. M., et al., 2015. The flavonoid quercetin ameliorates Alzheimer's disease pathology and protects cognitive and emotional function in aged triple transgenic Alzheimer's disease model mice. Neuropharmacology. 93C**,** 134-145.

Scatena, R., et al., 2012. Advances in mitochondrial medicine. Springer Verlag, Dordrecht ; New York.

Schapira, A. H., 1994. Evidence for mitochondrial dysfunction in Parkinson's disease--a critical appraisal. Mov Disord. 9**,** 125-38.

Scheider, W. L., et al., 1997. Dietary antioxidants and other dietary factors in the etiology of Parkinson's disease. Mov Disord. 12**,** 190-6.

Sian, J., et al., 1994. Alterations in glutathione levels in Parkinson's disease and other neurodegenerative disorders affecting basal ganglia. Ann Neurol. 36**,** 348-55.

Siler-Marsiglio, K. I., et al., 2005. Mitochondrially targeted vitamin E and vitamin E mitigate ethanol-mediated effects on cerebellar granule cell antioxidant defense systems. Brain Res. 1052**,** 202-11.

Smith, R. A., et al., 1999. Selective targeting of an antioxidant to mitochondria. Eur J Biochem. 263**,** 709-16.

Solesio, M. E., et al., 2013. The mitochondria-targeted anti-oxidant MitoQ reduces aspects of mitochondrial fission in the 6-OHDA cell model of Parkinson's disease. Biochim Biophys Acta. 1832**,** 174-82.

Sun, A. Y., et al., 2008. Botanical phenolics and brain health. Neuromolecular Med. 10**,** 259-74.

Sun, A. Y., et al., 2010. Resveratrol as a therapeutic agent for neurodegenerative diseases. Mol Neurobiol. 41**,** 375-83.

Szeto, H. H., 2006. Cell-permeable, mitochondrial-targeted, peptide antioxidants. AAPS J. 8**,** E277-83.

Szeto, H. H., 2008. Mitochondria-targeted cytoprotective peptides for ischemia-reperfusion injury. Antioxid Redox Signal. 10**,** 601-19.

Tang, B., et al., 2006. Association of PINK1 and DJ-1 confers digenic inheritance of early-onset Parkinson's disease. Hum Mol Genet. 15**,** 1816-25.

Tanner, C. M., 2003. Is the cause of Parkinson's disease environmental or hereditary? Evidence from twin studies. Adv Neurol. 91**,** 133-42.

Ullery, J. C., Marnett, L. J., 2012. Protein modification by oxidized phospholipids and hydrolytically released lipid electrophiles: Investigating cellular responses. Biochim Biophys Acta. 1818**,** 2424-35.

Uttara, B., et al., 2009. Oxidative stress and neurodegenerative diseases: a review of upstream and downstream antioxidant therapeutic options. Curr Neuropharmacol. 7**,** 65-74.

van der Vliet, A., et al., 1997. Oxidative stress in cystic fibrosis: does it occur and does it matter? Adv Pharmacol. 38**,** 491-513.

Weng, Y. H., et al., 2007. PINK1 mutation in Taiwanese early-onset parkinsonism : clinical, genetic, and dopamine transporter studies. J Neurol. 254**,** 1347-55.

Wu, X. F., et al., 2005. The role of microglia in paraquat-induced dopaminergic neurotoxicity. Antioxid Redox Signal. 7**,** 654-61.

Yang, L., et al., 2009. Mitochondria targeted peptides protect against 1-methyl-4-phenyl-1,2,3,6-tetrahydropyridine neurotoxicity. Antioxid Redox Signal. 11**,** 2095-104.

Yin, G., et al., 2015. Lipid peroxidation-mediated inflammation promotes cell apoptosis through activation of NF-kappaB pathway in rheumatoid arthritis synovial cells. Mediators Inflamm. 2015**,** 460310.

Yoritaka, A., et al., 1996. Immunohistochemical detection of 4-hydroxynonenal protein adducts in Parkinson disease. Proc Natl Acad Sci U S A. 93**,** 2696-701.

Zarkovic, K., 2003. 4-hydroxynonenal and neurodegenerative diseases. Mol Aspects Med. 24**,** 293-303.

Zhang, J., et al., 1999. Parkinson's disease is associated with oxidative damage to cytoplasmic DNA and RNA in substantia nigra neurons. Am J Pathol. 154, 1423-9.

Zhao, K., et al., 2003. Transcellular transport of a highly polar 3+ net charge opioid tetrapeptide. J Pharmacol Exp Ther. 304, 425-32.

Zhao, K., et al., 2004. Cell-permeable peptide antioxidants targeted to inner mitochondrial membrane inhibit mitochondrial swelling, oxidative cell death, and reperfusion injury. J Biol Chem. 279, 34682-90.

Zhu, J. T., et al., 2007. Flavonoids possess neuroprotective effects on cultured pheochromocytoma PC12 cells: a comparison of different flavonoids in activating estrogenic effect and in preventing beta-amyloid-induced cell death. J Agric Food Chem. 55, 2438-45.

ACKNOWLEDGMENTS

I would like to gratefully thank my major professor Dr. Anumantha G. Kanthasamy for providing me the opportunity to join his lab, his guidance and encouragement throughout my graduate studies. His profound knowledge in the field of neurodegenerative disorders, constructive comments and advices has been of great value for me and were critically important for completing this dissertation. I would also like to thank my committee members, Drs. Arthi Kanthasamy, Wilson Rumbeiha, Stephanie Hansen, and Sanjeevi Sivasankar for their help and comments to improve the quality of my research.

I would like to thank Dr. Vellareddy Anantharam for his help in getting the resources required for my study. Also, I would like to thank Dr. Huajun Jin and Gary Zenitsky for their assistance and support in the preparation of my manuscripts. It has been an absolute pleasure to work with the Kanthasamy group and I am grateful to have great mentors like Drs. Anamitra Ghosh, Afeseh Hilary and Huajun Jin. In addition, I would like to thank all my close collaborators particularly Matthew Neal, Dharmin Rokad, Shivani Ghaisas, Chi-Fu Yen, Dr. Nikhil Panicker and Souvarish Sarkar. I'm also indebted to the past and present current lab colleagues including, Vivek Lawana, Monica Langley, Poojya Anantharam, Dr. Muhammet Ay, Naveen Kondru, Sireesha Manne, Dongsuk Kim, Adhithiya Charli, Jie Luo, Ahmed Abdalla, Qi Xu, Emir Malovic, Carrie Berg, Dr. Richard Gordon, Dr. Dustin Martin, Dr. Arunkumar Asaithambi and Dr. Neeraj Singh.